



MAX-PLANCK-GESELLSCHAFT

TECHNISCHE UNIVERSITÄT MÜNCHEN
FAKULTÄT FÜR PHYSIK

Topological Phases, Symmetries and Open Systems

Caroline I. de Groot

Vollständiger Abdruck der von der Fakultät für Physik
der Technischen Universität München
zur Erlangung des akademischen Grades einer
Doktorin der Naturwissenschaften (Dr. rer. nat.)
genehmigten Dissertation.

Vorsitzender: Prof. Jonathan J. Finley, Ph.D.

Prüfer der Dissertation: 1. Prof. Dr. Norbert Schuch
2. Prof. Dr. Frank Pollmann

Die Dissertation wurde am 24.05.2022 bei der Technischen Universität München
eingereicht und durch die Fakultät für Physik am 16.06.2022 angenommen.

Abstract

The fundamental difference between classical and quantum phenomena in many-body systems arises from the notion of entanglement. This essential property emerges from microscopic interactions and leads to exotic collective phenomena. Entanglement plays a particularly significant role in linking both the fields of quantum information and quantum many-body physics. In quantum information, entanglement is a key resource in quantum computing [1], while in many-body physics, patterns of entanglement characterise the exotic quantum systems known as topological phases. These quantum phases are beyond the conventional Landau symmetry-breaking description and have gained much interest recently due to their potential applications in topological quantum computing (TQC) [2] and measurement-based quantum computing (MBQC) in the case of symmetry protected topological order (SPTO) [3]. SPTO is the simplest example of how symmetry enriches topological phases and enhances the accompanying entanglement structure.

The symbiotic relationship of quantum information and many-body physics has led to an expanding zoo of quantum phases at zero temperature. On the one hand, the classification of topological phases has been understood from the perspective of quantum information thanks to the toolbox given by tensor networks. On the other hand, the discovery of new phases with exotic properties has led to new platforms for quantum computing. Recently, there has been significant progress in understanding the robustness of quantum phases to noise, and classifying the phases of mixed states [4], complementing efforts to develop quantum technologies in the noisy intermediate scale quantum (NISQ) era [5]. In practice, dissipative processes determine the actual robustness of quantum phases and of their potential application towards technologies. Moreover, a symmetry protected topological (SPT) phase is equivalent to quantifiable computational power in MBQC [6], so describing a framework for noisy SPTO is an important goal.

The aims of this Thesis lie at the intersection of quantum information and many-body physics. We address how topological phases with symmetries are affected by the presence of a noisy environment, as witnessed through entanglement structure and order parameters.

Our first contribution is to introduce a new indicator for SPTO. We define the inaccessible entanglement of systems with SPTO, which determines how much entanglement is inextricable under the restrictions of symmetry. A previous work made the insight that SPTO is equivalent to computational power in MBQC, where entanglement is consumed in the computation [6]. We address how this entanglement emerges in SPT phases by considering the entanglement structure in the presence of symmetries. A common setting in quantum information is when two spatially-separated parties are able to perform local operations on their systems, and also communicate classically (i.e. over the telephone), which is called local operations and classical communication (LOCC). We find that a certain amount of entanglement is always inaccessible in non-trivial SPT phases. Namely, the inaccessible entanglement of states under symmetry-restricted LOCC is bounded,

when the local operations are required to commute with the symmetry. Further, SPT phases have a nontrivial lower bound.

Our main contribution in this Thesis is to determine how indicators of SPT phases in one-dimension can change under the effects of dissipation. We observe that there are two natural ways to enforce symmetry on noise, which we term weakly symmetric and strongly symmetric. Using these notions, we define a consistent set of state transformations preserving the manifold of SPT states. Recently, a rigorous framework for the classification of topological phases of mixed states which extends gapped phases of pure states has been given by Ref. [4]. However, it was suggested that SPTO cannot exist, as weak symmetry destroys SPTO instantly. We show the following: (i) Under evolution by a strongly symmetric channel, the SPTO of a state is generically preserved. We demonstrate this by studying various indicators of SPTO: string operators, topologically protected edge modes, twisted sector charges, and inaccessible entanglement. (ii) If SPTO is preserved by a channel, it must have been a convex combination of twisted strongly symmetric channels with appropriate twists. (iii) We determine how these twisted versions of strongly symmetric channels transform between different SPT phases. These channels may only preserve or reduce the complexity of the phase. Our analysis of robustness begins with single-site noise, and we generalize this to causal channels, which are closely related to local Lindbladians and Lieb-Robinson bounds. We conclude that strongly symmetric causal (or equivalently short-depth circuits of) channels are unable to generate sufficiently different patterns of entanglement which would destroy or change the phase.

Finally, we consider whether the above notion of robustness can be extended to intrinsic topological order, by applying the same recipe to symmetry enriched topological order (SETO). These systems are of interest since symmetry can augment intrinsic quantum error correcting properties [7–9]. We consider a two-dimensional system which is constructed from a Toric code decorated by cluster states [10], and analyse the robustness of an order parameter that detects symmetry fractionalisation in the anyons which is characteristic of and classifies SETO [11]. We conjecture that locally strongly symmetric causal channels preserve the symmetry enriched topological (SET) phase, supported by numerical evidence, and give steps towards demonstrating this analytically.

Zusammenfassung

Der grundlegende Unterschied zwischen klassischen und quantenmechanischen Phänomenen in Vielteilchensystemen ergibt sich aus dem Konzept der Verschränkung. Diese Eigenschaft entsteht durch mikroskopische Wechselwirkungen und führt zu exotischen kollektiven Phänomenen. Verschränkung spielt eine besonders wichtige Rolle bei der Verknüpfung der Bereiche Quanteninformation und Quantenvielteilchenphysik. In der Quanteninformation ist Verschränkung eine essentielle Ressource von Quantencomputern [1], während in der Vielteilchenphysik Verschränkungsmuster die exotischen Quantensysteme charakterisieren, die als topologische Phasen bekannt sind. Diese Quantenphasen lassen sich nicht durch die herkömmliche Landau-Symmetriebrechung beschreiben. Sie haben in letzter Zeit großes Interesse geweckt aufgrund ihrer potenziellen Anwendungen im topologischen Quantencomputing (TQC) [2] und im messungsbasierten Quantencomputing (MBQC) im Falle der symmetriegeschützten topologischen Ordnung (SPTO) [3]. SPTO ist das einfachste Beispiel dafür, wie Symmetrie topologische Phasen bereichert und die begleitende Verschränkungsstruktur erweitert.

Das symbiotische Verhältnis von Quanteninformation und Vielteilchenphysik hat zu einem wachsenden Zoo von Quantenphasen am absoluten Temperaturnullpunkt geführt. Einerseits gab der Werkzeugkasten der Tensornetzwerke Einsicht in die Klassifikation topologischer Phasen. Andererseits hat die Entdeckung neuer Phasen mit exotischen Eigenschaften zu neuen Plattformen für Quantencomputing geführt. Des Weiteren wurden kürzlich erhebliche Fortschritte beim Verständnis der Robustheit von Quantenphasen gegenüber Rauschen und bei der Klassifizierung von Phasen gemischter Zustände erzielt [4], begleitend zu allgemeinen Bemühungen zur Entwicklung von Quantentechnologien in der NISQ (Noisy Intermediate Scale Quantum) Ära [5]. In der Praxis bestimmen dissipative Prozesse die tatsächliche Robustheit von Quantenphasen und ihre potenziellen technologischen Anwendungen. Darüber hinaus entspricht eine symmetriegeschützte topologische Phase (SPT) einer quantifizierbaren Rechenleistung in MBQC [6], weshalb ein umfassendes Verständnis von SPTO mit Rauschen ein wichtiges Ziel ist.

Die Ziele dieser Arbeit liegen an der Schnittstelle von Quanteninformation und Vielteilchenphysik. Wir behandeln, wie topologische Phasen mit Symmetrien durch Kopplung zu einer verrauschten Umgebung beeinflusst werden, wobei wir ein besonderes Augenmerk auf die Verschränkungsstruktur und den Ordnungsparameter der Phase legen.

Unser erster Beitrag ist die Einführung eines neuen Indikators für SPTO. Wir definieren die unzugängliche Verschränkung von Systemen mit SPTO, die bestimmt, wie viel Verschränkung unter den Einschränkungen der Symmetrie unentwirrbar ist. Eine frühere Arbeit machte die Erkenntnis, dass SPTO der Rechenleistung in MBQC entspricht, wobei die Verschränkung in der Berechnung aufgebraucht wird [6]. Wir behandeln, wie diese Verschränkung in SPT-Phasen entsteht, indem wir die Verschränkungsstruktur im Beisein von Symmetrien betrachten. Wir betrachten dazu das in der Quanteninformation übliche Szenario lokaler Operationen

und klassischer Kommunikation (LOCC), in welchem zwei räumlich getrennte Parteien in der Lage sind, lokale Operationen auf ihren Systemen durchzuführen und auch klassisch (zum Beispiel telefonisch) zu kommunizieren. Wir stellen fest, dass ein gewisses Maß an Verschränkung in nicht-trivialen SPT-Phasen mit symmetriebeschränkter LOCC stets unzugänglich ist.

Der Hauptbeitrag dieser Dissertation besteht darin, die Auswirkungen von Dissipation auf verschiedene Indikatoren von SPT-Phasen zu bestimmen. Wir betrachten dazu zwei naheliegende Definitionen für symmetrisches Rauschen, welche wir als schwach symmetrisch und stark symmetrisch bezeichnen. Unter Verwendung dieser Begriffe definieren wir eine konsistente Menge von Zustandstransformationen, die die Mannigfaltigkeit von SPT-Zuständen bewahren. Kürzlich wurde durch Lit. [4] ein rigoroser Rahmen geschaffen, der die Klassifizierung topologischer Phasen von reinen auf gemischte Zustände erweitert. Es wurde jedoch vorgeschlagen, dass SPTO nicht existieren kann, da schwache Symmetrie SPTO sofort zerstört. Wir zeigen Folgendes: (i) Unter Evolution durch einen stark symmetrischen Kanal bleibt die SPTO eines Zustands generisch erhalten. Wir demonstrieren dies, indem wir verschiedene Indikatoren von SPTO untersuchen: String-Operatoren, topologisch geschützte Randmoden, verdrehte Sektorladungen und unzugängliche Verschränkung. (ii) Wenn SPTO durch einen Kanal erhalten bleibt, muss es sich um eine konvexe Kombination von verdrillten, stark symmetrischen Kanälen mit geeigneten Verdrillungen handeln. (iii) Wir bestimmen, wie diese verdrillten Versionen von stark symmetrischen Kanälen verschiedenen SPT-Phasen ineinander verwandeln. Dabei kann sich die Komplexität der Phase nicht vergrößern. Sie bleibt entweder gleich oder verringert sich. Unsere Analyse der Robustheit beginnt mit Einzelstellenrauschen und wir verallgemeinern dies auf kausale Kanäle, die eng mit lokalen Lindbladtermen und Lieb-Robinson-Grenzen zusammenhängen. Wir schlussfolgern, dass stark symmetrische, kausale Kanäle (oder, gleichwertig, kurze Schaltkreise von Kanälen) nicht in der Lage sind, ausreichend unterschiedliche Verschränkungsmuster zu erzeugen, die die Phase zerstören oder verändern würden.

Schließlich untersuchen wir, ob die obige Auffassung von Robustheit auf die intrinsische topologische Ordnung erweitert werden kann, indem wir dasselbe Rezept auf symmetrieangereicherte topologische Ordnung (SETO) anwenden. Diese Systeme sind von Interesse, da intrinsische Quantenfehlerkorrektoreigenschaften durch Symmetrie verstärkt werden kann [7, 8]. Wir betrachten ein System, das aus einem mit Clusterzuständen dekorierten torischen Code aufgebaut ist [10] und analysieren die Robustheit eines Ordnungsparameters, der die Symmetriefraktionierung in den Anyonen erkennt, welche für SETO charakteristisch ist und diese klassifiziert [11]. Unterstützt von numerischen Hinweisen mutmaßen wir, dass lokal stark symmetrische, kausale Kanäle die symmetrieangereicherte topologische (SET) Phase erhalten. Wir beschreiben die notwendigen Schritte, um dies analytisch zu zeigen.

Acknowledgements

This Thesis would never have been possible without the support of many individuals along the way who I am so grateful for.

Firstly, I would like to thank my supervisor Norbert Schuch for his mentorship throughout my PhD. You gave me freedom to explore the fascinating world of quantum physics, and have always been available to discuss science and other topics. I am very grateful for your insights and for our discussions from which I learned a lot. I am also thankful for the friendly, creative atmosphere of the group you created which is open to new ideas, promotes collaborations and gave me great friends.

I am also thankful to Ignacio Cirac for his leadership in the MPQ theory group, and in creating the inclusive, energetic group atmosphere there which is full of brilliant scientists and brilliant people. I am extremely grateful that you supported the last part of my PhD financially, as well as the consistent support in professional development and mentorship that you always offer.

I am extremely grateful to Sonya Gzyl for her consistent care as the IMPRS coordinator. The IMPRS program gave me invaluable opportunities for growth as a scientist and to develop myself personally and professionally. I am also very thankful to MCQST for countless opportunities, and in particular to staff such as Barbara Tautz for their support.

Thank you to the theory group secretaries Andrea Kluth, Regina Jasny and Elena Wiggert who play such a crucial role in the group, and who always show kindness and patience in helping with many administrative matters. I would also like to thank the administrative staff at MPQ including in particular Petra Mayrhofer, Marianne Kargl, Michaela Vey, Veronika Seidl and Lena Stachel.

I am very grateful for the support of collaborators and colleagues abroad who have shared many interesting and valuable discussions, including Alex Turzillo, José Garre-Rubio, Andras Molnar, Simon Lieu, Angela Capel Cuevas and David Perez-Garcia. I would also like to thank my Professors at St Andrews, including Jonathan Keeling, Brendon Lovett and Natalia Korolkova for guiding me as a young scientist.

This Thesis would never have been possible without David Stephen, my officemate, collaborator and mentor, but also my housemate and one of my dearest friends. Through David, I also made some of my closest friends: Annie, Ritika and Lorenzo. Thank you all for becoming my Garching family. I would like to thank my other officemates as well, Mohsin, Ivana, Jiří and Albert, for the fun times we have had, filled with many teas, interesting blackboard and life chats. Thanks also to David and Albert for their help in proofreading my Thesis.

I am also extremely thankful for the vibrant community in the MPQ theory group, which it has been a pleasure and privilege to be a part of. I'd like to thank in particular Daniel M., Giacomo G., Patrick, Christoph, Tommaso, Julian B., Cosimo, Anna, Johannes, Nicola, Henrik, Julian R., Asli, Eirini, Georgios,

Alvaro and Flavio. I'd also like to thank IMPRS colleagues for their friendship and sharing good science, including Ella, Noelia, Alex, Annabelle, Fabian, Toni and Tibor. Further I am thankful for the quantum information community at large which is so positive and friendly, and for the many moments of learning and fun memories shared at conferences with Elisa, David G., Armin, Jose C., Namit, Alex N., Andreas B. and Alexis. I am also grateful for the community I formed in industry, in my team at IBM Quantum who showed me another side to quantum science, including Elisa, Anamita, Fabio, Abraham, Hannah and Julia.

I'd like to thank the great friends I've made over the years in Munich who've kept me sane, including Umberto, Sam, Javi, Sofi, Sven, Anna, Esther, Fabian, Klara, Munan, and others in the swing dance community. I'd also like to thank friends from afar, including Pooneh, Klara, Louise, Nina, Charly, Raad and Kirsty. Thank you to my oldest friend Lucy for always being there for me, for being my constant partner in crime and many special times together, on our parallel PhD journeys.

Lastly, I am grateful for my family, my parents, brother and sister, for their unconditional support, sense of fun, and many lessons. You taught me to be brave, to always try my best and encouraged my curious and adventurous spirit. Finally, I am so grateful to Dom for the adventures together so far, and his warmth and kindness always in navigating this journey with me.

List of Acryonyms

AKLT: Affleck, Lieb, Kennedy and Tasaki
CPQC: causality-preserving quantum channel
GHZ: Greenberger-Horne-Zeilinger
irrep: irreducible representation
LOCC: Local Operations and Classical Communication
MBQC: measurement-based quantum computation
MPDO: Matrix Product Density Operator
MPO: Matrix Product Operator
MPU: Matrix Product Unitary
MPS: Matrix Product State
NISQ: Noisy Intermediate-Scale Quantum
PEPS: Projected Entangled Pair State
SD: Schmidt decomposition
sdQC: symmetric CPQC obtained by a Stinespring dilation
SCQM: self-correcting quantum memory
SET: Symmetry Enriched Topological
SF: Symmetry Fractionalization
SPT: Symmetry Protected Topological
SVD: Singular Value Decomposition
TN: Tensor Network
TQC: Topological Quantum Computing

Contents

1	Introduction	1
1.1	Structure of the Thesis	6
1.2	Publications	7
2	Background: Gapped quantum phases, tensor networks, and open systems	9
2.1	Gapped quantum systems	9
2.2	Beyond gapped phases of pure states	15
2.3	Tensor networks	19
2.4	Symmetry protected topological order	22
2.5	Intrinsic topological order	30
2.6	Symmetry enriched topological order	33
3	A new fingerprint for SPTO: inaccessible entanglement	41
3.1	Motivation	41
3.2	Summary	42
3.3	Accessible entanglement distillation	43
3.4	Bounds for the inaccessible entanglement	47
3.5	Investigation of the bounds	51
3.6	Outlook	60
3.7	Discussion & Conclusions	62
4	Symmetry protected topological phases in open systems	65
4.1	Motivation	65
4.2	Summary	67
4.3	Coherent SPT mixtures	69
4.4	A strong symmetry condition on channels	69
4.5	Strongly symmetric uncorrelated noise	77
4.6	Causal channels	87

4.7	Discussion & Conclusions	95
5	Transmuting symmetry protected topological phases under quantum channels	97
5.1	Motivation	97
5.2	Summary	99
5.3	The action of endomorphisms on SPT phases	100
5.4	Patterns of zeros under endomorphisms	105
5.5	Twisted symmetric channels	106
5.6	Transmutation of SPT phases	108
5.7	Discussion & Conclusions	115
6	Symmetry enriched topological order in open systems	117
6.1	Motivation	117
6.2	Summary	118
6.3	Swap order parameter with dissipation	120
6.4	SET order parameter under dissipation	127
6.5	Discussion & Conclusions	131
7	Conclusions	133

Chapter 1

Introduction

We have sought for firm ground and found none.
The deeper we penetrate, the more restless becomes
the universe... Not everything is knowable, still less
is predictable.

Max Born
The Restless Universe
1935.

The natural world is made up of astoundingly complex physical phenomena – from black holes, to superconducting levitation and the spontaneous creation of sub-atomic particles. What’s even more astounding is that much of this macroscopic emergent complexity in our universe is successfully described via a theory of complexity at the microscopic level. Systems are made up of discrete particles which are described by quantum mechanical laws. Nowadays we know that the emergent complexity of many-body systems is generated by the interactions between quantum particles, which is explained by a fantastic notion known as entanglement.

One of the most marvellous facts about quantum systems is that they cannot be understood by simply observing a single one of their constituents; indeed, the information in a quantum system is non-local and lies fundamentally in the bonds between their parts, rather than in the individual parts themselves. The study of entanglement and its ramifications underlies many of the central questions of modern quantum science and its applications today. In particular, entanglement is the essential link between the symbiotic fields of quantum information and many-body physics and plays a key role in several different ways. The first story in which entanglement is a main character is in explaining emergent quantum phenomena, which relates to the study of quantum phases of matter and the zoo of quantum phases [12]. A second story of entanglement is given by how quantum systems interact with a noisy environment, and the robustness of quantum coherence, which relates to the study of open quantum systems [13]. Both of these topics are becoming increasingly appreciated given the recent upsurge in interest in quantum technologies [14]. This Thesis combines both stories, living at the intersection of quantum information and many-body physics, and altogether illustrates the

intimate relationship these fields enjoy.

In the study of quantum phases of matter, quantum information has provided a new lens with which to study many-body systems through the realisation that they are characterised in terms of their entanglement structure [1]. This insight may seem surprising at first, since entanglement significantly complicates the description of quantum states, due to the mathematical fact that the number of possible quantum states grows exponentially in the number of particles. In fact, simulating some macroscopic, mole-sized system of 10^{23} two-level particles requires the storage of $2^{10^{23}}$ complex numbers. This is because quantum mechanical states, fundamentally different to classical states, are given by probability distributions on the possible measurement outcomes of qubits, according to Born's rule [15]. Further, observations are only explained by a theory which necessitates operators on a complex-valued Hilbert space [16]. How then can quantum systems be anything but intractable to study?

Fortunately, a key observation coming from quantum information has been that most interesting quantum many-body states live in just a small corner of the Hilbert space [17] which is characterised by a sweet spot in the amount of entanglement. Namely, ground states of certain quantum many-body Hamiltonians obey an area-law in entanglement, such that entanglement grows only slowly with the system size [18, 19], rather than volume-law which would be fast growing. This observation has led to tools in quantum information, such as tensor networks, which have allowed to greatly simplify the description of many-body states. Tensor networks leverage the inherent entanglement structure of interesting quantum states, providing a way to systematically construct quantum systems by building up entanglement locally. Further, this merges very naturally with symmetries by interplaying them with entanglement within this framework. As illustrated in Fig. 1.1(b), most generic states in the Hilbert space have too much entanglement (volume-law states) which creates non-universal behaviour through too many interactions to allow collective quantum coherences [20]. By contrast, a lack of entanglement (product states) creates classical behaviour since too few interactions do not allow quantum coherence at all. The quantum phases in the sweet spot of Hilbert space, which obey the area-law, are described by tensor networks and are characterised by non-trivial patterns of entanglement, are known as topological phases [12]. These will be our focus in this Thesis.

Facilitated greatly by the observations and tools from quantum information, developing a complete understanding of topological phases has become one of the most significant pursuits of modern day physics. On the one hand, the classification of quantum phases of matter leads to the discovery of new materials and new quantum phenomena [21–23]. On the other hand, the discovery of quantum many-body phases has led to new possibilities in quantum information, in the form of quantum technologies. Historically, the potential for advantages coming from quantum information was first perceived in applying simple quantum systems to study other harder-to-engineer many-body systems, namely in the application of quantum simulation [24]. It was realised that intrinsic properties of quantum particles (such as the spin of an electron or the polarisation of a photon) can be

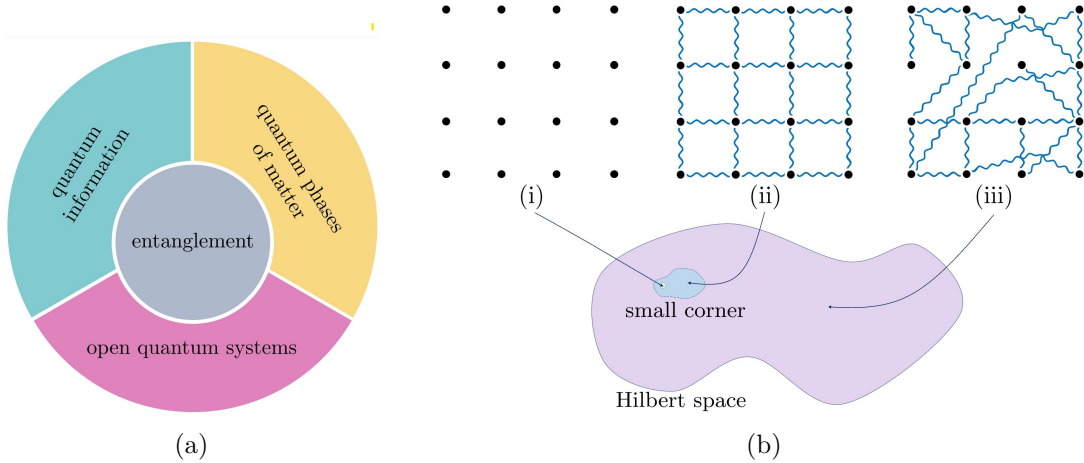


Figure 1.1: (a) The central question of this Thesis lies in how entanglement connects the fields of quantum information and many-body physics, and additionally open quantum systems. (b.i) Product states have no entanglement. (b.ii) States with a sweet spot of entanglement, namely those which obey an area-law, make up a small corner of Hilbert space. (b.iii) Most of the Hilbert space contains highly entangled states which obey a volume-law in entanglement.

leveraged to describe information, in the same way as classical bits (such as currents of electrons). Later, novel schemes of quantum computation were developed for quantum many-body states, harnessing their intrinsically quantum properties as an advantage over classical counterparts. For example, in Kitaev’s Toric code state [2] topological quasiparticles can be harnessed for topological quantum computing (TQC), while in the cluster state [25, 26], emergent quasiparticles living on the boundary of the state can be used for measurement-based quantum computing (MBQC).

The cluster state, which will be central throughout the Thesis, is a canonical example of a symmetry protected topological (SPT) phase. Furthermore, it is actually a computational phase of matter, since all states in the same phase as the cluster state can perform universal MBQC [6, 27, 28], meaning that the circuit model of quantum computing can be simulated efficiently. Notably, MBQC on the 1D cluster state can simulate all single qubit gates [27, 29–31], while MBQC on a 2D cluster state can simulate all two-qubit gates [32–34]. The computational power of the cluster phase in MBQC has been understood by its patterns of entanglement, which can in turn be directly related to its topological order. This fundamental relationship between SPT order and MBQC highlights once again the deep connection between quantum phases of matter and quantum information.

Preparing examples of such exotic quantum phases in experiment has been an impressive challenge in the generation and preservation of quantum coherence. For small numbers of qubits, the Toric code has been experimentally simulated in quantum systems based on superconducting qubits [35–38], photons [39, 40] as well as nuclear spin qubits [41, 42], while the cluster state has been realised in photons [43–48], in continuous-variable optical systems [49–51] and also in ultracold

atoms [52, 53]. This brings us to the second story of entanglement, which is of how quantum many-body systems interact with noise.

Entanglement is unfortunately very fragile under dissipation. The quantum coherence of many-body systems is easily destroyed under coupling to a dissipative environment. It is also impossible to completely isolate a quantum system in practice. Therefore any approach to engineering quantum phases or realising quantum technologies must grapple with the effects of noise. Since certain quantum algorithms were first demonstrated to solve some computational problems more efficiently than the best classical counterpart, such as Shor’s factorising algorithm just ca. 30 years ago [54], mitigating noise in quantum hardware has become an important problem at the forefront of current-day physics. Advances in hardware have been accelerating, driven by partnerships across academia, industry and government, beyond the limitations of the current available devices, which are the so-called Noisy Intermediate-Scale Quantum (NISQ) devices [5] due to their high error rates and low coherence times. This raises questions about the future of technology, which have not only scientific, but arguably also philosophical and social importance. However, the potential promise of quantum advantage is largely unresolved [55]. Fortunately for us, this still poses a fascinating challenge; of identifying both the strengths and limitations of quantum phases towards their applications in emerging technologies¹. This idea is encompassed by the study of phase robustness and fault-tolerance [56–59]. Further, understanding noisy quantum many-body phases is not only desirable for realising applications in quantum technologies, but is moreover motivated by the pursuit of fully classifying quantum phases.

Phase classification is important even in our everyday lives. Our brains naturally process information by grouping systems into simple classes which capture universal properties that are relevant to our context, i.e. the edibility of different kinds of forest berries. The same intuition applies in classifying quantum phases. Classes of quantum states can be understood by whether they share the same patterns of entanglement; this defines topological phases of pure states [60]. The zoo of topological phases contains useful information in the form of topological invariants, which form the labels for different topological phases. The classification of topological phases is well understood by now, where a phase corresponding to a particular topological invariant is given by families of quantum states connected by paths of particular unitary evolutions given by gapped, local Hamiltonians [61], and a change in topological invariant would signify a phase transition.

Since it has become increasingly important to understand the role of noise in classification of quantum phases, this requires studying quantum phases of mixed states as the generalisation from pure states, which are necessary to describe states in open quantum systems and beyond zero-temperature regimes. There have been significant contributions towards understanding beyond the zero-temperature regime in theory [61–69], but a fully satisfactory framework for classification of mixed state topological order has been elusive. Recently, a promising work has

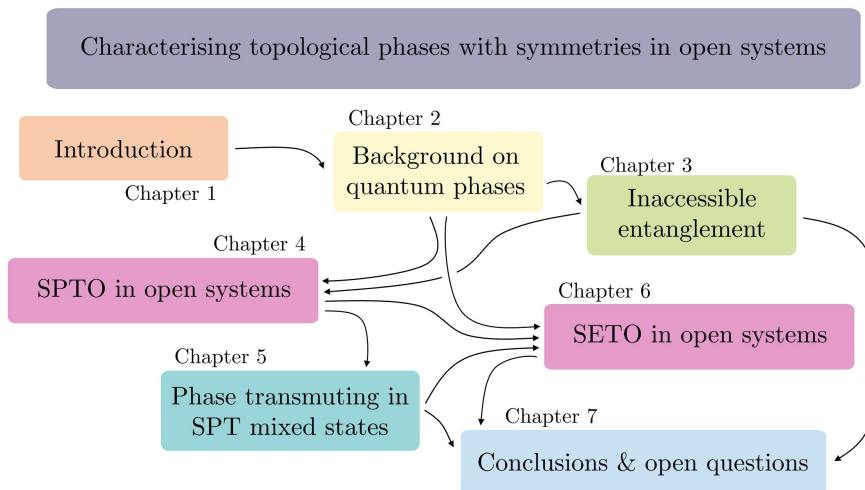
¹In the words of Scott Aaronson, “Like Achilles without his heel or Superman without kryptonite, a computer without any limitations would get boring pretty quickly” [55].

made significant steps in this direction [4]. It naturally extends gapped phases of pure states to phases of mixed states connected by short-depth circuits of channels, which generalise the unitary evolution of pure states to, in particular, an open system evolution called a Lindbladian. Also recently, SPT phases have been studied experimentally on noisy digital quantum computers, suggesting that the notion of SPT mixed states is sensible [70, 71].

The central question in this Thesis is of the robustness of topological phases to noise, and in particular of the interplay between symmetry and entanglement, which orchestrate the dance of collective quantum phenomena. We consider topological phases protected by symmetries, in particular symmetry protected topological (SPT) order and symmetry-enriched topological (SET) order. We ask the following, namely, *which are the topological phases of mixed states?* With such a notion of mixed state topological order in hand, we then consider *which invariants describe topological phases of mixed states?* and analyse the robustness of certain fingerprints, including a new fingerprint of SPTO which we have developed. Finally, we ask *which are the operations which map between topologically ordered mixed states?* Quantum information and quantum many-body physics continue to mutually benefit each other through their complementary studies of entanglement. We hope to convince the reader that the interweaving of these fields has raised and continues to raise important questions for science and society as a whole.

1.1 Structure of the Thesis

There are several possible paths a reader may take through this Thesis, which we visualise below. In each Chapter we have included a Motivation and Summary section which contain the most necessary take-aways, aimed at the reader with not a lot of time on their hands. The Motivation section aims to bring across an introduction to the context and significance of the main findings, while the Summary section is intended to be a short version of the work, describing the results and methodology.



We will begin by giving the relevant background in Chapter 2 on quantum phases of matter, tensor networks and open quantum systems. In Chapter 3, we will present a new quantity which measures the inaccessible entanglement in SPT phases, and which acts as a “fingerprint” of the SPT phase. Fingerprints, or order parameters, of topological phases will play a key role in coming discussions in the Thesis. In Chapter 4 we will reach the starting point for the main topic of the Thesis which is that of topological phases subject to noise. We will show that 1D SPTO is not robust to generic couplings to the environment, or even under couplings satisfying a weak symmetry condition. However, noise satisfying a stronger symmetry condition does preserve SPTO at finite times, which gives a promising starting point for the study of SPTO in open systems and phases of SPT mixed states. In Chapter 5 we will consider the question of which channels map between different coherent SPT phases of mixed states. In Chapter 6 we will discuss how our framework for the robustness of 1D SPTO may be applied to higher-dimensional topological orders, focusing on 2D symmetry enriched topological order. Finally, in Chapter 7 we will give conclusions and discuss several promising open questions.

1.2 Publications

During this PhD a number of manuscripts have been written. The manuscripts listed below are included in a modified form. Given also is a summary of the role of each publication in the Thesis and my contribution.

- Inaccessible entanglement in symmetry protected topological phases. **Caroline de Groot**, David T. Stephen, Andras Molnar, and Norbert Schuch. Journal of Physics A: Mathematical and Theoretical 53, 335302 (2020). [72]

We develop a new operationally-defined fingerprint for symmetry protected topological order. Contained in Chapter 3 of the Thesis, content revisited throughout the bulk of the Thesis. I am the main contributor and author.

- Symmetry Protected Topological Order in Open Systems **Caroline de Groot**, Alex Turzillo, and Norbert Schuch, arXiv:2112.04483v2 (submitted to Quantum). [73]

We study the robustness of symmetry protected topological order in open systems through its fingerprints. Main result of the Thesis, split into two separate stories, in Chapter 4 and Chapter 5. I share main contributions and authorship with Alex Turzillo.

- Symmetry Enriched Topological Order in Open Systems **Caroline de Groot** Jose Garre Rubio, and Alex Turzillo (in preparation). [74]

We study the robustness of symmetry enriched topological order in open systems. Contained in Chapter 6 of the Thesis, content draws from Chapter 4. I am the main contributor and author.

Chapter 2

Background: Gapped quantum phases, tensor networks, and open systems

Now we focus on introducing the background knowledge needed to complete the journey through this Thesis. We begin by discussing the core concept of gapped quantum systems and give the definition of a gapped quantum phase of matter in Section §2.1. We also introduce phases beyond pure states, which are important to Chapters 4, 5 and 6. We briefly discuss quantum channels, the notion of open quantum systems, and in particular the Lindblad master equation in Section §2.2.1. We then introduce some key notation in tensor networks in Section §2.3 which will be the main tool throughout the Thesis, and in particular is used for key calculations in Chapters 3 and 4. Section §2.4 introduces the main quantum phase we are interested in in this Thesis, which is symmetry protected topological phases. We give some particular examples, such as the cluster state, which have led to the main insights in this Thesis. Finally we discuss the notion of intrinsic topological order in Section §2.5, and in Section §2.6 introduce the notion of symmetry enriched topological order, as well as a model and order parameter which form the backbone of the results in Chapter 6.

For a more comprehensive review of these topics, the reader is referred to some personal favourites which include Ref. [75] for a textbook review on gapped quantum phases, Ref. [76] for an introductory course and Ref. [77] for a review on tensor networks, and Ref. [13] for a textbook review of open systems.

2.1 Gapped quantum systems

The quantum many-body systems we study in this Thesis are quantum spin lattices, which are discrete bosonic, rather than fermionic, systems. States live in a Hilbert space \mathcal{H} composed of a tensor product of N d -dimensional Hilbert spaces \mathbb{C}^d which represent (d -dimensional) spin degrees of freedom living on the lattice. From this we can see how the dimension of \mathcal{H} grows exponentially with the number of

spins N . Therefore, even a generic state in \mathcal{H} with just $N = 50$ can become very complicated indeed. Individual spins are called qudits, but we often consider only qubits, corresponding to $d = 2$ spins which have basis states $|0\rangle$ and $|1\rangle$. We will see later that defining a quantum system on a lattice often simplifies its study, for example through the use of tensor networks.

The first property which allows us to simplify the program is locality. The quantum spin lattices we consider here will be defined by local Hamiltonians, which have the form $H = \sum_{i=1}^N h_i$ where each local Hamiltonian h_i acts on a finite region r around a site i , and N is the system size. Local Hamiltonians require far fewer parameters to describe them, with only Nd^r parameters, compared a generic many-body Hamiltonian which has d^N [78].

A further property we will require is that of gappedness. A Hamiltonian H is called *gapped*, if, as the system size N grows to infinity, there is a finite gap Δ between the ground state manifold and the first excited state for each value of N [79]. In other words, the gap is bounded from above by a constant independent of N . Together, the properties of locality and gappedness lead the way for interesting phases of matter characterised by an area-law and non-trivial patterns of entanglement. Such quantum systems therefore are said to live in the small “physical corner” of Hilbert space, as depicted in Fig. 1.1(b).

Finally, the quantum spin lattices we will consider will only be commuting (non-frustrated) Hamiltonians, which are exactly solvable. Since all local Hamiltonian terms commute with each other, they share the same eigenstates, such that the system’s energies can be solved for exactly, without the need for approximation methods. Such systems are not naturally found in nature, but they capture universal features of many models relating to their entanglement. In particular, these systems can be described by a historically significant idea known as the renormalisation-group (RG) [80], first developed by K.G. Wilson in 1971, marrying ideas in statistical mechanics and quantum field theory. The RG method showed that by coarse-graining length scales, states flow towards a fixed point which has lost all local, microscopic details such as short-range entanglement or correlations and captures only the essential universal structure [81, 82]. This has been a profound insight which tells us that universal features of quantum phases of matter are emergent phenomena that have the same patterns within a phase [83]. This insight will be particularly useful in the paradigm of tensor networks, where universal features of gapped many-body phases universal features can be understood through entanglement. In particular, generic states in a many-body phase are perturbations around a fixed point with a particular entanglement structure [31].

2.1.1 Defining gapped quantum phases

Classical phases of matter such as solid, liquid and gas experience phase transitions in terms of macroscopic (extensive) properties such as pressure, temperature and volume, which rely only on the individual constituents of systems. Additionally, such systems always have a temperature, which can also describe their phase transitions. On the other hand, quantum phases of matter can’t be described by

their individual constituents due to entanglement, and can very conveniently be defined at zero temperature. We save non-zero temperature quantum phases for Section §2.2. Altogether, this means a new mechanism must be given for quantum phase transitions.

A very successful theory of quantum phase transitions was given by the idea of symmetry-breaking through the formalism of group theory by Landau in 1937 [84], which has led to the complete classification of the 230 kinds of crystals in 3D. Phase transitions between an ordered (symmetry-broken) and disordered (symmetry-preserving) phase are given by tuning parameters of the system such as the magnetic field strength or lattice spacing. However, with the discovery of the Berezinskii-Kosterlitz-Thouless (BKT) transition [85] in 1973 and the fractional quantum Hall effect [86] in 1982, it became clear that there was still more physics to be uncovered beyond the Landau paradigm. In 1989, the missing pieces were provided by a framework for gapped quantum phases, otherwise known as topological phases, which includes phases with and without symmetry-breaking [87–89].

The definition for a phase of gapped quantum matter is as follows:

Definition 1: *Two local, gapped Hamiltonians H, \widetilde{H} are in the same phase if there exists a continuous path of local, gapped Hamiltonians H_t with $t \in [0, 1]$, and $H_0 = H$ and $H_1 = \widetilde{H}$.*

Continuity of the path is meant in the sense that H_t is continuous, and further that the gap Δ_t doesn't close as a function of t . The path of local, gapped Hamiltonians is furthermore an adiabatic evolution. The presence of the gap guarantees that, if this evolution is done sufficiently slowly, the system will not leave the ground state, and hence observables will also only change continuously. This is described by the adiabatic theorem [90].

A *phase transition* occurs when the Hamiltonian path between H, \widetilde{H} has a gap closure, which is physically indicated by the divergence of quantities such as the correlation length [91]. The study of phase transitions is a field on its own [92–95].

Conversely, we may restate this definition for states. Two states $|\psi_0\rangle$ and $|\psi_1\rangle$ are in the same phase if they are the ground states of local, gapped Hamiltonians, $|\psi_t\rangle$ is also the ground state of H_t , and Definition 1 is satisfied. This defines an equivalence relation which leads to equivalence classes of states which we call phases. Note that the phase which contains only product states is called the trivial phase.

We may alternatively formalise the definition above via the notion of finite-depth quantum circuits (FDQC) which comes from the perspective of quantum information. This perspective allows us to directly interpret gapped quantum phases by their entanglement. Any time evolution of a local, time-dependent Hamiltonian H_t can be understood as a quantum circuit w.l.o.g. The FDQC is a unitary operator of the form

$$U = \prod_{k=1}^d \left(\prod_{i=1}^N u_{k,i} \right), \quad (2.1.1)$$

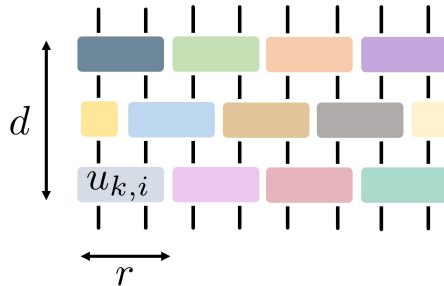


Figure 2.1: An example of a finite-depth quantum circuit with depth $d = 3$ and range $r = 2$.

where d is the circuit depth and where $u_{k,i}$ are local unitary operators acting on a site i with support on a region r . While r is allowed to be quasi-local, d should be independent of N [4]. The action of a FDQC is given in Fig. 2.1, where in general, each gate $u_{k,i}$ in the circuit may be different.

Definition 2: Two states $|\psi\rangle$ and $|\tilde{\psi}\rangle$ are in the same phase if there exists a unitary operator U which is a FDQC such that $U|\psi\rangle = |\tilde{\psi}\rangle$.

One can imagine separating states into two classes: those which can be connected to a product state by a FDQC, called short-range entanglement, and those which cannot be connected to a product by a FDQC, called long-range entanglement [91]. We depict this in Fig. 2.2.

2.1.2 Quasi-adiabatic evolution

How are the FDQC and the adiabatic Hamiltonian path related in the definition for gapped quantum phases? The notion which gives the connection is that of quasi-adiabatic evolution [96], which are also related to Lieb-Robinson bounds. We include the following discussion since it will be useful background in Section §2.2.

Firstly, consider an observation about the adiabatic Hamiltonian path. If we perform an adiabatic evolution with the original system Hamiltonian, the error scales as $t\Delta_N$, for the gap Δ_N of the Hamiltonian defined for a system size N . This implies that it would take an infinitely long time to exactly perform any time evolution, even between states in the same phase. Of course, this is bad news, since that seems to give a paradox with the FDQC which should be implementable in a finite time by definition. Fortunately, this can be resolved by replacing the adiabatic Hamiltonian evolution H_t by a quasi-adiabatic evolution [96]. At the price of approximating the actual Hamiltonian up to an exponentially small error with a particular quasi-adiabatic Hamiltonian H'_t , the desired evolution can be implemented in a shorter (and, crucially, finite) time, and still doesn't close the gap due to the adiabatic theorem. This means that the quasi-adiabatic evolution is able to approximately map between two states in the same gapped quantum phase in a finite time. We outline the procedure below.

Consider evolving a state under $|\tilde{\psi}\rangle = \mathcal{T}[e^{-i\int dt H'_t}]|\psi\rangle$, where \mathcal{T} is the time-ordering operator and where H'_t is an operator derived from H . The states $|\tilde{\psi}\rangle, |\psi\rangle$ are said to be quasi-adiabatically connected [91]. Furthermore, it's been shown that if H_t is local, then H'_t has the same locality up to corrections by exponential tails. Namely, the quasi-adiabatic Hamiltonian is also quasi-local, so that the support of each individual term in H'_t on the lattice decays exponentially [97]. This allows H'_t to spread correlations that much quicker than H_t , such that the time evolution can be implemented in a finite time.

Secondly, the quasi-adiabatic evolution can also be related to the FDQC. Take the quasi-adiabatic evolution operator above and trotterise it to express it as a sequence of unitary gates [98]. The size of the Trotter time step δt dictates the accuracy of the decomposition and also the depth of the circuit. The limit $\delta t \rightarrow 0$ gives the exact evolution, but requires again an infinite time. Fortunately, it's been shown that a FDQC is able to approximate the quasi-adiabatic evolution up to exponential accuracy in a finite amount of time [91]. This means that the FDQC corresponding to the adiabatic path of Hamiltonians which preserves a gapped phase has a circuit depth independent of system size, given that the unitary gates which make it up should each have finite support which scales as $\text{poly log}(N)$ [99].

Lieb-Robinson bounds

Lieb-Robinson bounds give additional intuitions to the discussion above and will appear later in this Thesis. The Lieb-Robinson bounds are a statement about how quickly information is allowed to spread in a locally-defined quantum system, which is bounded by a so-called light cone [100]. The effective light cone has been observed experimentally, for example in ultracold atoms in an optical lattice [101]. By a simple calculation, it takes a time of order $1/v$ for information to propagate information a distance ℓ under evolution by a local Hamiltonian, where v is the speed at which information propagates. This information can take the form of correlations which is very interesting in the context of topological phases. By allowing H'_t to be composed of quasi-local terms rather than be local like the original Hamiltonian, the speed v is increased, since at each time step, H'_t has a greater range than H_t .

We can see that this implies that it takes a time $t \sim \mathcal{O}(N/v)$ to produce topological order on a system of size N [96]. Local, gapped Hamiltonians have exponentially decaying correlations $\langle O_i O_j \rangle \sim \mathcal{O}(e^{-\ell})$ where O_i is a local operator on site i , and the distance between the two sites is ℓ . Concretely, when O_i is time evolved to some $O_i(t)$, this means that $O_i(t)$ can be written as an operator which acts only on a region $\ell = vt$ and implies a bound on the commutator $||[O_i(t), O_j]||$ at each time step t . The bound on the commutator in time provides the light cone. Now, in topologically ordered systems, the correlation functions of operators spanning the entire system (Wilson loops) are non-zero, and such correlations can only be generated in a time that scales with ℓ . Hence, generating topological order from trivial order requires a time which is at least linear in the system size.

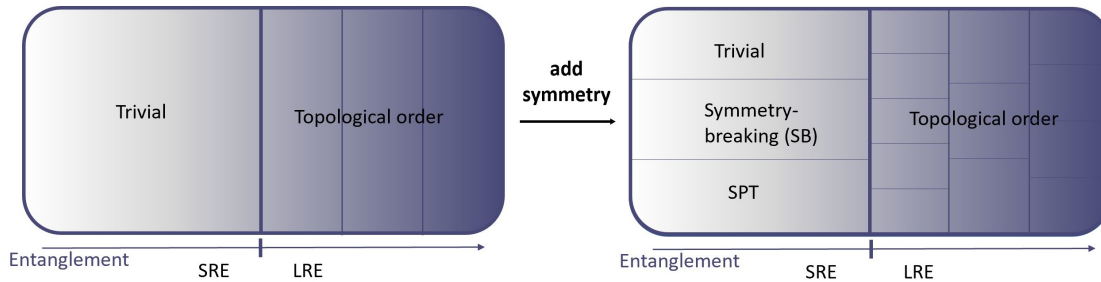


Figure 2.2: The phase diagram for gapped quantum phases can be understood by separating states into long-range entanglement (LRE) and short-range entanglement (SRE), or equivalently into topologically trivial and intrinsically topological states. The diagram becomes enriched by symmetries. Adding symmetries to SRE phases allows for symmetry-breaking phases and symmetry protected phases, and LRE phases can be further refined into different topological orders as well.

Overall, the notions of quasi-adiabatic evolution and Lieb-Robinson bounds, demonstrate the importance of maintaining the properties of locality and gappedness of system Hamiltonians in a phase. Together with the FDQC we see that universal properties should be described by continuity of observables such as correlation lengths [96]. This ensures that correlations, or, in our preferred language, the entanglement structure, is maintained within a phase.

Finally, let us make a note about the quasi-locality of the Hamiltonian H'_t which extends it from the original local Hamiltonian. The support of the individual terms in H'_t is not allowed to grow too quickly with the system size. Certainly it is not allowed to diverge, since this would lead to a gap closure or phase transition. Further, any two states can be connected by a path which takes an infinite amount of time, so in the classification of gapped phases we are not allowed either operations which take an infinite time or are completely non-local. Such operations do not have a causal light cone and the resulting phase diagram does not capture the universal features of entanglement. This observation will become particularly important in the coming Section §2.2.1 where we discuss the gapped phases beyond pure states, and will form the main motivation for Chapter 4.

2.1.3 Defining gapped quantum phases with symmetries

The classification of gapped phases is refined when symmetry is introduced, as illustrated in Fig. 2.2. If the phase has a symmetry, then so must the path which connects states in the same phase, be it a FDQC or an adiabatic path of Hamiltonians H_t .

Consider states with a global on-site symmetry $U_g = u_g^{\otimes N}$ of the group G , which acts locally on each site for a system of size N . The definition for a gapped quantum phase of matter with this symmetry is as follows [102]:

Definition 3: *Two states $|\psi\rangle$ and $|\tilde{\psi}\rangle$ satisfying a symmetry $U_g = u_g^{\otimes N}$ are in the same phase if there exists a unitary operator U which is a FDQC such that $|\tilde{\psi}\rangle = U|\psi\rangle$, and each gate u in U satisfies $[u, u_g] = 0$.*

Gapped phases without symmetry-breaking exist broadly in three different classes: symmetry protected topological order, intrinsic topological order, and symmetry enriched topological order. We will introduce these three different phases of matter in Section §2.4, Section §2.5 and Section §2.6 respectively.

At low temperatures, quantum phases of gapped systems can usually be very well described by just their ground states and low-energy excited states. This means that it suffices to study pure states in the Hilbert space. At high temperatures and beyond pure quantum states, however, it is necessary to consider other descriptions, such as (mixed) thermal states, or, more interesting to our context, steady states in open system dynamics, which we will elaborate on in the next Section. Note also that gapless systems are not well described in this way and require an altogether different treatment, for example with the use of order parameters [103–105].

2.2 Beyond gapped phases of pure states

In the following we give an overview of the study of gapped phases beyond pure states. The gapped phases of pure states were the subject of the previous Section and have been well studied. Their consistent generalisation to phases of mixed states has seen significant recent progress in the last decade. We begin with a short literature review and then give a definition which has been recently proposed for gapped phases of mixed states in Section §2.2.1.

Studying mixed states is important since these are the most general form of quantum states. They can describe an open system, while pure states only describe idealised quantum systems which are perfectly sealed off from the surrounding environment [13]. Certain mixed states of interest are the steady states of dissipative evolution and thermal states. Most recently, a formalism for classifying mixed state topological order was put forward by Coser and Perez-Garcia which will be the subject of the next Section [4]. It is still open as to how this new formalism connects with the previous works we will collect below.

In the context of topological phases, which are conventionally defined at zero temperature, it is interesting to ask whether universal properties, such as anyon braiding or topologically protected edge modes, survive being subjected to a temperature or other kinds of noise. The open systems setting is also relevant to quantum computing where dissipation determines the error rates and robustness of computational schemes. Experimentally, signatures of noisy SPTO have been observed to survive on current digital quantum computers by Refs. [71, 106, 107], so there is good reason to believe that these mixed state phases of matter are relevant.

When a quantum system is coupled to an environment describing thermal noise, the relevant class of mixed states are thermal (Gibbs) states, which are

in equilibrium and are defined by a temperature. The thermal robustness of the Toric code and other topologically ordered states have been studied in Refs. [62, 63, 108], and the cluster state in Refs. [109–113] where different properties have been shown to be robust up to certain temperature thresholds. In particular, entanglement quantities such as the localizable entanglement of the cluster state have been explored in Refs. [109–113]. Furthermore, states with symmetry protected topological order (SPTO), which is a known resource for the quantum computing scheme known as measurement based quantum computing (MBQC), have been shown to perform up until some critical temperature in the presence of dissipation. Meanwhile, in some set-ups this resource power is perhaps surprisingly shown to be enhanced by temperature [114–116]. It's also been recently suggested that only symmetries beyond global on-site can protect SPTO of mixed states [117], demonstrating that there is not yet a coherent vision of mixed state topological order.

Not all open quantum systems can be defined by a temperature. A certain class of these systems are out-of-equilibrium systems, in which drive and dissipation compete [13]. An example are Floquet phases, for which SPT versions have been defined [118–120].

A first definition for classification of mixed state topological order was given by Hastings in 2011 which defines a phase by how close a mixed state is to a thermal state under FDQC in the trace norm [61]. Under this definition, it is shown that any 2D local, commuting Hamiltonian is not topologically ordered at $T > 0$, and furthermore those thermal states cannot be used to store quantum information. Another definition was proposed at a similar time by Diehl, Bardyn and others for fermionic systems with steady states of a gapped Lindbladian in Refs. [66–68]. They focused on mixed state topological order for Gaussian, fermionic systems with pure steady states of a gapped quantum many-body Lindbladian, by studying topological phase transitions purely by dissipation. They identify two conditions necessary for the system to consistently contain topological order: the existence of a purity gap, and the existence of a dissipative gap. The former corresponds to the existence of a bulk spectral gap in the fictitious free-fermion Hamiltonian, while the latter corresponds to fast-enough relaxation to the steady state. This last work inspired the study of topological invariants for mixed states using the Uhlmann phase [64, 65]. Other studies have provided a classification for out-of-equilibrium topological insulators and superconductors [69, 121, 122].

This ends our short review of different works regarding gapped phases beyond pure states and we now go on to describe the framework for mixed state topological order given in Ref. [4].

2.2.1 Defining gapped phases in open quantum systems

The most general operation one can perform on a quantum state is a quantum channel, which is a completely positive and trace preserving (CPTP) map [15, 123]. These channels also include maps generated by an operator called a Lindbladian [124]. We are interested only in causal channels which have a finite light cone [125],

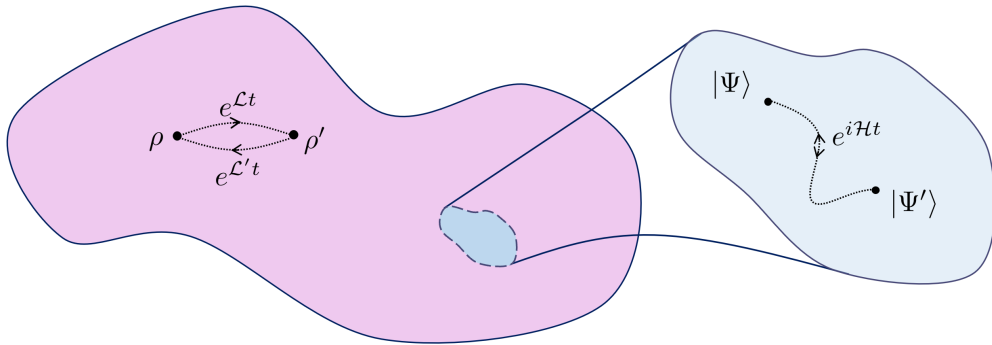


Figure 2.3: Framework give in Ref. [4] for the equivalence relations which preserve gapped phases of mixed states, as extending from gapped phases of pure states.

so the Kraus operators must be local or quasi-local.

There are many different equations describing evolution in an open quantum system, depending on assumptions about the noise model, and we will only focus on the Lindblad master equation [13]. This evolution describes semigroups of channels generated by continuous time evolution by a Lindbladian

$$\mathcal{L}(\rho) = -\frac{i}{\hbar}[H^S, \rho] + \sum_{i=1}^{\ell} \left(L_i \rho L_i^\dagger - \frac{1}{2} L_i^\dagger L_i \rho - \frac{1}{2} \rho L_i^\dagger L_i \right). \quad (2.2.1)$$

Here, the L_i are jump operators and H^S is the Hamiltonian of the system. This equation generalises the Schrödinger evolution for pure states to evolution of mixed states. It describes a small quantum system weakly coupled to a large environment. The derivation of the master equation assumes the Born approximation (that the system-bath coupling is sufficiently small) and the Markov property (that the bath has no memory), such that then one can apply the Lindblad master equation to an initially uncorrelated state of system and bath [13].

In defining phases of mixed states, it is desirable that the equivalence relations produce sensible equivalence classes on mixed states, and further that they reproduce the phases of pure states in a certain limit. As previously, it is therefore important to encode a balanced trade-off between circuit depth (which determines time or fastness) and locality of individual gates (which determines light cone or spread of correlations) such that a single phase contains only smooth observables.

A possible definition from adiabatic paths of local, gapped Hamiltonians and FDQCs is to fast, local Lindbladians. This definition for a gapped quantum phase of mixed states has been given in Ref. [4] as follows:

Definition 4: *Two states ρ and ρ' are in the same phase if there exists fast, local Lindbladians $\mathcal{L}, \mathcal{L}'$ which transform between them.*

The Lindbladians are defined by a sum of quasi-local terms, which act only on a subset of the lattice of size $\sim \text{poly log}(N)$, and are fast, meaning that the evolution takes a time $\sim \text{poly log}(N)$, up to an error ϵ which vanishes in the

thermodynamic limit¹. The Lindbladian paths interpolate smoothly between local observables. Then we say that two mixed states are in the same phase if they can be connected in either direction by evolution generated by such Lindbladians, as visualised in Fig. 2.3.

In order to see how this definition connects to the classification for gapped phases of pure states, it's useful to recall Definition 2 on FDQC. As an extra result, Ref. [4] shows that quasi-local quasi-adiabatic evolution corresponds to a FDQC whose depth is constant if the quasi-local gates are allowed to have support on a region of size $\text{poly log}(N)$. Now allow these gates to be noisy. Such a circuit has gates which are not necessarily unitaries, but are rather CPTP maps. Hence, the new setting is a circuit of channels. Then a Lindbladian that effectively implements this quantum circuit up to an error ϵ can be constructed with the help of the ancillas [4]. Finally, all states which are in the same gapped phase for pure states are shown to be in the same phase for mixed states with the resulting form of Lindbladians, so the definition consistently extends gapped phases of pure states. It is still open whether states in the same phase for mixed states may not be in the same phase for pure states, and whether there are mixed state phases within this framework for which there is no pure state analogy, as suggested elsewhere [69].

This definition is physically motivated. The conditions of locality and fast evolution on the Lindbladian ensure that new long range correlations cannot be created in the initial state, since the evolution is causally bounded by a light cone, and can't create correlations outside of it [127]. Hence, by this definition, equivalence classes contain states with the same kinds of long range correlations, which is necessary to be in the same phase.

Further, there is a partial order on states, which highlights that, in a hand-wavy sense, destroying correlations is generally easier than creating them. Imagine that given two states ρ_1 and ρ_2 , the long range correlations of ρ_1 are a subset of those in ρ_2 . On the one hand, we would expect that it is not possible by the fast, local Lindbladian evolution to transform from ρ_1 to ρ_2 since the evolution would need to generate new long range correlations. This is not allowed by the light cone argument given in the paragraph above. On the other hand, we could expect that we can transform from ρ_2 to ρ_1 with this evolution, since fast, local Lindbladian evolution can destroy correlations in a short time.

With this, we end the discussion on gapped phases, or topological phases, and before discussing particular topological orders, we introduce the tensor network formalism which will help us along the way.

¹Since $t \rightarrow \infty$ in the thermodynamic limit, non-analyticities may emerge in the path which may be remedied by requiring the Lindbladians to be additionally fast mixing [126]. Generally, one expects fastness and locality to be a strong enough assumption compared to requiring Lindbladians to additionally be fast mixing, since if channel has a finite light cone, it is generated by a local Lindbladian.

2.3 Tensor networks

We introduce some background on tensor networks (TN), which have provided a systematic approach to studying quantum many-body states. TN have emerged in the last the last 30 years as a favourite analytical and numerical tool to systematically investigate problems in modern condensed matter physics [77]. Importantly to this Thesis, they have a particularly powerful expressive ability of an interesting class of states, namely ground states of gapped, local Hamiltonians.

TN are ideal candidates for capturing states with topological order or symmetries, as they allow us to understand global properties of a states in terms of symmetries of the local tensors, which in turn describe the entanglement structure of the state [102, 128].

Intuitions behind the tensor network paradigm harken back all the way to 1941 studies in statistical mechanics with transfer matrix methods [129]. Later, this led to the construction of finitely-correlated states, and the idea that the structure of entanglement in states can characterise emergent physical phenomena. This links to the RG flow mentioned at the start of this Chapter [130, 131], through the description of fixed points of phases that contain all universal features of states in the phase. TN exploit this universality, which often combats a common problem of modelling natural systems which is that of overfitting, meaning that models have exceedingly many parameters in order to approximate the system well.

Further, TN efficiently approximate states obeying an entanglement entropy area-law, and as such are applicable to ground states of gapped, local Hamiltonians [132, 133]. Altogether, the expressive power of tensor networks has led to it being a fundamental keystone in the study of quantum many-body systems.

TN in 1D, which we will discuss in the next Section, were later applied to to understand important states such as the Affleck-Kennedy-Lieb-Tasaki (AKLT) state [134] as well as the cluster state [135], while TN in 2D, which we will discuss in Section §2.3.2 have been useful to understand states such as the Toric code [2].

2.3.1 Matrix Product States

A powerful tool to describe topological phases in 1D are matrix product states (MPS), in which the wave function is decomposed into a network of local tensors A^i associated to each site.

An MPS is defined by a single rank-three tensor A as

$$|\Psi[A]\rangle = \sum_{i_1, \dots, i_N} \text{Tr}(A^{i_1} \dots A^{i_N}) |i_1 \dots i_N\rangle, \quad (2.3.1)$$

where A^i are matrices such that $A = \sum_i A^i \otimes |i\rangle$. An MPS tensor is said to be *injective* if the transfer operator $T = \sum_i A^i \otimes (A^i)^\dagger$ has a unique eigenvalue of largest magnitude. For a physical dimension d of the MPS, bond dimension D , the number of parameters a translation-invariant state stores is D^2d , which is exponentially less than a generic state's d^N .

Injective MPS satisfy a fundamental theorem [77], which implies the following. If a state is invariant under a global symmetry $U_g^{\otimes N} |\Psi[A]\rangle = |\Psi[A]\rangle$, the action of the onsite symmetry U_g on its local tensor A results in an action on the virtual level

$$\sum_j (U_g)_{ij} A^j = e^{i\phi_g} V_g A^i V_g^\dagger, \quad (2.3.2)$$

where V_g is a projective representation of the symmetry [136], satisfying

$$V_g V_h = \omega(g, h) V_{gh}, \quad (2.3.3)$$

for some values $\omega(g, h)$ which are called cocycles. The projective representation clearly generalises the linear representation as $\omega(g, h)$ may be non-trivial. The cocycle will be particularly important in classifying SPT phases, which we describe in Section §2.4. Physically, the injectivity condition holds when the MPS is the unique ground state of its parent Hamiltonian, which is indeed the case for states in SPT phases without symmetry-breaking. As a tensor diagram, Eq. 2.3.2 is written as

$$\begin{array}{c} \downarrow U_g \\ \bullet \\ \text{---} A \end{array} = e^{i\phi_g} \begin{array}{c} \bullet \\ \text{---} V_g \end{array} \begin{array}{c} \bullet \\ \text{---} A \end{array} \begin{array}{c} \bullet \\ \text{---} V_g^\dagger \end{array}. \quad (2.3.4)$$

The fundamental theorem elucidates that the projective symmetry action of V_g occurs on the virtual level of each site tensor A , such that the entanglement structure and topological properties of the global state are encoded locally. Finally, note that we take A to be in canonical form so that V_g is unitary.

For a full refresher on MPS technology, we refer readers to more comprehensive introductory literature [76, 137, 138].

2.3.2 Projected entangled pair states

To aid our investigation of 2D topological phases, we introduce PEPS which is the analogue construction of MPS in higher dimensions. PEPS first emerged in the context of DMRG simulations to efficiently compute correlation functions [139–141]. PEPS do not have a canonical form which makes their use much more difficult, yet we will see that they still have an demonstrably expressive power.

Analogously to MPS, the PEPS is defined by a five-legged tensor (one physical and four virtual legs), defined as

$$A_{\alpha\beta\gamma\delta}^i = \begin{array}{c} i \\ \bullet \\ \alpha \text{---} \bullet \text{---} \beta \\ \delta \text{---} \bullet \text{---} \gamma \\ A \end{array}, \quad (2.3.5)$$

which can express any quantum state if D is allowed to grow arbitrarily large. For a fixed bond dimension, PEPS also fulfill the area-law; the entanglement entropy of a PEPS with boundary length L is $S(L) = O(L \log D)$. This property is satisfied by quantum states such as ground states and low-energy states of local Hamiltonians. Furthermore PEPS can also describe polynomially-decaying

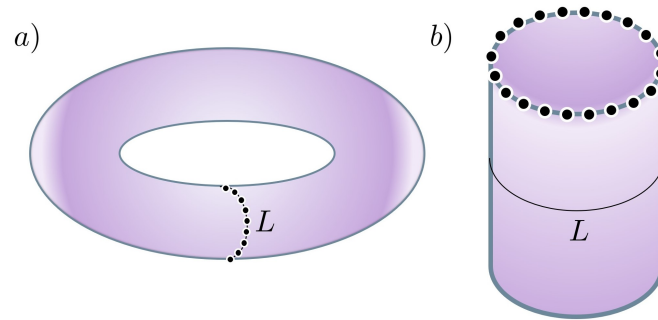


Figure 2.4: a) When a state is defined on an lattice with periodic boundary conditions, this is depicted as a torus. b) Defined on open boundary conditions, we can break open the torus which results in a cylinder.

correlations as compared to MPS which can only describe states with exponentially-decaying correlations [142].

The problem of exactly contracting a PEPS is unfortunately \sharp -P hard in terms of computational complexity [143]. Importantly, this means that for any arbitrary PEPS the contraction takes a time $t \sim O(e^N)$, even if we try to contract it in a smarter way. Evidently working with PEPS are hard.

Fortunately for us, it turns out that for interesting states such as the ground states of gapped, local Hamiltonians, we can approximately contract the PEPS to a high degree of accuracy, with the help of many different numerical methods. The numerical methods for contracting PEPS which will be most useful in this Thesis are the iPEPS algorithm [144, 145] and the corner transfer matrix method [146]. These all find their basis in the renormalisation group (RG) method [147] and White’s density matrix renormalisation group (DMRG) algorithm for finding ground states of 1D gapped Hamiltonians [148], which was realised later is really a variational algorithm searching over the class of MPS. Many algorithms also exist for simulating time evolution of TN states, such as the time-evolving block decimation algorithm (TEBD) [149], but we will be able to manage with Monte Carlo based simulations of quantum trajectories in 1D and also brute force simulation of channel evolutions.

We will define PEPS on a torus geometry to describe a 2D lattice on periodic boundary conditions, while a cylindrical geometry describes open boundaries in one dimension and periodic boundaries in the other dimension (Fig. 2.4).

G-injective PEPS

G-injective PEPS [150, 151] are remarkable in that they realise a particular family of states with topological order known as quantum double models [152]. This gives us a unified understanding of these models within the framework of tensor networks via the interplay of symmetry, locality and entanglement.

There are two important properties a tensor must possess to satisfy G-injectivity.

Firstly the tensor must have a local (gauge) symmetry

$$\begin{array}{c} | \\ \bullet \\ / \end{array} = \frac{1}{|G|} \sum_g \begin{array}{c} | \\ \bullet \\ / \end{array} \begin{array}{c} g \\ \bullet \\ g^{-1} \end{array} \quad \forall g \in G \quad (2.3.6)$$

This property is believed to be key to describing intrinsically topological models.

Secondly, the tensor must satisfy a variation on the injective property that we saw for MPS which is that the transfer operator

$$\begin{array}{c} A^{-1} \\ \bullet \\ / \\ \bullet \\ / \\ A \end{array} = \frac{1}{|G|} \sum_g \begin{array}{c} | \\ \bullet \\ / \\ | \\ \bullet \\ / \\ | \\ \bullet \\ / \\ A \end{array} \begin{array}{c} g \\ \bullet \\ g^{-1} \end{array} \quad (2.3.7)$$

A larger class of models which are believed to capture all non-chiral topological order are string-net models [83]. These can also be understood with tensor networks, by extending from simpler forms of PEPS G-injectivity and twisted-injectivity to MPO-injective PEPS [153].

TNs, and in particular PEPS, remain an active research field to this day. For example, chiral topological phases, such as the historical integer and Fractional Quantum Hall effects, are not yet fully understood within the TN framework which have worked so well to describe conventional topological orders (intrinsic and SPT). A barrier to the construction of a chiral PEPS is that they have algebraic bulk correlation functions which precludes them being the (efficiently simulable) ground states of gapped, local Hamiltonians. It is yet unknown whether it is possible to efficiently encode gapped chiral phases with PEPS.

With a description of tensor networks in hand, we go on to briefly introduce three different kinds of topological order. We will begin with the simplest one which is symmetry protected topological order.

2.4 Symmetry protected topological order

SPT order is defined by symmetric phases of short-range entangled (SRE) states, *i.e.* families of states which are connected by a FDQC respecting a particular symmetry, which corresponds to an adiabatic path of gapped, local Hamiltonians [12, 91, 154, 155]. As such, this order is called “topologically trivial”, but nevertheless intrinsically non-local properties prevail in presence of a symmetry, such as topologically protected edge mode degeneracy and string order [92, 156, 157]; this follows from the non-trivial symmetry action of the projective representation $V(g)$ on the edges [158, 159]. Hence, SPT order is intimately linked to the projective representation V_g , and remarkably demonstrates that global patterns of entanglement appear via a local mechanism, which emphasises the natural suitability of local tensor descriptions. Only the presence of appropriately defined symmetry in a system can allow SPTO to exist, allowing its characteristic topologically protected edge modes, ground state degeneracy on open boundary conditions, entanglement

spectrum degeneracy and string order [92, 156, 157]. Hence, G-symmetric FDQCs preserve SPTO in pure states. Finally, SPT states provide a link to quantum computation, as they are an ideal resource for measurement based quantum computing (MBQC), coming from the phase-protected entanglement [6, 160]. Other states without SPTO, such as the GHZ state (symmetry-breaking, SRE) and the Toric code (topological order, LRE) do not have the right kind of entanglement to achieve universal computation [112, 161].

SPT phases of local, gapped Hamiltonians in one dimension, for a symmetry group G , are classified by an invariant $[\omega]$, a class in the second group cohomology group $H^2(G, U(1))$ [102, 128, 162]. A useful method for determining the SPT invariant of a given Hamiltonian is to represent its ground state as a tensor network and study the symmetries of its tensor [77]. Let us review this procedure in 1D.

Recall the fundamental theorem we introduced in Eq. 2.3.2 which pulls a global symmetry to a virtual symmetry which is given by a projective representation V_g . For a given state, there is always a tensor in a canonical form, where V_g is unitary and $\omega(g, h)$ is a phase [77]. The collection of phases $\omega(g, h)$ constitutes a group cocycle and is defined up to a group coboundary, meaning it determines a cohomology class $[\omega]$ [102, 128]. It turns out that $[\omega]$ is invariant along smooth paths of gapped, local, symmetric Hamiltonians, which is to say it is an SPT phase invariant; moreover, it is a complete invariant [128]. Physically, the virtual space of the MPS tensor may be interpreted as the space of edge modes; the fact that there is a minimal bond dimension on which V_g can realise the invariant $[\omega]$ means that some of the edge modes are protected by the symmetry.

Essential to this definition of the SPT invariant $[\omega]$ is that the state is well-approximated by an MPS of bond dimension constant in the system size, a property which comes from the state being a ground state of a gapped, local Hamiltonian. Generic states in one dimension are not well-approximated by MPS, so for them a projective action V_g – and therefore an invariant $[\omega]$ – cannot be defined this way.

Throughout this Thesis, we will restrict to finite Abelian symmetries. This is not a severe restriction, as many physically relevant SPT phases protected by other groups remain non-trivial even when a finite Abelian subgroup of the symmetry is enforced [163]. One example is the Haldane phase, which may be defined as the non-trivial SPT phase protected by $SO(3)$ symmetry, but is effectively protected by a $\mathbb{Z}_2 \times \mathbb{Z}_2$ subgroup. The non-trivial phase protected by the latter symmetry is also called the cluster phase, as it contains the 1D cluster state [164]. Being the simplest non-trivial SPT phase, we will often refer to this example throughout the Thesis.

SPT phases with on-site symmetries are known as G-SPTO and are the simplest kind which will be the focus in this Thesis. Generally, d -dimensional SPT phases of matter are classified by the $d + 1$ group cohomology $H^{d+1}(G, U(1))$ [154], although models beyond group cohomology have also been studied in 3D and 4D [12, 165]. Other kinds of SPTO include subsystem-SPTO and most recently this has been generalised to matrix product operator (MPO) SPTO [166]. 2D G-SPTO is classified by $\mathcal{H}^3(G, U(1))$ (symmetry fractionalisation on edges) while 2D SSPTO is classified by $\mathcal{C}[G_s] = \mathcal{H}^2(G_s^2, U(1))/\mathcal{H}^2(G_s, U(1))^3$ for "strong" SSPT which is a

true subsystem SPT phase, or $\mathcal{H}^2(G, U(1))^N$ "weak" SSPT being N stacked 1D SPTs with global on site symmetries [167].

2.4.1 Example: the cluster state

In this Section we briefly introduce one of the simplest examples of SPT order, which is the 1D cluster state [135].

This state may be defined by a FDQC acting on a periodic chain of N qubits in a product state, which demonstrates that it is short-range entangled. This operational definition is

$$|\mathcal{CS}\rangle = \left(\prod_{i=1}^N CZ_{i,i+1} \right) |+\rangle^{\otimes N}, \quad (2.4.1)$$

where the state $|+\rangle$ is given by $|+\rangle = \frac{1}{\sqrt{2}}(|0\rangle + |1\rangle)$, and CZ is a 2-site unitary gate defined by $CZ_{ij} = |0\rangle\langle 0|_i \otimes \mathbb{1}_j + |1\rangle\langle 1|_i \otimes Z_j = \text{diag}(1, 1, 1, -1)$ acting on sites i, j [15]. We will refer to X, Y, Z as the Pauli X, Y, Z operators.

Since we used a mapping on the level of states to obtain the cluster state, we can use the same map on the level of Hamiltonians to obtain the cluster Hamiltonian, for which the cluster state is the unique ground state (on periodic boundaries). The Hamiltonian which has $|+\rangle^{\otimes N}$ as its ground state is the paramagnetic Hamiltonian $H = -\sum_{i=1}^N X_i$. We can then conjugate this H by the FDQC we implemented above $\prod_{i=1}^N CZ_{i,i+1}$ to arrive at the cluster Hamiltonian

$$H_{\mathcal{CS}} = -\sum_{i=1}^N Z_{i-1} X_i Z_{i+1}. \quad (2.4.2)$$

This form of the Hamiltonian is elucidating, as we see that the cluster state has $Z_{i-1} X_i Z_{i+1} |\mathcal{CS}\rangle = |\mathcal{CS}\rangle \forall i$, i.e. it is in the simultaneous $+1$ eigenbasis of all of the Hamiltonian terms. Such terms $S_i = Z_{i-1} X_i Z_{i+1}$ are known as stabilisers. Therefore, the cluster state is also a *stabiliser state*, which are states defined uniquely in the $+1$ eigenstate of a set of Pauli operators which generate a stabiliser space [168].

This Hamiltonian has symmetries given by the group $G = \mathbb{Z}_2 \times \mathbb{Z}_2$ generated by the action of $X_{\text{odd}} = \prod_{i=1}^{N/2} X_{2i-1}$ and $X_{\text{even}} = \prod_{i=1}^{N/2} X_{2i}$ on sites i . The reason why the product state and the cluster state are in different phases is that CZ gates do not commute with these symmetries, so the circuit is symmetry-breaking, although globally the FDQC does preserve the symmetry.

The cluster state is robust to weak perturbations. The idea is that the only operator which mixes the non-symmetry respecting states is a non-local operator which spans the whole chain of length N . We saw this before with topological order, and similarly in the cluster state, a local perturbation has an effect which is exponentially small in N [169].

The cluster state is an example of a maximally-non commutative (MNC) phase, as we discuss in the next Section. These phases are particularly interesting for

quantum computation; in this Thesis we will connect the facts that such MNC phases have maximal inaccessible entanglement, maximal SPT complexity, and also maximal topological edge mode degeneracy, which turn out to be intimately related.

2.4.2 Projective irreps of Abelian groups

We now introduce several properties about projective irreducible representations of finite Abelian groups that will be relevant in later calculations.

Let us introduce the term ω -irrep to refer to an irreducible representation with cocycle ω . Firstly, a general projective representation $V(g)$ of a finite group G with cocycle ω can be written as a direct sum over ω -irreps V_g^a

$$V_g = \bigoplus_a \left(\mathbb{1}_{n_a} \otimes V_g^a \right), \quad (2.4.3)$$

where n_a is the multiplicity for a given ω -irrep a [170]. The second property we make use of is the fact that any two ω -irreps of a finite Abelian group are projectively equivalent. Namely, if we fix $\tilde{V}(g)$ to be an arbitrary reference ω -irrep, every other ω -irrep $V_a(g)$ can be related to it by

$$V_a(g) = \mu_a(g) U_a \tilde{V}(g) U_a^\dagger, \quad (2.4.4)$$

where $\mu_a(g)$ can be thought of as a phase factor, as it is a linear character, and U_a is some unitary [171]. This allows us to simplify the general form of $V(g)$ in Eq. (2.4.3), which is a direct sum over the ω -irreps containing multiple tensor products, to a single tensor product when G is finite Abelian. Namely,

$$V(g) = \left(\bigoplus_a \mu_a(g) \mathbb{1}_{n_a} \right) \otimes \tilde{V}(g), \quad (2.4.5)$$

where we have removed the unitaries U_a through an appropriate choice of basis. This illustrates that, for finite Abelian groups, all ω -irreps for a given ω have the same dimension, which we call D_ω .

To calculate D_ω , we need to introduce the notion of the projective centre group k_ω . Given a cocycle ω under the group G , k_ω is defined by

$$k_\omega = \{s \in G \mid \omega(g, s) = \omega(s, g) \ \forall g \in G\}. \quad (2.4.6)$$

Then, D_ω is determined by the following equation [172],

$$D_\omega = \sqrt{|G|/|k_\omega|}. \quad (2.4.7)$$

For example, the Haldane phase has projective irreps given by the 2-dimensional Pauli operators. Conversely, for non-Abelian groups the irreps may have different dimensions, an example of which is S_4 , the symmetric group on four elements, which has 2- and 4-dimensional projective irreps.

Finally, we note that for any ω -irrep $V_\omega(g)$, the following condition about the trace holds up to a phase factor [170],

$$\mathrm{Tr}(V_\omega(g)) = \begin{cases} D_\omega, & \text{if } g \in k_\omega \\ 0 & \text{else.} \end{cases} \quad (2.4.8)$$

This will be helpful for calculations later on.

Maximal non-commutativity

SPT phases of special interest are the so-called maximally non-commutative (MNC) phases. These phases act as universal resources for MBQC [163, 164, 173–175]. A cocycle ω , along with the corresponding SPT phase, is called MNC if $k_\omega = \{e\}$, meaning it has a trivial projective centre. For such phases, D_ω takes the maximum value of $\sqrt{|G|}$. Since D_ω is equal to the topologically protected edge degeneracy of SPT phases [158], MNC phases therefore have the maximum edge degeneracy for a given group G . From now on, we will suppress the index ω in k_ω for notational simplicity.

For each MNC cocycle ω there is only one ω -irrep up to unitary equivalence [172], such that Eq. (2.4.5) becomes

$$V(g) = \mathbb{1} \otimes \tilde{V}(g). \quad (2.4.9)$$

The left part of the tensor product, which transforms trivially under symmetry, is referred to as the junk subspace. The size of this space determines the bond dimension and hence bounds the entanglement entropy of the state. We will also refer to the trivially transforming part of the MPS tensor in non-MNC phases as the junk subspace, although strictly there are multiple subspaces, corresponding to the existence of multiple projective irreducible representations.

We note that some symmetry groups host multiple MNC phases; such phases can't be distinguished by their edge mode degeneracy as the ω -irreps all have the same dimension. Order parameters as in Refs. [156, 157, 176, 177], however, can distinguish between them by microscopically probing the specific non-local action on the virtual level of the tensor network, which we discuss further in Section 3.4.3.

2.4.3 Fingerprints of symmetry protected topological order

Let us begin by reviewing the invariants of pure SPT states, including their manifestation in tensor networks and in patterns of zeros of string operators. After this review, we will discuss how these invariants appear in a special class of mixed states we dub *coherent SPT mixtures*.

In Chapter 3 we will introduce a new indicator of SPTO, which is the inaccessible entanglement.

String order

String order provides an alternate definition of the SPT invariant that does not rely on an MPS representation of the state. The string order parameter is a set of expectation values of string operators that can be defined on any state. On certain well-behaved states, such as the ground states of gapped Hamiltonians, it yields a well-defined pattern of zeros that uniquely determines the SPT invariant $[\omega]$.

Assume G is a finite abelian group, and let U_g denote the action of G on an individual site. The string operator is defined as

$$s(g, O_\alpha^l, O_\alpha^r) = \mathbb{1} \otimes O_\alpha^l \otimes U_g^{\otimes j} \otimes O_\alpha^r \otimes \mathbb{1} , \quad (2.4.10)$$

for some length j , where the end operators $O^{l,r}$ live in *opposite* irreps of the adjoint action

$$U_h^\dagger O_\alpha^l U_h = \chi_\alpha(h) O_\alpha^l , \quad U_h^\dagger O_\alpha^r U_h = \chi_\alpha^*(h) O_\alpha^r . \quad (2.4.11)$$

On some states, the string order parameter obeys a selection rule [157]. This rule says that, for each $g \in G$, there is a unique character α_g such that the expectation value $\langle s(g, O_\alpha^l, O_\alpha^r) \rangle$ vanishes, for all end operators, except for $\alpha = \alpha_g$. The values forced to vanish by the selection rule form what is called the *pattern of zeros* of the state. An SPT state can be defined as a state for which this selection rule holds; that is, a state with a well-defined pattern of zeros. The SPT invariant of an SPT state is extracted by defining the ratios ω/ω in terms of the unique character α_g for each g as follows:

$$\frac{\omega(h, g)}{\omega(g, h)} = \chi_{\alpha_g}(h) . \quad (2.4.12)$$

The invariant $[\omega]$ may then be recovered from these ratios, as we argue in §5.4. We remark that string order is also defined when G is nonabelian; however, it may not determine $[\omega]$ uniquely [157].

Now let us consider a state represented as an MPS and show that the definition of the SPT invariant $[\omega]$ by the projective action on edge modes agrees with its definition by string order parameters [157]. Injectivity may be achieved by blocking, which does not change the form of the string operator as long as its length is assumed to be large compared to the size of the blocks. On such a state, the string operator evaluates to

$$\langle s(g, O_\alpha^l, O_\alpha^r) \rangle = E_l(g, O_\alpha^l) E_r(g, O_\alpha^r) , \quad (2.4.13)$$

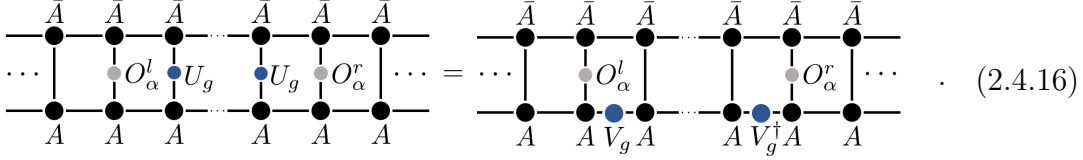
where

$$E_{l,r}(g, O_\alpha^{l,r}) = \text{Tr} [N_{l,r}^g O_\alpha^{l,r}] \quad (2.4.14)$$

are defined as

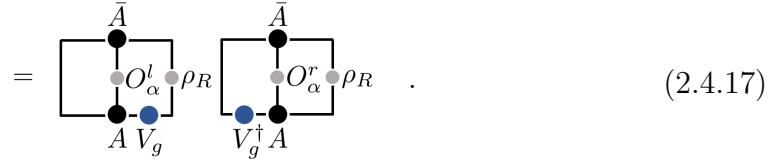
$$N_l^g = \begin{array}{c} \bar{A} \\ \bullet \\ \downarrow \\ \square \\ \uparrow \\ A \end{array} \rho_R, \quad N_r^g = \begin{array}{c} \bar{A} \\ \bullet \\ \downarrow \\ \square \\ \uparrow \\ V_g^\dagger A \end{array} . \quad (2.4.15)$$

Here, ρ_R is the unique (by injectivity) right fixed point of the MPS transfer matrix, and we have used the canonical form where the left fixed point is the identity. The evaluation (2.4.13) can be seen with the following diagrammatic argument (due to Ref. [157]):



$$\dots \begin{array}{ccccccc} \bar{A} & \bar{A} & \bar{A} & \bar{A} & \bar{A} & \bar{A} & \bar{A} \\ | & | & | & | & | & | & | \\ \dots & O_\alpha^l & U_g & \dots & U_g & O_\alpha^r & \dots \\ | & | & | & | & | & | & | \\ A & A & A & A & A & A & A \end{array} = \dots \begin{array}{ccccccc} \bar{A} & \bar{A} & \bar{A} & \bar{A} & \bar{A} & \bar{A} & \bar{A} \\ | & | & | & | & | & | & | \\ \dots & O_\alpha^l & V_g & \dots & V_g^\dagger & O_\alpha^r & \dots \\ | & | & | & | & | & | & | \\ A & A & V_g & A & A & V_g^\dagger & A \end{array} \dots \quad (2.4.16)$$

Evaluating the above



$$= \begin{array}{cc} \begin{array}{c} \bar{A} \\ | \\ O_\alpha^l \\ | \\ A \end{array} \rho_R & \begin{array}{c} \bar{A} \\ | \\ O_\alpha^r \\ | \\ V_g^\dagger A \end{array} \rho_R \end{array} \quad (2.4.17)$$

The operators $N_{l,r}^g$ transform as

$$U_h^\dagger N_l^g U_h = \frac{\omega(g,h)}{\omega(h,g)} N_l^g, \quad U_h^\dagger N_r^g U_h = \left(\frac{\omega(g,h)}{\omega(h,g)} \right)^* N_r^g, \quad (2.4.18)$$

The operators $N_{l,r}^{g\dagger}$ and $O_\alpha^{l,r}$ are orthogonal (and so $E_{l,r}$ is zero) unless they transform the same way; that is, unless the selection rule (2.4.12) is satisfied. This completes the argument.

If the operators $N_{l,r}^{g\dagger}$ and $O_\alpha^{l,r}$ transform the same way, then they are not orthogonal *generically* (and so $E_{l,r}$ is non-zero generically). This is because $N_{l,r}^g$ picks out a single direction in the multiplicity space for α , so the subspace orthogonal to this direction is codimension one in the full space of end operators $O_\alpha^{l,r}$. In other words, for a generic choice of end operators, the only expectation values $\langle s(g, O_\alpha^l, O_\alpha^r) \rangle$ that vanish are those that belong to the pattern of zeros determined by the SPT invariant. The non-zero values of the string order parameter depend on the choice of end operators, but the pattern of zeros does not. The string order will be discussed in Chapter 4.

Swap order

The swap order parameter is an alternative to the string order parameter, and uniquely detects the SPT invariant ω [176]. Similarly to the string order parameter, the swap order parameter is a set of expectation values that can be defined on any state. While the string order parameter has a *pattern of zeros*, the swap order parameter has a *pattern of signs* for gapped phases, where the signs are generally complex numbers. For the SPT phases of $\mathbb{Z}_2 \times \mathbb{Z}_2$, the signs are $+1, -1$.

The order parameter is attractive as it depends only on the symmetry of the state and doesn't require the construction of end-point operators (which are state-specific). This may make it more experimentally accessible: Refs. [176, 178]

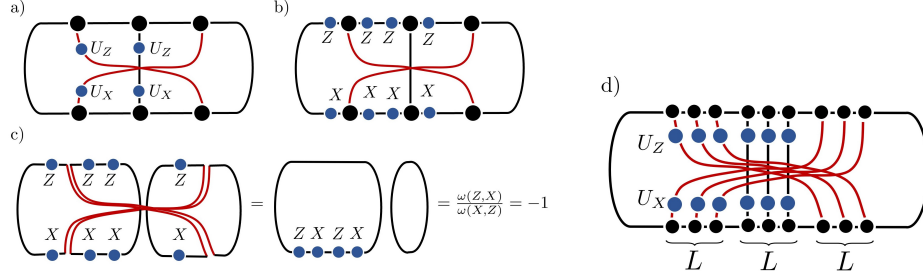


Figure 2.5: a) TN representation of the swap order parameter for $\text{SO}(3)$ symmetry, e.g. for the AKLT state. b) Applying the fundamental theorem. c) Computing the gauge-invariant quantity. We use injectivity on all sites and following the trace gives that the swap order parameter measures the anti-commutation of the symmetry on the virtual level. d) Depicts the blocked swap order parameter, where the length L is at least the blocking length to reach injectivity.

suggest methods for implementation aimed at cold atom setups in optical lattices. Finally, the swap order parameter has a nice interpretation. Just as the end-points of string operators can be understood as quasiparticles, the swap string operator can be understood as detecting the braiding class of those quasiparticles.

Assume G is a finite abelian group, and let U_g denote the action of G on an individual site. The swap operator is defined as

$$\mathcal{S}(g, h) = (U_g^{\otimes 2L} \otimes \mathbb{1}_L) \text{SWAP} (U_h^{\otimes 2L} \otimes \mathbb{1}_L), \quad (2.4.19)$$

for a length L which is greater than the correlation length (the blocking length required to become injective) and SWAP is a swap operation acting between L blocked sites of U_g, U_h . The diagrammatic representation for the order parameter given $\text{SO}(3)$ symmetry is provided in Fig. 2.5(b) (see also Ref. [179] for a different representation). For example, for the AKLT state, which is a renormalisation fixed point [158], the swap operator is

$$\mathcal{S}(g, h) = (U_z \otimes U_z \otimes \mathbb{1}) \text{SWAP}_{1,3} (U_x \otimes U_x \otimes \mathbb{1}) \quad (2.4.20)$$

If the site-wise representation of the AKLT is injective, then SWAP swaps the sites 1 and 3. Since actually only a subgroup of $\text{SO}(3)$ symmetry actually protects the Haldane phase, namely the subgroup $\mathbb{Z}_2 \times \mathbb{Z}_2$ which is generated by U_X and U_Z , the swap operator can be seen mathematically to extract the projective representations given by the Pauli operators X and Z , since at the RG fixed point the value of the quantity is $\frac{\omega(X,Z)}{\omega(Z,X)}$.

For MPS, the swap operator converges exponentially fast to this value. It is useful to remember that the length scale of convergence, or correlation length, is given by the gap of T^L , where T is the transfer matrix. These nice properties of the fixed point render it relatively simple to calculate the swap order parameter as well as to prove that for MPS which are RG fixed points (injective), the resulting quantity is gauge-invariant and hence determines the cocycle exactly.

One can normalise the swap order parameter so that it takes values $+1, -1$. This normalisation factor N is computed by setting $U_g, U_h = \mathbb{1}$ in Fig. 2.5(b)

so that $N = \mathcal{S}(\mathbb{1}, \mathbb{1})$. Then the normalised swap order parameter is the ratio $\hat{\mathcal{S}}(\psi) = \mathcal{S}(\psi)/\mathcal{N}(\psi) = \pm 1$.

The order parameter, its pattern of signs, and further details, e.g. pertaining to blocking, are discussed in Chapter 6.

2.5 Intrinsic topological order

We now introduce intrinsic topological order. Intrinsically topological phases are those which cannot be mapped to a product state by a FDQC, and are therefore characterised by patterns of long-range entanglement [60]. Referring to these phases as having intrinsic topological order separates them from symmetry protected topological, sometimes called trivial, (SPT) phases, whose topological order is conditional on the presence of symmetry.

The topological origin of these phases is that their ground state degeneracy depends on the topology of the manifold on which the system is defined. For example, the ground state of a topologically ordered Hamiltonian defined on a spherical lattice is unique; this is a topologically trivial manifold (with zero holes). However, a doughnut-shaped lattice would lead to an extensive ground state degeneracy on periodic boundary conditions, which is characteristic of topological phases on a nontrivial manifold. This also leads to the fact that local operators can't distinguish the different ground states, so these phases can't be detected by local order parameters; the phase is an emergent phenomena². They also contain low-energy excitations above the ground state, which are called anyons, in the bulk of the state. The topological properties are robust to perturbations which are smaller than the system size. Another final characteristic of topological phases is a correction to the entanglement entropy, called the topological entanglement entropy [180–182].

Topological phases have found application in quantum computing, in e.g. topological quantum computing and quantum error correction, by harnessing the braiding properties of anyons [2]. These applications come from several nice characteristic properties of topological order. If the goal is to encode information in an environment independent way, then one promising direction towards realising this is the observation that topological phases are non-local, and hence insensitive to local perturbations. The non-local patterns of (long-range) entanglement that define intrinsic topological ordered phases lead to several key characteristic properties. In particular, these properties make topological phases naturally amenable in application toward fault-tolerant quantum computation. Let us suggest why this might be the case.

First, topologically ordered phases possess a topology-dependent ground state degeneracy, e.g. the Toric Code has $d = 4^g$, where g is the genus. This suggests a natural possibility for such phases to act as a quantum memory, where the ground

²This is different to e.g. an Ising model in which the local magnetisations of individual spins are enough to determine the phase being ferro- or anti-ferromagnetic.

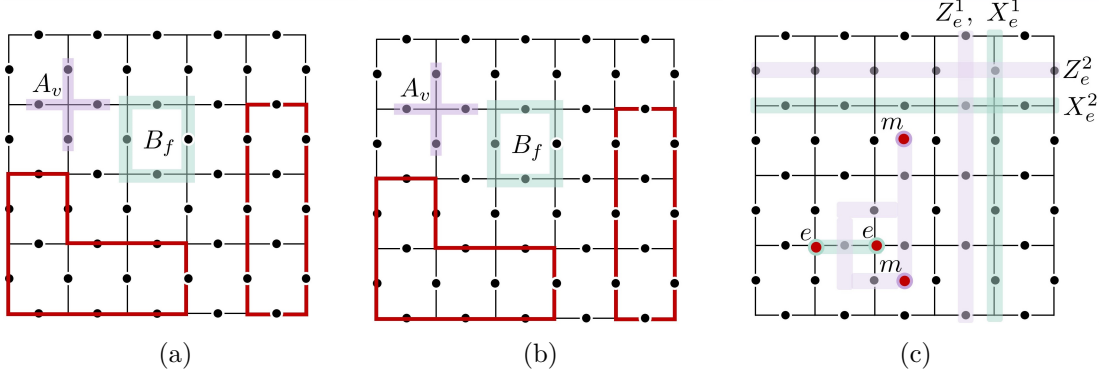


Figure 2.6: Physical operators on the Toric code making up the logical operators. Stable phase against weak local perturbations since see here that errors have to be $O(L)$ to transform between logical operators.

state space acts as the codespace with d logical operators with which quantum computation is allowed. These phases also host anyons, which are low-energy excitations above the ground state. Anyons can be moved around each other in a nontrivial manner which actually is described by the braid group following the rules of fusion category theory, and which can be leveraged for topological quantum computation. Furthermore, the topological phase is stable against weak perturbations, since only noise which acts on a region of size $O(L)$ is able to create a logical error. Altogether these properties make topological phases promising candidate platforms for quantum technologies.

Example: the Toric code

The Toric code is a canonical example of a many-body state which has topological order [183]. It has a topology-dependent ground state degeneracy, is a stable phase against weak perturbations, contains anyons in the bulk, and is constructed by G-injective PEPS.

The Toric code lives on a lattice with periodic boundary conditions where qubits live on the edge of the lattice. It is defined by the Hamiltonian

$$H_{TC} = - \sum_{v \in V} A_v - \sum_{e \in F} B_f, \quad (2.5.1)$$

where the edge and vertex terms are

$$B_f = \prod_{e \in F} X_e = X \cdot X \cdot X \cdot X, \quad A_v = \prod_{e \ni v} Z_e = Z \cdot Z \cdot Z \cdot Z. \quad (2.5.2)$$

A_v acts on all edges surrounding a vertex v , and B_f acts on all faces of the lattice, which is given in Fig. 2.6(a). Since each qubit can be in either basis state $|0\rangle$ or $|1\rangle$, we can depict the ground state pictorially by visualising a qubit in state $|1\rangle$ as

a line and a qubit in state $|0\rangle$ as the absence of a line. States can be represented on the lattice as a configuration of lines, which may either be in closed loops or open strings.

It turns out that the H_{TC} is exactly solvable, and that the ground state can be written as the equal weight superposition of such closed loops

$$|TC\rangle = \frac{1}{\mathcal{N}} \sum_{\mathcal{C}} |\mathcal{C}\rangle, \quad (2.5.3)$$

where each \mathcal{C} is a subset of edges that form closed loops, Hence each state $|\mathcal{C}\rangle$ has an even numbers of 1s (or equivalently 0s) written in the computational basis. In Fig. 2.6(a) we draw an example state configuration with loops of edges in state $|1\rangle$ as red lines. All other edges which have no red line touching them are in state $|0\rangle$.

We can quite easily convince ourselves that $|TC\rangle$ is the ground state of H_{TC} . Consider how to minimise the two different terms in H_{TC} . A_v enforces that the ground state has an even number of 1s since an odd configuration of 1s would give a -1 sign as depicted in Fig. 2.6(a). Therefore every configuration of closed loops is in the $+1$ eigenspace of A_v . Since B_f flips all edges on a face f between 1s and 0s, its clear that it moves loops around, transforming between states in the eigenspace. Since we can apply B_f at no energy cost (only $+1$ s from closed loops), every configuration is equally viable. This tells us that the Toric code must be an equal weight superposition over all loops.

Note that the Toric code, like the cluster state, is a stabiliser state, so all of the terms in the Hamiltonian commute which makes it very nice to work with since most quantities, such as entanglement entropy [184], become easier to compute.

What about excitations? Recall that any state configuration of open strings is in the -1 eigenspace of A_v , so it has an energy above the ground state energy. These open string configurations are created by string-like operators which violate Hamiltonian terms A_v or B_f and give a -1 . There are two types of excitations, called magnetic (m) or electric (e), which are depicted in Fig. 2.6(c). For some set of edges in the string Γ the string operator $S^{(m)} = \prod_{e \in \Gamma} Z_e$ creates magnetic anyons on the faces of the lattice by violating the A_v term, while $S^{(e)} = \prod_{e \in \Gamma} X_e$ creates electric anyons by violating the B_f term in the Hamiltonian.

A profound observation is that one thing that we can do some engineering to the system and move an $S^{(e)}$ string around a $S^{(m)}$ string. If we do this, notice that at some point an X and Z operator must interweave. At the crossing point, we have to anti-commute them through each other, gaining a -1 sign. By moving end-points of strings around each other, the state can be seen to pick up signs, e.g., as an m-anyon moves around an e-anyon in Fig. 2.6(c). This is what is now known as the phenomenon of braiding which allows topological computation.

Notice that if any of the four possible strings S is the length of the system, then the anyons of the Toric code may annihilate each other, since the loop now closes. Such states are globally distinguishable, though not locally distinguishable. We can use these states to form a logical subspace, and the logical operators are robust against weak, local perturbations up to $O(L)$.

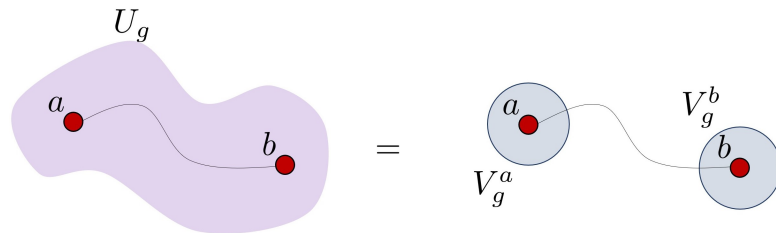


Figure 2.7: Symmetry fractionalisation of two anyons a and b . The physical symmetry U_g acting globally on some patch of the state manifests as a local symmetry V_g^a, V_g^b acting locally on the anyons.

The Toric code has the following PEPS

$$T_{\alpha\beta\gamma\nu}^i = \alpha \begin{array}{c} i \\ | \\ \bullet \\ / \quad \backslash \\ \nu \quad A \quad \beta \\ \backslash \quad / \\ \gamma \end{array} \gamma = \delta_{i,\alpha+\beta} \delta_{\beta,\gamma} \delta_{\alpha,\alpha+\nu} , \quad (2.5.4)$$

first derived in [139], which is an example of a G-injective states. Finally, note that the Toric code can be viewed as a \mathbb{Z}_2 gauge theory which leads to the conservation rule of having an even number of anyons in any excited state.

2.6 Symmetry enriched topological order

Symmetry enriched topological order (SETO) comes from the enrichment of intrinsic topological order with symmetry protection, so the phase hosts topological anyons. In 2D these excitations are point-like, but can be moved around. What can these anyons do in the new setting of symmetry? In general, there are two possibilities. First, the anyons can fractionalise the symmetry, much like the edge modes of SPTO. Symmetry fractionalisation (SF) occurs in intrinsic topological phases when anyons carry a non-trivial symmetry charge, meaning that they transform under a non-trivial projective representation. This is explained diagrammatically in Fig. 2.7. The second possibility is that anyons can be permuted between each other under the action of symmetry. Additionally, symmetry fractionalisation and permutation can be combined.

The requirements that the projective representations V_g^a must fulfill are described equivalently by braiding properties of the anyons [185]. It has been shown that for symmetry groups G , their cocycles are classified by the second cohomology group $H^2(G, \mathcal{Q})$, with the gauge group \mathcal{Q} [10]. This comes from the fact that the braiding of anyons has to be labelled by $U(1)$ phase factors [186]. This is a refined classification as compared to SPT phases, since $H^2(G, \mathcal{Q}) > H^2(G, U(1))$, meaning that the set of 2D SET phases is in general larger than the set of 1D SPT phases, for a given G-symmetric system and non-trivial anyon group \mathcal{Q} . For example, symmetry groups G which have no non-trivial SPT phases can support non-trivial SET phases such as $G = \mathbb{Z}_2$. Another relevant example is $G = \mathbb{Z}_2 \times \mathbb{Z}_2$, which supports only two SPT phases but supports four SET phases. We do not consider

the case where anyons are non-abelian; then it's necessary to consider the further interplay between the set of anyons and the symmetry [187].

The understanding of symmetry enriched topological (SET) phases has reached insofar as they have been classified both in the language of category theory for global on-site symmetries [185], as well as in the language of tensor networks through MPO-injective PEPS [188]. These fully describe the classification of the SF classes of anyons. An example of a state with SET order is the resonating valence bond (RVB) state on a kagome lattice [189].

SET phases have been explored in the context of quantum error correction, and in particular towards self-correcting quantum memories (SCQM) [190]. Unlike in active error correction, in which systems coupled to a thermal bath are maintained through an externally applied error-correcting procedure, systems which are SCQM have an intrinsic (“passive”) error-correcting ability. In other words, in SCQM all stored information has a lifetime that grows unboundedly in system size³. It's proven difficult in the community to describe a class of models which are SCQM. More recently, it's been suggested that topologically ordered systems are a promising candidate for SCQM due to their robustness to local noise and degenerate ground states. Moreover, symmetries may provide further advantages towards SCQM. Candidates are non-commuting Hamiltonians such as the Bacon-Shor code or Bombin's color code [9, 192]. Other candidates are commuting Hamiltonians which require a high dimension. For example, the 2D Toric code requires active error correction; however, the 4D Toric Code is a canonical example of self-correcting quantum memory [61].

2.6.1 A simple model of 2D SETO

An example of SETO in 2D has been constructed in Refs. [193] which can be understood as a 2D Toric code decorated with cluster states [10]. This model will be a main character in Chapter 6. It is particularly elegant as the SET order can be understood very simply as the overlap of properties of two famous examples of SPT order and intrinsic topological order. In particular, this model has its intrinsic topological order inherited from the Toric code (giving anyons in the bulk), and is enriched with extra symmetries from entangling with cluster states. The description with 2D PEPS allows us to interpret this via projective representations on the virtual level. This useful recipe leads to non-trivial action of the anyons, which can be fractionalised under the symmetries of the cluster state. Decorating by 1D SPTO and gauging the symmetry is by now an established procedure to study SET orders [189].

We briefly describe the recipe to construct the Hamiltonian H_{SET} from the Toric code Hamiltonian H_{TC} from Ref. [10]. The recipe starts with the Toric code Hamiltonian set on a honeycomb lattice with qubits living on the edges [183]. The

³The Caltech rules detail the hypothesized requirements for models of SCQM [191], including a nontrivial codespace and perturbative stability.

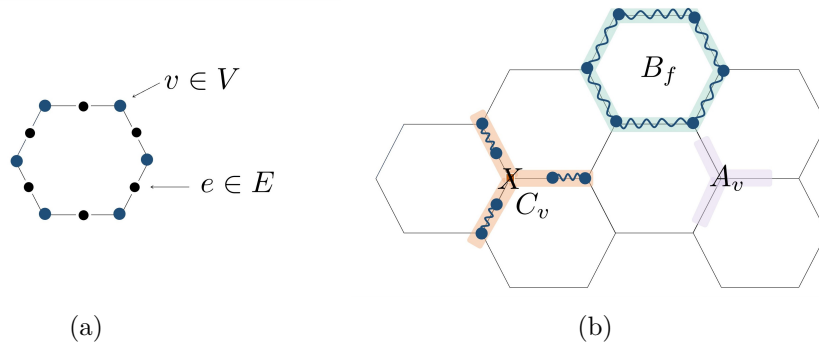


Figure 2.8: a) Hilbert space for $|SET\rangle$ consists of Toric code qubits living in E and cluster state qubits living in V . b) Terms of the Hamiltonian H_{SET} on a patch of the lattice. We omit the sites for visual simplicity. The red wavy lines indicate a CZ operation between the sites (which are either vertex-vertex or edge-vertex connections).

Hamiltonian has the same form as previously 2.5.1,

$$H_{TC} = - \sum_{v \in V} A_v - \sum_{f \in F} B_f, \quad (2.6.1)$$

but now where A_v is a 3-body operator acting on all the edges incident on a vertex v and B_f is a 6-body operator acting on all the edges around a face f . The ground state is $|TC\rangle$.

We now couple $|TC\rangle$ to an additional Hilbert space by placing qubits on the vertices of the honeycomb lattice (shown in Fig. 2.8(a)). We initialise each vertex qubit in the state $|+\rangle$, and couple them to the edge qubits via a circuit U of CCZ gates acting between all edges e and the vertices on either side which are denoted v_e^+, v_e^- . Applying U_{CCZ} to $|TC\rangle$ on the entire lattice leads to the SET ordered state

$$|SET\rangle = U_{CCZ}(|TC\rangle \otimes |+\rangle^{|V|}). \quad (2.6.2)$$

The CCZ gate is defined here to act on $\{e, v_e^+, v_e^-\}$ so the edge is a control bit. It does nothing if it touches an edge in state $|0\rangle$ but acts on the vertices as CZ if it touches a state $|1\rangle$. This means it acts on the Toric code as CZ s between the vertices in closed loops and acts trivially on qubits which are not in loops. Recall that CZ s on $|+\rangle^{\otimes |V|}$ between nearest neighbours generates the 1D cluster state. Finally, we can understand the resulting state is made up of an equal-weight superposition of closed loops \mathcal{C} decorated by cluster states $|CS\rangle$

$$|SET\rangle = \frac{1}{\mathcal{N}} \sum_{\mathcal{C}} |CS_{\mathcal{C}}\rangle. \quad (2.6.3)$$

The circuit which maps between the ground states $|SET\rangle$ and $|TC\rangle$ similarly leads to a mapping to H_{SET} . We first add the paramagnetic Hamiltonian term $\sum_{v \in V} X_v$ which has $|+\rangle^{\otimes |V|}$ as its ground state on all vertices. Then applying the unitary transform of CCZ s to H_{TC} results in the desired Hamiltonian which has

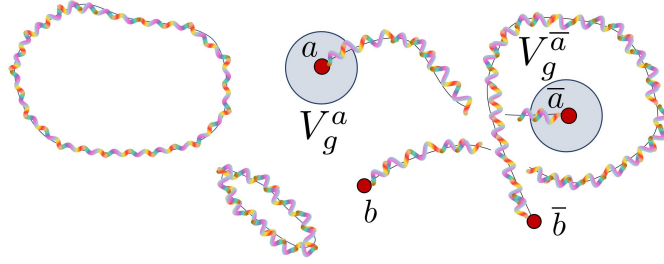


Figure 2.9: The connection between SF and the braiding of anyons is used to detect SETO in the state $|SET\rangle$ in 2.6.3. In the ground state, the Toric code loops are decorated by cluster states, depicted here as wavy rainbow-coloured lines in one such configuration. We omit the edge qubits. By acting on the state with string operators we create excitations which are open loops. Here we first create one pair of anyons a, \bar{a} and then act with a global symmetry which fractionalises on the anyons as a projective symmetry. This is equivalent to braiding a with a second anyon type b . All blank space corresponds to vertex qubits not in loops, which are in the $|+\rangle$ state.

ground state $|SET\rangle$

$$H_{SET} = - \sum_{v \in V} A_v - \sum_{f \in F} B_f - \sum_{v \in V} C_v \frac{1 + A_v}{2}, \quad (2.6.4)$$

where A_v is just the same, B_f is a modified version of 2.6.1 with CZ operators acting between each pair of vertices surrounding an edge and $C_v = U_{CCZ} X_v U_{CCZ}$. This evaluates to

$$B_f = \prod_{e \in f} X_e CZ_{v_e^+, v_e^-}, C_v = X_v \prod_e CZ_{v_e^+, v_e^-}, \quad (2.6.5)$$

where v_e^+, v_e^- are the two vertices attached to an edge e . The action of the projector $\frac{1 + A_v}{2}$ is to project the state onto one with only closed loops. This enforces the third term to be symmetric, since C_v otherwise doesn't commute with the endpoint terms. Hence H_{SET} then has the full $\mathbb{Z}_2 \times \mathbb{Z}_2$ symmetry group generated by X_A and X_B (which flip spins on the vertices of the sublattices A and B of the honeycomb lattice)⁴. More details can be found in Ref. [10].

How do we characterise the symmetry fractionalisation effect? This is the most relevant point that we will need to understand for this Thesis, which tells us how SETO manifests in the model. It turns out that the decoration structure by cluster states provides a natural way to see this.

We saw that H_{SET} and its ground state $|SET\rangle$ inherit the symmetries from the cluster state. In the Toric code, we can create excitations which manifest as the local end-points of open strings (see Fig 2.6(c)). Any configuration of strings in this model now corresponds to cluster states, so an open string has the edge modes of a cluster state on its boundary. The symmetry on the boundary manifests

⁴The Hamiltonian also has time-reversal and inversion symmetry.

projectively. Therefore the anyons at the ends of strings inherit the fractionalisation property from the cluster state.

We can also see this from the explicit construction of the string operator for this model which creates open strings [10]. We apply a unitary transform CCZ to S^m for some set of edges Γ which gives

$$S_\Gamma = \prod_{e \in \Gamma} X_e C Z_{v_e^+, v_e^-}. \quad (2.6.6)$$

This string operator doesn't commute with the term A_v so a state by excited applying the string violates this term in the Hamiltonian. The string's end-points (vertex qubits) are in the $A_v = -1$ eigenspace. Then the projector $\frac{1+A_v}{2} = 0$ and all Hamiltonian terms C_v are annihilated. This was the only term acting with X s on vertices, so notice that no energies are changed by adding some Z s onto the string end-points at locations v_i and v_f (all other terms commute with Z on vertices). The dressed string operator is

$$S_\Gamma(a, b) = Z_{v_i}^a Z_{v_f}^b S_\Gamma, \quad (2.6.7)$$

for $a, b \in \{0, 1\}$ indicating 0 or 1 Z s acting on an anyon on site v_i or v_f . The degeneracy of the string operators for different values of a, b leads to a four-fold degenerate subspace of the excited states which can be written

$$|a, b\rangle = S_\Gamma(a, b) |SET\rangle. \quad (2.6.8)$$

The operators which transform between these excited states are X_A and X_B which either permute basis states $|a, b\rangle$ or contribute a phase. The action of this symmetry realised locally on a single anyon generates a projective representation of $\mathbb{Z}_2 \times \mathbb{Z}_2$ given by $V_{(\alpha, \beta)} = X^\alpha Z^\beta$ where the labels (α, β) are $\alpha, \beta = \{0, 1\}$. By writing out the commutation rules

$$V_q V_k = \omega(q, k) V_{qk}, \quad (2.6.9)$$

with $\{q, k\} = (0, 0), (0, 1), (1, 0), (1, 1)$ we see that the SF pattern on the anyons is given by

$$\omega(q, k) = \begin{pmatrix} +1 & +1 & +1 & +1 \\ +1 & +1 & -1 & -1 \\ +1 & +1 & +1 & +1 \\ +1 & +1 & -1 & -1 \end{pmatrix}. \quad (2.6.10)$$

A trivial SF pattern would have a different pattern of $+1, -1$. By considering the elements of the table (q, k) , the SF pattern detects the class $[\omega(q, k)]$.

2.6.2 An order parameter for SETO

For our investigations we make use of a particular order parameter in 2D which has been recently developed for SETO in the framework of TN [11]. The goal of the order parameter is to capture the projective representation characterising the SF class of the anyons. Similarly to the swap order parameter for SPTO 2.4.19, this

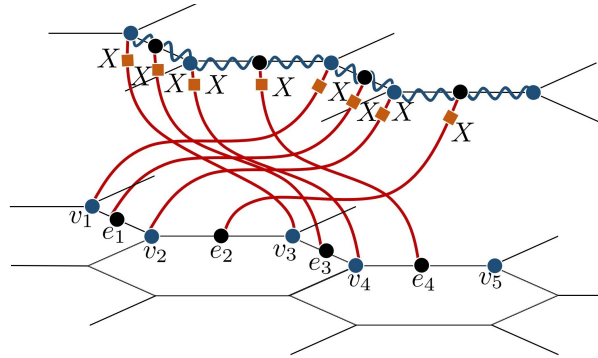


Figure 2.10: Order parameter detecting SETO via SF in the model of Ref. [10]. Black dots are edge qubits and blue dots are vertex qubits. The orange square denotes an X operator on an edge qubit. Wavy lines depict CZ gates between next-neighbour vertices. The SWAP operation is represented pictorially by linking the physical legs between different sites.

order parameter detects the realisation of the symmetry locally on quasiparticles which is given by a projective representation. The order parameter is designed for quantum double models on a 2D lattice enriched with a global on-site symmetry, and in particular defined for G -injective projected entangled pair states (PEPS)⁵. The key ideas and the model of the order parameter for the SETO model are visualised in Fig. 2.9 and Fig. 2.10.

A nice way to understand the action of the order parameter is via its equivalence to braiding; by creating two different pairs of anyons, applying the global symmetry, and braiding one type of anyon around another, the action of the projective symmetry can be captured. The key insight is that braiding probabilities can be measured by taking an expectation value of the braiding operation on an anyon. The braiding operation is achieved by SWAP operators. The anyon pairs are created by S_Γ at both ends of a chain of symmetry operators, and then the symmetry operators X are applied. By applying the rules of G -injectivity and that the state is a fixed point, one can derive the gauge-invariant quantity [11].

What advantages of TNs can we leverage to write an order parameter? Consider a state of size N with a global onsite symmetry $U_g^{\otimes N} |\psi[A]\rangle = |\psi[A]\rangle \forall g \in G$ where U_g is a unitary representation of the group \mathcal{G} . Another way to view G -injectivity is that the physical symmetry U_g pulls through to the virtual degrees of freedom

$$\begin{array}{c} u_q \\ | \\ \bullet \\ | \\ \text{---} \end{array} = \begin{array}{c} v_q \\ | \\ \bullet \\ | \\ v_q^\dagger \\ | \\ \text{---} \end{array} \quad \forall q \in \mathcal{Q} \quad , \quad (2.6.11)$$

where v_q is invertible [199, 200]. Notice that the virtual operators v_q do not necessarily need to form a linear representation; the phase freedom on a single site

⁵We note that other existing order parameters can consider different classes of states, including the elusive chiral spin liquids, by probing effective 1D systems through dimensional compactification [194–198].

means they can form a projective representation as in Eq. 2.6.9. For a system on periodic boundary conditions, the operators v_q cancel each other out on the virtual level. However, when anyons are introduced into the system, the symmetry on the virtual level can interact with them and their braiding properties.

Consider how acting with the global symmetry is realised locally on the tensor network when an anyon is present

$$(2.6.12)$$

We can see from this that $v_q^\dagger a v_q$ is allowed to be projective as long as v_q and v_q^{-1} have opposite sign, since we assumed that the global symmetry was linear. This is satisfied easily for abelian anyons a whose anti-particles \bar{a} transform with the inverse projective representation (which is just v_q^\dagger).

If we apply another symmetry u_k then conjugation by v_q on the anyon a can either permute the anyon or add a phase; it turns out that the allowed actions have to agree with the fusion rules of the system defined by category theory and the classification of SF [201].

Overall, we can interpret the classifying SF pattern equivalently through braiding, which gives the intuition for how the order parameter of Ref. [11] is constructed. The order parameter can be expressed (in a simplified form) as

$$\Lambda := \langle \mathcal{O}_a^\dagger P_\pi \bigotimes_{s_i}^{s_m} U_g^{s_i} \mathcal{O}_a^\dagger \rangle, \quad (2.6.13)$$

where P_π is a permutation operator on some finite m sites, \mathcal{O}_a creates an anyon pair a, a^\dagger at some location and \mathcal{O}_a^\dagger creates another pair some place else. The idea is that the action of P_π is the same as a braiding operation of the anyon with the symmetry and so can capture the SF effect. It is possible to normalise this quantity as follows

$$\hat{\Lambda} := \Lambda / \langle \mathcal{O}_a^\dagger P_\pi \mathcal{O}_a^\dagger \rangle, \quad (2.6.14)$$

which promotes Λ to a gauge-invariant quantity that actually distinguishes between inequivalent cocycles that label the SF classes.

One might wonder whether order parameters built for SETO which detect the class $H^2(G, \mathcal{Q})$ could detect SPTO as well. This is not the case, as although SPT systems experience a fractionalisation of the edge modes they cannot resolve all SPT phases, due to their lack of anyon classes, and hence the 2D SET order parameter on a 1D SPT phase would set some phases equal. Conversely one could consider whether SPT order parameters can detect SETO, which this time doesn't resolve the SF classes of anyons and sets them equal.

For the case of the SETO model defined in the previous Section, the following form of the order parameter applies

$$\Lambda = S_{\Gamma=e_1, \dots, e_6}^\dagger [X_{e_1}^a X_{e_2}^b X_{e_3}^a X_{e_4}^b] \times \quad (2.6.15)$$

$$[\text{SWAP}_{e_1, e_3} \text{SWAP}_{e_3, e_4} \text{SWAP}_{v_1, v_3} \text{SWAP}_{v_2, v_4}] S_{\Gamma=e_5, e_6}, \quad (2.6.16)$$

$$(2.6.17)$$

where S_Γ is the string operator defined in 2.6.6, $\text{SWAP}_{i,j}$ denotes contracting the physical legs on two different sites i, j which can be edges or vertices, and $a, b \in \{0, 1\}$ are the physical symmetry operators. By decomposing the string operators the expression simplifies

$$= (\prod_{i=1}^4 CZ_{i,i+1} X_{e_i}) [X_{e_1}^a X_{e_2}^b X_{e_3}^a X_{e_4}^b] \times \quad (2.6.18)$$

$$[\text{SWAP}_{e_1, e_3} \text{SWAP}_{e_3, e_4} \text{SWAP}_{v_1, v_3} \text{SWAP}_{v_2, v_4}], \quad (2.6.19)$$

so we arrive at the order parameter drawn for the honeycomb lattice in Fig. 2.10.

The normalised order parameter is given by the set

$$\mathcal{O}^{[a,b]} = \frac{\Lambda^{[a,b]}}{\Lambda^{[0,0]}}. \quad (2.6.20)$$

Note that the order parameter is defined with respect to the fixed point representation of a state with zero correlation length. A generalisation to deal with states with non-zero correlation lengths has been given where the order parameter acts not just on lines but on faces has been given in Ref. [10].

We can focus on the case $a = 1, b = 1$ which gives $\mathcal{O}^{[1,1]} = -1$ in the SET phase of the decorated Toric code model, and $+1$ otherwise.

Chapter 3

A new fingerprint for SPTO: inaccessible entanglement

This Chapter contains the publication

- Inaccessible entanglement in symmetry protected topological phases. **Caroline de Groot**, David T. Stephen, Andras Molnar, and Norbert Schuch. *Journal of Physics A: Mathematical and Theoretical* 53, 335302 (2020). [202]

3.1 Motivation

Entanglement is the essential resource which allows for tasks beyond the restrictions of local operations and classical communication (LOCC). Certain tasks in the quantum world are impossible to implement classically, such as quantum teleportation, dense coding and secure cryptography [203–205]. A fascinating realisation in the quantum information community was that entanglement governs state conversion, through the mathematical structure of majorisation and quantified by the von Neumann entropy, [15]. More recently, it has been interesting to study how additional restrictions to LOCC reshape the non-local resources that emerge, as well as the tasks they allow.

In a seminal work Wiseman and Vaccaro found that entanglement under superselection rule (SSR) is reduced, for indistinguishable particles subject to fixing the total particle number [206]. This observation led to studies of SSR in varying contexts across the quantum information community [206–213]. SSR occurs in natural physical phenomena where particular state transitions are forbidden in the Hilbert space due to some physical rule. It can be described by global symmetry groups or local gauge symmetry groups but is a broader notion. Examples of SSR include disallowing a superposition across different electronic charge sectors, which would violate the inherent parity symmetry of fermions [214], or restrictions due to particle number conservation [215].

The interplay between entanglement and SSR in physical systems has yet to be fully explored. Bridging this gap necessitates modifying the rules of LOCC

to include the SSR. This requires enforcing a further structure (by the SSR) on the majorisation criterion which defines the partial order of states [215]. SSR were shown to even produce additional non-local resources, *e.g.* to permit perfect quantum data hiding protocols [216]. This motivated exploring the entanglement under restricted settings in various contexts, such as the symmetry-resolved entanglement [211, 217–220], as well as conservation laws in fermionic systems with parity symmetry and ultracold atoms with particle number conservation, for both critical and gapped systems [221–223]. This has also been applied to lattice gauge theories, in which the additional local symmetry restrictions changes the entanglement distillation rules [224–226]. Here we consider symmetry protected topological (SPT) phases [12, 91, 102, 128, 154, 158, 159].

The motivation of this Chapter is to apply insights from quantum information about entanglement under SSR, to SPT phases. Our main question is the following: *what is the connection between SPTO and SSR entanglement?* It is natural to expect a connection between entanglement distillation and topological order, as topological phases are determined by global patterns of entanglement beyond the Landau description of symmetry breaking [227–229]. In particular, topological phases are classified through non-local order, rather than local order parameters. The many-body entanglement picture of topological order sorts phases into two classes; topological phases have long range entanglement (i.e. have topological order), while others have short range entanglement (i.e. have SPT order). We are concerned with the latter, which only host topological properties in the presence of symmetry, such as topological insulators and the Haldane chain [12, 154, 227]. The development of quantities which detect SPT order is of particular interest in improving intuitions about these phases [230, 231], such as the string order parameter and SPT-entanglement which characterize the phase in terms of the global entanglement structure [156, 157, 176, 177, 232]. Here we impose a global symmetry as our SSR and consider the impact on entanglement distillation in SPT phases.

3.2 Summary

We study the entanglement of SPT ordered systems under local operations commuting with a global onsite symmetry G , which we call G -LOCC. This setting is naturally suggestive of SPT phases which are only defined with respect to the symmetry group G protecting the order, since the classification breaks down when considering scenarios with no symmetry. In G -LOCC, the amount of accessible entanglement is naturally reduced as compared to LOCC. We therefore show that, in the presence of non-trivial SPT order under G , there is always some entanglement that is inaccessible under G -LOCC. We give this quantity operational meaning by showing that it is consistent with entanglement distillation under G -LOCC. In §3.3, we firstly formalise the definition of inaccessible entanglement via entanglement distillation with G -LOCC.

In Section 3.4, we present our proofs of the bound on inaccessible entanglement

for all SPT phases under finite Abelian symmetry groups, and the connection to string order parameters. This leads to the following bound

$$\log(D_\omega^2) \leq E_{inacc} \leq \log(|G|), \quad (3.2.1)$$

where D_ω is the topologically protected part of the edge mode degeneracy and the dimension of the projective irreducible representation defining the SPT phase ω . Of particular interest are a class of phases called maximally non-commutative (MNC) phases (introduced previously in §2.4.2), such as the Haldane or cluster phase for the symmetry $\mathbb{Z}_2 \times \mathbb{Z}_2$, which saturate the upper bound on inaccessible entanglement. This is connected to the fact that MNC phases maximise the number of topologically protected degenerate edge modes. Importantly, trivial SPT phases always have zero as the lower bound, while non-trivial phases have a non-zero lower bound.

Through a numerical investigation in §3.5 we confirm that the bound is tight, and examine properties of SPT phases living in particular regions of the bound by performing interpolations in the MPS tensor. To better understand the inaccessible entanglement of typical states, we numerically study particular random distributions of MPS. We demonstrate that the bound is tight by interpolating through a path of states from the lower bound to the upper bound in Fig. 3.4. Intriguingly, we find that both trivial and non-trivial SPT systems typically have near maximal inaccessible entanglement. However, the irrep probabilities, which are the weights of the state on the individual symmetry sectors, have different structure, and can thus be used to distinguish these phases. We study the implication of effective reduced symmetries in a non-trivial SPT system, where we interpolate a state with a symmetry G to effectively a lower symmetry $H \subset G$. The interpolation causes the inaccessible entanglement and the irrep probabilities to lose the structure due to G and the final state displays only structure due to H . On the other hand, we also study the effect of reduced G -LOCC, so that the local operations commute with some $H \subset G$ where G is still the symmetry protecting the SPT phase, as opposed to the effective reduced symmetry scheme. We argue that the accessible entanglement depends on the dimension of the subspace of the MPS which transforms trivially under the symmetry, previously termed the junk subspace [174]. We can increase the dimension of the junk subspace for a given bond dimension by giving an uneven irrep structure to the projective representation, which causes a greater spread in the distribution of inaccessible entanglement.

In §3.7 we discuss the implications on computational power, 2D subsystem SPT phases [233, 234], restricting operations to a subgroup of G , and also how they relate to the characterization of states as resources for measurement-based quantum computation (MBQC) [164].

3.3 Accessible entanglement distillation

How much entanglement can be extracted from a state obeying a symmetry G under LOCC respecting the same symmetry? In this Section we define the accessible

entanglement in the presence of G -symmetric LOCC (G -LOCC) and derive an expression through multi-shot entanglement distillation which is consistent with previous works *e.g.* Refs. [206, 208–211]. We will first define G -LOCC and motivate why we might expect this to effect the entanglement which is accessible under these operations.

We define G -LOCC by restricting LOCC protocols to positive-operator valued measure (POVM) sets $\{M_\alpha^\dagger M_\alpha\}$ that commute with the global symmetry $U(g) = u(g)^{\otimes N}$ such that $[U(g), M_\alpha] = 0 \forall g \in G$, where α are the measurement outcomes. Note that the M_α are not necessarily orthogonal measurements. The accessible entanglement we will motivate that exists under such POVM sets is given by

$$E_{acc}(\rho) = \sum_{\alpha} p_{\alpha} E(\rho_{\alpha}), \quad (3.3.1)$$

where $p_{\alpha} = \text{Tr}(M_{\alpha}\rho M_{\alpha}^{\dagger})$ are measurement probabilities corresponding to the post-measurement state $\rho_{\alpha} = M_{\alpha}\rho M_{\alpha}^{\dagger}$ up to normalisation and the entanglement entropy $E(\rho_{AB})$ of a bipartite state ρ_{AB} is given by the von Neumann entropy $S(\rho_A)$, where $\rho_A = \text{Tr}_B(\rho_{AB})$ is the reduced density operator [15]. We will now argue that the entanglement entropy overestimates the physical entanglement E_{acc} due to the structure imposed by symmetry. This line of thought leads naturally into the entanglement distillation protocol of the next Section, in which we will derive Eq. (3.3.1).

A simple argument considers that local operations may not mix symmetry sectors, and that local operations can only decrease entanglement. As the state ρ is symmetric under the symmetry G which imposes the G -LOCC, enforcing $[u(g)^{\otimes N}, \rho] = 0$, the reduced density ρ^A also has the symmetry $[u(g)^{\otimes N_A}, \rho^A] = 0$. In the following we will make use of a particular POVM set to directly measure the symmetry and capture properties of the SPT phase under G -LOCC. We utilise the projective measurement Π_{α} onto the irrep sectors given by

$$\Pi_{\alpha} = \frac{1}{|G|} \sum_g \chi_{\alpha}(g) u(g)^{\otimes N_A}, \quad (3.3.2)$$

where $\chi_{\alpha}(g)$ is the character corresponding to irrep α and N_A are the sites in the A -subsystem (see also [156]). Due to the symmetry, the reduced state can be written as $\rho^A = \bigoplus_{\alpha} p_{\alpha} \rho_{\alpha}^A$, where p_{α} are the measurement probabilities defined above for the POVM operators $M_{\alpha} = \Pi_{\alpha}$, and where $\rho_{\alpha}^A = \Pi_{\alpha} \rho^A \Pi_{\alpha}^{\dagger} / p_{\alpha}$.

All allowed operations commute with the symmetry and hence operate only within single sectors α which can be written as $\rho_{\alpha, out} = \Lambda_{\alpha}(\rho_{in})$ with the map $\Lambda_{\alpha}(\cdot) = M_{\alpha}(\cdot)M_{\alpha}^{\dagger}$, and M_{α} defining an element of a POVM set obeying the symmetry and acting on a single sector. These operations are local by definition. Since operations which mix the symmetry sectors of states are not supported, any entanglement between different sectors is erased by G -LOCC. Hence, only the entanglement within individual symmetry sectors contributes. The accessible entanglement defined in Eq. (3.3.1) is therefore the sum over the entanglement within each symmetry sector α . Clearly the entanglement in each sector $E(\rho_{\alpha})$ is less than the total entanglement, but so is the weighted sum of $E(\rho_{\alpha})$ over α . As

this defines the accessible entanglement, it is therefore also smaller or equal to the entanglement,

$$E_{acc} \leq E. \quad (3.3.3)$$

Hence G -LOCC leads to a reduced accessible entanglement. Note that this expression ensures that product states have $E_{acc} = 0$. The considerations above naturally lead to an operational definition of the accessible entanglement.

3.3.1 Entanglement distillation under G -LOCC

We now present how entanglement distillation under G -LOCC leads us to the accessible entanglement in Eq. (3.3.1). Entanglement distillation is the process of distilling Bell pairs from asymptotically many copies of a state under LOCC, and is consistent with a partial order on states through the majorisation criterion [15, 235]. This leads to the equivalence of the conversion ratio M/N , between N copies of a pure state $|\Psi\rangle$ to M copies of the Bell state in the asymptotic limit $N \rightarrow \infty$, to E the entanglement entropy [236]. We now consider entanglement distillation under G -LOCC.

We measure the POVM set $\{\Pi_\alpha^\dagger \Pi_\alpha\}$ with Π_α as defined in Eq. (3.3.2) the projector onto each irrep α of the symmetry G imposing the G -LOCC, such that on average we get every channel containing the normalised output state ρ_α with a probability p_α in the asymptotic limit. This action splits the state into the symmetry sectors which impose the super-selection rule, so that operations are restricted to within these subspaces. This makes it possible to act with LOCC within each subspace. Then the entanglement entropy of the output state at each branch α computes the number of Bell pairs distilled from the α -channel. Clearly, the total entanglement extracted from this procedure is the weighted sum of the entanglement from each branch, giving the expression in Eq. (3.3.1).

Furthermore, as the LOCC can be defined free of SSR within each sector, each branch contains an optimal distillation within each symmetry sector such that the full distillation is optimal [15], *i.e.* the maximal possible ratio M/N of M Bell pairs produced from N copies of $|\Psi_\alpha\rangle$ is achieved. This concludes the description of entanglement distillation under G -LOCC, which employs the full rigour of distillation under LOCC, and as such is of itself complete.

3.3.2 Symmetry measurement

In order to carry out calculations later on, we rewrite the irrep probabilities in tensor network notation through some simple manipulations which we sketch here. We consider a system on a ring with N sites in the limit of the number of sites going to infinity which allows us to use properties of the fixed point, such that bipartitioning cuts the ring in half and results in two boundaries. Using $p_\alpha = \text{Tr}(\Pi_\alpha \rho)$, and inserting the form of the symmetric projection operator from Eq. (3.3.2), we should recall that Π_α acts only on the A -subsystem, so the rest is traced over, leaving the fixed point action on the remaining half.

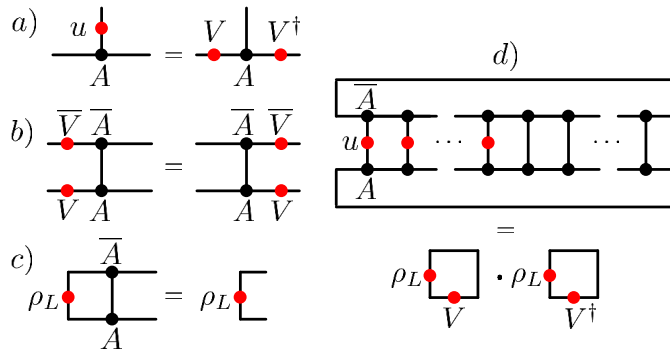


Figure 3.1: In this figure, u and V have a dependence on g which is omitted. 1a) Reminder of the fundamental theorem, given in Eq. 2.3.2. 1b) Symmetries of the transfer operator T . 1c) Definition of the left-fixed point ρ_L . 1d) Graphical calculation of the trace part of the irrep probabilities leading to (3.3.5).

By using the fact that the symmetry action in Π_α acts locally, we can pull the sum out and by engaging the fundamental theorem, Eq. (2.3.2), we find an effective action of the symmetry group on the virtual system. Due to the cross-cancellation of all $V(g), V(g)^\dagger$ except for the action at the edges, the rest of the expression becomes

$$p_\alpha = \frac{1}{|G|} \sum_g \chi_\alpha(g) \langle L | (\mathbb{1} \otimes V(g)) T^{N_A} (\mathbb{1} \otimes V(g)^\dagger) | R \rangle. \quad (3.3.4)$$

Now recall the transfer operator T introduced in Section §2.3, which inherits the symmetries of A as shown in Fig. 3.1 b). The transfer operator is an important object in coming calculations, so we give some further notation. Let $|R\rangle$ and $\langle L|$ denote the right and left eigenvectors of T corresponding to the largest eigenvalue, which we can set to be equal to 1 with normalisation, such that $T|R\rangle = |R\rangle$ and $\langle L|T = \langle L|$. It can be convenient to express T as a quantum channel \mathbb{T} defined as $\mathbb{T}(\rho) = \sum_i A^i \rho A^{i\dagger}$. This allows us to easily define $|R\rangle$ and $\langle L|$ as the fixed-points ρ_R and ρ_L of \mathbb{T} and $\mathbb{T}^\dagger(\rho) = \sum_i A^{i\dagger} \rho A^i$, respectively, see Fig 3.1 c).

We now use that $T^{N_A} \rightarrow |R\rangle \langle L|$ as $N_A \rightarrow \infty$, and for simplicity we switch from the language of vectors $\{|L\rangle, |R\rangle\}$ to matrices $\{\rho_L, \rho_R\}$ which are the same object, the fixed point of the MPS, considered either as vectors or as matrices. Then the remaining expression is

$$p_\alpha = \frac{1}{|G|} \sum_g \chi_\alpha(g) \text{Tr}(\rho_L V(g)) \text{Tr}(\rho_L V(g)^\dagger), \quad (3.3.5)$$

using right-canonical form such that ρ_R is the identity [237]. The part of the summand involving the trace in the calculations leading to Eq. (3.3.5) is shown pictorially in Fig. 3.1.

3.3.3 Inaccessible entanglement

Having defined the accessible entanglement by distillation under G -LOCC earlier, we now conversely define the inaccessible entanglement as the amount of

entanglement that the G -LOCC prevents access to:

$$E_{inacc} = E - E_{acc}. \quad (3.3.6)$$

While the accessible entanglement captures the physical entanglement of a system with SPT order, inaccessible entanglement measures the entanglement protected by the presence of symmetry and stored in the state. We show below that the inaccessible entanglement can be written as

$$E_{inacc}(\rho) = - \sum_{\alpha} p_{\alpha} \log(p_{\alpha}), \quad (3.3.7)$$

where p_{α} are the irrep probabilities defined above. In the following we will use \log to signify \log base-2. Note that Eq. (5.6.8) is the entropy of the probability distribution corresponding to the irrep weights of the symmetry group G on the state, $E_{inacc} = S(\{p_{\alpha}\})$.

Recall that the reduced density ρ^A has the symmetry $[u(g)^{\otimes N_A}, \rho^A] = 0$, and therefore can be written as $\rho^A = \bigoplus_{\alpha} p_{\alpha} \rho_{\alpha}^A$ where $\rho_{\alpha} = \Pi_{\alpha} \rho^A / p_{\alpha}$. Therefore the entanglement entropy of the state is

$$E(\rho) = - \sum_{\alpha} p_{\alpha} \rho_{\alpha}^A \log(p_{\alpha} \rho_{\alpha}^A) = \sum_{\alpha} p_{\alpha} E(\rho_{\alpha}) - p_{\alpha} \log p_{\alpha}. \quad (3.3.8)$$

Then Eq. (5.6.8) follows since the first term in the second equality is the accessible entanglement, and subtracting this gives the relation for inaccessible entanglement. Notice that since $E \geq E_{inacc}$, the presence of entanglement is a necessary condition for inaccessible entanglement.

Given the irrep probabilities in Eq. 3.3.5, we now have a tensor network formulation of E_{inacc} . In the following, we explore how different classes of SPT phases behave with regards to inaccessible entanglement.

3.4 Bounds for the inaccessible entanglement

In this Section we derive bounds on the entanglement that is inaccessible due to SPT order. It is trivial to deduce that $E_{inacc} = 0$ for a product state (which has no entanglement) or a state with no symmetry (which has no SSR). We show, however, a non-zero lower bound in the presence of symmetries for states with non-trivial SPT order. This bound, together with the upper bound, reads as

$$\log\left(\frac{|G|}{|k|}\right) \leq E_{inacc} \leq \log(|G|), \quad (3.4.1)$$

where G is the symmetry group protecting the topological order and k is the projective centre of G associated to the cocycle characterizing the SPT phase (defined in Eq. (2.4.6)). We thereby develop a prescription for all SPT phases under finite Abelian groups by showing that non-trivial SPT phases remarkably incur a non-zero lower bound on the inaccessible entanglement.

3.4.1 Maximal inaccessible entanglement in the MNC phase

We first consider the simpler case of MNC phases, which obey a strong condition on inaccessible entanglement where the lower bound meets the upper bound

$$E_{inacc} = \log(|G|), \quad (3.4.2)$$

given the symmetry G . MNC phases therefore maximise the inaccessible entanglement. The irrep probabilities are $p_\alpha = \frac{1}{|G|} \forall \alpha$, which produces maximal entropy $S(\{p_\alpha\})$, and hence Eq. (3.4.2). We first give an example to illustrate this result.

The Haldane or cluster phase is a canonical example of the MNC phase, which is protected by the symmetry $G = \mathbb{Z}_2 \times \mathbb{Z}_2$ for which the cohomology group is known to be $H^2(G, U(1)) = \mathbb{Z}_2$, indicating one trivial and one SPT phase [174, 228]. One valid symmetry representation is given by $u(g) = \bigoplus_\alpha \chi_\alpha(g)$, where χ_α is the character of the irrep α , and the projective representation in the MNC phase is given by the Pauli operators including the identity, $V(g) = \sigma(g)$. States satisfying this symmetry have an MNC cocycle as all the Pauli operators mutually anti-commute, so the projective centre k contains only the identity. Since the Pauli matrices are traceless, $\text{Tr}(\sigma(g)) = 0 \forall g \in G$, the only contribution to p_α in Eq. (3.3.5) is from the identity element and hence $p_\alpha = \frac{1}{4} \forall \alpha$. Therefore in the Haldane phase the inaccessible entanglement is 2.

To derive a similar result for all states in an MNC phase, we start from Eq. (3.3.5). We first use symmetries of the left fixed point. The main step will be to use the simplified form of the projective representation in Eq. (2.4.9). We begin by fixing the form of the left fixed point according to the symmetry imposed by Eq. (2.4.3). Inherited from the symmetries of the transfer matrix T , the left fixed point is also symmetric under $V(g) = \mathbb{1} \otimes \tilde{V}(g)$, *i.e.* $\rho_L = (\mathbb{1} \otimes \tilde{V}(g))\rho_L(\mathbb{1} \otimes \tilde{V}(g)^\dagger)$. By Schur's Lemma, ρ_L can therefore be written as $\rho_L = \tilde{\rho}_L \otimes \mathbb{1}$, for some matrix $\tilde{\rho}_L$ carrying correlations and corresponding to the junk subspace. We choose normalisation $\text{Tr}(\rho_L) = 1$ which implies that $\text{Tr}(\tilde{\rho}_L) = 1/D_\omega$.

Inserting back the above form of the fixed point ρ_L into Eq. (3.3.5), the irrep probabilities can be expressed as

$$p_\alpha = \frac{1}{|G|} \sum_g \chi_\alpha(g) \text{Tr}\left((\tilde{\rho}_L \otimes \mathbb{1})(\mathbb{1} \otimes \tilde{V}(g))\right) \text{Tr}\left((\tilde{\rho}_L \otimes \mathbb{1})(\mathbb{1} \otimes \tilde{V}^\dagger(g))\right). \quad (3.4.3)$$

Now multiplying out the corresponding parts of the tensor product, and reducing the trace over it,

$$p_\alpha = \frac{1}{|G|} \sum_g \chi_\alpha(g) \text{Tr}(\tilde{\rho}_L)^2 \text{Tr}(\tilde{V}(g)) \text{Tr}(\tilde{V}^\dagger(g)). \quad (3.4.4)$$

Using now Eq. (2.4.8) and that $\text{Tr}(\tilde{\rho}_L) = 1/D_\omega$, the above equation becomes

$$p_\alpha = \frac{1}{|G|} \frac{1}{D_\omega^2} \sum_g \chi_\alpha(g) D_\omega^2 \delta_{g,e}. \quad (3.4.5)$$

Using $\chi_\alpha(e) = 1$, p_α finally takes the same value for all irreps α ,

$$p_\alpha = \frac{1}{|G|}. \quad (3.4.6)$$

The irrep probabilities are degenerate, meaning that the weight of each sector contributes equally to E_{inacc} , and the entropy is maximised which confirms $E_{inacc} = \log(|G|)$. This demonstrates that MNC phases have the maximal set of topologically protected degenerate edge modes $D_\omega = |G|$ from Eq. (2.4.7), which is reflected in the inaccessible entanglement.

*

3.4.2 Generalisation of bounds to non-MNC phases

We generalise the inaccessible entanglement to describe all SPT phases, and crucially show that for non-MNC phases there exists a non-zero lower bound,

$$\log\left(\frac{|G|}{|k|}\right) \leq E_{inacc} \leq \log(|G|), \quad (3.4.7)$$

for the group G and projective centre group k defined in Eq. (2.4.6). We will first outline the steps taken to prove this. We use the general form of $V(g)$ in Eq. (2.4.5), and thus are prevented from easily evaluating the trace over ρ_L . However, much of the following proof remains in the same vein as in the previous Section, by simplifying the expression for p_α as much as possible by symmetry under $V(g)$. Finally we make an argument with entropy configurations from which we deduce the lower bound.

First we use the symmetry of ρ_L under $V(g)$ to deduce the fixed point. By Schur's Lemma, the fixed point is again $\rho_L = \tilde{\rho}_L \otimes \mathbb{1}$, where now $\tilde{\rho}_L = \bigoplus_a \tilde{\rho}_{L,a}$, and each $\tilde{\rho}_{L,a}$ has dimension $n_a \times n_a$. Again we choose the normalisation $\text{Tr}(\tilde{\rho}_L) = 1/D_\omega$ for convenience. Recalling the form of $V(g)$ from Eq. (2.4.5), the measurement probability then is written

$$p_\alpha = \frac{1}{|G|} \sum_g \chi_\alpha(g) \text{Tr} \left(\tilde{\rho}_L \bigoplus_a \mu_a(g) \mathbb{1}_{n_a} \otimes \tilde{V}(g) \right) \text{Tr} \left(\tilde{\rho}_L \bigoplus_a \overline{\mu_a(g)} \mathbb{1}_{n_a} \otimes \tilde{V}^\dagger(g) \right). \quad (3.4.8)$$

Separating the trace over the tensor product,

$$p_\alpha = \frac{1}{|G|} \sum_g \chi_\alpha(g) \text{Tr} \left(\tilde{\rho}_L \bigoplus_a \mu_a(g) \right) \text{Tr} \left(\tilde{\rho}_L \bigoplus_{a'} \overline{\mu_{a'}(g)} \right) \text{Tr}(\tilde{V}(g)) \text{Tr}(\tilde{V}^\dagger(g)). \quad (3.4.9)$$

Using Eq. (2.4.8), we can evaluate the traces over the projective representation, such that p_α further simplifies to

$$p_\alpha = \frac{D_\omega^2}{|G|} \sum_{s \in k} \chi_\alpha(s) \text{Tr} \left(\tilde{\rho}_L \bigoplus_a \mu_a(s) \right) \text{Tr} \left(\tilde{\rho}_L \bigoplus_{a'} \overline{\mu_{a'}(s)} \right). \quad (3.4.10)$$

Crucially, at this point, p_α depends only on the value that χ_α takes in $k \subset G$. This will lead to degeneracy in the different p_α , giving our lower bound of E_{inacc} . To derive a simplified expression for p_α , we insert $\tilde{\rho}_L \oplus_a \mu_a(g) = \oplus_a \mu_a(g) \tilde{\rho}_{L,a}$, and $D_\omega = \sqrt{|G|/|k|}$ to arrive at

$$p_\alpha = \frac{1}{|k|} \sum_{s \in k} \chi_\alpha(s) \sum_a \mu_a(s) \text{Tr}(\tilde{\rho}_{L,a}) \sum_{a'} \overline{\mu_{a'}(s)} \text{Tr}(\tilde{\rho}_{L,a'}). \quad (3.4.11)$$

We now use that the $\mu_a(g)$ are linear characters of G , *i.e.* there is a function $u(a)$ such that $\mu_a(g) = \chi_{u(a)}(g) \forall g \in G$. Then, we can write $\chi_\alpha(s) \mu_a(s) \overline{\mu_{a'}(s)} = \chi_\alpha(s) \chi_{u(a)}(s) \overline{\chi_{u(a')}(s)}$. Combining the first two characters as $\chi_\alpha(g) \chi_{u(a)}(g) = \chi_{\alpha \cdot u(a)}(g)$, we can now use the row character orthogonality relation $\sum_{g \in G} \chi_\alpha(g) \chi_\beta(g) = |G| \delta_{\alpha\beta}$ to simplify the sum $\sum_{s \in k} \chi_{\alpha \cdot u(a)}(g) \overline{\mu_{a'}(s)} = |k| \delta_{\alpha \cdot u(a), u(a')}$ [170]. This leaves us with the final expression:

$$p_\alpha = \sum_a \text{Tr}(\tilde{\rho}_{L,a}) \text{Tr}(\tilde{\rho}_{L, u^{-1}(\alpha \cdot u(a))}). \quad (3.4.12)$$

We hereby arrive at the final expression above in Eq. (3.4.12). To calculate the lower bound on inaccessible entanglement we use the fact that the probabilities p_α depend only on the values that χ_α takes in k , which means that each value of p_α occurs $\frac{|G|}{|k|}$ times. When p_α have such a degeneracy, the configuration with lowest possible entropy is that for which $\frac{|G|}{|k|}$ of the p_α are equal to $\frac{|k|}{|G|}$, and the rest are 0. This leads to the lower bound on $E_{inacc} = \log\left(\frac{|G|}{|k|}\right)$ for non-MNC phases. Combining this with the upper bound given by the size of the symmetry group, leads to the main result presented in Eq. (3.4.7).

3.4.3 Comparison with string order parameter

We show here that the string order parameter for 1D SPT phases [157] can be related to the inaccessible entanglement E_{inacc} . The probabilities p_α for each symmetry sector α are the Fourier transform of the string order parameter with identities as the end operators,

$$p_\alpha = \frac{1}{|G|} \sum_g \chi_\alpha(g) s(g, \mathbb{1}, \mathbb{1}), \quad (3.4.13)$$

where the string order is defined

$$s(g, O^A, O^B) = \text{Tr}(\rho_L O^A V(g)) \text{Tr}(\rho_L O^B V(g)^\dagger), \quad (3.4.14)$$

and O^A, O^B are in a set of carefully chosen operators specific to the symmetry and projective representation which allow a particular selection rule to be detected. The rule changes at the phase transition point and allows unique determination of the phase, even distinguishing different MNC phases [92, 157].

This has allowed us to give an operational interpretation to string order as well as more concretely linking E_{inacc} to phase detection. The expression in Eq. (3.4.13)

clarifies why inaccessible entanglement is not directly an order parameter; the missing end operators in inaccessible entanglement mean that the full information of the phase cannot be captured due to the lack of additional structure afforded, which the string order still possesses.

3.5 Investigation of the bounds

In this Section we explore the bounds on the inaccessible entanglement in SPT states, and present numerical results to consolidate our findings. We consider the following main questions. Firstly, can states be constructed to explore the whole bound? Secondly, where do states typically live in the bound? We consider how to explicitly construct states both on the lower and upper bound, and probe the SPT phase and entanglement properties of the state. Lastly, we examine the effect of varying bond and physical dimension on the inaccessible entanglement.

We first introduce some conventions we will use in this Section. When performing interpolations between states of interest, we will filter certain components of the state $|\Psi[A(\lambda)]\rangle$, i.e. we choose $A(\lambda)$ in the form

$$A(\lambda) = \sum_{j \in I} A^j |j\rangle + \lambda \cdot \sum_{j \notin I} A^j |j\rangle, \quad (3.5.1)$$

for some set of indices I . Here and in the rest of this Section, the basis set $\{|j\rangle\}$ is that which diagonalises $u(g)$, such that $u(g)|j\rangle = \chi_j(g)|j\rangle$. The path defined by tuning parameter $\lambda \in [0, 1]$ for the state $|\Psi[A(\lambda)]\rangle$ is a particular adiabatic evolution where each MPS is the ground state of some Hamiltonian $H(\lambda)$. By interpolating λ acting on a particular symmetry sector we can filter out the state's support on that sector, and effectively eliminate that symmetry action, which enables us to manipulate the symmetry of the state in a smooth, controlled manner.

Throughout this numerical investigation we mainly employ an MPS construction which generates random states in a particular SPT phase by inputting $u(g)$ and $V(g)$ and symmetrising a random MPS tensor. This allows us to construct generic families of states in a chosen SPT phase and to study their properties. We first generate the random, injective tensor M sampled from a Gaussian distribution of mean 0 and variance 1 over the complex numbers. We then sum over M^i with elements of the symmetry as follows,

$$A^i = \sum_g \sum_j u(g)_{ij} (V(g)M^jV(g)^\dagger). \quad (3.5.2)$$

The MPS tensor defined above naturally satisfies the symmetries in Eq. (2.3.2) imposed by the fundamental theorem. The two crucial ingredients of the construction are the physical representation of the symmetry $u(g)$, written as a direct sum over its linear irreps $\chi_\alpha(g)$ with multiplicity m_α , and the projective representation $V(g)$, built from projective irreps $V_a(g)$ with multiplicity n_a . The dimension of $V(g)$ is the bond dimension $D = \sum_a n_a \dim(V_a(g))$ while the dimension of $u(g)$ is the physical dimension $d = \sum_\alpha m_\alpha$. Note that all figures presented will display a sample of 10^6 states.

3.5.1 Tight bound for the inaccessible entanglement

We demonstrate that there exists no tighter bound for E_{inacc} in the trivial phase by interpolating from an example in an SPT-trivial phase to a product state, which adiabatically connects the upper and lower bound, as shown in Fig. 3.2. We will use a toy MPS construction as our example for an SPT-trivial maximally entangled state with zero accessible entanglement. With this construction, we can interpolate to a product state and hence demonstrate the tightness of the bound. The MPS tensor is given by

$$A_{ij}^{(ij)} = |i\rangle \langle j|, \quad (3.5.3)$$

where the indices i and j run from 1 to D , and the physical index (ij) runs from 1 to $d = D^2$. This state is a product of maximally entangled pairs. The MPS generated by this tensor satisfies the symmetry condition of Eq. (2.3.2) with $u(g) = V(g) \otimes \overline{V(g)}$ and therefore $V(g)$ can be any invertible matrix satisfying the group relations of G . For convenience we will use $V(g) = \bigoplus_{\alpha=0}^D \chi_{\alpha}(g)$ to study the trivial SPT phase. Then, by the Clebsch-Gordan series the linear representation is written $u(g) = \bigoplus_{\alpha=0}^D (\mathbb{1}_D \otimes \chi_{\alpha}(g))$.

We consider $\mathbb{Z}_2 \times \mathbb{Z}_2$ symmetry by using the MPS tensor introduced in Eq. (3.5.3) with bond dimension $D = 4$ and physical dimension $d = 16$. The path we choose is the interpolation $|\Psi[A(\lambda)]\rangle$ as defined in Eq. (3.5.1) with $I = \{0\}$ to filter all but the trivial irrep which connects the highly entangled state $|\Psi[A(\lambda = 1)]\rangle$ to the product state $|\Psi[A(\lambda = 0)]\rangle$ in the trivial irrep, while respecting the symmetry. This interpolation smoothly connects $E_{inacc} = 2$ to $E_{inacc} = 0$ tuning through an irrep probability distribution $p_{\alpha} = \{\frac{1}{4}, \frac{1}{4}, \frac{1}{4}, \frac{1}{4}\}$ to $p_{\alpha} = \{1, 0, 0, 0\}$. The example state we give is but one of many possible examples which could have produced this. As we will later show, indeed states typically saturate the upper bound, while having (close to) zero inaccessible entanglement or residing in the middle region is rare.

3.5.2 Typical behaviour in the MNC and trivial phase

In this Section we discuss the inaccessible entanglement of states in the trivial and non-trivial (MNC) SPT phase of $\mathbb{Z}_2 \times \mathbb{Z}_2$. We begin by discussing the cluster state as a canonical example of a state in an MNC phase (the cluster phase). We comment on the allowed irrep probabilities in trivial and non-trivial SPT phases in this simple case; trivial order has no restrictions, whereas the MNC phase is fixed.

We first more exhaustively discuss the inaccessible entanglement of the cluster state, which we have calculated in §3.4.1. The cluster state has $p_{\alpha} = 1/4 \forall \alpha$, so $E_{inacc} = 2$ which is the upper bound on inaccessible entanglement for this symmetry group. The cluster state is the unique ground state of the stabiliser Hamiltonian $H_C = -\sum_n \sigma_n^z \sigma_{n+1}^x \sigma_{n+2}^z$ for sites n , and it can be prepared by a finite depth circuit of $CZ = \text{diag}(1, 1, 1, -1)$ gates between neighbouring pairs of sites each initialised in the state $|+\rangle^{\otimes N}$; hence it is short-range entangled [164, 238, 239]. An MPS description of the cluster state can be given by the Pauli matrices σ^i , $i = 1, x, y, z$ which has bond dimension $D = 2$ and physical dimension $d = 4$,

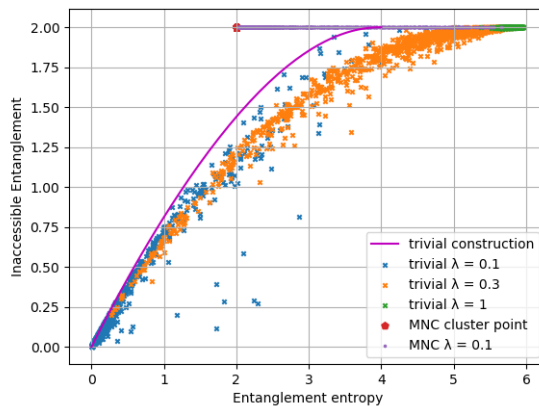


Figure 3.2: Inaccessible entanglement of states $|\Psi[A(\lambda)]\rangle$ for a filter λ . This is implemented in two ways: firstly, for families of random states and a certain λ (scattered dots) defined by the MPS tensor in Eq. (3.5.2), and secondly an interpolation in λ on a particular trivial MPS construction defined in Eq. (3.5.3) (solid magenta line). The tensors are constructed with $\mathbb{Z}_2 \times \mathbb{Z}_2$ symmetry and the interpolation on any MPS tensor $A(\lambda)$ as defined in Eq. (3.5.1), where $I = \{0\}$ is the trivial irrep. For reference, the cluster state is also displayed (red dot).

so the linear representation has multiplicity $m_\alpha = 1$ for each irrep such that $u(g) = \bigoplus_\alpha \chi_\alpha(g)$. Note that we use the notation σ^i for MPS constructions and $\sigma(g)$ for representations, where both refer to the set of Pauli matrices. The Schmidt values of the state are $(\frac{1}{2}, \frac{1}{2})$, so $E(\rho) = 2S(\rho_A) = 2$. Therefore the accessible entanglement is zero; all the entanglement is inaccessible. Note that the factor of two comes from periodic boundary conditions; partitioning the system cuts through two bonds.

Let us now consider the rest of the cluster phase. The inaccessible entanglement persists throughout the cluster phase, as demonstrated in Fig. 3.2 by studying random states with a non-trivial multiplicity in the physical representation. In this figure we use the MPS tensor A from Eq. (3.5.2), where SPT-trivial states are constructed with $n_a = 4$, $m_\alpha = 2 \forall a, \alpha$ (bond dimension $D = 8$ and physical dimension $d = 16$), while the MNC phase is constructed with $n_a = 4$, $m_\alpha = 2 \forall a, \alpha$ ($D = 4$ and $d = 16$). We can view E_{inacc} as an invariant in a particular sense since it takes the same value throughout this phase, being independent of the correlations within the junk subspace and only dependent on the part of the state in which symmetries act non-trivially. States in the cluster phase with larger bond dimension can allow more entanglement due to a non-trivial junk subspace, which allows non-zero accessible entanglement. These results provide a new angle on the cluster phase.

Let us compare the trivial phase to the MNC phase. Fig. 3.2 demonstrates that trivial SPT order displays less restricted combinations of (E_{inacc}, E) compared to the MNC phase; this originates from a lack of enforced structure in irrep

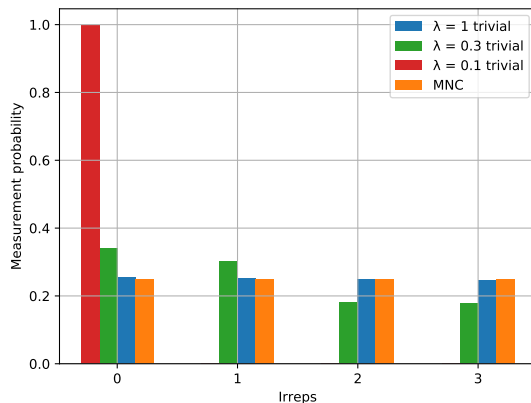


Figure 3.3: Irrep measurement probability distributions for a selection of four random states from the families displayed in Fig. 3.2, three with trivial SPT order with a filtering λ , where $\lambda \rightarrow 0$ denotes tuning the state towards a product state, and one with MNC order. The MNC phase strictly contains states with a degenerate irrep distribution, whereas trivial states can have entirely different irrep probabilities. The interpolation is from an almost degenerate irrep distribution, which mimics the MNC phase, to an irrep distribution weighted only on the trivial irrep, corresponding to zero inaccessible entanglement; notice that between the $\lambda = 1$ state and the MNC phase the probabilities are not quite equal due to the different SPT order.

probabilities, while the MNC phase has a fixed, degenerate probability distribution. Despite this key difference, a random state in the SPT trivial phase typically has similar (E_{inacc}, E) -values compared to the MNC phase value, as they are generally close to the upper bound. The closer we tune random states in either phase towards the product state, the lower the entanglement gets on average, but while for the trivial phase the inaccessible entanglement also decreases on average, the MNC phase has a fixed inaccessible entanglement. Since the entanglement entropy can't decrease below the fixed E_{inacc} in the MNC phase, the path tuning an MNC phase to a product state would see a phase transition.

We now explore the irrep probability distributions, which can reveal crucial information about the composition of the inaccessible entanglement, as displayed in Fig. 3.3. While the MNC phase can only be realised by a degenerate probability distribution, the trivial phase is unconstrained. Although typically random trivial states have near maximal inaccessible entanglement, one can distinguish it from an MNC ordered state given enough precision on the irrep probabilities. Additionally, we emphasise that while the MNC phases of a system with a symmetry G have a fixed value for the inaccessible entanglement, this is not enough to distinguish two MNC phases from the same group G . While two such phases are mathematically inequivalent, some of their physical properties, such as the topologically protected edge mode degeneracy and entanglement spectrum, are unchanged.

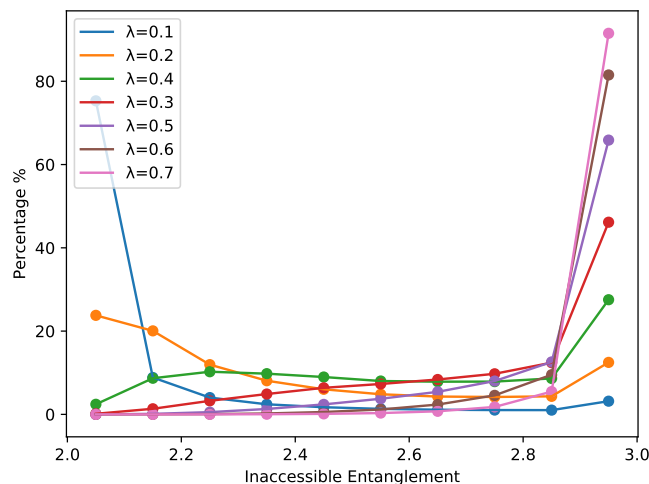


Figure 3.4: Histogram of the inaccessible entanglement for the non-MNC phase of $\mathbb{Z}_4 \times \mathbb{Z}_2$ in families of the random MPS tensor A with a filter λ which drives states towards an effective $\mathbb{Z}_2 \times \mathbb{Z}_2$ symmetry as $\lambda \rightarrow 0$. Moving through each λ value illustrates how states are gradually forced from the upper bound onto the lower bound, which corresponds to the upper bound of the trivial phase with $\mathbb{Z}_2 \times \mathbb{Z}_2$ symmetry.

3.5.3 Exploring a non-MNC phase

How does the inaccessible entanglement behave for non-MNC phases? In this part of our Investigation, we explore the properties of non-MNC phases, which have interesting characteristics compared to MNC or trivial phases, since states with this SPT order live in a finite region of the bound which is fully restricted, having a non-zero, symmetry dependent lower and upper bound, which are not equal to each other. We study the simplest symmetry hosting a non-MNC phase $G = \mathbb{Z}_4 \times \mathbb{Z}_2$, which has $H^2(G, U(1)) = \mathbb{Z}_2$.

The first point of interest is the possibility to drive states towards the lower bound by reducing the symmetry of the state to effective sub-symmetries. Secondly, we observe very little difference in the inaccessible entanglement between the trivial and non-trivial phase for random states; they both reside near the upper bound. As before, the trivial and non-trivial phases are still discriminated by the structure of irrep measurement probabilities. Finally, we make an analysis on the effect of bond dimension on the patterns of inaccessible entanglement in random states, and show that increasing D increases the variance and mean of the inaccessible entanglement. We will clarify that this is due to a significant dependence on the structure of the junk subspace.

Reduced effective symmetries

While in §3.5.2 we showed that states in the trivial phase can be driven to the lower bound ($E_{inacc} = 0$ for trivial states) simply by interpolating towards a product state, we now show that considering a larger sub-symmetry allows additional interesting behaviour. Indeed, both the trivial and the non-MNC phase can be driven towards $E_{inacc} = 2$ by effectively enforcing a $\mathbb{Z}_2 \times \mathbb{Z}_2$ symmetry through suppression of particular A^i in the MPS tensor A as introduced in Eq. (3.5.3), with $u(g) = \bigoplus_{\alpha} \chi_{\alpha}(g)$ where $m_{\alpha} = 1 \forall \alpha$, and with $V(g)$ constructed with $n_a = 2$ for $a \in \{0, 1\}$ since there are two projective irreps. We refer to $E_{inacc} = 2$ as the lower bound, although it is only the lower bound for the non-trivial phase.

The non-MNC phase is depicted in Fig. 3.4. As $\lambda \rightarrow 1$, random states typically live near the upper bound $E_{inacc} = 3$ in either phase, while as $\lambda \rightarrow 0$ states get trapped nearer the lower bound. The latter happens at comparatively low values of λ , illustrating further that typical states tend to have high inaccessible entanglement. As an aside, we do not include the value $\lambda = 0$ for which the symmetry is actually enforced, in order to be consistent with assumptions made in the derivation of the bounds, since these states will not be injective.

Let us describe how we determine which irreps are filtered. We denote elements g of $\mathbb{Z}_4 \times \mathbb{Z}_2$ by $g = (x, y)$ where $x = 0, 1, 2, 3$ and $y = 0, 1$. Then, the irreps can be labelled by a pair $\alpha = 0, 1, 2, 3$ and $\beta = 0, 1$ such that

$$\chi_{\alpha,\beta}(x, y) = (i)^{\alpha x} (-1)^{\beta y}. \quad (3.5.4)$$

The irreps we filter are those for which $\alpha = 1$ or 3 , such that the unfiltered irreps are only faithful to a $\mathbb{Z}_2 \times \mathbb{Z}_2$ subgroup generated by $(x, y) = (2, 0)$ and $(0, 1)$. Therefore in the limit $\lambda \rightarrow 0$ the MPS effectively only has a $\mathbb{Z}_2 \times \mathbb{Z}_2$ symmetry.

Comparing trivial to non-trivial phase

We discuss how the inaccessible entanglement is characterised in the non-MNC and trivial phase of $\mathbb{Z}_4 \times \mathbb{Z}_2$, as illustrated by the following numerical results. We show that SPT trivial states generally have high inaccessible entanglement, which makes them hard to distinguish from the non-trivial states, but the lack of degeneracy in the irrep probabilities (present in the non-trivial phase) reveals their triviality. The SPT-trivial states are constructed with $n_a = 1$, $m_{\alpha} = 2 \forall a, \alpha$ (bond dimension $D = 8$ and physical dimension $d = 16$), while the non-MNC phase is constructed with $n_a = 2$, $m_{\alpha} = 1 \forall a, \alpha$ ($D = 8$ and $d = 8$).

Studying Fig. 3.5, there are some main remarks. From Eq. (3.4.7), the non-trivial SPT phase is bounded by $2 \leq E_{inacc} \leq 3$ whereas the trivial SPT can get arbitrarily close to zero inaccessible entanglement. Since states in the trivial phase can reach values below $E_{inacc} = 2$, decreasing λ drives states towards approaching this value from below, rather than from above. States with non-MNC order meanwhile become increasingly clustered above the bound, as they can't pass below it, as we saw earlier displayed in Fig. 3.4.

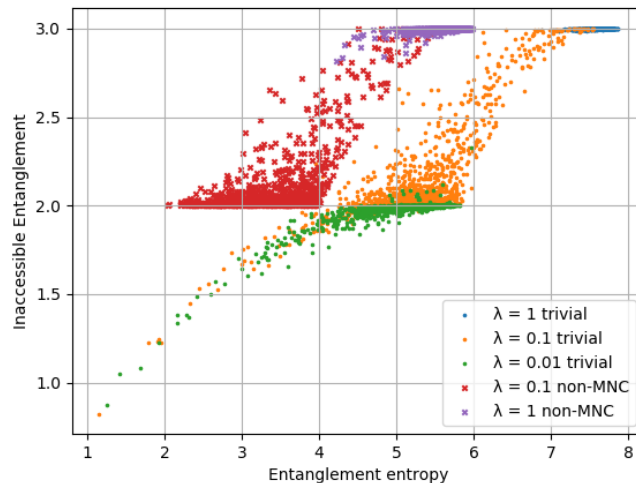


Figure 3.5: Inaccessible entanglement versus entanglement of states in the SPT phases of $G = \mathbb{Z}_4 \times \mathbb{Z}_2$. We study random states $|\Psi[A(\lambda)]\rangle$ generated with the construction in Eq. (3.5.2) with a particular filtering λ effecting the sub-symmetry $\mathbb{Z}_2 \times \mathbb{Z}_2$ as in Fig. 3.4, acting on three trivial and two non-MNC families of states. The non-MNC phase is restricted to within the bound $2 \leq E_{inacc} \leq 3$ whereas the trivial phase is lower bounded by zero.

We demonstrate that one can actually infer SPT triviality or non-triviality from the irrep probability distributions, displayed in Fig. 3.6. Notice that non-MNC phase irrep probabilities are four-fold degenerate; this is due to only two inequivalent irreps which contribute to the calculation for the measurement probabilities p_α . By contrast each irrep probability can be different in the trivial phase.

Let us consider the physical insights offered by three example parameters. In each, the difference between trivial and non-trivial phase is apparent. Firstly, recall from §3.5.3 that all states with $\lambda = 1$ have a near maximal inaccessible entanglement. The closer to saturating this value a state is, the closer to degenerate the irrep probabilities become. Therefore in the non-MNC phase, the probabilities are approximately $p_\alpha = \frac{1}{8}\forall\alpha$. Notably, this still differs from the behaviour in an MNC phase, as the irrep probabilities are still not completely flat, having instead a four-fold degeneracy. The degeneracy in the non-MNC phase becomes more apparent for $\lambda = 0.3$, and even more prominently with $\lambda = 0.01$ which generates the effective sub-symmetry, and echoes the irrep probabilities of the cluster phase, where $p_\alpha = \frac{1}{4}$ for half the irreps α , with the other half being zero. For all three examples, the trivial phase may have eight different irrep probabilities, which are quite similar to the non-trivial probabilities but are very unlikely to be exactly degenerate; although such states may have indistinguishable inaccessible entanglement on average compared to the non-trivial phase, it is remarkable that due to a trivial projective representation characterising the state, they lose crucial symmetry structure in the irrep probabilities.

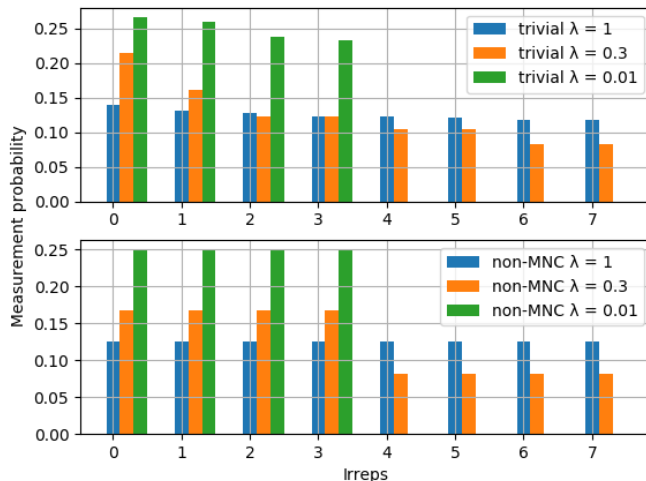


Figure 3.6: Irrep measurement probabilities of a selection of random states picked from distributions as in Fig. 3.5 with filtering λ where $\lambda \rightarrow 0$ drives states towards an effective $\mathbb{Z}_2 \times \mathbb{Z}_2$ symmetry, comparing the trivial phase to the non-MNC phase of $\mathbb{Z}_4 \times \mathbb{Z}_2$. The non-MNC phase irrep probabilities are four-fold degenerate for any filtering, whereas the trivial phase gives different probabilities to each irrep in general. However, for both phases, as $\lambda \rightarrow 0$ the irrep probabilities increasingly resemble the degeneracy of the MNC phase of $\mathbb{Z}_2 \times \mathbb{Z}_2$.

Accessible entanglement in the junk subspace

We examine how inaccessible entanglement depends on the bond dimension. Clearly increasing bond dimension shifts states to a larger entanglement entropy by virtue of the tensor network construction, but it also leads to a higher average inaccessible entanglement. We consider the non-trivial SPT phase of $\mathbb{Z}_4 \times \mathbb{Z}_2$, which has two projective irreps. We argue that an imbalance in the multiplicities of the two irreps leads to larger proportions of states near the upper bound of inaccessible entanglement compared to equal multiplicities. The numerics for this study are displayed in Fig. 3.7, where we construct states as in Eq. (3.5.2) with a constant $u(g) = \bigoplus_{\alpha} \chi_{\alpha}(g)$ where $m_{\alpha} = 1 \forall \alpha$ but where we vary the multiplicities of $V(g)$ and hence the junk subspace.

Let us first explain the significance of the junk subspace, introduced in Eq. (2.4.9), by considering the simple case of the MNC phase. The cluster state is represented by the MPS tensor $A^i = \sigma^i$ which has a trivial junk subspace. In the MNC phase, the accessible entanglement is determined only by the junk subspace of the MPS tensors; a trivial junk subspace has $E_{acc} = 0$, and non-trivial subspace allows non-zero accessible entanglement. A large junk subspace, effected by higher bond dimension, has the potential to host more entanglement since the upper bound on entanglement entropy is given by the Schmidt rank which is $\log(D)$; in other words, there are more free parameters and hence more correlations are possible. By increasing the junk subspace and exploring the cluster phase $A^i = B^i \otimes \sigma^i$

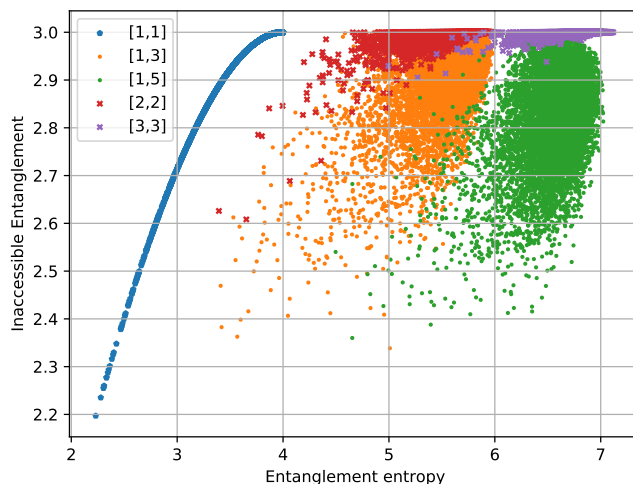


Figure 3.7: Effects of different irrep distributions of $V(g)$ for random states constructed as in Eq. (3.5.2) in the non-MNC phase of $\mathbb{Z}_4 \times \mathbb{Z}_2$, with a constant $u(g) = \bigoplus_{\alpha} \chi_{\alpha}(g)$ where $m_{\alpha} = 1 \forall \alpha$. The labels $[n_0, n_1]$ are the multiplicities of the two irreducible projective representations in $V(g)$. The first example (blue dots) has a trivial junk subspace and is therefore limited to a line. States with uneven multiplicities on the irreps have less possible inaccessible entanglement compared to the same bond dimension which has equal multiplicities. Larger bond dimension allows more entanglement but the inaccessible entanglement remains capped at $E_{inacc} = 3$, as this upper bound depends only on G .

for some non-trivial B^i , the inaccessible entanglement remains the same, since it depends only on the part of the state which transforms non-trivially under the symmetry, yet the entanglement and accessible entanglement can grow. We now extend this argument to a more general case.

In non-MNC phases, as opposed to MNC phases, the inaccessible entanglement is not fixed, so there is greater freedom in how the total entanglement is divided into accessible and inaccessible parts. However, the importance of the junk subspace for the accessible entanglement is still clear. As the total size of the junk subspaces in each block increases, so does the possible values of the inaccessible entanglement for a given total entanglement. Indeed, the family $n = [1, 1]$ has no junk subspace, and we see that the inaccessible entanglement is uniquely determined by the total entanglement. Comparing the two families $n = [1, 5]$ and $n = [3, 3]$ reveals the same effect. Even though total bond dimension is the same, the structure of the junk subspaces is different, with the number of free parameters in the junk subspace being $1 + 5 \times 5 = 26$ compared to $2 \times 3 \times 3 = 18$ respectively. In the former case, the larger number of parameters means more possible values of accessible entanglement, leading to the more spread-out distribution in Fig. 3.7. This highlights the power of the inaccessible entanglement to also capture properties due to symmetry structure on the virtual level.

3.6 Outlook

3.6.1 Restricting symmetry to a subgroup

Up until this point, we have fixed a symmetry group G and considered the inaccessible entanglement under G -LOCC for different G -symmetric states. Now, we consider the inverted scenario, in which we fix a particular state and consider G -LOCC for different symmetries G . Intuitively, reducing the number of enforced symmetries should reduce E_{inacc} . To see this explicitly, let us take a state in an MNC phase of G and determine E_{inacc} under H -LOCC where H is a subgroup of G . Following the calculation in §3.4.1, we find that $p_\alpha = \frac{1}{|H|}$ for all α , where α now runs over the $|H|$ irreps of H . Therefore, Eq. (5.6.8) gives $E_{inacc} = \log(|H|)$. As expected, we find that E_{inacc} decreases as smaller symmetry groups are enforced, corresponding to more of the entanglement in our fixed state becoming accessible as our LOCC becomes less restricted.

Restricting symmetries to a subgroup also effects the SPT order of a state; a state with SPT order under G symmetry may be trivial under H symmetry for $H \subset G$. Yet, as demonstrated above, if we begin with a state in an MNC phase, the inaccessible entanglement under H -LOCC will always take the maximum value. For example, consider a state in an MNC phase of $G = \mathbb{Z}_4 \times \mathbb{Z}_4$. If we restrict to the subgroup $H = \mathbb{Z}_2 \times \mathbb{Z}_2$, the SPT order becomes trivial, but we nonetheless have $E_{inacc} = \log(|H|) = 2$. This provides an example of a state in a trivial SPT phase which, due to the “hidden” presence of SPT order under a larger symmetry group, maximises E_{inacc} in the way that would normally be expected from a state in the MNC phase. The maximal inaccessible entanglement therefore captures the underlying MNC behaviour, even though the actual SPT order is destroyed by operations which do not protect the symmetry.

3.6.2 Subsystem SPT order

Our results immediately apply to certain 2D subsystem SPT (SSPT) phases [233, 234]. SSPT order generalises the concept of SPT order to include subsystem symmetries, which act on rigid subsystems such as lines or fractals. As an example, the 2D cluster state [164] has subsystem symmetries corresponding to flipping every spin along a line [26, 233, 240]. These systems can often be analysed with dimensional reduction which translates the subsystem symmetry group in 2D to an extensive global on-site symmetry group of an effective 1D system [26, 234, 241, 242]. Because of this, we can immediately apply our results to these phases as well.

For example, if we place the 2D cluster state on a cylinder of circumference N such that the line symmetries wrap diagonally along the cylinder periodically, we can consider each block of $N \times N$ spins as a single site, such that we get an effective 1D chain with symmetry group $G = (\mathbb{Z}_2 \times \mathbb{Z}_2)^N$ [26]. For each N , this 1D system is in an MNC phase with respect to G , so our general results can be applied to show that the inaccessible entanglement will be equal to N . For the 2D cluster state, this is all of the entanglement, which shows that there is no accessible

entanglement in the state if the subsystem symmetries are enforced. The above analysis, which extends to the general family of fractal subsystem SPT phases defined in Refs. [234, 242], shows that E_{inacc} for these subsystem SPT phases satisfies an area law in 2D.

3.6.3 Relation to computational power

The study of SPT order shares a remarkably symbiotic relationship with quantum computation via the paradigm of measurement-based quantum computation (MBQC) [164]. In MBQC, quantum computation is performed using single-site projective measurements on an entangled many-body state. A state is called a universal resource for MBQC if these measurements allow the circuit model of quantum computation to be efficiently simulated, with the cluster state being a canonical example. Characterizing universal resource states is a fundamental open problem in MBQC. Remarkably, there is a deep connection between the MBQC universality of a state and its SPT order: Many SPT phases in 1D and 2D are computational phases of matter, meaning that every state within the phase is a universal resource [26, 163, 173–175, 234, 241, 242]. A question which arises naturally due to their separate connections to SPT order is the following: can inaccessible entanglement predict whether a state is computationally universal for MBQC?

One intriguing connection comes from the importance of MNC phases in each setting: these are the phases which are universal for MBQC in 1D [163, 173, 174], and they are also the phases in which E_{inacc} is maximised in the entire phase. This connection extends to the 2D SSPT phases discussed in the previous Section [26, 234, 241, 242]. This suggests that a maximised value of E_{inacc} may imply that a state is universal. However if we more closely analyze the MBQC scheme in Ref. [163], which utilises 1D MNC SPT phases, we see that the connection might not always be certain. In each phase, there are certain measure-zero subsets of states which are not universal, even though E_{inacc} remains maximised within these subsets. Of course, this does not preclude the existence of a different MBQC scheme for which these subsets are universal. Indeed, a similar scheme from Ref. [175] comes with a different set of non-universal states which covers some of the holes left by the scheme of Ref. [163].

When we consider non-MNC phases, the connection becomes less clear still. In Ref. [243], a scheme of MBQC is introduced which utilises non-MNC phases. Crucially, unlike the MNC case, universality is not guaranteed in non-MNC phases, and is determined principally by the on-site symmetry representation $u(g)$. To check whether the universal states within a phase can be distinguished from the non-universal ones, we took random states from each case and computed their E_{inacc} . However, we found that there was no clear differentiating behaviour of E_{inacc} between the two cases. This suggests that E_{inacc} does not relate strongly to computational power beyond the MNC case.

3.7 Discussion & Conclusions

We demonstrated that investigating the properties of G -LOCC is deeply connected to questions about phases of matter. We defined the accessible entanglement $E_{acc} = \sum_{\alpha} p_{\alpha} E_{\alpha}$ in this setting operationally, and thereby showed that the inaccessible entanglement corresponds to the number of Bell pairs inextricable under symmetry-restricted local operations. The main result of this work is that, given a 1D system with a global onsite (finite Abelian) symmetry, there is a tight bound on the inaccessible entanglement $\log\left(\frac{|G|}{|k|}\right) \leq E_{inacc} \leq \log(|G|)$, which depends on the symmetry group and SPT phase (via k) in question. This shows that there is always some entanglement present in non-trivial SPT phases which cannot be extracted via symmetry-respecting operations. In the maximally non-commutative SPT phases, which play an important role in measurement-based quantum computation [163, 174], we have $|k| = 1$, such that every state in these phases has $E_{inacc} = \log(|G|)$. In particular, the 1D and 2D cluster states, which are highly entangled by certain measures [238, 244], have zero accessible entanglement under G -LOCC for suitable G .

We studied these bounds numerically by constructing random states in different SPT phases and calculating E_{inacc} . We find that the whole bound can be explored, although typical states tend to have near maximal E_{inacc} , even in the trivial phase. We characterised those states near the lower bound as those which have low weight in certain symmetry sectors, and therefore have an effective subgroup symmetry. Although it is difficult to distinguish trivial from non-trivial SPT phases by E_{inacc} alone, we show that they can be distinguished by their irrep probabilities, which exhibit an exact degeneracy in non-trivial phases. We demonstrate that the inaccessible entanglement is the entropy of the irrep probability distribution corresponding to the Fourier transform of the string order parameter, which allows E_{inacc} to harness some of the properties of the order parameter, and the irrep probabilities themselves are a good contender to access this information. Recent studies have accessed the entanglement spectrum of the cluster state on a noisy, intermediate-scale quantum (NISQ) computer [217, 245], and we believe a similar study could be done with our method which might prove more able to identify topological phases beyond the cluster state and illuminate their computational power.

We also affirmed the question: can “latent” inaccessible entanglement appear due to the presence of a larger symmetry, which the description misses out on? We show that an MNC phase protected by some symmetry G can become SPT-trivial by partially violating the symmetry through restricting operations to a symmetry $H \subset G$. This “hidden” order is detected by the inaccessible entanglement, since E_{inacc} still contains the information of the SPT phase under the original symmetry that is not detected by the entanglement alone.

Throughout this work, we have focused on 1D SPT phases, as well as 2D subsystem SPT phases via dimensional reduction. For 2D SPT phases with global symmetries, the classification is given by the third cohomology group $H^3(G, U(1))$, and it is not clear what bounds may exist for the inaccessible entanglement.

Therefore a natural future direction for investigation is to extend E_{inacc} to PEPS. In the outlook we also discussed how our work immediately applies to subsystem-symmetry protected SPTO, and the relation to MBQC.

An intriguing question is whether the inaccessible entanglement acts as a resource for a task in quantum information processing, in analogy to the superselection induced variance (SIV) which can be viewed as a resource for quantum data hiding, introduced in Ref. [215]. It was found that states obeying particle number conservation can be distilled into a part containing pure SIV and a disjoint part containing pure entanglement, which we can now confirm is the accessible entanglement. The presence of SIV is a necessary condition for perfect data hiding, a protocol where classical data is hidden in such a way that it cannot be recovered by LOCC without quantum communication [216, 246]. One can ask whether these non-local quantities can be formalised into the framework of a resource theory. It is also natural to ask about the connection between the inaccessible entanglement and SIV, by extending the definition of SIV to arbitrary symmetries.

Chapter 4

Symmetry protected topological phases in open systems

This Chapter contains the first part of the publication

- Symmetry Protected Topological Order in Open Systems **Caroline de Groot**, Alex Turzillo, and Norbert Schuch. arXiv:2112.04483v2 [73]

4.1 Motivation

The realization that the interplay of symmetries and entanglement can give rise to novel physics beyond the Landau paradigm has led to an expanding zoo of topologically-ordered phases of matter. A particularly prominent role among those phases, in particular in one dimension (1D), is played by symmetry protected topological (SPT) phases, which have their root in Haldane’s original work elucidating the gapped nature of the spin-1 Heisenberg chain and its topological origin, nowadays known as the Haldane phase [247–249].

SPT phases consist of systems with a unique ground state and a gap, yet which are distinct from the trivial (mean-field) gapped phase, as witnessed by a number of characteristic fingerprints: most prominently, string order [157, 177, 250], specific degeneracies in the entanglement spectrum [157], and fractionalized edge excitations [249]. A key step toward the comprehensive understanding of SPT phases was made by using Matrix Product State (MPS) representations [77, 237] of their ground states. This step was based on the fact that MPS faithfully approximate ground states of gapped systems [132, 251, 252] and that they allow one to realize global symmetries locally on tensors that carry physical and entanglement degrees of freedom [77, 150]. Namely, it was understood that in non-trivial SPT phases, the physical symmetry that protects the phase acts on entanglement as a projective, rather than linear, representation. This insight was key in several ways. First, it provided a unified explanation for the aforementioned fingerprints of SPT phases in terms of this projective action. Second, it allowed one to obtain a comprehensive classification of SPT phases, based on the classification of projective representations

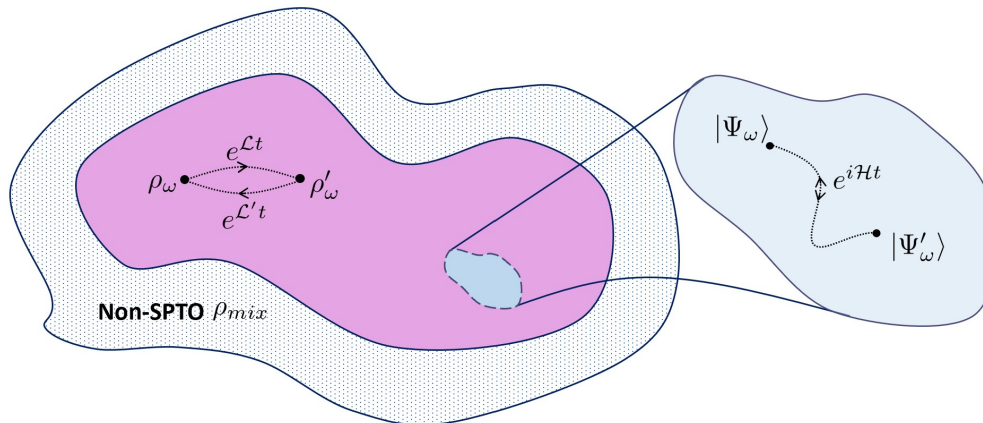


Figure 4.1: Equivalence relations which preserve gapped phases of coherent SPT mixtures, as extending from gapped phases with pure state SPTO, based on the formalism in Ref. [4], given in Definition 4.

by group cohomology. And finally, it connected the characterization of SPT phases based on fingerprints like string order and edge modes to the characterization based on the equivalence relation by which two systems are in the same phase if they can be connected by a path of gapped, symmetric Hamiltonians [102, 128, 162]. Altogether, the representation of SPT states by MPS clarified and unified the various definitions for SPT order (SPTO) for the ground states of gapped Hamiltonian systems and allowed for their complete classification [77, 253].

The situation becomes much less clear when moving from pure ground states to mixed states, which are the states we expect to appear in realistic physical systems. Several questions arise. *First*, which states should we consider? Depending on the scenario, relevant states might be thermal states of Hamiltonians [61, 109, 117], equilibrium states of dissipative evolutions (steady states of Lindbladians) [66, 68, 254–256], or states – for instance, originally pure states with SPT order – which have been subjected to noise, which could be either Markovian or discrete-time non-Markovian noise. *Second*, what is the correct generalization of the symmetry condition? For Lindbladian noise, at least two different symmetry conditions have been considered [8, 257–259]; they differ in how the symmetry is imposed on the joint system-bath interaction, and for discrete noise, even further symmetry conditions are conceivable. *Third*, which notion should one use for SPTO? The various fingerprints of SPTO could give divergent results, or might even be ill-defined, on mixed states. String order parameters can be defined for any state, but it is a priori not clear whether the patterns they exhibit are meaningful. For other fingerprints, such as entanglement spectra or edge modes, it is even unclear how to define them for mixed states. *Fourth*, are any of these fingerprints, which are defined on individual systems, compatible with the notion of SPT phase based on equivalence relations, analogous to paths of symmetric gapped Hamiltonians? All in all, in the quest to understand SPTO in the presence of noise, any approach must address these questions.

4.2 Summary

In this Chapter, we systematically investigate the robustness of SPTO under various types of symmetric noise. To this end, we characterize SPTO through string order parameters. These are constructed by placing local order parameters (labeled by irreducible representations) at the endpoints of strings of symmetry operators (labeled by group elements). In gapped phases, any string order parameter either decays exponentially to zero as the separation of the endpoints is increased, or converges to a constant whose value depends on the specific order parameter chosen, and which is generically non-zero. For ground states, the resulting pattern of zeros and non-zeros, as a function of the irrep and group element labels of the string, is a fingerprint of the SPT phase. In many cases, including all abelian symmetry groups, the pattern is in one-to-one correspondence with the SPT phases protected by the symmetry [157]. We say that a mixed state has some SPT order if it exhibits the same pattern of zeros and non-zeros as pure states with the same SPTO; if a symmetric mixed state (such as a mixture of different pure SPT phases) exhibits a pattern which cannot appear in pure symmetric states, it is said to have no SPTO at all (not even trivial SPTO). This definition has several advantages: it coincides with the pure state definition in the limit of pure states, and, being an expectation value of an operator with tensor product structure, it is both simple to compute and to measure.

We study the robustness of SPTO, as witnessed by the string order parameter (2.4.10), for systems subject to evolution by general symmetric and locality-preserving noise. We consider discrete-time evolutions described by quantum channels, as well as continuous noise described by Lindbladians. The Lindbladian evolution forms a special case of quantum channels, where the semigroup structure constrains the possibilities for the action of the symmetry on the channels at finite times. Locality-preservation encompasses both noise obtained from local Lindbladians and locality-preserving evolutions which are not locally generated but which appear, for example, at the boundaries of two-dimensional systems, in driven systems, and via coupling to non-Markovian baths. We introduce two different notions of symmetry of quantum channels – strong symmetry (4.4.8) and weak symmetry (4.4.2). We study several SPT order parameters – string operators, twisted sector charges, edge modes, and irrep probabilities – analytically and numerically. With the use of these unique “fingerprints” which detect the SPT phase, we prove that strong symmetry is necessary and sufficient for a noisy evolution to preserve SPTO, which builds on the formalism for mixed state topological order given in Ref. [4]. The notion of phases extends from SPT phases in closed systems, as depicted in Fig. 4.1.

In particular, we define a class of states called *coherent SPT mixtures* in Section §4.3, for which a relevant fingerprint of SPTO, namely the string order parameter, is well-defined. This is a relevant class of mixed states with SPTO which extend naturally from pure states since SPTO is uniquely characterized through the string order parameter’s *pattern of zeros*. This encodes the cocycle which classifies all 1D SPT phases of finite abelian groups. Moreover, coherent

SPT mixtures are the ground states of gapped, local Hamiltonians, and therefore have an MPS description. These states are particularly nice to study thanks to the ease of TN methods.

In Section §4.4 we introduce the symmetry conditions. We discuss their interpretations in terms of conservation laws, purifications, and couplings between the system and the environment, and finally investigate the form of the symmetry conditions when applied to Lindbladians. Weakly symmetric channels are invariant under the symmetry action, which seems the natural definition of a symmetric channel, and corresponds to symmetric system-bath interactions where the symmetry acts simultaneously on the system and the bath. Strongly symmetric channels, on the other hand, have the property that each Kraus operator individually commutes with the symmetry up to a constant phase factor, and correspond to symmetric system-bath interactions where the symmetry only acts on the system. Specializing these concepts to Lindbladian channels, where the semigroup structure imposes additional restrictions, we recover the notions of strong and weak symmetry studied by Albert and others [8, 257–259].

In Section §4.5 we give the main result that SPTO is robust to channels which are strongly symmetric, focused on uncorrelated noise for which there is a decomposition of the channel as a tensor product over sites of the lattice. To be precise, we prove that the (local) strong symmetry condition on locality-preserving noise is *sufficient* to preserve SPTO (Lemma 2) and, conversely, that strong symmetry is *necessary* for channels generated in finite time by strictly local Lindbladian evolution (Theorem 1), which we conjecture to hold for all local Lindbladian evolutions (4.6.4). This result might appear surprising in light of the work of Coser and Pérez-García, who show that symmetric local Lindbladian noise, applied for a short amount of time, destroys SPTO [4]. As we demonstrate, this is due to the fact that their noise is only weakly symmetric, and not strongly symmetric. We thus find that SPTO is robust to noise that satisfies a sufficiently strong yet natural symmetry condition; namely that the system-bath coupling is invariant under the symmetries acting on the system alone, as opposed to jointly on the system and bath.

We study the string order numerically under channels in Section §4.5.2. We consider two examples of strong symmetry (given by the dephasing channel) and weak symmetry (given by the depolarising channel). We observe a numerical agreement with the main Theorem. Evolutions with strong symmetry preserve string order, while weakly symmetric channels do not. Through the example of an infinite time evolution, given by the fully dephasing channel, which destroys SPTO despite being strongly symmetric, we demonstrate the importance of the finite time assumption in Theorem 1. We also demonstrate that fingerprints of SPTO such as twisted sector charges, topologically protected edge modes, irreducible probabilities and SPT complexity also agree with the analytical results.

Finally, in Section §4.6, we discuss the extension of this result from uncorrelated noise to causal (that is, locality-preserving) noise, which includes the case of fast, local Lindbladians. We give a generalisation of the preservation of string operators by locally-SS channels in Lemma 2 and an analogue to Theorem 1 which is left

open as a conjecture (Conjecture 3). A nice intuition behind the Conjecture comes from analysing edge modes; these survive only under a fastness assumption which means that the range r of the MPO is small compared to the system size.

4.3 Coherent SPT mixtures

Now we turn to SPT invariants of open systems. In the formalism of Lindbladian evolution [4], phases of open systems are defined in terms of states, as opposed to with some open systems analogue of gapped paths of Hamiltonians. We do not attempt to answer the questions of which mixed states generalize the ground states of gapped, local Hamiltonians and what is their phase classification under an appropriate equivalence relation. Instead we seek to motivate the strong symmetry condition on Lindbladian evolution by focusing on a special class of mixed states for which we can define an invariant:

Definition: *A coherent SPT mixture is a mixed state with a well-defined pattern of zeros.*

(4.3.1)

Such states have a well-defined SPT invariant $[\omega]$ that can be extracted from the pattern of zeros, as discussed above. Mixed states that are ensembles

$$\rho = \sum_i p_i |\psi_i^\omega\rangle\langle\psi_i^\omega| \quad (4.3.2)$$

of SPT pure states $|\psi_i^\omega\rangle$ all in the same SPT phase $[\omega]$ are examples of coherent SPT mixtures. We leave open the possibility that there exist exotic coherent SPT mixtures that are not covered by this example.¹

The main claim of the paper is that translation-invariant pure SPT states (and more generally, states of the form (4.3.2) where each component $|\psi_i^\omega\rangle$ is translation-invariant) are transformed into coherent SPT mixtures (4.3.1) with the same SPT invariant by a Lindbladian evolution if and only if the evolution is strongly symmetric. We prove this claim for uncorrelated noise in Section §4.5 and show its ‘if’ direction (while conjecturing its ‘only if’ direction) for fast, local Lindbladians in Section §4.6. In particular, this result means that SPTO of pure states is robust in open systems described by strongly symmetric Lindbladians.

4.4 A strong symmetry condition on channels

We begin by introducing the *weak* (4.4.2) and *strong* (4.4.8) *symmetry conditions* and discussing their various formulations. The latter is motivated by showing that weak symmetry is insufficient to preserve SPTO. The argument that strong

¹Components of the ensemble that have a different SPTO or no SPTO at all could cancel exactly the expectation values of the string operators, yielding a well-defined pattern of zeros.

symmetry is necessary and sufficient to preserve SPTO is reserved for Section §4.5 (uncorrelated noise) and Section §4.6 (causal channels).

The symmetry conditions are first formulated and studied for arbitrary quantum channels. Then in 4.4.4, for the particularly important case of Lindbladian evolution $\mathcal{E}_t = e^{t\mathcal{L}}$, the conditions are reformulated in terms of \mathcal{L} ; the Lindbladian formulations have been discussed previously [8, 257–259]. The definitions and results in this section apply to general systems on finite-dimensional Hilbert spaces, not just spin chains; U_g denotes the action of the symmetry on the full system, not on a single site of a spin chain.

4.4.1 Weak and strong symmetry conditions

A channel \mathcal{E} is said to satisfy the *weak symmetry (WS) condition* if it commutes, as a superoperator, with the symmetry-implementing channels

$$\mathcal{U}_g(\rho) = U_g \rho U_g^\dagger ; \quad (4.4.1)$$

that is, if

$$\boxed{\mathcal{U}_g \circ \mathcal{E} \circ \mathcal{U}_g^\dagger = \mathcal{E} , \quad \forall g .} \quad (\text{weak symmetry condition}) \quad (4.4.2)$$

The channel \mathcal{E} can be expressed in terms of a Kraus representation, $\mathcal{E}(\rho) = \sum K_i \rho K_i^\dagger$, where we can interpret the K_i as representing different trajectories. In terms of a Kraus representation of \mathcal{E} , the weak symmetry condition reads

$$\sum_i (U_g K_i U_g^\dagger) \rho (U_g K_i U_g^\dagger)^\dagger = \sum_i K_i \rho K_i^\dagger , \quad \forall g . \quad (4.4.3)$$

Since K_i and $U_g K_i U_g^\dagger$ define Kraus representations of the same channel, they are related by a unitary x^g [15]:

$$U_g K_i U_g^\dagger = \sum_j x_{ji}^g K_j , \quad \forall i, g . \quad (4.4.4)$$

Since U_g forms a representation of G , so does x^g :

$$\sum_k x_{ki}^{gh} K_k = U_{gh} K_i U_{gh}^\dagger = U_g U_h K_i U_h^\dagger U_g^\dagger = \sum_{jk} x_{ji}^h x_{kj}^g K_k = , \quad \forall i, g . \quad (4.4.5)$$

In a basis of Kraus operators K_i^g that diagonalizes x^g as a collection of phases $\theta_i(g)$, (4.4.4) amounts to

$$U_g K_i^g U_g^\dagger = e^{i\theta_i(g)} K_i^g , \quad \forall i, g . \quad (4.4.6)$$

The existence of a basis K_i^g , for each g , such that this relation holds is equivalent to the WS condition.

Observe that the phases θ_i in the WS condition (4.4.6) may differ across the trajectories (labeled by i). It will be demonstrated in Section §4.5 that this

interference between the trajectories is the source of the destruction of SPTO, as eliminating it by setting the phases equal is sufficient to ensure that a channel preserves SPTO. Let us now take the phases to be equal: $\theta_i(g) = \theta(g)$ for all i, g . Under this restriction, the condition (4.4.6) is independent of the basis of Kraus operators because $K_i^{g'} = \sum_j v_{ij} K_j^g$ (for any unitary v_{ij}) satisfies

$$U_g K_i^{g'} U_g^\dagger = \sum_j v_{ij} U_g K_j^g U_g^\dagger = e^{i\theta(g)} \sum_j v_{ij} K_j^g = e^{i\theta(g)} K_i^{g'} . \quad (4.4.7)$$

Basis-independence means we can also drop the group label on the Kraus operators: $K_i^g = K_i$ for all i, g . We arrive at what we call the *strong symmetry (SS) condition*:

$$U_g K_i U_g^\dagger = e^{i\theta(g)} K_i , \quad \forall i, g . \quad (\text{strong symmetry condition}) \quad (4.4.8)$$

Note that there is no distinction between the WS and SS conditions for a reversible (unitary) channel, as such a channel is realized by a single Kraus operator, and so it has only a single phase $\theta(g)$.

By Schur's lemma, the SS condition (4.4.8) may be restated as the condition that each K_i is block-diagonal in the irrep basis: $K_i = \oplus_\alpha K_i^\alpha$, where K_i^α acts on the multiplicity space of the (isomorphism class of the) irrep α . The completeness relation $\sum_i K_i^\dagger K_i = \mathbf{1}$ is equivalent to a completeness relation on each block, so the channel decomposes as $\mathcal{E} = \oplus_\alpha \mathcal{E}_\alpha$, where \mathcal{E}_α is the channel with Kraus operators K_i^α . This decomposition is a stronger constraint than the decomposition of WS channels, which, when viewed as matrices on the space of operators, have a block-diagonal form $\mathcal{E} = \sum_\alpha \Phi_\alpha$ in the irrep basis of the action $U_g \otimes U_g^\dagger$; note that the operators Φ_α are different from \mathcal{E}_α and are not themselves channels.

4.4.2 Charge conservation

The strong symmetry condition may be alternatively characterized as

$$\mathcal{E}^\dagger(U_g) = e^{i\theta(g)} U_g , \quad \forall g . \quad (\text{strong symmetry condition}) \quad (4.4.9)$$

where the dual channel \mathcal{E}^\dagger is the channel with Kraus operators K_i^\dagger , $\mathcal{E}^\dagger(X) = \sum K_i^\dagger X K_i$. This alternative statement may be interpreted as conservation of symmetry charge. The charge of a state under a symmetry g is the expectation value $\langle U_g \rangle_\rho = \text{Tr}[\rho U_g]$ of the operator U_g on the state, and the strong symmetry condition means this expectation value is the same (up to a phase) for ρ and $\mathcal{E}(\rho)$:

$$\langle U_g \rangle_{\mathcal{E}(\rho)} = \langle \mathcal{E}^\dagger(U_g) \rangle_\rho \stackrel{SS}{=} e^{i\theta(g)} \langle U_g \rangle_\rho . \quad (4.4.10)$$

The connection between strong symmetry and conservation laws has been noted previously [257].

The equivalence of the two statements may be seen as follows. If a channel satisfies Eq. (4.4.8), then

$$\mathcal{E}^\dagger(U_g) = \sum_i K_i^\dagger U_g K_i = e^{i\theta(g)} \sum_i K_i^\dagger K_i U_g = e^{i\theta(g)} U_g , \quad (4.4.11)$$

which is Eq. (4.4.9). For the converse, we need a lemma: if $\mathcal{E}^\dagger(X) = Y$ and $\mathcal{E}^\dagger(X^\dagger X) = Y^\dagger Y$, then $XK_i = K_i Y$. If this is true, the statement that Eq. (4.4.9) implies Eq. (4.4.8) follows from taking $X = U_g$ and $Y = e^{i\theta(g)}U_g$. The lemma is proved by borrowing the argument for Theorem 6.13 of Ref. [260]:

$$\sum_i (XK_i - K_i Y)^\dagger (XK_i - K_i Y) = \mathcal{E}^\dagger(X^\dagger X) - \mathcal{E}^\dagger(X^\dagger)Y - Y^\dagger \mathcal{E}^\dagger(X) + Y^\dagger \mathcal{E}^\dagger(\mathbb{1})Y = 0. \quad (4.4.12)$$

Then, since the left hand side is a sum of positive terms, each of them must individually vanish: $XK_i = K_i Y$.

4.4.3 Symmetric purifications

The symmetry conditions can be restated in terms of purifications:

Claim: *A channel is weakly symmetric if it has a purification to a unitary that commutes, up to a phase, with some diagonal symmetry $U_g \otimes U_g^A$, for which the action U_g^A on the ancillary space leaves the ancilla state invariant.* (4.4.13)

Claim: *A channel is strongly symmetric if and only if it has a purification to a unitary that commutes, up to the phase $e^{i\theta(g)}$, with the symmetry $U_g \otimes \mathbb{1}^A$.* (4.4.14)

We do not prove a converse to the first claim, though we expect it or a similar statement to hold. The second claim means that one may take $U_g^A = \mathbb{1}^A$ precisely when the channel is strongly symmetric. These statements will come in handy in Section §4.6, when we discuss causal channels in terms of their purifications to matrix product unitaries. The statements also have interpretations in terms of couplings between the system and environment, which we discuss here. First let us review the basics of purifications and justify the claims.

Let \mathcal{E} be a channel on a system with Hilbert space \mathcal{H} . A purification of \mathcal{E} is a unitary W on a space $\mathcal{H} \otimes A$ – the original space appended with an ancillary space – such that, for some ancilla state $|a\rangle \in A$,

$$\text{Tr}_A(W(\rho \otimes |a\rangle\langle a|)W^\dagger) = \mathcal{E}(\rho). \quad (4.4.15)$$

A purification W always exists. Given a set of Kraus operators K_i , indexed in a set \mathcal{I} , form the ancillary space A spanned by an orthonormal basis $|e_i\rangle$, $i \in \mathcal{I}$ and the operator $V : \mathcal{H} \rightarrow \mathcal{H} \otimes A$ that acts as

$$V : |\psi\rangle \mapsto \sum_i K_i |\psi\rangle \otimes |e_i\rangle. \quad (4.4.16)$$

The operator V is called a Stinespring dilation of \mathcal{E} and is an isometry since

$$\langle \phi | V^\dagger V | \psi \rangle = \sum_{ij} \langle e_i | \langle \phi | K_j^\dagger K_i | \psi \rangle | e_j \rangle = \sum_i \langle \phi | K_i^\dagger K_i | \psi \rangle = \langle \phi | \psi \rangle. \quad (4.4.17)$$

Then use the fact that any isometry V on $\mathcal{H} \cong \mathcal{H} \otimes |a\rangle$, $|a\rangle \in A$, can always be extended to a unitary W on $\mathcal{H} \otimes A$. Conversely, if we expand the expression (4.4.15) in an orthonormal basis $|e_i\rangle$ of A to obtain

$$\sum_i \langle e_i | W | a \rangle \rho \langle a | W^\dagger | e_i \rangle = \mathcal{E}(\rho) , \quad (4.4.18)$$

we see that $K_i := \langle e_i | W | a \rangle$ are candidates for a set of Kraus operators for \mathcal{E} . To see that they are actually Kraus operators, check completeness:

$$\sum_i K_i^\dagger K_i = \sum_i \langle a | W^\dagger | e_i \rangle \langle e_i | W | a \rangle = \langle a | (\mathbb{1} \otimes \mathbb{1}^A) | a \rangle = \mathbb{1} . \quad (4.4.19)$$

The purification can be expressed diagrammatically as a tensor

$$K_i = \begin{array}{c} | \\ \text{---} \\ | \end{array} \text{---} i = \begin{array}{c} | \\ \text{---} \\ | \\ \text{---} \\ | \\ \text{---} \\ | \end{array} \begin{array}{c} a \\ W \\ i \end{array} , \quad \mathcal{E}(\rho) = \begin{array}{c} K_i^\dagger \\ \rho \\ K_i \end{array} = \begin{array}{c} | \\ \text{---} \\ | \\ \text{---} \\ | \\ \text{---} \\ | \\ \text{---} \\ | \end{array} \begin{array}{c} W^\dagger \\ \rho \\ W \\ a \end{array} . \quad (4.4.20)$$

The claim (4.4.13) about weak symmetry (4.4.2) may be expressed as

$$\begin{array}{c} U_g^\dagger \\ | \\ \text{---} \\ | \\ \text{---} \\ | \\ \text{---} \\ | \end{array} \begin{array}{c} U_g^A \\ | \\ \text{---} \\ | \\ \text{---} \\ | \\ \text{---} \\ | \end{array} \begin{array}{c} W \\ | \\ \text{---} \\ | \\ \text{---} \\ | \\ \text{---} \\ | \end{array} = e^{i\theta(g)} \begin{array}{c} | \\ \text{---} \\ | \\ \text{---} \\ | \\ \text{---} \\ | \end{array} \begin{array}{c} W \\ | \\ \text{---} \\ | \\ \text{---} \\ | \\ \text{---} \\ | \end{array} \implies WS , \quad (4.4.21)$$

while the claim (4.4.14) about strong symmetry (4.4.8) may be expressed as

$$\begin{array}{c} U_g^\dagger \\ | \\ \text{---} \\ | \\ \text{---} \\ | \\ \text{---} \\ | \end{array} \begin{array}{c} W \\ | \\ \text{---} \\ | \\ \text{---} \\ | \\ \text{---} \\ | \end{array} = e^{i\theta(g)} \begin{array}{c} | \\ \text{---} \\ | \\ \text{---} \\ | \\ \text{---} \\ | \end{array} \begin{array}{c} W \\ | \\ \text{---} \\ | \\ \text{---} \\ | \\ \text{---} \\ | \end{array} \iff SS . \quad (4.4.22)$$

Let us now prove the claim (4.4.13). Suppose W is symmetric with the symmetry $U_g \otimes U_g^A$ and the state $|a\rangle$ is invariant: $U_g^A |a\rangle = |a\rangle$. Then the $K_i = \langle e_i | W | a \rangle$ satisfy weak symmetry (4.4.4):

$$U_g K_i = \begin{array}{c} | \\ \text{---} \\ | \\ \text{---} \\ | \\ \text{---} \\ | \end{array} \begin{array}{c} |a\rangle \\ W \\ |e_i\rangle \end{array} = \begin{array}{c} | \\ \text{---} \\ | \\ \text{---} \\ | \\ \text{---} \\ | \end{array} \begin{array}{c} |a\rangle \\ W \\ U_g^A (U_g^A)^\dagger |e_i\rangle \end{array} = e^{i\theta(g)} \begin{array}{c} U_g \\ | \\ \text{---} \\ | \\ \text{---} \\ | \\ \text{---} \\ | \end{array} \begin{array}{c} U_g^A |a\rangle \\ W \\ (U_g^A)^\dagger |e_i\rangle \end{array} = x_{ji}^g \begin{array}{c} U_g \\ | \\ \text{---} \\ | \\ \text{---} \\ | \\ \text{---} \\ | \end{array} \begin{array}{c} |a\rangle \\ W \\ |e_j\rangle \end{array} = x_{ji}^g K_j U_g , \quad (4.4.23)$$

where x_{ji}^g are the matrix elements $x_{ji}^g = e^{i\theta(g)} \langle e_i | (U_g^A)^\dagger | e_j \rangle = e^{i\theta(g)} (U_g^A)_{ji}^*$.

One direction of the claim (4.4.14) follows from a similar argument. Suppose W is symmetric with $U_g \otimes \mathbb{1}^A$. Then the $K_i = \langle e_i | W | a \rangle$ satisfy the strong symmetry condition (4.4.8):

$$U_g K_i = \begin{array}{c} | \\ \color{red}{a} \\ \boxed{W} \\ | \\ \color{red}{i} \\ U_g \end{array} = e^{i\theta(g)} \begin{array}{c} U_g \\ | \\ \color{red}{a} \\ \boxed{W} \\ | \\ \color{red}{i} \end{array} = e^{i\theta(g)} K_i U_g. \quad (4.4.24)$$

Conversely, suppose the Kraus operators satisfy the SS condition and construct a symmetric W as follows. Without loss of generality, take $|a\rangle$ to be $|e_1\rangle$. A unitary extension of the Stinespring dilation V is a square matrix W consisting of blocks K_i^j , where the blocks of the first column are the Kraus operators $K_i^1 := K_i$, and we choose the remaining blocks so that W is unitary:

$$\sum_i K_i^{j\dagger} K_i^k = \delta^{jk} \mathbb{1}_{\mathcal{H}}. \quad (4.4.25)$$

The remaining blocks may be chosen to be symmetric (so that W is symmetric) as follows. Build linear independent columns by adding signs like $K_i^j := (-1)^{\delta(i < j)} K_i$, then make them orthogonal by applying the Gram-Schmidt process, and finally normalize. The result is manifestly symmetric.

The claims (4.4.13) and (4.4.14) may be interpreted in terms of the coupling between the system and the environment (the ancillary space). Suppose W represents unitary evolution by a Hamiltonian:

$$W = e^{-itH/\hbar}, \quad H = \sum_i H_i^S \otimes H_i^E, \quad (4.4.26)$$

where the H_i^S and H_i^E are each assumed to be linearly independent. If the unitary evolution W satisfies the formulation of the weak symmetry condition in the claim (4.4.13) at all times t , then $U_g \otimes U_g^A$ is a symmetry of H . If the unitary evolution W satisfies the strong symmetry condition (4.4.14) at all times t , then

$$0 = (U_g \otimes \mathbb{1}^A) H - e^{i\theta(g)} H (U_g \otimes \mathbb{1}^A) = \sum_i (U_g H_i^S - e^{i\theta(g)} H_i^S U_g) \otimes H_i^E, \quad \forall g, \quad (4.4.27)$$

which, since the H_i^E are linearly independent, implies $U_g H_i^S = e^{i\theta(g)} H_i^S U_g$, $\forall i, g$. By conjugating both sides of the equation, we find that $e^{i\theta(g)} = e^{-i\theta(g)}$, so $\theta(g) = 0, \pi$. Since W is a continuous function of t , the phase $\theta(g)$ must vary continuously from zero at $t = 0$ to its values at nonzero times (this can be formalized by including the constant order in the expansion of (4.4.26) in the symmetry condition (4.4.27)); this means it must be zero at all times. Therefore, for channels arising from a continuous coupling of system to environment,

$$U_g H_i^S = H_i^S U_g, \quad \forall i, g, \quad (4.4.28)$$

which is to say that the system alone, rather than merely its composite with the environment, is symmetric.

4.4.4 Symmetry conditions on Lindbladians

Let us now discuss semigroups of channels generated by continuous time evolution by a Lindbladian (2.2.1), which we introduced in Section §2.2.1.

If a semigroup consists of channels satisfying the weak or strong symmetry condition, the Lindbladian generating it satisfies, respectively,

$$\boxed{\mathcal{U}_g \circ \mathcal{L} \circ \mathcal{U}_g^\dagger = \mathcal{L}, \quad \forall g.} \quad (\text{WS condition on } \mathcal{L}) \quad (4.4.29)$$

$$\boxed{U_g L_i = L_i U_g, \quad U_g H^S = H^S U_g, \quad \forall i, g,} \quad (\text{SS condition on } \mathcal{L}) \quad (4.4.30)$$

where the L_i are jump operators and H^S is the Hamiltonian of the system (2.2.1). In particular, this implies that semigroups of strongly symmetric channels generated by Lindbladian evolution necessarily have $\theta(g) = 0, \forall g$ at all times.

To see the weak symmetry condition (4.4.29), observe that the channels $\mathcal{E}_t = e^{t\mathcal{L}}$ commute with \mathcal{U}_g at all times t if and only if \mathcal{L} commutes with \mathcal{U}_g . To see the strong symmetry condition (4.4.30), observe that

$$\begin{aligned} \mathcal{E}_{\delta t}(\rho) &= \rho + \delta t \mathcal{L}(\rho) \\ &= \rho + \delta t \left[\left(-\frac{i}{\hbar} H^S - \frac{1}{2} \sum_{i=1}^{\ell} L_i^\dagger L_i \right) \rho + \rho \left(\frac{i}{\hbar} H^S - \frac{1}{2} \sum_{i=1}^{\ell} L_i^\dagger L_i \right) \right] + \sum_{i=1}^{\ell} \delta t L_i \rho L_i^\dagger, \end{aligned} \quad (4.4.31)$$

at small times δt , and thus

$$\mathcal{E}_{\delta t}(\rho) = \sum_{i=0}^{\ell} K_i(\delta t) \rho K_i(\delta t)^\dagger \quad (4.4.32)$$

with Kraus operators

$$K_0(\delta t) = \mathbb{1} + \delta t \left(-\frac{i}{\hbar} H^S - \frac{1}{2} \sum_{i=1}^{\ell} L_i^\dagger L_i \right), \quad K_{i>0}(\delta t) = \sqrt{\delta t} L_i. \quad (4.4.33)$$

This relationship between Kraus operators and jump operators lets us translate our strong symmetry condition (4.4.8) on channels into the strong symmetry condition (4.4.30) on the Lindbladians that generate them: First, from the commutation relation $U_g K_{i>0} = e^{i\theta(g)} K_{i>0} U_g$, we infer that $U_g L_i = e^{i\theta(g)} L_i U_g$. It follows that $X := \mathbb{1} - \delta t \frac{1}{2} \sum L_i^\dagger L_i$ commutes with U_g . Second, from the commutation relation $U_g K_0 = e^{i\theta(g)} K_0 U_g$, we get $U_g (-i/\hbar) H^S \delta t + X U_g^\dagger = e^{i\theta(g)} (-i/\hbar) H^S \delta t + X$. Taking the Hermitian part and using that X commutes with U_g , we obtain $X = U_g X U_g^\dagger = \cos \theta(g) X + \sin \theta(g) (\delta t/\hbar) H^S$, or

$$(1 - \cos \theta(g)) X = \sin \theta(g) (\delta t/\hbar) H^S. \quad (4.4.34)$$

As this must hold for all $g \in G$ simultaneously, the proportionality factor $(1 - \cos \theta(g))/\sin \theta(g)$ must not depend on g , which is only possible if $\theta(g)$ is constant.

As $\theta(g)$ is a representation, this implies $\theta(g) \equiv 0$ for all $g \in G$ (and in particular, the above equation then imposes no constraints on X and H^S).² It thus follows that both L_i and H^S must commute with U_g . We conclude that a Lindbladian generates a family of SS channels if and only if it satisfies the condition (4.4.30).

We also obtain a characterization of strong symmetry for Lindbladians by applying the charge conservation condition (4.4.9) to $\mathcal{E}_{\delta t} = e^{\delta t \mathcal{L}}$ (using that we now know that $\theta(g) \equiv 0$ for Lindbladian channels):

$$U_g = \mathcal{E}_{\delta t}^\dagger(U_g) = U_g + \delta t \mathcal{L}^\dagger(U_g) , \quad (4.4.35)$$

and thus

$$\boxed{\mathcal{L}^\dagger(U_g) = 0 . \quad (\text{SS condition on } \mathcal{L})} \quad (4.4.36)$$

The Lindblad master equation (2.2.1) can also be recovered from the Hamiltonian that couples the system to the environment, under the Born (weak coupling, large environment) and Markov (memoryless environment) approximations. We refer readers to Chapter 6.2.1 of Ref. [261] for a detailed analysis of this procedure. The jump operators appear in the coupling Hamiltonian as

$$H = H^S \otimes \mathbf{1}^E + \mathbf{1}^S \otimes H^E + \sum_{i>0} L_i \otimes B_i . \quad (4.4.37)$$

In this picture, the strong symmetry condition (4.4.30) on Lindbladians is equivalent to our previous result about the strong symmetry condition on purifications (4.4.28).

Destruction of SPTO by weakly symmetric coupling

Let us now demonstrate that having merely weakly symmetric noise is insufficient to preserve SPTO. Specifically, the fast, local Lindbladian evolution defined by Coser and Pérez-García [4], which they showed to destroy SPTO, is weakly symmetric. However, as we will also see, it lacks the strong symmetry condition, leaving open the possibility that the latter preserves SPTO.

The local Lindbladian of Ref. [4] is given as a sum over sites on a spin chain

$$\mathcal{L} = \sum_s \mathcal{L}_s , \quad (4.4.38)$$

where

$$\mathcal{L}_s = \mathcal{T}_s - \mathbf{1}_s , \quad \mathcal{T}_s(\rho) = \text{Tr}_s[\rho] |\phi\rangle_s \langle \phi| \quad (4.4.39)$$

for some single-site state $|\phi\rangle$. It is shown to drive any one-dimensional SPT state toward the product state $|\phi\rangle^{\otimes L}$, approximating it well in short time. This result suggests that no SPTO is robust in open systems.

²There is an alternative topological argument for $\theta(g) = 0$. Since the $K_i(t)$ are continuous functions in t , the phase $\theta(g)$ in their commutation relations must also be continuous in t . But $e^{i\theta}$ is a one-dimensional representation of G , and there are only discretely many of these (even if G is continuous), so $\theta(g)$ must be a constant function in t . Then, since $\theta(g) = 0$ for all g at $t = 0$ (because $W(t=0) = \mathbf{1}$), the condition $\theta(g) = 0$ must also be true at all times t .

Any time \mathcal{L} is given as a sum of single site terms (4.4.38), the SS condition (4.4.36) reads

$$0 = \mathcal{L}^\dagger(U_g^{\otimes L}) = \sum_s \mathcal{L}_s^\dagger(U_g^{\otimes L}) = \sum_s \mathcal{L}_s^\dagger(U_g^{(s)} \otimes \mathbb{1}^{(L \setminus s)}) \otimes U_g^{(L \setminus s)}, \quad (4.4.40)$$

where U_g now denotes the action of the symmetry on a single site. This condition is equivalent to each of the single site terms satisfying the local condition $\mathcal{L}_s^\dagger(U_g^{(s)} \otimes \mathbb{1}^{(L \setminus s)}) = 0$. The channel (4.4.39) has $\mathcal{L}_s^\dagger(X) = \langle \phi | X | \phi \rangle_s \otimes \mathbb{1}^{(L \setminus s)} - X$, so it fails this condition for any $g \neq 1$ and therefore is not SS. On the other hand, \mathcal{L} commutes with \mathcal{U}_g and so is WS, as long as $|\phi\rangle$ is taken to be symmetric.

4.5 Strongly symmetric uncorrelated noise

We begin by considering uncorrelated noise – channels that decompose into onsite operations as $\mathcal{E} = \otimes_s \mathcal{E}_s$. If $\{K_{i_s}^s\}$ is a Kraus representation of \mathcal{E}_s , a Kraus representation of \mathcal{E} is by operators

$$K_i = \otimes_s K_{i_s}^s. \quad (4.5.1)$$

The full channel satisfies the WS or SS condition if and only if all of the single site channels do. Uncorrelated noise is the simplest class of channels, and include the example of 4.4.4, so they are a natural place to start.

The following subsections consider several typical probes of SPTO, in particular, string order, twisted sector charges, edge modes, and irrep probabilities. We demonstrate that these probes are preserved by strongly symmetric uncorrelated noise, indicating that SPTO is preserved. We show in [Theorem 1](#) that, for semigroups of noise generated by Lindbladians, the strong symmetry condition on the Lindbladians is both necessary and sufficient for string order to be preserved at all finite times. We present analytical arguments as well as numerical investigations of example states and channels.

4.5.1 Preservation of string order by strongly symmetric channels

The first indicator of SPTO we consider is the string order parameter, which was introduced in 2.4.3. A channel \mathcal{E} preserves string order if the evolved state $\mathcal{E}(\rho)$ has the same pattern of zeros as the initial state ρ . In the Heisenberg picture, this means that the collection of values $\langle \mathcal{E}^\dagger(s(g, O_\alpha^l, O_\alpha^r)) \rangle$ has the same pattern of zeros as $\langle s(g, O_\alpha^l, O_\alpha^r) \rangle$, where \mathcal{E}^\dagger is the dual channel to \mathcal{E} . We save for 5.6 the question of precisely which channels preserve the string order of a state in a given SPT phase. For now, we show

Lemma 1: *A channel of uncorrelated noise maps string operators to other string operators of the same type (g, α) if and only if the channel is strongly symmetric.*

Note that the evolved string operators are not guaranteed to be nonvanishing.³

To see the lemma, consider evolving the string operator (2.4.10) by the uncorrelated noise. It becomes

$$\mathcal{E}^\dagger(s(g, O_\alpha^l, O_\alpha^r)) = \mathbf{1} \otimes \mathcal{E}_l^\dagger(O_\alpha^l) \otimes \left(\bigotimes \mathcal{E}_s^\dagger(U_g) \right) \otimes \mathcal{E}_r^\dagger(O_\alpha^r) \otimes \mathbf{1} . \quad (4.5.2)$$

If \mathcal{E}_s is SS, each of the terms in the bulk of the string becomes $\mathcal{E}_s^\dagger(U_g) = e^{i\theta_s(g)}U_g$. Since an SS channel is in particular WS (4.4.2), it maps the end operators to other end operators with the same charge: $\tilde{O}_\alpha^{l,r} := \mathcal{E}_s^\dagger(O_\alpha^{l,r})$ has $U_g^\dagger \tilde{O}_\alpha^l U_g = \chi_\alpha(g) \tilde{O}_\alpha^l$ and similarly for \tilde{O}_α^r . Then in total, we have

$$\mathcal{E}^\dagger(s(g, O_\alpha^l, O_\alpha^r)) = e^{i \sum_s \theta_s(g)} s(g, \tilde{O}_\alpha^l, \tilde{O}_\alpha^r) . \quad (4.5.3)$$

Conversely, asking that $\mathcal{E}^\dagger(s(g, O_\alpha^l, O_\alpha^r))$ is a string operator of type (g, α) for all (g, α) requires,⁴ in particular, that $\mathcal{E}_s^\dagger(U_g)$ is proportional to U_g , which is the strong symmetry condition.

A necessary and sufficient condition on Lindbladians

Our discussion has so far focused on the string operators. We now turn toward analyzing their expectation values, which encode the invariant of SPT states. In the following, a coherent SPT mixture is a mixed state with a well-defined pattern of zeros (and thus a well-defined invariant $[\omega]$), in the sense of Definition (4.3.1). A “coherent SPT phase” is a class consisting of all coherent SPT mixtures with a given invariant. Preserving a phase means that every mixture of translation-invariant pure SPT states in the phase (states of the form Eq. (4.3.2)) is mapped to a coherent SPT mixture in the same phase.⁵

Our main result is stated as a theorem:

Theorem 1: *Fix any coherent SPT phase. A semigroup of channels of uncorrelated noise generically preserves the phase at all finite times if and only if the semigroup is generated by a strongly symmetric Lindbladian.*

In other words, the notion of coherent SPT phase defined by patterns of zeros coincides with the notion of phase defined by strongly symmetric Lindbladian evolution.

³It is possible that a strongly symmetric channel annihilates some string operators by mapping their end operators to zero. This phenomenon is unrelated to the symmetry selection rules for string order, discussed in 2.4.3, which happens on the level of expectation values. For channels that are generic in the sense of Eq. (5.6.1), it does not occur for generic end operators.

⁴The choice $O_\alpha^{l,r} = \mathbf{1}$ always results in nonvanishing $\tilde{O}_\alpha^{l,r}$, so the bulk $\mathcal{E}_s^\dagger(U_g)$ can be compared to U_g .

⁵We expect that strongly symmetric Lindbladian evolution takes every coherent SPT mixture to a coherent SPT mixture in the same phase; however, we restrict ourselves to initial states that are mixtures of translation-invariant pure SPT states in order to make use of tensor network methods in the proof of the theorem.

To make a claim as strong as [Theorem 1](#), it is necessary to work on the level of phases rather than the states (equivalently, systems) that compose them. A phase protected by a symmetry G consists of systems together with the data of embeddings of G into the systems' full groups of symmetries. For example, the AKLT system may be regarded as lying in a $G = \mathbb{Z}_2 \times \mathbb{Z}_2$ SPT phase if one specifies this group's embedding into the system's larger $SO(3)$ intrinsic symmetry group. Also, there is no restriction on the physical degrees of freedom, or the symmetry action on these degrees of freedom, that a system in a phase may have. For example, the $\mathbb{Z}_2 \times \mathbb{Z}_2$ SPT phase to which the AKLT system belongs also contains systems that are not built of spin-1 degrees of freedom. Whether two systems lie in the same phase has not to do with their intrinsic symmetry groups or degrees of freedom but on the values taken by their order parameters. This means that MPS representations of states within the phase will have tensors of various physical dimensions and symmetries. The theorem concerns which symmetry condition channels must satisfy so that they preserve the string order of *every system in the SPT phase*. To do this, we consider generic states, whose MPS tensors have exactly the symmetry G , are injective, and have physical Hilbert space no larger than the tensor's image. We emphasize that this result does not preclude the possibility of nongeneric systems within the phase for which a condition weaker than strong symmetry is sufficient.

With these remarks behind us, we are ready to prove the theorem, starting with the 'if' direction. If the semigroup is generated by a strongly symmetric Lindbladian, each channel \mathcal{E}_t is itself strongly symmetric. Then by [Lemma 1](#), \mathcal{E}_t preserves the type of string operators. Moreover, finite time Lindbladian evolution defines channels that are invertible as linear maps⁶ since $\det(e^{t\mathcal{L}}) = e^{\text{Tr}(t\mathcal{L})} \neq 0$ for finite t , so these channels do not annihilate any string operators. Thus the pattern of zeros of the expectation values of string operators is preserved, as long as one uses end operators that are generic in the sense of [2.4.3](#) – namely, that $O_\alpha^{l,r}$ is orthogonal neither to $N_{l,r}^{g\dagger}$ nor to $\mathcal{E}(N_{l,r}^{g\dagger})$. The assumption that the end operators are generic can be dropped if one is interested in generic evolution times. This is because the expectation value of a string operator is analytic as a function of time, and so it either vanishes at all times – as occurs where the initial pattern of zeros has a zero – or is zero only at isolated points in time. The assumption of finite time cannot be dropped, as an infinite time evolution may annihilate some string operators and therefore alter the pattern of zeros. An evolution for which this phenomenon occurs is the fully dephasing channel introduced below.

Next we turn to the 'only if' direction. We show it for initial states that are translation-invariant pure SPT states. Then it also holds for their mixtures. If a channel \mathcal{E} preserves the string order of an SPT state, there is, for every symmetry g , a string operator with g in the bulk whose expectation value is nonvanishing. This expectation value may be written as $\langle L | T_{\mathcal{E}_s^\dagger(U_g)}^j | R \rangle$, where $T_{\mathcal{E}_s^\dagger(U_g)}$ is the transfer

⁶Note that invertibility of the channel as a linear map is a weaker condition than reversibility of the channel, as the inverse linear map is not required to be a channel.

matrix

$$\mathcal{E}_s^\dagger(U_g) = \begin{array}{c} \bar{A} \\ \text{---} \\ \bullet \\ | \\ \text{---} \\ \bullet \\ | \\ \text{---} \\ A \end{array} = \begin{array}{c} \bar{A} \\ \text{---} \\ \bullet \\ | \\ \text{---} \\ \bullet \\ | \\ \text{---} \\ A \end{array} \quad (4.5.4)$$

This operator must have $\lambda = 1$ as its maximum eigenvalue in order for the expectation value to be nonvanishing in the thermodynamic limit.⁷ By Lemma 2 of Ref. [76], for injective MPS, in order for T_X to have $\lambda = 1$, X must be a symmetry of the MPS, which by assumption is some element $h_g \in G$. Thus $\mathcal{E}_s^\dagger(U_g) = e^{i\theta(g)}U_{h_g}$. Taking $X = U_g$ and $Y = e^{i\theta(g)}U_{h_g}$ in the argument at the end of 4.4.2, we see that $U_g K_i = e^{i\theta(g)}K_i U_{h_g}$ for all i . The map $\sigma : g \mapsto h_g$ is an endomorphism⁸ of G since U is faithful and, up to phases θ ,

$$\begin{aligned} U_{\sigma(g)}U_{\sigma(h)} &= \sum_i K_i^\dagger K_i U_{\sigma(g)}U_{\sigma(h)} \sim \sum_i K_i^\dagger U_g U_h K_i \\ &= \sum_i K_i^\dagger U_{gh} K_i \sim \sum_i K_i^\dagger K_i U_{\sigma(gh)} = U_{\sigma(gh)}. \end{aligned} \quad (4.5.5)$$

If \mathcal{E} is connected to the trivial channel by a semigroup of channels \mathcal{E}_t satisfying the above at all times, the endomorphism σ must be connected to the identity endomorphism $\sigma = 1$ by a continuous path σ_t . Since we have assumed G is abelian, the only identity-connected endomorphism is $\sigma = 1$ itself. Thus, we have $\mathcal{E}_s^\dagger(U_g) = U_g$, which is the strong symmetry condition (4.4.9) on the site s . This holds for all s , so the full channel \mathcal{E} is strongly symmetric. It holds at all finite times, so by the discussion in 4.4.4, the Lindbladian that generates it is strongly symmetric. This completes the proof of [Theorem 1](#).

It is interesting to note that, by [Theorem 1](#) and [Lemma 1](#), any semigroup that preserves an SPT phase, even the trivial SPT phase, also preserves the type of all string operators. This reflects how special SPT states, even trivial SPT states, are among mixed states, most of which lack valid patterns of zeros.

The proof of [Theorem 1](#) involved only the identity-connected endomorphisms of the symmetry group. In [Chapter 5](#) we lift the restriction that the channel belongs to a semigroup of SPT-preserving channels; in this broader setting, more general group endomorphisms play an important role.

Let us comment on the generalization to a nonabelian symmetry group G . Recall that in this case, string order is not guaranteed to capture the full SPT invariant ω ; nevertheless, we can ask about which channels preserve string order. If G is a finite group, the only identity-connected endomorphism is again $\sigma = 1$ itself.

⁷At finite string lengths, the difference between strongly symmetric and non-strongly symmetric Lindbladians is reflected in the length-dependence of the order parameters: only for the latter is there decay as a function of length.

⁸An endomorphism is a map from the group to itself that is compatible with the group structure.

On the other hand, if G is a semisimple Lie group, the only identity-connected endomorphisms are *inner automorphisms* [262]. An automorphism σ is said to be inner if there exists an element $h \in G$ such that

$$\sigma(g) = \text{conj}_h(g) := h^{-1}gh, \quad \forall g \in G. \quad (4.5.6)$$

The element h is defined up to elements of the center. An example of a channel with automorphism $\sigma = \text{conj}_h$ is the symmetry-implementing channel \mathcal{U}_h (4.4.1), which has a single Kraus operator $K = U_h$ satisfying

$$U_{\sigma(g)} := K^\dagger U_g K = U_h^{-1} U_g U_h = U_{h^{-1}gh}. \quad (4.5.7)$$

Any channel \mathcal{E} with inner automorphism $\sigma = \text{conj}_h$ may be expressed as the composition of the symmetry-implementing channel \mathcal{U}_h and a strongly symmetric channel \mathcal{E}_{SS} :

$$\mathcal{E} = \mathcal{E}_{SS} \circ \mathcal{U}_h. \quad (4.5.8)$$

To see this, let K_i denote the Kraus operators for \mathcal{E} and define Kraus operators for \mathcal{E}_{SS} as

$$K'_i = U_h^{-1} K_i. \quad (4.5.9)$$

One can easily verify that the latter define a strongly symmetric channel \mathcal{E}_{SS} . The semigroup of channels of the form (4.5.8) is generated by the sum of a strongly symmetric Lindbladian \mathcal{L}_{SS} and a generator \mathcal{Q} of the continuous symmetry $\mathcal{U}_h = e^{\mathcal{Q}}$. We obtained this condition by asking that a string operator expectation value not vanish, which is weaker than asking that string order is preserved; in fact, string order may be modified by such channels. The \mathcal{U}_h factor changes the bulks of string operators from U_g to $\mathcal{U}_h^\dagger(U_g) = U_{h^{-1}gh}$ and the ends from O_α to $\mathcal{U}_h^\dagger(O_\alpha)$, which transform as $(\sigma^{-1})^*\alpha$. It may happen, however, that string order is preserved despite the permutation of string operators; this phenomenon is discussed in Chapter 5.

4.5.2 Numerical study of string order under channels

In this subsection, we simulate the behavior of string order under the action of two example channels – the depolarizing channel and the dephasing channel. We find, in agreement with the analytical results, that evolutions with strong symmetry preserve string order, while weakly symmetric channels do not. We also use the example of the fully dephasing channel, which destroys SPTO despite being strongly symmetric, to demonstrate the importance of the finite time assumption in the theorem. All end operators are annihilated BY this channel and string order is destroyed (in particular, the channel is not invertible).

The depolarising channel is a severely noisy channel, as it contracts the Bloch sphere to the origin, driving states towards the maximally mixed state. This channel is written as

$$\mathcal{E}(\rho) = (1 - \lambda) \rho + \lambda (\text{Tr } \rho) \frac{1}{d} \mathbb{1}, \quad (4.5.10)$$

with the decay rate parametrized by $\lambda \in [0, 1]$ [13]. The value $\lambda = 1$ gives the fully depolarising channel. The channel satisfies the weak symmetry condition (4.4.2) for any symmetry.

The Kraus decomposition for this channel can be written as a twirling operation since the normalised d -identity can be decomposed as an average over the generators of the Lie algebra of $SO(d)$ [15]. In $d = 2$, these operators are Paulis, while in higher d they are the Heisenberg-Weyl matrices: the shift operator $X |j\rangle = |j + 1 \bmod d\rangle$ and the phase operator $Z |j\rangle = e^{i2\pi j/d} |j\rangle$, which have commutation relation $Z^m X^n = e^{i2\pi nm/d} X^n Z^m$. The Kraus decomposition for spin-1 ($d = 3$) systems such as the AKLT state is given by

$$\mathcal{E}(\rho) = (1-\lambda)\rho + \frac{\lambda}{9} \sum_i N_i \rho N_i^\dagger, \quad N_i = \{\mathbb{1}, Z, Z^2, X, ZX, Z^2X, X^2, ZX^2, Z^2X^2\}. \quad (4.5.11)$$

A $G = \mathbb{Z}_2 \times \mathbb{Z}_2$ symmetry acts on the spin-1 system as $U_g = e^{i\pi S_j}$, where S_j are the spin-1 operators. Since the Kraus operators $K_i \sim N_i$ only commute with the symmetry action up to different phases, the channel does not satisfy the strong symmetry condition (4.4.8); it is only weakly symmetric.

The second channel we discuss is given by

$$\mathcal{E}(\rho) = (1-\lambda)\rho + \frac{\lambda}{4} \sum_j N_j \rho N_j^\dagger, \quad N_j = \{\mathbb{1}, e^{i\pi S_x}, e^{i\pi S_y}, e^{i\pi S_z}\}, \quad (4.5.12)$$

where S_j are the spin-1 operators. Since the Kraus operators $K_j \sim N_j$ commute with the symmetry action, the channel is strongly symmetric (4.4.8). The channel is the fully dephasing channel when $\lambda = 1$.

String order after a single time-step

Let us consider the AKLT state, which belongs to the Haldane SPT phase. This state has nontrivial $SO(3)$ SPT order, but can be protected by just the subgroup $\mathbb{Z}_2 \times \mathbb{Z}_2$ [157, 176]. The AKLT state has an exact tensor network representation given by the Pauli operators in the basis $\{|+\rangle, |0\rangle, |-\rangle\}$.

The $|G|^2 = 16$ string operators s_{ij} for the symmetry $G = \mathbb{Z}_2 \times \mathbb{Z}_2$ are built out of end operators $O_\alpha^{l,r} = S_i$ and bulk operators $U_g = e^{i\pi S_j}$, where S_i are the spin-1 matrices with $j = \{e, x, y, z\}$. On the AKLT state, the diagonal string operators take nonzero values $s_{zz}, s_{xx}, s_{yy} = -4/9$ and $s_{\mathbb{1},\mathbb{1}} = \mathbb{1}$ independent of string length in the limit of infinite system size, while the off-diagonal string operators elements $s_{ij}, i \neq j$ have vanishing expectation values in the limit of long string length.

Recall that the string order parameter may be manipulated into the form (2.4.17)

$$\langle s(g, O_\alpha^{l,r}) \rangle = \text{Tr}(\rho_l T_{O_\alpha^l} (T_{U_g})^{N-2} T_{O_\alpha^r} \rho_r), \quad (4.5.13)$$

where T is the transfer matrix $T = \sum_i A^i \otimes \bar{A}^i$ for the MPS tensor A , and $\rho_{l,r}$ are its fixed points. Now consider evolving the string operator under a channel. The

operator becomes

$$\langle \mathcal{E}^\dagger(s(g, O_\alpha^l, O_\alpha^r)) \rangle = \text{Tr}(\rho_l T_{\mathcal{E}^\dagger(O_\alpha^l)} T_{\mathcal{E}^\dagger(U_g)}^{N-2} T_{\mathcal{E}^\dagger(O_\alpha^r)} \rho_r). \quad (4.5.14)$$

For the SS channel (4.5.12), the evolved string order pattern for the AKLT state as a function of the decay rate λ is

$$\langle \mathcal{E}^\dagger(s(e^{i\pi S_j}, S_i)) \rangle = \begin{pmatrix} 1 & -\frac{4}{9}(1-\lambda)^2(-\frac{1}{3})^N & -\frac{4}{9}(1-\lambda)^2(-\frac{1}{3})^N & -\frac{4}{9}(1-\lambda)^2(-\frac{1}{3})^N \\ (-\frac{1}{3})^N & -\frac{4}{9}(1-\lambda)^2 & -\frac{4}{9}(1-\lambda)^2(-\frac{1}{3})^N & -\frac{4}{9}(1-\lambda)^2(-\frac{1}{3})^N \\ (-\frac{1}{3})^N & -\frac{4}{9}(1-\lambda)^2(-\frac{1}{3})^N & -\frac{4}{9}(1-\lambda)^2 & -\frac{4}{9}(1-\lambda)^2(-\frac{1}{3})^N \\ (-\frac{1}{3})^N & -\frac{4}{9}(1-\lambda)^2(-\frac{1}{3})^N & -\frac{4}{9}(1-\lambda)^2(-\frac{1}{3})^N & -\frac{4}{9}(1-\lambda)^2 \end{pmatrix}. \quad (4.5.15)$$

In the limit of large string length $N \rightarrow \infty$, the diagonal entries are nonzero while the off-diagonal entries are zero, which indicates that the string order of the AKLT state was preserved, as is expected for SS channels. Note that if we were to repeatedly evolve the state by \mathcal{E} a large number of times, the entire string order set would be sent to zero, so the preservation of the pattern is only visible at finite times. The finite-time decay is minimal (outside of the nongeneric cases discussed in the next section) since it occurs locally at the ends of the string and receives no contribution from the bulk.

In contrast, consider the WS depolarising channel (4.5.11). The string order for the evolved state is

$$\langle \mathcal{E}^\dagger(s(e^{i\pi S_j}, S_i)) \rangle = \begin{pmatrix} 1 & -\frac{4}{9}(1-\lambda)^2(-\frac{1}{3})^N & -\frac{4}{9}(1-\lambda)^2(-\frac{1}{3})^N & -\frac{4}{9}(1-\lambda)^2(-\frac{1}{3})^N \\ (-\frac{1}{3})^N & -\frac{4(1-\lambda)^2}{9}(1-\frac{8\lambda}{9})^N & -\frac{4(1-\lambda)}{9}(-\frac{1}{3}+\frac{4\lambda}{9})^N & -\frac{4(1-\lambda)}{9}(-\frac{1}{3}+\frac{4\lambda}{9})^N \\ (-\frac{1}{3})^N & -\frac{4(1-\lambda)}{9}(-\frac{1}{3}+\frac{4\lambda}{9})^N & -\frac{4(1-\lambda)^2}{9}(1-\frac{8\lambda}{9})^N & -\frac{4(1-\lambda)}{9}(-\frac{1}{3}+\frac{4\lambda}{9})^N \\ (-\frac{1}{3})^N & -\frac{4(1-\lambda)}{9}(-\frac{1}{3}+\frac{4\lambda}{9})^N & -\frac{4(1-\lambda)}{9}(-\frac{1}{3}+\frac{4\lambda}{9})^N & -\frac{4(1-\lambda)^2}{9}(1-\frac{8\lambda}{9})^N \end{pmatrix}. \quad (4.5.16)$$

For any $\lambda > 0$, the string order goes to zero instantaneously (with a single time-step, application of \mathcal{E}) in the limit $N \rightarrow \infty$. This is because, in contrast to the SS channel, this WS channel receives an exponential contribution to its decay from the bulk of the string.

Master equation simulation of string order

We simulate the time-evolved master equation on pure SPT states by acting with the channel at each time-step

$$\mathcal{E}_t = \mathcal{E}_T \circ \dots \circ \mathcal{E}_{t_1} \circ \mathcal{E}_{t_0}. \quad (4.5.17)$$

Figure 4.2 depicts the results of simulating the evolution of the s_{zz} component of the string order parameter under the following channels: the dephasing channel (4.5.12) with $\lambda = 0.5$, the dephasing channel with $\lambda = 1$ (fully dephasing), and the depolarising channel (4.5.11). The first two of these channels are SS, while the third is only WS. The first exhibits slow decay, while the others exhibit instantaneous decay.

The reason that the fully dephasing channel fails to preserve SPT order despite being SS can be traced to how it annihilates the end operators S_i with nontrivial

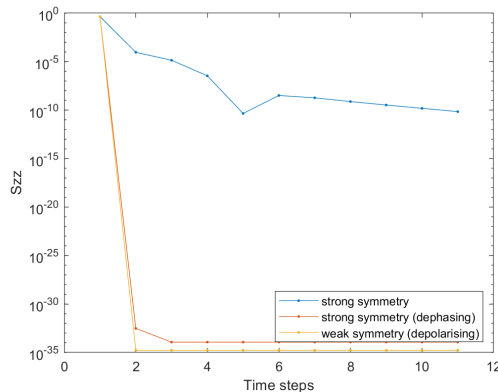


Figure 4.2: Evolution of the s_{zz} component of the $\mathbb{Z}_2 \times \mathbb{Z}_2$ string order parameter for the AKLT state.

labels and thus sets the corresponding rows of the pattern of zeros to zero. This phenomenon cannot occur for finite time evolutions, as these channels are invertible as linear maps, so [Theorem 1](#) is safe. The fully dephasing channel, however, is only realized as an *infinite* time evolution, so SS is insufficient to protect SPTO.

Let's show that the fully dephasing channel really corresponds to an infinite time evolution. First, notice that all end operators corresponding to a non-trivial α are annihilated by the channel, as the only operators it preserves are diagonal. Hence, the fully dephasing channel is not invertible since its Kernel is nonempty. Now we want to show that it is the fixed point of the dephasing channel describing infinite time evolution. First derive the Lindbladian \mathcal{L} that generates the channel $\mathcal{E}_t(\rho) = e^{t\mathcal{L}}(\rho)$, with $\lambda = 1 - e^{-t}$. Since

$$\mathcal{L}(\rho) = \frac{\partial \rho}{\partial t} \Big|_{t=0} = \lim_{\delta t \rightarrow 0} \frac{\mathcal{E}_{\delta t}(\rho) - \rho}{\delta t},$$

and performing an expansion of the fully dephasing channel $\mathcal{E}_{\delta t}(\rho)$ in δt up to $O(\delta t^2)$, we can show that $\mathcal{L}(\rho) = \frac{1}{4} \sum_j N_j \rho N_j^\dagger$. Hence $\mathcal{L}(\rho)$ is given by the fully dephasing channel which is defined by $\lambda = 1$ corresponding to $t = \infty$ so $\mathcal{L}(\rho) = \mathcal{E}_{t=\infty}(\rho)$. This highlights that at infinite times, SS channels may destroy the SPT phase.

In [5.6](#), we discuss a genericness condition on SS channels, failed by the fully dephasing channel, that says whether or not they preserve SPTO.

4.5.3 Twisted sector charges

The SPTO of a state may alternatively be detected in the charges of its twisted sector states [\[263, 264\]](#). Consider a state on a closed chain, represented as an MPS

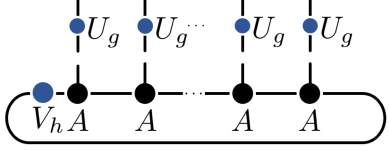
$$\langle i_1 \cdots i_L | \psi \rangle = \text{Tr} \left[A^{i_1} \cdots A^{i_L} \right], \quad (4.5.18)$$

with the symmetry represented projectively on the virtual space by operators V_g . The states

$$\langle i_1 \cdots i_L | \psi_h \rangle = \text{Tr} \left[V_h A^{i_1} \cdots A^{i_L} \right] \quad (4.5.19)$$

are the twisted sector states. In closed systems, they appear as ground states of the Hamiltonians obtained by twisting the original Hamiltonian by the insertion of a symmetry flux through the closed chain.

The charge of a twisted sector state is obtained by acting on the state with the charge operator $U_g^{\otimes L}$:



$$(4.5.20)$$

For simplicity, assume G is abelian. The charges of the twisted sector states are given by

$$\langle i_1 \cdots i_L | U_g^{\otimes L} | \psi_h \rangle = \text{Tr} \left[V_g^{-1} V_h V_g A^{i_1} \cdots A^{i_L} \right] = \frac{\omega(h, g)}{\omega(g, h)} \text{Tr} \left[V_h A^{i_1} \cdots A^{i_L} \right]. \quad (4.5.21)$$

As we saw in the previous subsection, this ratio ω/ω determines the cohomology class $[\omega]$. This means that the collection of twisted sector charges completely characterizes the SPTO.

The twisted sector charges of an initial state and the state reached by evolving by a channel are the expectation values of $U_g^{\otimes L}$ and $\mathcal{E}^\dagger(U_g^{\otimes L})$, respectively, on the initial twisted sector states $|\phi_h\rangle$. Since for a strongly symmetry channel (4.4.9) these are equal, such a channel preserves the SPTO.

4.5.4 Protected edge modes

SPT phases are also characterized by their topologically protected edge modes. Consider a pure state $|\psi^\omega\rangle$ in an SPT phase characterized by a cocycle ω . The SPT invariant is encoded in the projective action of the symmetry on the edge introduced by cutting the system:

$$(\mathbb{1}^l \otimes U_g^r) |\psi^\omega\rangle = \sum_a |\psi_{l,a}^\omega\rangle \otimes U_g^r |\psi_{r,a}^\omega\rangle = \sum_{a,b} (V_g)_{ab} |\psi_{l,a}^\omega\rangle \otimes |\psi_{r,b}^\omega\rangle, \quad V_g V_h = \omega(g, h) V_{gh}. \quad (4.5.22)$$

After evolving through a channel, $|\psi^\omega\rangle$ becomes a mixture of the (unnormalized) states $K_i |\psi^\omega\rangle$. We claim that, if the channel is strongly symmetric and onsite, each of these states has SPT invariant ω . To see this, write the Kraus operators as $K_i^l \otimes K_i^r$, so that $K_i |\psi^\omega\rangle = \sum_a K_i^l |\psi_{l,a}^\omega\rangle \otimes K_i^r |\psi_{r,a}^\omega\rangle$. Then, since K_i^r commutes with U_g^r , the projective representation V_g on this cut is the same as for $|\psi^\omega\rangle$; in particular, ω is the same.

4.5.5 Irrep probabilities and SPT complexity

In this section, we investigate the behavior of another probe of SPTO – the irrep probabilities that compose the inaccessible entanglement which we introduced

in Chapter 3 – under channels, strongly symmetric and not. Irrep probabilities measure the weight of the state in each symmetry sector. They are given by Fourier transforms of the string operators with identity end operators

$$p_\alpha = \frac{1}{|G|} \sum_g \chi_\alpha(g) \langle s(U_g, \mathbb{1}, \mathbb{1}) \rangle, \quad (4.5.23)$$

Using orthogonality of characters, one can confirm that the irrep probabilities sum to 1:

$$\sum_\alpha p_\alpha = \frac{1}{|G|} \sum_g \langle s(U_g, \mathbb{1}, \mathbb{1}) \rangle \sum_\alpha \chi_\alpha(g) = \frac{1}{|G|} \sum_g \langle s(U_g, \mathbb{1}, \mathbb{1}) \rangle |G| \delta_{g,1} = \langle s(\mathbb{1}, \mathbb{1}, \mathbb{1}) \rangle = 1, \quad (4.5.24)$$

We are now ready to formally introduce the *SPT complexity*. Irrep probabilities partially distinguish SPT phases by capturing their complexities

$$D_\omega = \sqrt{|G|/|K_\omega|}, \quad (4.5.25)$$

where

$$K_\omega = \{g : \omega(g, h) = \omega(h, g) \ \forall h\} \quad (4.5.26)$$

is subgroup of G called the *projective center*. Recall that a phase with $K_\omega = \{1\}$ has maximum complexity and is said to be *maximally noncommutative* (MNC) [240], which we introduced previously in Section §2.4.2. On the other end of the spectrum is the trivial phase $\omega = 1$, with complexity $D_1 = 1$. The complexity of a generic MPS was shown numerically to appear in the degeneracy D_ω^2 of the irrep probabilities [72]. In an MNC phase, the probabilities are all $p_\alpha = 1/|G|$ with degeneracy $|G|$; in the trivial phase, they are generically distinct. The value D_ω also appears as the degree of the projective representation V_g (c.f. [172], theorem VI.6.39), which means D_ω^2 is the number of topologically protected edge modes. For a given symmetry G , there may be multiple phases with the same complexity and these cannot be distinguished from each other by their irrep probabilities; nevertheless, because they can distinguish phases with different complexities, irrep probabilities are a useful tool.

The values of the irrep probabilities are preserved by strongly symmetric channels. To see this, observe that such channels preserve that the string operators $s(U_g, \mathbb{1}, \mathbb{1})$, and therefore their Fourier transforms, exactly. The exact preservation of irrep probabilities stands in contrast with general string order parameters, whose end operators $\mathcal{O}_\alpha \neq \mathbb{1}$ may cause decay toward zero in infinite time.

In contrast with strongly symmetric channels, non-SS Lindbladian channels map all irrep probabilities to the maximally degenerate values $p_\alpha = 1/|G|$, for any phase. This is because, as was established in 4.5.1, such channels annihilate all of the string order parameters except for those with $g = 1$. The result is

$$p_\alpha = \frac{1}{|G|} \sum_g \chi_\alpha(g) \delta_{g,1} = \frac{1}{|G|}. \quad (4.5.27)$$

This means that, outside of states which already have maximally degenerate irrep probabilities (for example, states in MNC phases), the effect of a Lindbladian

channel on irrep probabilities is a diagnostic for whether or not a channel is strongly symmetric. In 5.6.2, we discuss non-Lindbladian channels, some of which preserve irrep probabilities and complexity despite not being SS.

4.6 Causal channels

Let us extend our analysis from uncorrelated noise to causal channels. A channel is said to be *causal* if there is a range r such that it maps operators supported on a compact region A to operators supported on the region of sites within distance r of A [125].⁹ Channels that are not causal can create long-range correlations, and so are expected to destroy topological order and SPTO, no matter the symmetry condition imposed on them. For this reason, we will not consider non-causal channels here.

A subset of causal channels, labeled “dQC” in Ref. [125], have purifications that are causal. In addition, one can consider their convex combinations, which are also causal. It has been suggested that these convex combinations might constitute all causal channels, but this remains an open question [125]. Another open question is whether every channel in dQC that has a symmetric purification (and so by Claim (4.4.13) is weakly symmetric) has a purification that is *both* causal and symmetric with respect to an on-site symmetry. Rather than attempting to answer this question, we let “sdQC” denote the channels with such a purification. We restrict our focus to channels in dQC (in 4.6.1) and sdQC (in Section §4.6.2 and 4.6.3) and leave open the possibility that channels outside of these classes exhibit different behaviors. As we remark in 4.6.4, our expectation is that only channels in these classes are relevant to local Lindbladian evolution.

Low depth circuits of local unitary gates are a special class of unitary causal channels. Causal unitaries have a topological index¹⁰ that takes values $\log(p/q)$ for natural numbers p, q , capturing the flow of information to the left and to the right [267], and low depth circuits of local unitary gates are precisely the causal unitaries for which this topological index vanishes. From the perspective of phase classification, circuits are the only causal unitaries one should care about, as they approximate fast local unitary evolution. Nevertheless, it is most convenient for us to work with causal unitaries in general – forgetting whether or not they are circuits – because causal unitaries have convenient tensor network representations (which we will describe shortly). Similarly, a special class of causal channels is given by low depth circuits of local channels.¹¹ It may be the case that these are the causal channels which approximate fast local Lindbladian evolution, just as unitary circuits do for unitary evolution, and that they are in dQC and are characterized by a vanishing topological index of their purification. We do not attempt to prove

⁹The terms “causal” and “locality-preserving” have different meanings in Ref. [125], and we are interested in the former.

¹⁰This index may be computed locally from the tensor of the MPU discussed below [265, 266].

¹¹By this, we mean that the channel consists of a small number of layers of disjoint channels supported on small intervals.

this conjecture. Regardless, our analysis considers causal channels in general, even if most of them are unrelated to Lindbladian evolution.

4.6.1 Tensor network representations of causal channels

Causal unitary operators, which in this context are the purifications of channels in dQC, have finite bond dimension tensor network representations called matrix product unitaries (MPUs) [265, 266]:

$$W = \cdots \text{---} \square \text{---} \square \text{---} \square \text{---} \square \text{---} \square \text{---} \cdots \quad (4.6.1)$$

Here, unlike in the previous section, we simplify the analysis by restricting to channels that are translation invariant, which means that the tensor network representations of their purifications consist of the same tensor at every site. We expect, however, that our results hold without this assumption.

The theory of MPUs says that there exists a length $r \leq \delta^4$ (where δ is the bond dimension of W) such that on blocks of r sites, the tensor satisfies the following “simpleness relations” [265]:

$$\begin{array}{c} \square \cdots \square \\ \vdots \\ \square \cdots \square \end{array} \Big|_{\substack{r \\ r}} = \begin{array}{c} \square \cdots \square \\ \vdots \\ \square \cdots \square \end{array} \Big|_{\substack{r \\ r}} \bullet \Lambda \begin{array}{c} \square \cdots \square \\ \vdots \\ \square \cdots \square \end{array} \Big|_{\substack{r \\ r}}, \quad \begin{array}{c} \square \cdots \square \\ \vdots \\ \square \cdots \square \end{array} \Big|_{\substack{r \\ r}} \bullet \Lambda = \left| \begin{array}{c} \cdots \\ \vdots \\ \cdots \end{array} \right|_{\substack{r \\ r}}, \quad (4.6.2)$$

where Λ denotes the right fixed point of the MPU transfer matrix.

The fact that the causal unitaries have tensor network representations means that channels in dQC do as well. The Kraus operator K_i is realized as the matrix product operator obtained by plugging in the ancilla state $|a\rangle = \otimes_s |a_s\rangle$ (take all a_s to be the same) and the ancillary space basis vector $|e_i\rangle = \otimes_s |e_{i_s}\rangle$:

$$K_i = \text{---} \square \text{---} \square \text{---} \square \text{---} \square \text{---} \square \text{---} \cdots \text{---} \square \text{---} = \text{---} \square \text{---} \Big|_{\substack{i_s \\ a}} \quad (4.6.3)$$

Then, in terms of the tensors for the Kraus operators, the simplicity relations become

$$\begin{array}{c} \square \cdots \square \\ \vdots \\ \square \cdots \square \end{array} \Big|_{\substack{r \\ r}} = \begin{array}{c} \square \cdots \square \\ \vdots \\ \square \cdots \square \end{array} \Big|_{\substack{r \\ r}} \bullet \Lambda \begin{array}{c} \square \cdots \square \\ \vdots \\ \square \cdots \square \end{array} \Big|_{\substack{r \\ r}}, \quad \begin{array}{c} \square \cdots \square \\ \vdots \\ \square \cdots \square \end{array} \Big|_{\substack{r \\ r}} \bullet \Lambda = \left| \begin{array}{c} \cdots \\ \vdots \\ \cdots \end{array} \right|_{\substack{r \\ r}} \quad (4.6.4)$$

The uncorrelated noise considered in Section §4.5 appears here as the channels

whose MPUs have $\delta = 1$:

$$(4.6.5)$$

4.6.2 Local realization of the symmetry conditions

It will be demonstrated in the following subsections that a causal channel preserves SPTO if it satisfies not just the strong symmetry condition, but the strong symmetry condition *realized locally* (4.6.9). The present subsection is dedicated to describing what is meant by local realization of the symmetry conditions and to motivating it. We consider channels in the class sdQC we defined earlier, meaning that the causal purification is symmetric under acting with the symmetry operator $U_g \otimes U_g^A$ on every site.

As always, the symmetry conditions refer to how the Kraus operators transform under conjugation by a symmetry. If the Kraus operators do not decompose as products of uncorrelated terms, we must work out what these global conditions mean locally, in terms of their tensor network representation. Local properties of a symmetry action may be studied by cutting the spin chain into two halves, so that the purified channel decomposes as $W = \sum_{\mu} W_l^{\mu} \otimes W_r^{\mu}$, and acting with the symmetry on the right half:

$$(\mathbf{1}^l \otimes (U_g \otimes U_g^A)^r) W (\mathbf{1}^l \otimes (U_g \otimes U_g^A)^r)^{\dagger} = \sum_{\mu, \nu} (Q_g)_{\mu\nu} W_l^{\mu} \otimes W_r^{\nu}. \quad (4.6.6)$$

The operators Q_g are defined up to redefinition by phases and form a projective representation: $Q_g Q_h = \nu(g, h) Q_{gh}$. By folding the MPU representing the purification W into a normal MPS [265] and applying the usual arguments [76, 77], it can be shown that the Q_g satisfy¹²

$$(4.6.7)$$

In particular, when the channel is SS, we have $U_g^A = \mathbf{1}$, so the Kraus operators satisfy

$$(4.6.8)$$

¹²The version of the Fundamental Theorem of MPS in Theorem IV.4 of Ref. [77] can be used to show that this condition holds not just on blocks of size r but on individual sites; however, we will not require this stronger condition in our arguments.

We note that symmetric MPUs have been studied previously [268].

Now we can state the condition of local realization of the symmetry:

$$\boxed{Q_g Q_h = Q_{gh}, \quad \forall g, h, \quad \text{up to redefinition by phases.}} \quad (4.6.9)$$

Under redefinition of Q by phases, the cocycle ν that captures the projectivity of Q shifts by a coboundary, so local realization is the condition that $[\nu]$ is trivial in cohomology. In the case of uncorrelated noise, the symmetry conditions are automatically realized locally because Q acts on a one-dimensional space. When a channel is WS or SS and its symmetry is realized locally, we say it is “locally-WS” or “locally-SS”.

To build intuition for local realization, let us see that it is satisfied by the circuits of symmetric gates that define phase equivalence for states of closed systems. For a circuit, symmetry of the gates means that Q can be extracted from a single gate by acting on half of its legs with the symmetry g :

$$(4.6.10)$$

Since the adjoint action of U_g on half of the gate is a linear (non-projective) representation, Q is linear as well. More generally, consider the circuits of local channels that were mentioned briefly above. In analogy to the condition that the unitary gates are symmetric, these local channels can be made to satisfy the weak or strong symmetry condition. If they satisfy the WS or SS condition, the argument we just used for unitary circuits demonstrates that the causal channel as a whole is locally-WS or locally-SS, respectively.

4.6.3 String operators

Let us generalize Lemma 1 of 4.5.1 to causal channels by showing the following lemma.

Lemma 2: *A channel in sdQC maps string operators to sums of string operators of the same type (g, α) if and only if the channel satisfies the local strong symmetry condition.*

Doing so requires working with a slight generalization of string operators where the end operators are supported intervals, rather than sites. It is assumed that the system size and the length of the string are large compared to the length of these intervals and the range r of the channel.

After evolution by the channel, the string operator (2.4.10) becomes

$$(4.6.11)$$

If the SS condition is satisfied, the symmetry pulls through at the cost of operators Q_g :

$$(4.6.12)$$

which cancel except near the ends of the string. Then the simpleness relations (4.6.4) can be applied to obtain

$$(4.6.13)$$

This is a string operator with the symmetry g in the bulk. The new end operators are the result of acting on the original end operators by the superoperators (generalizing the $\mathcal{E}_{l,r}^\dagger$ of uncorrelated noise)

$$(4.6.14)$$

and are supported on $2r$ more sites than the original end operators. The superoperators \mathcal{S}_l^g and \mathcal{S}_r^g transform in the representations $h \mapsto \nu(g, h)/\nu(h, g)$ and

$h \mapsto (\nu(g, h)/\nu(h, g))^*$, respectively:

$$(4.6.15)$$

This means that, if and only if ν is trivial, as is the case when the symmetry condition is locally realized, the new end operators $\mathcal{S}_{l,r}^g(\mathcal{O}_\alpha^{l,r})$ transform in the same representations as the original ones $\mathcal{O}_\alpha^{l,r}$. We conclude that the evolved string operator is of type (g, α) if the channel satisfies the locally realized SS condition. Note that, in contrast with the case of uncorrelated noise, WS is not enough to ensure the correct transformation of the end operators. This is because the WS condition states only that the charge of operators is conserved *globally*. When correlations between sites are present, charge can flow between regions of the system, such as between the two end operators, changing their individual charges.

It remains to show the converse: that, assuming the evolved string operator (4.6.11) is a string operator of type (g, α) , the channel must have been locally SS. The string operator with bulk $U_g^{\otimes j'}$ evolves into

$$(4.6.16)$$

Compose it with $(U_g^\dagger)^{\otimes j'}$ on the string bulk and take the trace to obtain

$$(4.6.17)$$

neglecting the part of the tensor network outside the support of the evolved string. Meanwhile, doing the same to some string operator results in

$$(4.6.18)$$

where $j = j' - 2r'$ for r' the spread of the end operators under the channel (which turns out to be $r' = r$ due to SS). Setting (4.6.17) and (4.6.18) equal (by our assumption), and defining

$$\mathbb{E} := \text{diagram} \quad (4.6.19)$$

we find that $\langle \rho_\ell | \mathbb{E}^j | \rho_r \rangle = v d^j$ for some relative normalization $v \neq 0$, where $\langle \rho_\ell |$ and $| \rho_r \rangle$ are the boundary conditions imposed by the end operators in Eq. (4.6.17). Expressing \mathbb{E} in terms of its distinct nonzero eigenvalues λ_k , this amounts to the condition $\sum w_k \lambda_k^j = v d^j$ for all $j \geq 1$, which implies that there must be an eigenvalue $\lambda_1 = d$.¹³ On the other hand, considering the MPU W on a periodic ring of length N , we have – using Cauchy-Schwarz – that

$$\begin{aligned} \left| \sum_k \lambda_k^N \right| &= \left| \text{tr } \mathbb{E}^N \right| = \left| \text{Tr} [U_g^{\otimes N} W (U_g^{\otimes N})^\dagger W] \right| \\ &\leq \sqrt{\left| \text{Tr} [(U_g^{\otimes N} W (U_g^{\otimes N})^\dagger) (\dots)^\dagger] \right| \left| \text{tr} [W W^\dagger] \right|} = d^N. \end{aligned} \quad (4.6.20)$$

Thus, $\left| m_1 d^N + \sum_{k>1} \lambda_k^N \right| \leq d^N$ for all N , where $m_1 \geq 1$ is the multiplicity of $\lambda_1 = d$ and the $\lambda_{k>1} \neq d$ are the other eigenvalues. This implies that \mathbb{E} has one nondegener-

¹³First, note that by moving the $v d^j$ to the other side of the equation, one obtains $\sum w_k \lambda_k^j - v d^j = 0$ for all $j \geq 1$, and thus, one is left with showing the following

Lemma. *Given K distinct $\mu_k \neq 0$, then*

$$\sum_{k=1}^K c_k \mu_k^j = 0 \quad \forall j = J_0, \dots, K + J_0 - 1 \quad \Rightarrow \quad c_k = 0 \quad \forall k = 1, \dots, K. \quad (\star)$$

Proof. The matrix with entries $M_{jk} \equiv (\mu_k^j)_{jk}$ is the product of the diagonal matrix $\text{diag}(\mu_1^{J_0}, \dots, \mu_K^{J_0})$ with the Vandermonde matrix $(\mu_k^{j-J_0})_{jk}$, both of which are invertible. Thus, the linear system (\star) , $M \vec{c} = \vec{0}$, has the unique solution $c_k \equiv 0$. \square

Note that this also provides a concise proof of the often-used Lemma in the MPS literature that $\sum a_k^j = \sum b_k^j$ implies that the a_k and b_k must be pairwise equal.

ate eigenvalue $\lambda_1 = d$, and all other eigenvalues are 0.¹⁴ Thus, the Cauchy-Schwarz inequality (4.6.20) is saturated, which implies that $U_g^{\otimes N} W (U_g^{\otimes N})^\dagger = e^{i\phi} W$, which is to say that the channel with purification W is strongly symmetric. To see that the SS condition is realized locally, apply the ‘if’ direction to obtain the evolved end operators. By assumption, they transform in the same irrep α as the initial end operators; therefore, the local-SS condition $[\nu] = 0$ must hold.

4.6.4 Preservation of string order by strongly symmetric Lindbladians

The preservation of string operators by locally-SS channels in sdQC (Lemma 2) means that we can state the following analogue to Theorem 1, where short times are times that are small compared to the system size.

Conjecture: *Evolution generated by a local Lindbladian preserves SPTO at short times if and only if the Lindbladian is strongly symmetric.*

The conjecture is inspired by a plausible connection between local Lindbladians and causal channels. Just as local unitary evolution is approximated by locally-symmetric causal unitaries (in particular, circuits of symmetric local unitary gates) precisely when the generating Hamiltonian is symmetric, we expect that

$$\begin{aligned} \text{Evolution by a local Lindbladian is approximated by} \\ \text{locally-WS/SS channels in sdQC precisely when the} \\ \text{Lindbladian is WS/SS.} \end{aligned} \tag{4.6.21}$$

Let us motivate this statement nonrigorously. Local Lindbladian evolution is subject to Lieb-Robinson bounds [4], so we expect it to be described by causal channels (with range r linear in time), up to exponentially small errors outside of the lightcone. Moreover, we expect such causal channels to live in dQC since nontrivial convex combinations of channels in dQC (which plausibly are arbitrary causal channels [125]) seem to introduce unphysically long-range correlations. We established in 4.4.4 that WS/SS of a Lindbladian implies WS/SS of the channels it generates, but the question remains whether locality of the symmetric Lindbladian implies that the channel is in sdQC and that the symmetry of the channel is locally realized. As mentioned previously, it may be the case that causal channels approximating local Lindbladian evolution are circuits of local channels, just as causal unitaries approximating local unitary evolution are circuits of local unitaries, and that these local ‘gates’ are WS/SS precisely when the generating Lindbladian is WS/SS. Then an argument like Eq. (4.6.10) would translate the symmetry of the gates into locally realized symmetry of the channel.

¹⁴To see this, write $\lambda_k = e^{2\pi i \xi_k} |\lambda_k|$, and fix $M = 8^K$. Dirichlet’s approximation theorem states that there are integers p_k and $1 \leq q \leq M$ such that $|\xi_k - p_k/q| \leq 1/(qM^{1/K})$. Then, $|2\pi(q\xi_k - p_k)| \leq \pi/4$, and thus $\text{Re}[(e^{2\pi i \xi_k})^q] > 0$. It follows that $\text{Re}[\sum_{k>1} \lambda_k^q] > 0$ and thus $|m_1 d^q + \sum_{k>1} \lambda_k^q| > d^q$, unless $m_1 = 1$ and there are no other nonzero eigenvalues $\lambda_k \neq 0$.

Taking the statement (4.6.21) for granted and neglecting the issue of approximation, the ‘if’ direction of the conjecture follows from Lemma 2. The strongly symmetric local Lindbladian generates locally-SS channels in sdQC, which by Lemma 2 preserve the types of string operators and therefore their patterns of zeros with generic end operators. The short time of the evolution is a crucial assumption, as it was necessary in Lemma 2 that the ranges of the causal channels were small compared to the string length; otherwise, the bulks of the strings were swallowed up by the end operators. The ‘only if’ direction of the conjecture might require analyzing the transfer matrix of the expectation value of the evolved string operator, as in 4.5.1.

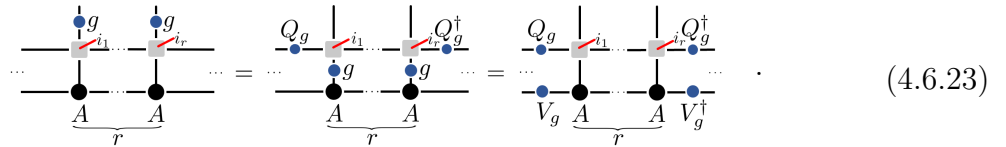
4.6.5 Protected edge modes

As in 4.5.4, consider a pure state $|\psi^\omega\rangle$ in an SPT phase characterized by the invariant ω . Under the channel, it evolves into a mixture of states $K_i|\psi^\omega\rangle$. The SPT invariant will be obtained by cutting the system into left and right halves and acting on the right half by the symmetry. Across the cut, the state and Kraus operators decompose as $|\psi^\omega\rangle = \sum_a |\psi_{l,a}^\omega\rangle \otimes |\psi_{r,a}^\omega\rangle$ and $K_i = \sum_\mu K_{i,l}^\mu \otimes K_{i,r}^\mu$. The SS condition means that Eq. (4.6.6) holds. Therefore, the states in the mixture transform as

$$(\mathbb{1}^l \otimes U_g^r)K_i|\psi^\omega\rangle = \sum_{a,b,\mu,\nu} (V_g)_{ab}(Q_g)_{\mu\nu}K_{i,l}^\mu|\psi_{l,a}^\omega\rangle \otimes K_{i,r}^\nu|\psi_{r,b}^\omega\rangle, \quad (4.6.22)$$

so their SPT invariants are captured by the projectivity class $[\omega\nu]$ of $V \otimes Q$. If the SS condition is realized locally, $[\nu]$ is trivial, so the SPT invariant $[\omega\nu] = [\omega]$ is unchanged.

This argument has a simple diagrammatic representation when the state $|\psi^\omega\rangle$ is an MPS. In this case, the MPO tensor for K_i is contracted with the MPS tensor for $|\psi^\omega\rangle$ to obtain an MPS tensor for $K_i|\psi^\omega\rangle$. The virtual space of the new MPS tensor has symmetry action $V \otimes Q$ on blocks of size r .



Crucial to the preservation of protected edge modes is the fastness assumption, which means that the range r of the MPO is small compared to the system size; without it, there is no invariant to be extracted locally.

4.7 Discussion & Conclusions

Our main result is to show that SPTO is preserved by fast evolution of a local Lindbladian precisely if the Lindbladian satisfies a strong symmetry condition; in other words, SPTO is robust to coupling to an environment if and only if

the coupling is strongly symmetric. There are at least two ways to interpret this finding. First, it may be taken simply as a rule for determining how order parameters such as string order will transform under a coupling of interest: rather than calculate the full dynamics of a system, one need only look at the symmetry of its generator. Second, the result may be taken as motivation for strong symmetry as the appropriate symmetry condition for classifying symmetry protected phases of open systems. Just as the Lindbladian phase equivalence of Ref. [4] was designed so that local observables are analytic within phases, the strong symmetry condition is chosen so that SPT order parameters are constant within phases.

We have focused on a special class of mixed states: coherent SPT mixtures. These are mixed states that, according to the phase diagram defined by strongly symmetric evolution, lie in the same phase as some pure SPT state and share its SPT invariant $[\omega] \in H^2(G, U(1))$. A question left for the future is what the rest of the phase diagram looks like in one dimension. It would also be interesting to study strong symmetry of SPT phases in higher dimensions, for example with the use of membrane string order in 2D [269]. Another relevant question is whether [Theorem 1](#) (for SPTO) can be extended to phases protected by general symmetries. A classification of the 1D phases protected by matrix product operator symmetries has recently been given in Ref. [166].

As a separate result, we determined how causal channels, including those not generated by Lindbladians, interact with SPTO. We found that those satisfying twisted symmetry conditions map between coherent SPT phases, sometimes decreasing but never increasing their complexity. Since the complexity of an SPT phase determines its computational power in measurement-based quantum computing [243], it would be interesting to study twisted strongly symmetric channels as equivalence relations for a resource theory.

This research raises several other questions for future investigation. Firstly, since string orders are experimentally tractable [71, 107], one can ask how to detect mixed state SPTO in experiment. Secondly, our work considers SPTO at finite time, as at infinite times fingerprints of SPTO such as string order get washed out. This raises the question of whether coherent SPT mixtures arise as steady states of Lindbladians. Also, what are the implications of our findings for SPTO at finite temperature? This would clarify further the nature of SPT mixed states. And finally, it would be interesting to explore further how our findings relate to other properties of SPT phases, their boundaries and transitions, as studied in previous work [4, 68, 256].

Chapter 5

Transmuting symmetry protected topological phases under quantum channels

This Chapter contains the second part of the publication

- Symmetry Protected Topological Order in Open Systems **Caroline de Groot**, Alex Turzillo, and Norbert Schuch. arXiv:2112.04483v2 [73]

5.1 Motivation

Order parameters are key to our understanding of phases of matter. Not only do they enable the classification of phases by labeling them with invariants [84, 120, 176, 270], but they also allow the study of phase transitions [92–95]. The classification of phases and phase transitions are topics which are two sides of the same coin; the former tells us about properties within the boundary of an equivalence class, while the latter provides information about the nature of the boundary itself. In phase transitions of gapped quantum phases, demarcating critical points has long been a core goal in condensed matter physics. Importantly, order parameters, and in particular their correlations, play a major role. Correlations give a complete characterisation of the phase transition, since at the critical point all typical correlation lengths of the system diverge exponentially with some particular critical exponent [271]. In Landau-type order, phase transitions are enacted through spontaneous symmetry breaking by tuning parameters in the system Hamiltonian.

However in gapped phases without symmetry-breaking, different mechanisms for phase transitions are possible. To be precise, we introduce the more general term of “phase transmutation”, which is a mapping between two phases but does not imply anything about closure of the gap. This differs from “phase transition” which is conventionally meant to be synonymous with gap closure. This phenomenon occurs in symmetry protected topological (SPT) phases, where one may transform from one phase to another either by operations which preserve the symmetry protecting

the SPT phase and cause a gap closure (a phase transition)¹ or by operations which break that symmetry but do not cause gap closure (a phase transmutation). SPT phase transmutations (with or without gap closure) may be characterised by certain invariants of the phase, such as string order parameters and inaccessible entanglement [272–274].

By contrast, the SPT phase transmutations of mixed states have been relatively unexplored (in part because a more thorough understanding of open systems topological order has been lacking until recently [4, 73]). Dissipation has long been considered the enemy of quantum phases since it causes decoherence; coherence being taken to mean the nontrivial entanglement patterns which are necessary to have in a nontrivial phase. It is therefore perhaps surprising that dissipation can actually be harnessed as a resource, countering previous intuitions. Namely, dissipative processes can be used to prepare relevant classes of states which are ground states of frustration-free Hamiltonians, such as matrix product states [254, 255] and PEPS [275], which describe graph states, and certain topological codes such as the Levin-Wen string-net models or Kitaev quantum double models. This has even led to a new form of quantum computation called dissipative quantum computation [275], which can be considered robust since the evolution can be chosen such that the steady state is the desired outcome of the computation, which is a stable point of the evolution. Given that dissipation has been found to engineer interesting quantum phases, creating coherence, we might expect that such dissipation can be described systematically.

The main question we address here is: *is there a framework to describe the SPT phase transmutations of mixed states?* This would give an outline of the phase boundaries of SPT mixed states, as well as shed light on their physical properties. We consider which operations transform between different SPT phases in the open system setting, as witnessed by order parameters. In Chapter 4 we previously we asked which equivalence relations map between states in the same phase by preserving the same invariants (order parameters). The answer is that strongly symmetric channels preserve SPTO. We now consider building from the framework of Chapter 4 to describe SPT phase transmutations in open systems. In particular, we address which channels map between states in different SPT phases.

We confirm that dissipation can be structurally interesting in the open system setting by giving a systematic description of operations which transform between particular SPT phases by breaking symmetries. The prescription for transmuting² between SPT phases follows the rules of group theory which determine precise patterns of entanglement. As suggested in [4], we show that the entanglement pattern may only be changed according to particular rules. We visualise how a pattern of entanglement may be broken down in Fig. 5.1 by an interplay between symmetry and entanglement. This finding is the open systems equivalent of symmetry-breaking unitary circuits which can transform between pure state SPT

¹Further, SPT phase transitions exist in three different kinds, either continuous quantum critical points, first order phase transitions, or spontaneous symmetry breaking [95].

²We do not consider whether *transmutation* can be considered on the same footing as SPT phase *transition*, and leave this problem open.

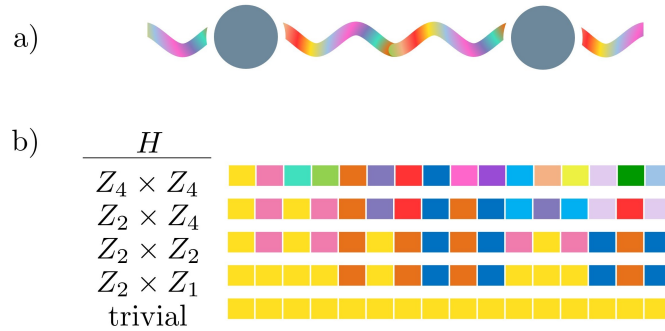


Figure 5.1: a) Visualising a “pattern of entanglement” encoded in the virtual degrees of freedom of TN states. The rainbow wavy lines depict entangled bonds between two sites. b) Colours encode the symmetry group $G = \mathbb{Z}_4 \times \mathbb{Z}_4$ in a bond. All of its subgroups $H \subset G$ are also valid patterns. Twisted strongly symmetric channels may map to simpler patterns which are already encoded in the state, which is visualised by mapping certain colours to other colours. They may not generate new colours, nor can they increase the complexity of patterns.

orders [276].

5.2 Summary

We extend our analysis of SPTO in open systems to the scenario where the noise does not commute with the symmetry but rather acts by exchanging symmetries, either permuting them or identifying their group actions. We term channels with this property *twisted strongly symmetric*. We introduce versions of the symmetry conditions introduced in the previous Chapter that are twisted by an endomorphism $\sigma : G \rightarrow G$ of the symmetry group. The twisted conditions are stated in Eqs. (5.5.1), (5.5.2), and (5.5.3).

In the case of permutation of symmetries, we demonstrate that the noise acts by permuting SPT phases with the same complexity, and otherwise the noise reduces complexity (Theorem 2). Symmetric channels with a nontrivial twist cannot be generated by continuous evolution by a symmetric Lindbladian in finite time; in other words, for σ that are not identity-connected (every nontrivial σ when G is finite and all but those of the form (4.5.6) otherwise [262]), channels twisted by σ are not generated by continuous symmetric Lindbladian evolution in finite time. These channels therefore describe infinite time evolution (for example in §5.6.3) and discrete noise.

First we discuss an action of group endomorphisms σ on the SPT invariant $[\omega]$ in Section §5.3. Then we argue in Theorem 2 that σ -twisted SS channels have the effect of changing the SPTO according to this action. In particular, when an endomorphism σ does not change $[\omega]$, channels satisfying the σ -twisted SS condition preserve the phase with invariant $[\omega]$. This allows us to answer a question we had previously deferred – of the *necessary* condition for a channel to preserve a given SPTO. The answer is that the channel must be a mixture of σ -twisted SS

channels for σ that fix the SPTO. We also discuss the general situation where a channel does not preserve the phase but rather transmutes it into one of equal or lesser complexity. We illustrate several examples for allowed different SPT phase transformations, and illustrate the general case in Fig. 5.2.

We investigate this in terms of the inaccessible entanglement which was introduced in Chapter 3, and find that the degeneracy of the inaccessible entanglement depends on both the initial phase and the endomorphism σ . In other words, order parameters reflect the changed SPT order that is brought about by the channel which is twisted strongly symmetric by the twist σ .

5.3 The action of endomorphisms on SPT phases

Here we collect necessary facts about endomorphisms as they relate to SPT phases. An endomorphism $\sigma : G \rightarrow G$ acts on the cocycle ω as a pullback. Concretely this means

$$\sigma : \omega \mapsto \sigma^* \omega, \quad (\sigma^* \omega)(g, h) = \omega(\sigma(g), \sigma(h)). \quad (5.3.1)$$

The action of endomorphisms has the following property:

$$\textit{An automorphism preserves the complexity of phases.} \quad (5.3.2)$$

This is because, if σ is an automorphism, the transformed projective center

$$K_{\sigma^* \omega} = \{ g : \omega(\sigma(g), \sigma(h)) = \omega(\sigma(h), \sigma(g)) \ \forall h \}. \quad (5.3.3)$$

equals $\sigma^* K_\omega$, since $\sigma(h)$ runs over the whole G , and this in turn is isomorphic to K_ω by σ^* . The converse to Claim (5.3.2) is false because noninvertible endomorphisms may also preserve complexity. As a counterexample, take any G, σ with $\omega = 1$. Less trivially, take $G = H_1 \times H_2$ and $\omega = P^* \omega_1$, where P projects onto H_1 and ω_1 is any cocycle on H_1 . The endomorphism $\sigma = P$ is not an automorphism, yet it fixes ω and its complexity. Despite the lack of a full converse, one can make the following weaker claim:

$$\textit{An endomorphism maps MNC phases, and only MNC phases, to MNC phases if and only if it is an automorphism.} \quad (5.3.4)$$

In other words, an endomorphism preserves the distinction between MNC and non-MNC phases precisely when it is an automorphism. The ‘if’ direction follows from Claim (5.3.2). To see the ‘only if’ direction, note that the kernel of σ is contained in $K_{\sigma^* \omega}$, so the MNC condition $K_{\sigma^* \omega} = \{1\}$ implies that $\ker \sigma = \{1\}$. The properties (5.3.2) and (5.3.4) appear in Figure 5.5 as constraints on the arrows between nodes. The special case of $G = \mathbb{Z}_{12} \times \mathbb{Z}_{12}$ is explored in complete detail in Figure 5.6.

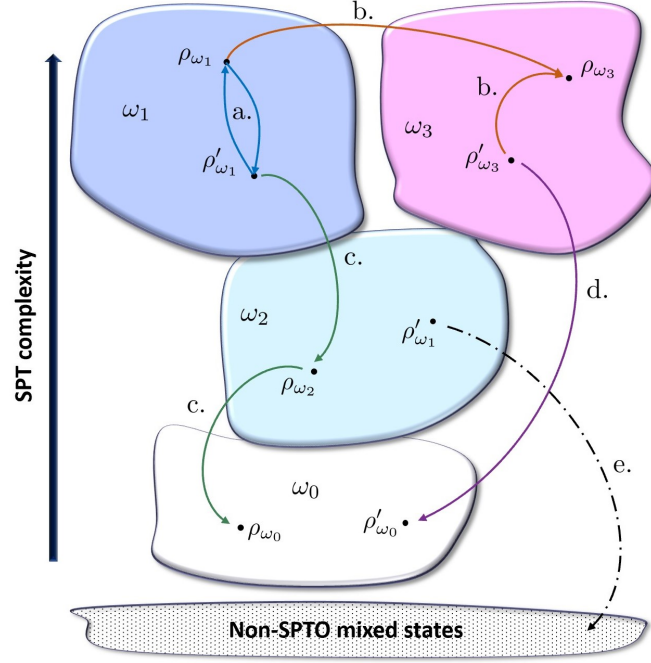


Figure 5.2: Five kinds of channels acting on the spaces of SPT phases. The four coloured lines map between SPT phases as they are twisted-SS, while the dotted line maps out of the manifold of coherent SPT states. These maps change patterns of entanglement.

Changing SPT phase by σ -SS

Which SPT phases get mapped between by σ -SS given a group $G = \mathbb{Z}_n \times \mathbb{Z}_n$? We will go through how to construct all allowed endomorphisms of SPT phases given a G of this kind. There are four classes of maps: SS, automorphism-twisted SS (which is not also SS), endomorphism-twisted (which is not also automorphism-twisted SS) and e -SS. The SS channels map an SPT phase to itself, which is given by multiplication by $1 \pmod n$, and e -SS maps all SPT phases to the trivial phase, which is given by multiplication by $0 \pmod n$. The depolarising channel (4.5.10) introduced in §4.5.2 is only WS, while the dephasing example (4.5.12) is e -SS. Automorphism-twisted SS maps SPT phases to different SPT phases with the same notion of complexity (same size of projective centre subgroup K_ω) which are generated by multiplication by $m \pmod n$ for $\gcd(m, n) = 1$, m coprime to n , and finally endomorphism-twisted SS maps SPT phases to phases with less complexity, which is generated by multiplication by $m \pmod n$ where $m \mid n$, m divides n .

To examine this more closely, we depict the possible maps given a group G by a directed graph. Each phase is represented by a vertex, and the possible maps are directed edges between vertices. The complexity of the phase will be given by the position in a tiered structure calculated by the projective centre K_ω , with lowest complexity at the bottom, which is always the trivial phase, and with highest complexity at the top.

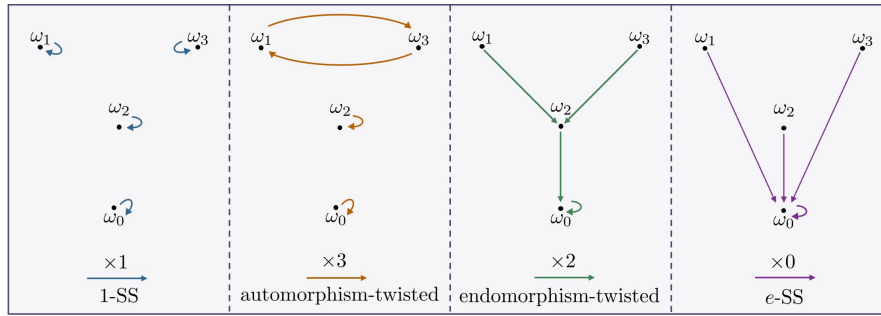


Figure 5.3: The allowed σ -SS maps with $G = \mathbb{Z}_4 \times \mathbb{Z}_4$ are endomorphisms between the four SPT phases ω_n , with n in \mathbb{Z}_4 , labelling the elements of the cohomology group. We indicate which tiers of SPT phases the four main classes of SS map between. SS is generated by multiplication $\times 1$, automorphism is generated by $\times 3$, endomorphism is generated by $\times 2$, and e -SS is generated by $\times 0$. The third tier are MNC phases, the second tier are non-MNC phases, and the first tier is the trivial phase, with the order of complexity dictated by the projective centre $|k|$.

Consider a first example, the maps between different phases of $G = \mathbb{Z}_4 \times \mathbb{Z}_4$ which are allowed under σ -SS channels, illustrated in Figure 5.3. There are four possible SPT phases: two MNC phase ($|K_{1,3}| = 1$), one non-MNC phase ($|K_2| = 4$), one trivial phase ($|K_0| = |G|$). We can immediately deduce that all σ -SS channels map between SPTOs given G , but while exact SPTO-preserving maps are SS, all other σ s map to different, but still valid SPTOs which are hosted by G . Automorphisms map between MNC phases, while endomorphisms always reduce the complexity of the SPT phase and e -SS takes all phases to trivial. For a physical example, consider a spin-1 system ($d = 3$), with representation of the symmetry which acts with a Kraus operator K_1 which takes the trivial irrep to itself, but K_2 permutes between the two elements.

In Figure 5.4 we consider a richer example, namely the endomorphisms of SPT phases given $G = \mathbb{Z}_8 \times \mathbb{Z}_8$. Then there are eight SPT phases: four MNC ($|k_{1,3,5,7}| = 1$), two non-MNC ($|k_{2,6}| = 16$), one non-MNC ($|k_4| = 32$), and one trivial phase ($|k_0| = |G|$). The allowed endomorphisms here are interesting as, since G is relatively large, this class can be subdivided into two by quantifying the reduction in complexity. The first type of endomorphism, given by $\times 2, \times 6$ maps down by maximally one tier such that only two of the seven non-trivial SPT phases can survive, whereas the second type, given by $\times 4$, maps down by maximally two tiers, which destroys all the non-trivial SPT order but one.

Let us examine in detail one of the most studied settings for investigations of one-dimensional SPT phases – that of symmetry group $G = \mathbb{Z}_n \times \mathbb{Z}_n$, where phases are classified by $H^2(G; U(1)) = \mathbb{Z}_n$.

Elements of $\mathbb{Z}_n \times \mathbb{Z}_n$ are “vectors” (w, x) with $w, x \in \mathbb{Z}_n$. Endomorphisms of $\mathbb{Z}_n \times \mathbb{Z}_n$ are matrices with entries in \mathbb{Z}_n that act on these vectors by matrix

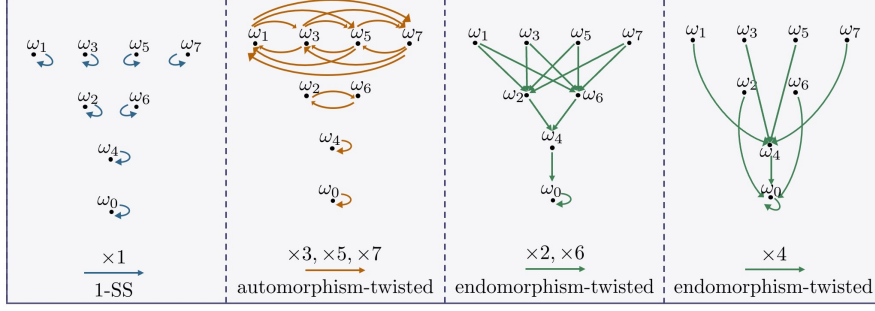


Figure 5.4: Similarly to Fig. 5.4, we calculate an example with $G = \mathbb{Z}_8 \times \mathbb{Z}_8$ for allowed σ -SS maps between SPT phases, which are labelled by ω_n with n in \mathbb{Z}_8 . Now two types of endomorphisms exist, one which maps down in complexity of SPT phase by one tier, and another that can map down by two tiers. Automorphisms preserve the complexity of the phase, while endomorphisms can have varying strengths to map to phases of lower complexity, either down one or two tiers. We omit the e -SS maps which are again generated by $\times 0$.

multiplication:

$$\text{End}(\mathbb{Z}_n \times \mathbb{Z}_n) = M_2(\mathbb{Z}_n) = \left\{ \begin{pmatrix} a & b \\ c & d \end{pmatrix} : a, b, c, d \in \mathbb{Z}_n \right\}, \quad (5.3.5)$$

$$g = \begin{pmatrix} w \\ x \end{pmatrix}, \quad \sigma(g) = \begin{pmatrix} a & b \\ c & d \end{pmatrix} \begin{pmatrix} w \\ x \end{pmatrix} = \begin{pmatrix} aw + bx \\ cw + dx \end{pmatrix}.$$

Automorphisms are those with invertible matrix, i.e. where the determinant $ad - bc$ is relatively prime to n .

Now let's discuss cocycles. The n classes of $H^2(\mathbb{Z}_n \times \mathbb{Z}_n; U(1)) = \mathbb{Z}_n$ are represented by cocycles

$$\omega_k[(w, x), (y, z)] = \exp\left(\frac{2\pi i}{n} k xy\right). \quad (5.3.6)$$

Note that $\exp\left(\frac{2\pi i}{n} (-k) wz\right)$ is cohomologous to ω_k by the coboundary of $\phi[w, x] = \exp\left(\frac{2\pi i}{n} wx\right)$ and that $\exp\left(\frac{2\pi i}{n} wy\right)$ and $\exp\left(\frac{2\pi i}{n} xz\right)$ are trivialized by $\phi[w, x] = \exp\left(\frac{2\pi i}{n} w\right)$ and $\phi[w, x] = \exp\left(\frac{2\pi i}{n} x\right)$, respectively.

An endomorphism σ on $\mathbb{Z}_n \times \mathbb{Z}_n$ induces an endomorphism σ^* on $H^2 = \mathbb{Z}_n$ as follows:

$$\begin{aligned} (\sigma^* \omega_k)[(w, x), (y, z)] &= \omega_k[\sigma(w, x), \sigma(y, z)] \\ &= \omega_k[(aw + bx, cw + dx), (ay + bz, cy + dz)] \\ &= \exp\left(\frac{2\pi i}{n} k (cw + dx)(ay + bz)\right) \\ &= \exp\left(\frac{2\pi i}{n} k (acwy + bcwz + adxy + bdxz)\right) \\ &\sim \exp\left(\frac{2\pi i}{n} k (ad - bc) xy\right) \\ &= \omega_{k(ad-bc)}[(w, x), (y, z)]. \end{aligned} \quad (5.3.7)$$

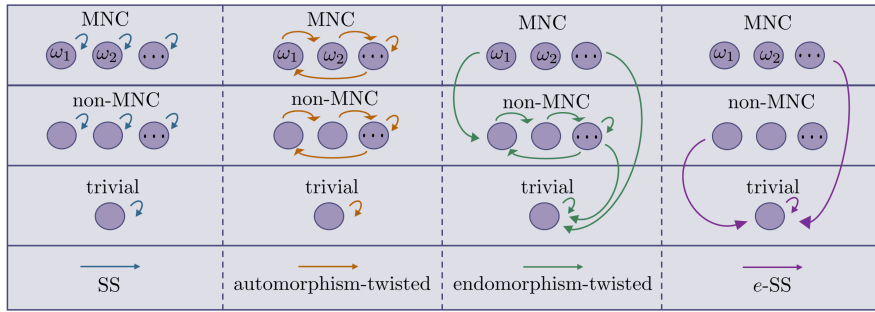


Figure 5.5: Phases ω appear as nodes and the action of endomorphisms σ as arrows between nodes. From left to right, the columns depict the identity endomorphism, automorphisms, noninvertible endomorphisms, and the constant endomorphism. In anticipation of the implementation of these endomorphism actions by twisted symmetric channels (c.f. §5.6), the columns are labeled by the corresponding symmetry conditions.

The penultimate line holds up to coboundaries. We conclude that the action of σ^* on the group of SPT phases is multiplication of the SPT index k by the determinant $(ad - bc)$ of σ .

Endomorphisms of \mathbb{Z}_n are given by multiplication by an element of \mathbb{Z}_n , while automorphisms are those where the multiplication is by a generator of \mathbb{Z}_n , i.e. by a number relatively prime to n . This means that σ^* is an automorphism of the group of SPT phases precisely when σ is an automorphism of G .

For example, the automorphism $\sigma(w, x) = (x, w)$ that exchanges the two factors has the effect of inverting SPT phases since it has determinant -1 . (For $n = 2$, inversion is the identity, so the two phases – trivial and Haldane – are fixed by the exchange automorphism.) On the other hand, the endomorphism $\sigma(w, x) = (w, e)$ that collapses the second factor to the identity has determinant 0, so it destroys all SPT phases.

Let us compute the projective center K_{ω_k} , the set of elements (w, x) such that

$$\exp\left(\frac{2\pi i}{n} k xy\right) = \omega_k[(w, x), (y, z)] = \omega_k[(y, z), (w, x)] = \exp\left(\frac{2\pi i}{n} k wz\right), \quad \forall (y, z), \quad (5.3.8)$$

i.e. such that $kxy \equiv kwz \pmod{n}$, $\forall y, z$. Taking $z = 0$ while varying y and vice versa, we find

$$K_{\omega_k} = \{(w, x) \in \mathbb{Z}_n \times \mathbb{Z}_n : k \cdot (w, x) \equiv 0\}. \quad (5.3.9)$$

In particular, when k is coprime to n , the projective center is trivial, so the cocycle ω_k is MNC. The invariant $(\det \sigma)k$ of the transformed phase is coprime to n precisely when k and $(\det \sigma)$ and both coprime to n ; that is, when the original phase is MNC and σ is an automorphism, in agreement with Claim 5.3.4.

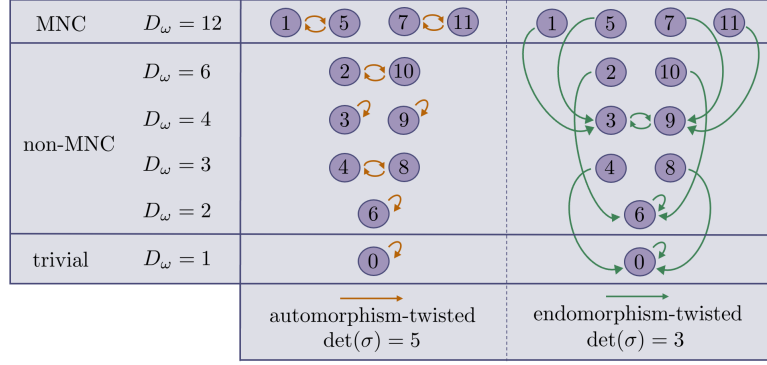


Figure 5.6: The 12 phases of the group $G = \mathbb{Z}_{12} \times \mathbb{Z}_{12}$ are depicted as nodes. Arrows represent the actions of two endomorphisms: on the left, an automorphism with $\det \sigma = 5$; on the right, a noninvertible endomorphism with $\det \sigma = 3$. Observe that the automorphism preserves complexity, as required by Claim (5.3.2), by preserving phases 3, 6, 9, 0 and exchanging the remaining phases with others of equal complexity. On the other hand, the noninvertible endomorphism reduces the complexity of all MNC phases (1, 5, 7, 11), as required by Claim (5.3.4) but nevertheless preserves the complexity of phases 3, 6, 9, even fixing phase 6.

5.4 Patterns of zeros under endomorphisms

Let G be abelian. The cocycle ω defines a “pattern of zeros” $\zeta_\omega : G \rightarrow G^*$ given by

$$\zeta_\omega : g \mapsto \chi_g^\omega(\cdot) = \frac{\omega(\cdot, g)}{\omega(g, \cdot)}. \quad (5.4.1)$$

The image is indeed linear characters (one-dimensional representations) since

$$\chi_g^\omega(h)\chi_g^\omega(k) = \frac{\omega(h, g)\omega(k, g)}{\omega(g, h)\omega(g, k)} = \frac{\omega(k, g)\omega(h, gk)}{\omega(g, h)\omega(hg, k)} \stackrel{\text{abelian}}{=} \frac{\omega(k, g)\omega(h, kg)}{\omega(g, h)\omega(gh, k)} = \frac{\omega(hk, g)}{\omega(g, hk)} = \chi_g^\omega(hk). \quad (5.4.2)$$

The kernel of ζ_ω is the projective center K_ω (4.5.26).

The pattern of zeros ζ_ω determines the cohomology class $[\omega]$ of the cocycle ω . To see this, note that the map $\omega \mapsto \zeta_\omega$ is a group homomorphism: $\zeta_{\omega_1}\zeta_{\omega_2} = \zeta_{\omega_1\omega_2}$; therefore, it suffices to check that its kernel consists of coboundaries. Suppose $\omega \mapsto 1$, i.e. $\omega(g, h) = \omega(h, g)$ for all g, h . Then any projective representation with class ω satisfies $V_gV_h = V_hV_g$. By Schur’s lemma, V_g must be proportional to the identity by a scalar $\lambda(g)$. Then ω is the coboundary of λ since

$$\lambda(g)\lambda(h)\mathbf{1} = V_gV_h = \omega(g, h)V_{gh} = \lambda(gh)\omega(g, h)\mathbf{1}. \quad (5.4.3)$$

It is convenient to represent a pattern of zeros ζ_ω as a two-dimensional array with columns indexed by group elements g and rows indexed by linear characters α . The entry (g, α) in this array is \star if $\zeta_\omega(g) = \chi_\alpha$ and zero otherwise. Since $\zeta_\omega(g)$ is a particular linear character, there is exactly one \star per column. The row indexed by α has either $|K_\omega|$ or zero \star ’s depending on whether χ_α is in the image

of ζ_ω . The rank of the array is $|G|/|K_\omega|$. For example, the two phases of symmetry $G = \mathbb{Z}_2 \times \mathbb{Z}_2$ have patterns of zeros

$$\zeta_{\text{trivial}} = \begin{pmatrix} \star & \star & \star & \star \\ 0 & 0 & 0 & 0 \\ 0 & 0 & 0 & 0 \\ 0 & 0 & 0 & 0 \end{pmatrix}, \quad \zeta_{\text{Haldane}} = \begin{pmatrix} \star & 0 & 0 & 0 \\ 0 & \star & 0 & 0 \\ 0 & 0 & \star & 0 \\ 0 & 0 & 0 & \star \end{pmatrix}, \quad (5.4.4)$$

with columns indexed by $g = (0, 0), (0, 1), (1, 0), (1, 1)$ and rows by α with $\frac{1}{\pi i} \log \chi_\alpha(w, x) = 0, w, x, w + x$. Now consider the action of an endomorphism σ . It acts on ω as Eq. (5.3.1) and on ζ_ω as

$$\sigma \cdot \zeta_\omega = \zeta_{\sigma^* \omega} : g \mapsto \chi_g^{\sigma^* \omega} = \sigma^* \chi_{\sigma(g)}^\omega. \quad (5.4.5)$$

This rule tells us how the array for ω transforms into the array for $\sigma^* \omega$:

$$\begin{aligned} & \text{For each group element } g, \text{ look up the unique row } \beta \text{ of the} \\ & \text{old pattern } \zeta_\omega \text{ such that the entry } (\sigma(g), \beta) \text{ is } \star. \text{ Then} \\ & \text{compose } \beta \text{ with } \sigma \text{ to obtain the row } \alpha \text{ of the new pattern} \\ & \sigma \cdot \zeta_\omega \text{ such that the entry } (g, \alpha) \text{ is } \star. \end{aligned} \quad (5.4.6)$$

Using this rule for transforming patterns of zeros, one can check the examples of endomorphisms introduced above. The exchange automorphism swaps the middle two rows and swaps the middle two columns, fixing both the trivial and Haldane patterns. On the other hand, the endomorphism that collapses the second factor copies the first the third columns, which have g in the image of σ , and moves their \star entries up according to σ ; the result is that both patterns are mapped to the trivial one.

The MNC property has a meaning in terms of patterns of zeros: the only column with a \star in the $\alpha = 1$ row is the $g = 1$ column. Claim 5.3.4 can be shown in this language. Consider the ‘if’ direction. We wish to find the entries $(g, 1)$ of the new pattern that are \star . If σ is an automorphism, these entries are the entries $(\sigma(g), (\sigma^{-1})^* 1) = (\sigma(g), 1)$ of the old pattern. Precisely when the old pattern is MNC, the only of these entries with \star is the one with $\sigma(g) = 1$ and so, since σ is an automorphism, $g = 1$ is the only solution and the new pattern is MNC. Consider the ‘only if’ direction. The entry $(\sigma(g), 1)$ of the old pattern is the entry $(g, \sigma^* 1) = (g, 1)$ of the new pattern. When the new pattern is MNC, it has a \star in this row only for $h = 1$. Precisely when the old pattern is MNC, it does only for $\sigma(g) = 1$, which means the new pattern does for all $h \in \ker \sigma$; therefore, precisely in this case do we have $\ker \sigma = \{1\}$, which is to say that σ is an automorphism.

5.5 Twisted symmetric channels

Having understood the action of group endomorphisms on phases, we turn to studying the channels that implement it. Here, we introduce twisted symmetry conditions and discuss the structure of Kraus operators of twisted symmetric channels. Later we will argue that the σ -SS condition implements the action of σ .

The σ -twisted weak symmetry (σ -WS) condition is

$$\mathcal{U}_g \circ \mathcal{E} \circ \mathcal{U}_{\sigma(g)}^\dagger = \mathcal{E} , \quad \forall g . \quad (\sigma\text{-twisted weak symmetry condition})$$

(5.5.1)

By setting the phases θ_i equal as before, we obtain the σ -twisted strong symmetry (σ -SS) condition:

$$U_g K_i U_{\sigma(g)}^\dagger = e^{i\theta(g)} K_i , \quad \forall i, g . \quad (\sigma\text{-twisted strong symmetry condition})$$

(5.5.2)

Using the argument from before but with $X = U_g$, $Y = e^{i\theta(g)} U_{\sigma(g)}$, we obtain the alternative statement

$$\mathcal{E}^\dagger(U_g) = e^{i\theta(g)} U_{\sigma(g)} , \quad \forall g . \quad (\sigma\text{-twisted strong symmetry condition})$$

(5.5.3)

The untwisted SS condition means that the channel decomposes as a sum of channels on irrep blocks, acting only within multiplicity spaces. A similar statement holds for σ -SS channels: each Kraus operator has a block decomposition $K_i = \bigoplus_{\alpha\beta} K_i^{\alpha\beta}$ such that the component $K_i^{\alpha\beta}$, which is a map from the multiplicity space of β to that of α , vanishes unless $\alpha = \sigma^* \beta$. This is because the σ -SS condition says that K_i maps to a space where g acts as $\sigma(g)$ did before mapping. This means the completeness condition on \mathcal{E} implies

$$\sum_i (K_i^{\sigma^* \alpha, \alpha})^\dagger K_i^{\sigma^* \alpha, \beta} = \sum_i (K_i^\dagger K_i)^{\alpha\beta} = \mathbf{1} \delta^{\alpha\beta} , \quad (5.5.4)$$

which in particular enforces a completeness condition on the channels

$$\mathcal{E}_\alpha(\rho) = \sum_i (K_i^{\sigma^* \alpha, \alpha})^\dagger \rho K_i^{\sigma^* \alpha, \alpha} . \quad (5.5.5)$$

When σ is not an automorphism, each term $K_i^\dagger K_i$ may have off-diagonal components: K_i maps α to $\sigma^* \alpha$, which K_i^\dagger maps back to any β in the preimage. Eq. (5.5.4) implies these must cancel in the sum.

Extending the untwisted class sdQC of causal channels, one can define σ -sdQC as the set of channels with a purification that is both causal and σ -twisted symmetric under an on-site symmetry. The folded MPS of the MPU representing the purification has a symmetry $U_g \otimes U_{\sigma(g)}^\dagger \otimes U_g^A \otimes (U_{\sigma(g)}^A)^\dagger$, which defines a projective representation Q . Local realization of the symmetry is again the condition that Q is linear.

While strong symmetry twisted by an automorphism is possible in reversible channels, strong symmetry twisted by a noninvertible endomorphism is not.³ To see this, suppose g belongs to the kernel of σ . Then the single Kraus operator K of the reversible channel satisfies $K^\dagger U_g K = \mathbf{1}$, but this implies $U_g = \mathbf{1}$, so $g = 1$ by

³A stronger statement also holds: noninvertible twists are impossible not just in reversible channels but in all channels that are invertible as linear maps. To see this, note that \mathcal{E}^\dagger annihilates $U_g - \mathbf{1}$ for $g \in \ker \sigma$ and that \mathcal{E} is invertible iff \mathcal{E}^\dagger is.

faithfulness. In light of [Theorem 2](#) (below), this means that reduction of complexity – as opposed to change of phase at a fixed complexity level – is a phenomenon unique to irreversible channels. On the other hand, any automorphism can be realized by a reversible channel: let U_g contain one copy of each irrep and let K be the permutation matrix that implements the induced action σ^* on irreps.

The impossibility of noninvertible twists for reversible channels is reflected in purifications. If σ is an automorphism, the construction in [§4.4.3](#) yields purifications W of σ -SS channels that satisfy

$$(U_g \otimes \mathbf{1}^A)W = W(U_{\sigma(g)} \otimes \mathbf{1}^A) . \quad (5.5.6)$$

However, if σ is not invertible, the irrep block structure of the Kraus operators means that some rows of W constructed this way must be zero, meaning it is not unitary and so not a valid purification.

Endomorphisms compose contravariantly under the composition of channels. If \mathcal{E} is a σ -WS channel and \mathcal{E}' a σ' -WS channel, their composition $\mathcal{E} \circ \mathcal{E}'$ has WS twisted by $\sigma' \circ \sigma$, as can be seen by

$$U_g \circ \mathcal{E} \circ \mathcal{E}' \circ \mathcal{U}_{(\sigma' \circ \sigma)(g)}^\dagger = U_g \circ \mathcal{E} \circ \mathcal{U}_{\sigma(g)}^\dagger \circ \mathcal{E}' = \mathcal{E} \circ \mathcal{E}' . \quad (5.5.7)$$

If both \mathcal{E} and \mathcal{E}' have σ - and σ' - twisted-SS, respectively, the composition $\mathcal{E} \circ \mathcal{E}'$ has $(\sigma' \circ \sigma)$ -SS since

$$(\mathcal{E} \circ \mathcal{E}')^\dagger(U_g) = (\mathcal{E}'^\dagger \circ \mathcal{E}^\dagger)(U_g) = \mathcal{E}'^\dagger(U_{\sigma(g)}) = U_{(\sigma' \circ \sigma)(g)} . \quad (5.5.8)$$

We also note that convex combinations and tensor products of σ -WS/SS channels are σ -WS/SS.

5.6 Transmutation of SPT phases

This section is dedicated to showing that certain σ -twisted strongly symmetric channels have the effect of transmuting one coherent SPT phase into another, according to the action of σ on the SPT invariants.

It is not the case that all σ -SS channels perform transmutation of SPT phases, but most of them do. We state our result for σ -SS channels satisfying a genericness condition

$$\Phi_\alpha \neq 0 , \quad \forall \alpha \in \text{im } \sigma , \quad (5.6.1)$$

where Φ_α is the α -labeled component of \mathcal{E} in the irrep block decomposition of \mathcal{E} discussed in [§4.4.1](#). This condition excludes, for example, the fully dephasing channel of [??](#), which destroys SPT order despite having strong symmetry. It includes all channels generated by Lindbladians in finite time. In the following theorem, “coherent SPT phase” means a class of coherent SPT states with a given pattern of zeros (which, by [Theorem 1](#) and the conjecture of [§4.6.4](#), is a phase defined by strongly symmetric Lindbladians). Mapping an SPT phase to another refers to mapping every state in one phase to a state in the other.

Theorem 2: *Generic locally σ -twisted strongly symmetric channels map the coherent SPT phase with invariant ω to the phase with invariant $\omega' = \sigma^*\omega$.*

For uncorrelated noise, the converse holds: if a channel maps the coherent SPT phase with invariant ω to the phase with invariant ω' , it is σ -twisted strongly symmetric for some σ with $\sigma^\omega = \omega'$.*

As we will discuss later, the converse statement is false for causal channels.⁴

A consequence of [Theorem 2](#) is that, among channels of uncorrelated noise, twisted strongly symmetric channels are precisely those that map within the space of SPT states. Focusing on the MNC phases discussed in §5.4, we can also conclude that, among channels of uncorrelated noise, *automorphism-twisted* strongly symmetric channels are precisely those that map within the space of MNC SPT states.

[Theorem 2](#) tells us when a channel preserves a given SPTO:

Corollary: *The SPTO with invariant ω is preserved by generic locally σ -twisted strongly symmetric channels with σ that fix ω . Among channels of uncorrelated noise, σ -twisted strongly symmetric channels with such σ are the only channels that preserve this SPTO.*

To prove the theorem, we need the following lemma, which generalizes [Lemma 1](#) (for uncorrelated noise, not necessarily symmetric) and [Lemma 2](#) (for channels in σ -sdQC, which in particular are σ -WS) by adding a twist σ . Let $s(g, \alpha_l, \alpha_r)$ denote a string operator with end operators transforming in α_l and α_r^* , respectively.⁵

Lemma 3: *Consider either a channel of uncorrelated noise or a causal channel in σ -sdQC.*

The channel satisfies the σ -twisted (local) strong symmetry condition if and only if it maps each string operator $s(g, \alpha, \alpha)$ to a sum of string operators $s(\sigma(g), \beta_l, \beta_r)$, where $\sigma^\beta_{l,r} = \alpha$ (if no $\beta_{l,r}$ exists, the sum is empty).*

⁴We also remark about the converse statement that the genericness condition (5.6.1) is sufficient but not necessary: a weaker ω' -dependent genericness condition on only the subset of the α that appear in the pattern of ω' is enough.

⁵We previously considered only string operators with $\alpha_l = \alpha_r$ since these are the ones with nonvanishing patterns of zeros.

Let us now prove the lemma. The label on the string bulk is changed from g to $\sigma(g)$ if and only if \mathcal{E} is σ -SS. In the case of uncorrelated noise, this is because each \mathcal{E}_s is σ -SS and so $\mathcal{E}_s^\dagger(U_g) = e^{i\theta(g)}U_{\sigma(g)}$. For a channel in σ -sdQC, the argument is essentially that of §4.6.3. The label on the ends of the string are changed from α to a sum of irreps $\beta_{l,r}$ satisfying $\sigma^*\beta_{l,r} = \alpha$. This is because the superoperators $S_{l,r}^g$ (4.6.14) (which are simply $\mathcal{E}_{l,r}^\dagger$ for uncorrelated noise) are invariant under acting on the inner legs with U_h and on the outer legs with U_k for $\sigma(k) = h$, as can be seen by an argument like Eq. (4.6.15). This means that they map the representation space α on the inner legs to its preimage under σ^* on the outer legs. We have shown that the string operator evolves into an operator $s(\sigma(g), \mathcal{S}_l^g(\mathcal{O}_\alpha^l), \mathcal{S}_r^g(\mathcal{O}_\alpha^r))$ and that $\mathcal{S}_{l,r}^g(\mathcal{O}_\alpha^{l,r})$ is a sum of end operators that transform with $\beta_{l,r}$ such that $\sigma^*\beta_{l,r} = \alpha$, proving the lemma. For uncorrelated noise, an alternative way of understanding the change in representation labeling the end operators is with the block decomposition of the Kraus operators. Since $\mathcal{E}_{l,r}$ are σ -SS, their Kraus operators vanish outside of the irrep blocks $K_i^{\lambda\tau}$ with τ in the preimage of λ under σ^* . Meanwhile $\mathcal{O}_\alpha^{l,r}$ have nonvanishing blocks for irreps λ', λ such that $\lambda' \otimes \lambda^* = \alpha$. Putting these together, the nonvanishing blocks of each term $K_i^\dagger \mathcal{O}_\alpha^{l,r} K_i$ in the evolved end operator occur at irreps τ', τ in the preimage of λ', λ with $\lambda' \otimes \lambda^* = \alpha$. Each of these blocks has $\tau' \otimes \tau^*$ in the preimage of α , so we conclude that $\mathcal{E}_{l,r}^\dagger(\mathcal{O}_\alpha^{l,r})$ lives in the sum of irreps β with $\sigma^*\beta = \alpha$.

With Lemma 3 in hand, let us turn toward proving Theorem 2 by first reformulating it in terms of patterns of zeros. The pattern ζ_ω of a state is understood as the collection of pairs (g, α) such that $\langle s(g, \alpha, \alpha) \rangle$ is generically nonvanishing on the state. By the rule (5.4.6), the pattern of zeros $\sigma \cdot \zeta_\omega$ consists of pairs (g, α) such that $\alpha = \sigma^*\beta$ for the (unique) β for which $(\sigma(g), \beta)$ appears in the pattern ζ_ω . The theorem demonstrates how this new pattern can be understood as expectation values of evolved operators $\mathcal{E}^\dagger(s(g, \alpha, \alpha))$ evaluated on the original state. To be precise, the first half of the theorem states that, on an SPT state,

$$\begin{aligned} & \text{If } \mathcal{E} \text{ is a generic locally } \sigma\text{-SS channel, then generically} \\ & \langle \mathcal{E}^\dagger(s(g, \alpha, \alpha)) \rangle \neq 0 \text{ precisely for the pairs } (g, \alpha) \text{ such that} \\ & \alpha = \sigma^*\beta \text{ for the (unique) } \beta \text{ with } \langle s(\sigma(g), \beta, \beta) \rangle \neq 0. \end{aligned} \quad (5.6.2)$$

To see why this is true, apply Lemma 3 to write $\mathcal{E}^\dagger(s(g, \alpha, \alpha))$ as a sum of terms $s(\sigma(g), \beta_l, \beta_r)$ with $\sigma^*\beta_{l,r} = \alpha$. Due to the condition (5.6.1), these terms do not vanish (though the sum may be empty if no $\beta_{l,r}$ exist). A pattern of zeros of an SPT state has a unique entry β per column, so the expectation values of the terms in the sum vanish unless $\beta_l = \beta_r = \beta$; either zero or one terms do not vanish. We have $\langle \mathcal{E}^\dagger(s(g, \alpha, \alpha)) \rangle \neq 0$ when the nonvanishing term $\langle s(\sigma(g), \beta, \beta) \rangle$ appears in the sum. This can only happen when $\alpha = \sigma^*\beta$, and in this case it generically happens, since generically the β -components of the end operators are nonzero.

It remains to prove the second half of Theorem 2. The argument follows that of §4.5.1, except that σ is no longer constrained to be connected to the identity endomorphism. Now the condition that the transfer matrix (4.5.4) has $\lambda_{\max} = 1$ implies that $\mathcal{E}_s^\dagger(U_g) = U_h$, which is to say that \mathcal{E}_s is σ -SS for some σ with $\sigma(g) = h$. Then apply the first half of Theorem 2 to see that the channel maps the phase ω

to the phase $\sigma^*\omega$, which by assumption is ω' ; therefore, σ satisfies $\sigma^*\omega = \omega'$, as claimed.

As we mentioned earlier, the second half of [Theorem 2](#) does not generalize from uncorrelated noise to all causal channels. This is because there are causal channels that are not locally σ -SS yet nevertheless transmute SPT phases. For example, the phase ω is mapped to ω' by convex combinations of locally σ_i -SS channels where each $\sigma_i^*\omega$ equals ω' . Additionally, one can add to the convex combination a channel that is not σ -SS for any σ . This extra factor annihilates string operator expectation values and so does not alter the effect of the channel on string order. Finally, there are channels that are σ -SS but not *locally* σ -SS. These change the bulk labels of strings from g to $\sigma(g)$ and the end labels from χ_α to $\chi'_g\chi_\alpha$, where ν is the projectivity cocycle of Q . In doing so, they transform the pattern of zeros in a way that endomorphism actions cannot; for example, if $\sigma = 1$, the cohomology invariant of the channel is simply added to that of the state: $\omega \mapsto \omega + \nu$ [268].⁶

5.6.1 Edge modes perspective

The transformation of the SPT invariant ω under a σ -SS channel can also be seen in terms of edge modes:

$$\dots = \dots = \dots \quad (5.6.3)$$

The σ -SS condition means that U_g is hit by σ upon pulling through K_i , and local realization means that Q is linear. Then the edge modes of the evolved MPS state transforms like $\sigma^*V \otimes Q$, which has cocycle $\sigma^*\omega$.

5.6.2 Irrep probabilities perspective

Irrep probabilities were introduced in §4.5.5, where it was shown that SS Lindbladian evolution preserves them while non-SS Lindbladian evolution maps them to the fully degenerate value $1/|G|$. In this section, we consider the effects of (not necessarily Lindbladian) causal channels on irrep probabilities.

We find that strongly symmetric channels twisted by automorphisms preserve the degeneracies of irrep probabilities (though permute the irrep probabilities themselves) for all SPT phases, while those twisted by noninvertible endomorphisms reduce the degeneracy if the initial state is in an MNC phase and either reduce or preserve it (depending on the phase) for non-MNC phases. In light of the claim of Ref. [72] that the degeneracy of irrep probabilities measures SPT complexity, this result reflects the behaviour of complexity we observed in §5.3; in particular, in Figure 5.5. Meanwhile, channels that are not σ -SS for any endomorphism σ

⁶This is not surprising. In closed systems, 1D SPT phases can be prepared by symmetric causal unitaries with index $\nu = \omega$.

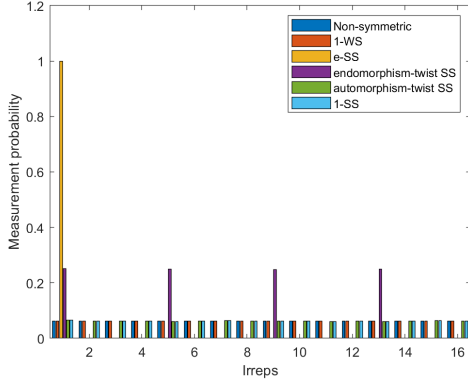


Figure 5.7: A random state in trivial phase of $\mathbb{Z}_4 \times \mathbb{Z}_4$. Under non- σ -SS channels the irrep probabilities become exactly fully degenerate. For σ -SS channels, the nondegeneracy of the trivial phase is preserved.

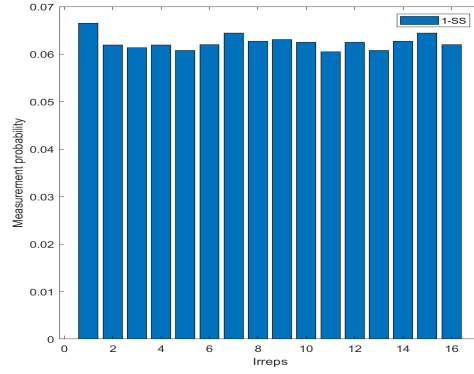


Figure 5.8: A close-up of the irrep probabilities of a random state in the trivial phase evolved by a σ -SS channel shows that they have no enforced degeneracy.

send the degeneracy to to the maximal value $|G|$, regardless of the initial state. This result means that irrep probabilities and their degeneracy detect whether a channel is twisted strongly symmetric.

To see that automorphism-twisted SS channels permute irrep probabilities, use what we learned in §5.6 about the transformation of the string operators $\langle s(U_g, \mathbb{1}, \mathbb{1}) \rangle$ to compute

$$p_\alpha \mapsto \frac{1}{|G|} \sum_g \chi_\alpha(g) \langle s(U_{\sigma(g)}, \mathbb{1}, \mathbb{1}) \rangle = \frac{1}{|G|} \sum_g \chi_\alpha(\sigma^{-1}(g)) \langle s(U_g, \mathbb{1}, \mathbb{1}) \rangle = p_{(\sigma^{-1})^* \alpha}. \quad (5.6.4)$$

A similar computation can be performed for endomorphisms. Fix a set of elements $h \in G$ that represent the cosets of the quotient $G/\ker \sigma$. Then

$$\begin{aligned} p_\alpha \mapsto & \frac{1}{|G|} \sum_g \chi_\alpha(g) \langle s(U_{\sigma(g)}, \mathbb{1}, \mathbb{1}) \rangle \\ & = \left(\frac{|\ker \sigma|}{|G|} \sum_h \chi_\alpha(h) \langle s(U_{\sigma(h)}, \mathbb{1}, \mathbb{1}) \rangle \right) \left(\frac{1}{|\ker \sigma|} \sum_{k \in \ker \sigma} \chi_\alpha(k) \right). \end{aligned} \quad (5.6.5)$$

Orthogonality of characters means that the sum over $k \in \ker \sigma$ enforces the constraint that α restricted to $\ker \sigma$ is trivial. For the characters α without this property (of which there is at least one if σ is noninvertible), the corresponding irrep probability p_α must vanish. When at least one of the p_α 's vanishes, they cannot be fully degenerate, so there is less degeneracy than for a MNC state. We conclude that SS channels twisted by noninvertible endomorphisms reduce the degeneracy of MNC phases. Finally, channels that are not σ -SS for any σ annihilate the string order parameters without $g = 1$, so we get again the result (4.5.27) that the irrep probabilities become maximally degenerate, regardless of the initial state.

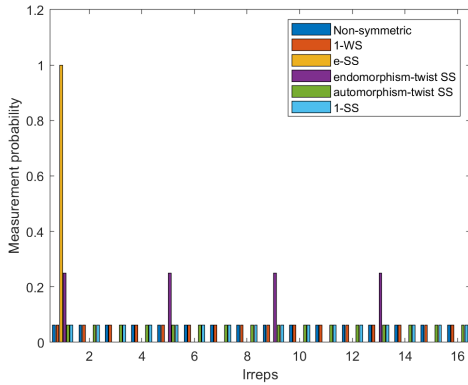


Figure 5.9: Irrep probabilities for a random state in a $\mathbb{Z}_4 \times \mathbb{Z}_4$ MNC SPT phase after evolution by channels satisfying various symmetry conditions.

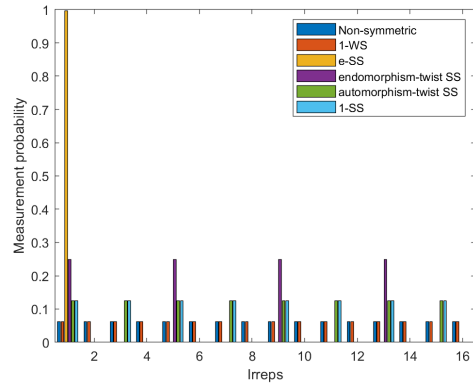


Figure 5.10: Irrep probabilities for a random state in a $\mathbb{Z}_4 \times \mathbb{Z}_4$ non-MNC SPT phase after evolution by channels satisfying various symmetry conditions.

To illustrate these results, we perform numerical checks on example SPT states with symmetry $G = \mathbb{Z}_4 \times \mathbb{Z}_4$. We generate random, injective, symmetric MPS of bond dimension $D = 16$ in a particular SPT phase, with support in all irrep sectors. Then we act on them with channels satisfying various symmetry conditions. The resulting irrep probabilities are depicted in Figures 5.7, 5.8 (trivial phase) and Figures 5.9, 5.10 (nontrivial phases). For $\mathbb{Z}_4 \times \mathbb{Z}_4$, the automorphisms are those σ with $\det \sigma = 1, 3$, while the noninvertible endomorphisms are those with $\det \sigma = 0, 2$. Each Kraus operator of our example channels is a 16×16 matrix. The WS but non-SS channel we consider is the depolarizing channel (4.5.11), and the SS channel we consider is the dephasing channel (4.5.12). The SS channel twisted by the constant endomorphism (in particular, $\det \sigma = 0$) is given by Kraus operators $(K_i)_{ab} = \delta_{ai}\delta_{b1}$. The channel with SS twisted by an automorphism with $\det \sigma = 3$ is given by two Kraus operators, each expressed in terms of 4×4 blocks as $K_i = (\tilde{K}_i)^{\oplus 4}$, where

$$\tilde{K}_0 = \begin{pmatrix} 1 & 0 & 0 & 0 \\ 0 & 0 & 0 & 0 \\ 0 & 0 & 0 & 0 \\ 0 & 0 & 0 & 0 \end{pmatrix}, \quad \tilde{K}_1 = \begin{pmatrix} 0 & 0 & 0 & 0 \\ 0 & 0 & 1 & 0 \\ 0 & 1 & 0 & 0 \\ 1 & 0 & 0 & 0 \end{pmatrix}, \quad (5.6.6)$$

The channel that enacts a $\det(\sigma) = 2$ endomorphism twist is given by four Kraus operators with blocks

$$\tilde{K}_i = \left\{ \begin{pmatrix} 1 & 0 & 0 & 0 \\ 0 & 0 & 0 & 0 \\ 0 & 0 & 0 & 0 \\ 0 & 0 & 0 & 0 \end{pmatrix}, \begin{pmatrix} 0 & 0 & 0 & 0 \\ 0 & 0 & 0 & 0 \\ 0 & 1 & 0 & 0 \\ 0 & 0 & 0 & 0 \end{pmatrix}, \begin{pmatrix} 0 & 0 & 1 & 0 \\ 0 & 0 & 0 & 0 \\ 0 & 0 & 0 & 0 \\ 0 & 0 & 0 & 0 \end{pmatrix}, \begin{pmatrix} 0 & 0 & 0 & 0 \\ 0 & 0 & 0 & 0 \\ 0 & 0 & 0 & 1 \\ 0 & 0 & 0 & 0 \end{pmatrix} \right\}. \quad (5.6.7)$$

Irrep probabilities let one compute the entanglement of a state that is not accessible to local operations and classical communication (LOCC) that respect

the symmetry G [72]. The inaccessible entanglement is given by the entropy of the irrep probabilities

$$E_{\text{inacc}} = - \sum_{\alpha} p_{\alpha} \log_2 p_{\alpha}. \quad (5.6.8)$$

The lower bound on this quantity over pure states in an SPT phase is determined by the complexity of the phase and is $\log_2(D_{\omega}^2) = \log_2(|G|/|K_{\omega}|)$, while the upper bound is given by $\log_2(|G|)$.

While the upper bound on E_{inacc} is unchanged by evolution under any (weakly symmetric) channel, the lower bound may decrease or remain the same according to the symmetry condition satisfied by the channel. If the channel is σ -SS, it changes the SPTO from $[\omega]$ to $[\sigma^*\omega]$ and the lower bound to $\log_2(D_{\sigma^*\omega}^2)$. Then, since the lower bound decreases as complexity decreases, SS and automorphism-twisted SS channels leave the lower bound unchanged, while the lower bound is decreased under SS channels twisted by noninvertible endomorphisms. In particular, channels twisted by the constant endomorphism $\sigma : g \mapsto e$ send the lower bound to zero (since $D_{\sigma^*\omega} = 1$). In fact, by Eq. (5.6.5), states evolved by e -SS channels saturate the lower bound by concentrating their support in the trivial irrep.

5.6.3 Revisiting the example of the SPTO-destroying Lindbladian

Our investigation into the strong symmetry condition was motivated in §4.4.4 by Coser and Pérez-García's example [4] of a weakly symmetric Lindbladian that destroys SPTO. Let us now revisit this example and discuss how it fits into the theory of twisted symmetric channels that we have developed in this section.

Recall that this Lindbladian (4.4.39) is not strongly symmetric, which means by Theorem 1 that it does not preserve SPTO. Moreover, by Theorem 2, the only channels that map within the space of SPT states are σ -SS channels, so the channels this Lindbladian generates at finite times must destroy SPTO altogether. To see how this assertion is consistent with the claim of Ref. [4] that their Lindbladian maps one SPT phase to another in finite time, notice that they are interested in matching states only approximately (albeit exponentially well), whereas we require exact matching in order to preserve string order.

At infinite time, however, the channel generated by this Lindbladian maps arbitrary states *exactly* to a product state, which has a well-defined SPTO – the trivial order. This means that the infinite time evolution satisfies the strong symmetry condition twisted by the constant endomorphism $\sigma : g \mapsto e$. This can be seen explicitly by writing out the channel on each site s :

$$\mathcal{E}_{s,t} = e^{t\mathcal{L}_s} = e^{t(\mathcal{T}_s - \mathbb{1})} = \mathcal{T}_s - e^{-t}\mathcal{L}_s \xrightarrow{t \rightarrow \infty} \mathcal{T}_s, \quad \text{for } \mathcal{T}_s(\rho) = \text{Tr}[\rho]|\phi\rangle\langle\phi|, \quad (5.6.9)$$

where we used $\mathcal{T}_s^2 = \mathcal{T}_s$. This channel has dual $\mathcal{T}_s^\dagger(X) = \langle\phi|X|\phi\rangle\mathbb{1}$, which, since the state $|\phi\rangle$ is chosen to be symmetric, satisfies $\mathcal{T}_s^\dagger(U_g) = \mathbb{1}$, the twisted strong symmetry condition for $\sigma : g \mapsto e$. We remark that the channel \mathcal{T}_s is generic, in the sense of Eq. (5.6.1), despite arising as an infinite time evolution.

The transformation of one SPT phase into another by this Lindbladian is considered in Ref. [4]. Let $|\omega\rangle$ denote a state in the phase labeled by ω . Any state $|\omega_1\rangle$ may be transformed into any $|\omega_2\rangle$ by appending a $|\omega_2^{-1}\rangle \otimes |\omega_2\rangle$, then acting with $\mathcal{E}_\infty \otimes \mathbb{1}$, and finally discarding the product state that is reached after infinite time:

$$|\omega_1\rangle \sim |\omega_1\rangle \otimes |\omega_2^{-1}\rangle \otimes |\omega_2\rangle \xrightarrow{\mathcal{E}_\infty} |\phi\rangle^{\otimes L} \otimes |\omega_2\rangle \sim |\omega_2\rangle . \quad (5.6.10)$$

At first glance, this procedure may seem to suggest that the channel is capable of transforming between arbitrary G -SPTOs ω_1 and ω_2 , in violation of [Theorem 2](#) and the rule that SPT complexity cannot be increased. This apparent paradox is dissolved by realizing that the full symmetry group of these states is $G \times G \times G$, rather than just the diagonal subgroup G . The fact that $\mathcal{E}_\infty \otimes \mathbb{1}$ changes the $G \times G \times G$ -SPTO according to the action of the endomorphism $\sigma : (g_1, g_2, g_3) \mapsto (e, e, g_3)$ is consistent with it being strongly symmetric with this twist. It is not possible to reduce the symmetry group to the diagonal factor: either $|\phi\rangle$ is taken to be symmetric (resulting in a copy of G on each factor) or it is taken to be nonsymmetric, in which case the full symmetry group is a copy of G on the third factor. If the states are chosen so that only the third factor of G remains a symmetry, the channel (which acts trivially on the third factor) may be regarded as having untwisted strong symmetry; indeed, the G_3 -SPTO is ω_2 on either side of the transformation.

5.7 Discussion & Conclusions

This Chapter answers a general question interesting to the condensed matter community regarding topological phase transmutation. We consider the question of the mechanism for SPT phase transmutation in a non-unitary setting. We provide a concrete framework to answer this question, with twisted-SS channels. By restricting channels to not only be weakly but strongly symmetric, the SPT phase remained well-defined under finite amounts of noise. By evolving with twisted-SS channels, this suggested defining the SPT complexity which may either stay the same or be reduced; when the twist is non-trivial, the SPT phase changes. This is detected by hallmarks of the SPTO such as the string order parameter, edge modes and inaccessible entanglement. In the following we will discuss some implications of the work, as well as some more nebulous connections as food for thought.

While in closed system settings, several procedures are known which engineer topological phase transmutation, this work gives a first attempt at developing a framework to describe SPT phase transmutation in open systems. In closed systems, it's known that applying symmetric filters on a pure state may reduce the complexity of the entanglement pattern and lead the state to have a different pattern, e.g. by the condensing or confinement of anyons [94, 277, 278]. This induces a topological phase transition, due to the remarkable fact that topological phases are defined by the pattern of entanglement. Intuitively, reducing the symmetry in a meaningful way, by restricting to a subgroup, gives non-trivial

entanglement patterns, where the symmetries refer to the SF class of the topological quasi-particles. That only certain topological orders can be transformed between is intuitive, since entanglement cannot be created without a cost (even with dissipation) [127].

The twisted-SS framework allows us to easily interpret how changing patterns of entanglement changes the topological phase. In the setting of G -LOCC, when one restricts the problem by reducing the symmetry of the operations to a subgroup, inaccessible entanglement can detect a hidden SPT phase by its latent entanglement pattern as we saw in Chapter 3. In the setting of open systems, restricting channels to those with twisted-SS may cause an SPT phase transmutation by physically changing the system's pattern of entanglement. The different possible phase transmutations may be derived mathematically, since they are simply the different permitted endomorphisms of G acting on the SPT phase, and these are nicely detectable through the various hallmarks of SPTO. This emphasizes the role that patterns of entanglement occupy, by the interplay of symmetry and locality.

An interesting connection is the link to thermodynamics. Open system dynamics can describe the coupling of a system to a thermal environment. Classically, the second law of thermodynamics tells us there is an arrow of time in the operations that classical systems experience naturally which increases the sum total entropy in the universe, while a quantum second law of thermodynamics is not fully agreed-upon, in part due to the difficulty of defining a consistent notion of work and entropy [279–282]. We also see a unidirectionality and ‘arrow of time’ under twisted-SS channels since SPT complexity can only be reduced. Does SPT complexity relate to a quantum notion of entropy, in that twisted-SS increases entropy? One may ask whether channels which are not twisted-SS can decrease entropy. Most channels in the natural world can be expected to destroy SPT complexity, such as weakly symmetric channels. However, channels can be engineered that create SPTO from the trivial phase [254, 255]; such channels increase the SPT complexity and would be thought of as decreasing entropy.

Perhaps more natural for the quantum information scientist to consider is the connection to resource theory. Consider the resource of the SPT phase, which provides the computational power in MBQC [26, 115, 135, 243, 283–286]. Resource theories describe how a partial order is induced on states by defining allowed operations. Certain states have no resource, and are useless under the allowed operations, while other states are resourceful, and allow to overcome the limited operations. Entanglement theory is a canonical example of a resource theory, in which entanglement is the resource we are interested in and the allowed operations are LOCC. Consider bipartite entanglement. The possible state transformations are given a partial order which is determined by majorization [15]. While product states have no entanglement and so cannot transform to any entangled state under LOCC, the Bell states are the most entangled (most resourceful) states, and from these states we can transform to any other bipartite state. If twisted-SS are the allowed operations, what is a resulting resource theory? Since MBQC is a useful task, an interesting and potentially useful question to answer is which states are resourceful and how one may do state transformations between them.

Chapter 6

Symmetry enriched topological order in open systems

This Chapter contains the publication in preparation:

- Symmetry Enriched Topological Order in Open Systems **Caroline de Groot** Jose Garre Rubio, Alex Turzillo (in preparation) [74].

6.1 Motivation

The zoo of quantum phases expands with growing dimension. Higher-dimensional systems can host intrinsic topological order as well as SPTO in dimensions greater than one. By adding symmetries to intrinsic topological phases, the phase diagram becomes further refined, and families of states which could previously be classified in the same phase can now be in distinct phases. Such topological phases are called symmetry enriched topological (SET) phases. These phases are classified by the symmetry fractionalisation (SF) properties of its anyons, which also describes their braiding. Then the anyons in the bulk of the system are allowed to fractionalise or be permuted under the action of the symmetry.

The realisation that anyon braiding can be harnessed as a tool for quantum computing has led to applications such as topological quantum computing and quantum error correction [152, 183]. A further widespread subject of interest is whether topological phases can act as a self-correcting quantum memory (SCQM) in which a system is able to passively perform error correction [7, 8]. SCQM store information with a memory time τ_{mem} that grows in the system size. However, for commuting Hamiltonians, this almost certainly requires an unattractively high dimension. For example, the 4D Toric code is a canonical example of a SCQM, while the 2D Toric code requires active error correction. Enrichment by symmetries has provided another way to circumvent the issue of high-dimensionality [61]. SET phases have been particularly interesting in this direction, as adding symmetries to topological phases may strengthen the inherent perturbative stability [287, 288]. It's been suggested that phases enriched by symmetry can support fault-tolerant

quantum computing even under coupling to a thermal environment, in particular through higher-form symmetries [190]. In general, the mixing time τ_{mix} , the time for the state to transform to a thermal Gibbs state, is longer than the memory time τ_{mem} , the time in which the logical subspace is protected; τ_{mem} is upper-bounded by τ_{mix} . To study systems which admit SCQM, it is arguably important to understand the robustness of relevant quantum phases to noise, in which there is a growing interest for fundamental reasons as well.

While SET phases are fully classified for phases of pure states, an understanding of SET phases of mixed states is lacking. A significant and relatively unexplored question is that of the robustness of SET phases on coupling to an open system. The subject of the previous two Chapters has been to systematically investigate the open system paradigm in which a notion of 1D SPTO is robust to noise, given by locally strongly symmetric Lindbladian channels [73]. It is natural to ask whether the same reasoning can be applied to other phases which rely on symmetry, such as SETO, namely by asking the following: *what is the robustness of fingerprints of SETO to noise?* For 1D SPTO the string order parameter acts as a unique fingerprint by detecting the symmetry fractionalisation classifying the edge modes, for finite groups. This is conveniently studied within the framework of MPS. In the case of 2D SETO, the simplest case of topological enrichment, it is already quite difficult to compute quantities, so a reasonable restriction is to focus on G-injective PEPS which describe quantum double models of finite abelian groups. Then an order parameter has been developed which measures the symmetry fractionalisation (SF) pattern of anyons [10] which can reasonably act as a fingerprint. 2D SETO and 1D SPTO are both classified by a second cohomology group, which can be traced back to both being determined by symmetry fractionalisation (SF), either on the boundary, in the case of SPTO, or on the anyons, in the case of SETO. Therefore, their order parameters reflect some similarities. With this connection in mind, exploit the methods developed in Chapter 4 and Chapter 5 to study our fingerprint of SETO and consider the question of the robustness of SETO to noise.

6.2 Summary

In this Chapter, we study the robustness of symmetry enriched topological order (SETO) in open systems, as witnessed by a particular order parameter, under general symmetric, single-site noise. We consider the two different notions of symmetry of quantum channels which have been introduced previously in this Thesis – strong symmetry (4.4.8) and weak symmetry (4.4.2). We show numerically that 2D SETO is robust only to strongly symmetric noise which fits with our previous results for 1D SPTO. This motivates us to demonstrate this claim analytically and we give a discussion in this direction.

In Section §6.3 we begin by investigating the swap order parameter \mathcal{S} , which was defined previously in (2.4.19) for 1D SPT phases, which captures the SF of edge modes in spin chains [176]. The order parameter is equivalent to the SPT phase since it uniquely encodes the cocycle $\omega(g, h)$ via a *pattern of signs*. Intuitively,

\mathcal{S} makes use of a swap gate to capture the anti-commutation properties of the projective representation at the virtual level which classifies the SPTO. Advantages of \mathcal{S} are that it does not suffer from a pattern of zeros as the string order parameter does; in the latter, certain evolutions, such as infinite time evolutions or those which destroy the end operators, often send the whole pattern to zero which means no order can be detected. In Section §6.3.1 we demonstrate the equivalence of the swap order pattern of signs and the SPT phase.

We then provide a numerical study in Section §6.3.2 of the time evolution of the swap order parameter under channels representing uncorrelated noise, calculated for the AKLT state. In particular, we investigate its dependence on strong symmetry and weak symmetry, which is depicted in Fig. 6.2. The numerical evidence motivates us to suggest that the swap order parameter is robust under strongly symmetric channels at finite times. We observe that \mathcal{S} decays sub-exponentially in time under strongly symmetric channels. Moreover, \mathcal{S} decays exponentially fast in time under weakly symmetric channels. The unnormalised version of \mathcal{S} is simulated in Fig. 6.3.

In Section §6.3.3 we present work in progress towards proving the above claim, which is formalised in Conjecture 2. We discuss a reformulation of Theorem 1 in terms of the swap order parameter \mathcal{S} . The idea is to replace Lemma 1, which says that string order parameters characterises open system SPTO, with a similar statement leveraging the swap order parameter given in Conjecture 2. We can divide the swap order parameter into two separate operators: one of which is a string of symmetry operators and the other of which is a swap operator. This is described in Eq. 6.3.4. The symmetry string is preserved if and only if the channel is strongly symmetric, but the swap part requires further work. The Conjecture is unproven at this stage.

In Section §6.4 we turn to the robustness of SETO. We study a simple model of 2D SETO H_{SET} (2.6.4) with $|SET\rangle$ as its ground state (2.6.2), which is constructed by decorating a 2D Toric code with cluster state loops [10]. We explore it through the order parameter Λ (2.6.15), similarly based on a swap gate, which was developed for quantum double models of finite groups in Ref. [11]. It was shown that Λ detects the SF pattern of anyons uniquely, which gives it a unique correspondence to the SET phase $\omega(q, k)$.

We present a numerical study in Section §6.4.1 of the SET order parameter Λ under general symmetric, single-site channels. We find strong numerical evidence that SETO is robust only to strongly symmetric noise. Fig. 6.5 suggests that SETO is preserved by a family of strongly symmetric channels representing dephasing noise, as witnessed by Λ not changing sign for finite times. For a family of weakly symmetric channels representing depolarising noise Λ changes sign which indicates a phase change. In the steady state $\text{sgn}[\Lambda] = +$, which is expected in the trivial phase. Conversely, for strongly symmetric channels $\text{sgn}[\Lambda] = -$ at all times including at infinite time, which is indicative of the non-trivial SET phase.

Finally in Section §6.4.2 we discuss how to formalise the claim that SETO is robust under coupling to strongly symmetric noise in ongoing work. We give a reasonable statement of this in Conjecture 3, and a possible description of a proof in order to promote the Conjecture to a Theorem. We can analogously split Λ

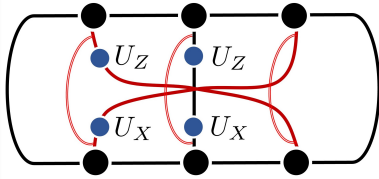


Figure 6.1: Tensor network diagram of the swap order parameter (defined in Eq. 2.4.19) for 1D SPTO evolved under channels. The evolution by the noisy channel $\varepsilon(\cdot) = \sum_i K_i(\cdot)K_i^\dagger$ is depicted as a doubled red line going from a physical leg for a site on the bra to a physical leg for the same site on the ket, where we omit the tensor corresponding to the Kraus operators K_i, K_i^\dagger .

into two parts made up of a string of symmetry operators and a swap operator (6.4.5). A key piece of analysis to facilitate the proof would come from successfully showing Conjecture 2 for the 1D swap order parameter \mathcal{S} .

6.3 Swap order parameter with dissipation

While the string order parameter had a *pattern of zeros*, the swap order parameter has a *pattern of signs* for gapped phases, where by signs we mean complex phases. In the simple case of $\mathbb{Z}_2 \times \mathbb{Z}_2$, the pattern of signs only contains $+, -$.

Here we consider the ground states of gapped Hamiltonians, namely MPS, such that states yield a well-defined pattern of signs that uniquely determine the SPT invariant $[\omega]$. We can follow a very similar reasoning as what was done previously in [73], which we consider in the next Section. The graphical representation of the string order acted on by a channel is given in Fig 6.1.

6.3.1 Equivalence of pattern of signs and SPT phase

How does the swap order parameter distinguish the inequivalent projective representations, and in so doing detect the SPT phase? It captures their anti-commutation properties through the SWAP operator, which leads to a gauge-invariant quantity. In Fig. 2.5(b) we demonstrated that the order parameter computes the cocycle for the special case of the AKLT state. By replacing U_Z and U_X (which together form the generators for $\mathbb{Z}_2 \times \mathbb{Z}_2 = \langle X, Z \rangle$) with U_g and U_h , this becomes a general order parameter for finite abelian symmetries G and $g, h \in G$ [176].

The swap order parameter encodes the SPT invariant directly, and computing its value gives exactly the quotient $\omega(g, h)/\omega(h, g)$. Unlike string order, the order parameter pattern is hence not given by selection rules of zeros and non-zeros, but rather of complex numbers. We can define an SPT state to be a state which has a well-defined swap order pattern of signs, equally as well a string order parameter pattern of zeros. Since the states we consider are MPS, they obey the fundamental theorem, and the physical symmetry U_g acts on the virtual level as $U_g = V_g \otimes \bar{V}_g$. We remind the reader that the invariant $[\omega]$ is recoverable from these ratios, as we

argued in §5.4.

The cocycle ω defines a “pattern of signs” $\xi_\omega : G \rightarrow G^*$ given by

$$\xi_\omega : g \mapsto \chi_h^\omega(g) = \frac{\omega(h, g)}{\omega(g, h)}. \quad (6.3.1)$$

This definition is similar to that of the string order pattern of zeros ζ_ω in Sec. §5.4, which leads ξ_ω to share some of the same properties. First, the image of ξ_ω is linear characters (one-dimensional representations) and the kernel of ξ_ω is the projective center K_ω (4.5.26). Further, the map $\omega \mapsto \xi_\omega$ is a group homomorphism $\xi_{\omega_1}\xi_{\omega_2} = \xi_{\omega_1\omega_2}$, and the kernel consists of coboundaries. Therefore the pattern of signs ξ_ω determines the cohomology class $[\omega]$ of the cocycle ω .

Here it will be convenient to represent a pattern of signs ξ_ω as a two-dimensional array with columns and rows indexed by group elements g and h , rather than with irreps as in the pattern of zeros. Then the entry (g, h) in this array is “+” if $\xi_\omega(g) = 1$, i.e. $g, h \in K_\omega$, and is a complex phase \star otherwise. For abelian groups, the pattern of signs is a symmetric matrix, Then it is sufficient to consider any single column (row) of the pattern of signs which does not begin with the identity element. The number of complex phases in those columns (rows) is $\sqrt{|G|/|K_\omega|}$, which is the SPT complexity. For example, the two phases of symmetry $G = \mathbb{Z}_2 \times \mathbb{Z}_2$ have patterns of signs

$$\xi_{\text{trivial}} = \begin{pmatrix} + & + & + & + \\ + & + & + & + \\ + & + & + & + \\ + & + & + & + \end{pmatrix}, \quad \xi_{\text{Haldane}} = \begin{pmatrix} + & + & + & + \\ + & + & \star & \star \\ + & \star & + & \star \\ + & \star & \star & + \end{pmatrix}, \quad (6.3.2)$$

with columns and rows indexed by $\{g, h\} = (0, 0), (0, 1), (1, 0), (1, 1)$. Here $\sqrt{|G|/|K_\omega|} = 2$, so there are two \star in every column (row). In this simple case of the Haldane phase $\star = -1$. Note that for non-abelian groups, the pattern of signs is not symmetric. The pattern of signs is an observable, and like any observable it can be sent to zero (by a non-invertible superoperator). We consider a valid pattern of signs to be one that does not have any zeros.

An example of states which do not satisfy this are gapless phases which may exhibit zero swap order parameter¹. An example more relevant to our context of gapped quantum phases of mixed states are the steady states of channels corresponding to a Lindbladian evolution at infinite time.

6.3.2 Numerical study

The numerical experiments of channel evolutions on the AKLT state are depicted in Fig. 6.2 and in Fig. 6.4(b), for the normalised and unnormalised versions of

¹Ref. [176] studies the phase diagram of the bilinear-biquadratic Hamiltonian. The order parameter returns a distinct zero signature for the two gapless regimes, converging exponentially in L for the ferromagnetic phase, and converging algebraically with L in the other phase.

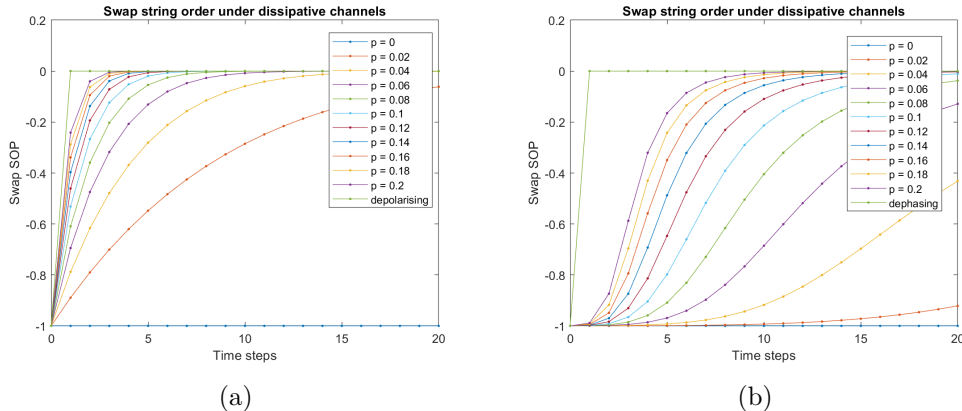


Figure 6.2: Time evolution of the swap order parameter under two different channels for different decay rates p , with respect to the AKLT state. a) the strongly symmetric channel given by the dephasing channel 4.5.12) has very different behaviour compared to b) the weakly symmetric channel (given by the depolarising channel 4.5.10), for which the order parameter decays instantly to the steady state value, while strong symmetry allows the swap order parameter to persist at finite times, and only disappears as time gets long. The order parameter is normalised to ± 1 at $t = 0$ by the normalisation factor N .

the swap order parameter \mathcal{S} , which we introduced thoroughly in Section §2.4.3 respectively. These indicate that SPTO coupled to a noisy environment may be described in a similar manner to the way we did in Chapter 4. This suggests that we may reformulate Theorem 1 from Chapter 4 for the swap order parameter and its pattern of signs. Different from the string order parameter, the steady state values for \mathcal{S} are not zero but rather finite positive reals close to zero (see Table 6.1) which indicates a trivial pattern of signs.

We investigated the swap order parameter with respect to two different noise models, with our focus on the AKLT state and order parameter depicted as in Fig. 2.5(b). We consider the depolarising channel and the dephasing channel, as in Section §4.5.2. We find numerically that weakly symmetric channels cause exponential decay of the pattern of signs with the decay rate p , while strongly symmetric channels cause slower decay at finite times.

We observe a difference between the weakly symmetric and strongly symmetric channels in the convergence to the steady state value with the decay rate p . While for evolutions under the depolarising channel the convergence of \mathcal{S} is exponential in time for all p , for the dephasing channel the convergence of \mathcal{S} is sub-exponential in time (when \mathcal{S} is appropriately normalised).

We may understand the origin of the distinction in their behaviour from how the strong symmetry condition manifests in the constituents of the order parameter, as we investigate more explicitly in Fig. 6.4. Consider that we can split up the

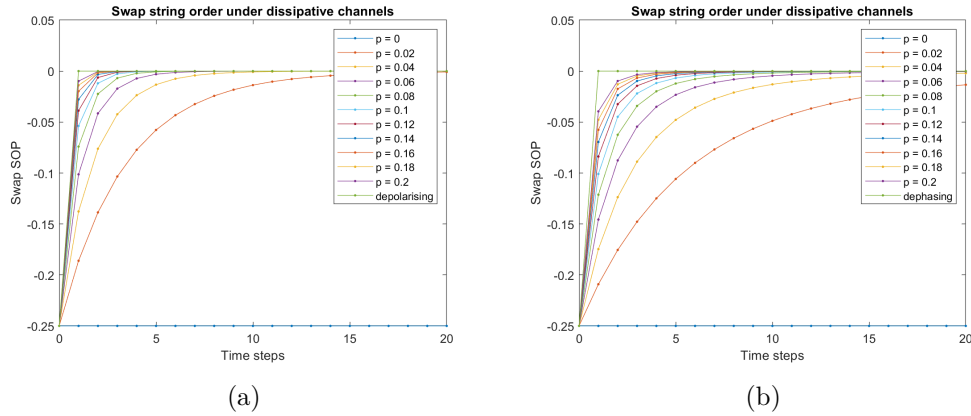


Figure 6.3: Unnormalised time evolution of the swap order parameter with evolution given by a) weakly symmetric depolarising channel and b) strongly symmetric dephasing channel.

swap order parameter into the following constituent pieces

$$\begin{array}{c}
 \text{a)} \\
 \begin{array}{c}
 \bullet \quad \bullet \\
 | \quad | \\
 \text{---} U_Z \text{---} \\
 | \quad | \\
 \bullet \quad \bullet \\
 \text{---} U_X \text{---} \\
 | \quad | \\
 \bullet \quad \bullet
 \end{array}
 \end{array}
 \quad , \quad
 \begin{array}{c}
 \text{b)} \\
 \begin{array}{c}
 \bullet \\
 | \\
 \text{---} U_Z \text{---} \\
 | \\
 \bullet \\
 \text{---} U_X \text{---} \\
 | \\
 \bullet
 \end{array}
 \end{array}
 \quad , \quad (6.3.3)$$

where (a) contains the swapped sites which play the role of braiding the quasi-particles created at the ends of the symmetry string and (b) is the middle part which contains the symmetry. In fact, we've seen (b) before in the string order parameter where it is also the middle part. By seeing these operators as matrices, we can study their spectrum or take their trace. Although it may seem an artificial exercise, this division will allow us to make useful insights as the two operators take different roles. We observe that decay from strongly symmetric channels only occurs due to the swap part of the order parameter, while the middle part remains constant for all time. Under weakly symmetric channels, both constituent parts decay with time.

The SWAP operation allows the order parameter to detect the anti-commutation of the projective representation corresponding to the SPT phase, and in this sense acts in the same way as the end operators \mathcal{O}_α in string order parameters. This observation suggests that channels which preserve the middle operator of the swap order parameter preserve the SPT phase, as long as the SWAP (which plays a similar role to that of end operators) doesn't vanish too quickly. Then we might expect that a version of [Theorem 1](#) in [Chapter 4](#) holds, with patterns of zeros replaced by patterns of signs.

Notice that under coupling to the noisy environment, the swap order parameter decays and saturates at a finite, positive value in the infinite time limit, since it has a pattern of signs. On the other hand, the string order parameter decays to zero at infinite time, with any finite amount of dissipation, since it has a pattern of

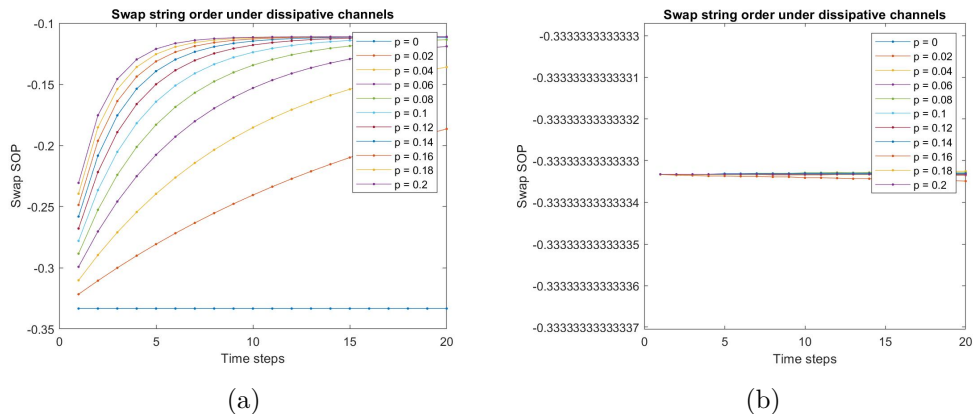


Figure 6.4: Time evolution of the swap order parameter (unnormalised) broken into two constituents, under the dephasing (strongly symmetric) channel with decay rates p for the AKLT state. We plot the evolution of the part of the order parameter which contains the swap operator (a) separately from the middle part of the order parameter (b). We demonstrate numerically what we expected analytically which is that all decay of the swap order parameter must come from the swap action.

zeros. This difference in steady state values corresponds to the difference between pattern of signs vs. the pattern of zeros. We believe this is explained by the fact that even with the channel acting on a SWAP, the resulting operator nevertheless has a well-defined norm, unlike the string order parameter which may be sent to zero as we discussed extensively in Chapter 4.

What happens at infinite time? The steady state values for the depolarising and dephasing channels are the same since both channels drive towards the trivial maximally mixed (diagonal) state as the steady state. The fully depolarising and fully dephasing channel destroy \mathcal{S}_{ss} instantly, at the same (positive) steady state value $\mathcal{S}_{ss} = 1.6935 \times 10^{-5}$ and $\mathcal{N} = 0.0041$. Since \mathcal{S} becomes positive, this reflects a phase transition from the non-trivial SPT phase to the trivial phase, as it changes the pattern of signs.

Finally, towards completing our analysis of the swap order parameter we remark on some unanswered points. Interestingly, the blocking length L does not affect \mathcal{S} after L has exceeded the correlation length. We have found no length dependence in either the normalisation or the swap order parameter beyond blocking $L > L_I$ sites to injectivity, as recorded in Table 6.1. This implies that the swap order parameter contains an interaction between the middle part, which should decay to zero when $L \rightarrow \infty$, and the swap part which counteracts the middle party decay. This then would explain the lack of dependence on L and only on t . This also suggests that the decay rate of \mathcal{S} is the correct quantity² to consider towards a statement about SPTO robustness with respect to the swap order parameter.

Last, surprisingly, while one might have expected that the depolarising channel

²The decay rate of \mathcal{S} under action of a channel depends on whether the channel is strongly or weakly symmetric, and on the decay rate p which defines a one-parameter family of channels.

t	\mathcal{N} depolarising	\mathcal{N} dephasing	\mathcal{S} depolarising	\mathcal{S} dephasing
0	0.25	0.25	-0.25	-0.25
1	0.209	0.101	-0.249	-0.101
2	0.176	0.025	-0.186	-0.045
3	0.14	0.023	-0.139	-0.022
4	0.125	0.013	-0.103	-0.012
5	0.105	0.009	-0.077	-0.007

Table 6.1: Values for the normalisation N and the unnormalised swap order parameter \mathcal{S} when evolving them with time steps t for the depolarising and dephasing channel ($p = 1$ and $L = 5$). Notice that the normalisation N changes with the decay rate p .

destroys non-trivial \mathcal{S} instantaneously as it does with the string order parameter, this is not the case. When one does not carefully normalise \mathcal{S} it might even appear that the decay is not all too different. After normalising, the exponential vs. sub-exponential decay behaviour which characterises the weakly symmetric vs. strongly symmetric channels is obvious.

6.3.3 Robustness under strongly symmetric uncorrelated channels

The aim of this section has been to motivate that the swap order parameter is a good invariant to consider in the study of noisy SPT phases. Crucially, order parameters are invariants of phases and so intuitively we might expect that we can switch between different order parameters and still extract the information about the phase that we want. In practice, there are subtleties that we encounter, so some order parameters will be unsuitable. For example, we saw that with the string order analysis of Chapter 4 we must be mindful of end operators, since certain choices may happen to send the pattern to zero by accident. Since swap order does not get sent to zero accidentally, this may make it a more convenient quantity to study in the open systems setting.

Can we reformulate a statement about robustness of SPTO in terms of the swap order parameter? We have seen that strongly symmetric channels cause a sub-exponential decay in the swap order while weakly symmetric channels cause an exponential decay of the swap order in time. This suggests that we may make our numerical evidence with swap order rigorous by formulating a version of the previous Chapters' [Theorem 1](#).

Now we hope to replace [Lemma 1](#) in the proof of [Theorem 1](#) by the following Conjecture:

Conjecture 2: *A channel of uncorrelated noise maps the swap order parameter to other swap order parameters with the same pattern of signs if and only if the channel is strongly symmetric.*

[Conjecture 2](#) is plausible as at least one direction of the statement can be shown to be true. At the time of writing, the “if” direction is missing, but we expect some version of it to hold. The other direction (the “only if”) is that if a swap order parameter is preserved, then the channel which preserved it must have been strongly symmetric, is straightforward as it partially follows from [Chapter 4](#). Consider writing the swap order compactly as

$$\mathcal{S} := \mathcal{S}(T_{\mathcal{E}^\dagger(U_g)}, \text{SWAP}(g)), \quad (6.3.4)$$

with a dependence on the two parts corresponding to the middle part and the swap operator. We know how the middle part behaves. Namely, symmetries are sent to other symmetries by strongly symmetric channels, so that then the transfer matrix $T_{\mathcal{E}^\dagger(U_g)}$ has its maximum eigenvalue preserved. This implies that any expectation value of this operator can be nonvanishing in the thermodynamic limit. Otherwise, such as for weakly symmetric channels, they are sent to zero in the thermodynamic limit.

Then, it remains to show that the evolution of the $\text{SWAP}(g)$ operator is not zero generically. However, proving the other direction, that if a channel is strongly symmetric, then the swap order parameter is preserved, is tricky since we work on the level of observables rather than operators, and we must consider the SWAP action explicitly. The SWAP operator is not preserved under channels in general, as only unitary channels are reversible. We have not yet answered the question of how weakly and strongly symmetric compare³.

Note that [Conjecture 2](#) involves an observable (the swap order parameter) explicitly, rather than just the swap operator itself, so [Conjecture 2](#) can’t simply be exchanged with [Lemma 1](#) in proving [Theorem 1](#).

For the string order parameter as an invariant of SPTO, we were able to prove that strongly symmetric channels send end operators to different end operators of the same type (representing the same group element and irrep) and vice versa in [Lemma 1](#). Since strongly symmetric channels do not necessarily transform a swap operator into another swap operator, we must take a different path to prove [Conjecture 2](#).

Another way of formulating the statement which we aim to show is that the sign of the swap order parameter is the same before and after it is acted upon by a strongly symmetric channel. Namely, notice that we can define a new operator

³A simple example of a strongly symmetric channel which doesn’t preserve SWAP is the following. Consider the channel composed of diagonal, orthogonal Kraus operators $K_1 = \text{diag}(1, 0)$ and $K_2 = \text{diag}(0, 1)$ have $\mathcal{E}^\dagger(\text{SWAP}) = K_1 \otimes K_1 + K_2 \otimes K_2$.

$\mathcal{W}_{g,h}$ and its conjugate $\overline{\mathcal{W}}_{g,h}$ as follows

$$\mathcal{W}_{g,h} = \left(\begin{array}{c} \bullet \\ \text{---} \\ \bullet \\ U_g \\ \text{---} \\ \bullet \\ U_h \\ \text{---} \\ \bullet \end{array} \right), \quad \overline{\mathcal{W}}_{g,h} = \left(\begin{array}{c} \bullet \\ \text{---} \\ \bullet \\ U_g \\ \text{---} \\ \bullet \\ U_h \\ \text{---} \\ \bullet \end{array} \right). \quad (6.3.5)$$

The swap order parameter in terms of these operators is $\mathcal{S} = \text{Tr}(\mathcal{E}^\dagger(\mathcal{W}_{g,h})\mathcal{E}^\dagger(\overline{\mathcal{W}}_{g,h}))$. The action of a channel on $\mathcal{W}_{g,h}$ and $\overline{\mathcal{W}}_{g,h}$ is simply

$$\mathcal{E}^\dagger(\mathcal{W}_{g,h}) = \left(\begin{array}{c} \bullet \\ \text{---} \\ \bullet \\ U_g \\ \text{---} \\ \bullet \\ U_h \\ \text{---} \\ \bullet \end{array} \right), \quad \mathcal{E}^\dagger(\overline{\mathcal{W}}_{g,h}) = \left(\begin{array}{c} \bullet \\ \text{---} \\ \bullet \\ U_g \\ \text{---} \\ \bullet \\ U_h \\ \text{---} \\ \bullet \end{array} \right). \quad (6.3.6)$$

For the statement of the Conjecture to be true, we require the condition

$$\text{sgn}[\text{Tr}(\mathcal{W}_{g,h}\overline{\mathcal{W}}_{g,h})] = \text{sgn}[\text{Tr}(\mathcal{E}^\dagger(\mathcal{W}_{g,h})\mathcal{E}^\dagger(\overline{\mathcal{W}}_{g,h}))] \quad (6.3.7)$$

to be satisfied if and only if \mathcal{E} is strongly symmetric.

6.4 SET order parameter under dissipation

We now turn to the main point of this Chapter which is to study the robustness of SETO to noise. In the previous section we motivated that we can investigate symmetry fractionalisation (SF) for SPT phases in open systems via an order parameter different than the one considered in Chapter 4. This order parameter is called the swap order parameter Λ . It is nice to use for many reasons, including its numerical ease, since it is based on a local swap operator (which has finite support) rather than on some arbitrarily long string as the string operator does. We went through the trouble of understanding the 1D swap order parameter since an order parameter with an analogous form was developed recently for SET phases in Ref. [11]. The order parameter Λ (2.6.15) detects the SF classes of anyons in the bulk of the state through a SWAP operator, symmetry operator and anyon creation operators which we introduced in Chapter 2.

We have motivated that swap order parameters are a good fingerprint for 1D SPTO in open systems, via their ability to detect the SF effects in the pattern of signs, so it is natural to expect that the analogous order parameter for 2D SETO will act similarly. We saw that the swap order parameter \mathcal{S} displays pronounced differences under channels with a weak symmetry compared to a strong symmetry. We now develop a similar intuition for SET phases with the order parameter Λ defined in 2.6.15 as our fingerprint of SETO to discuss the robustness of SETO in open systems.

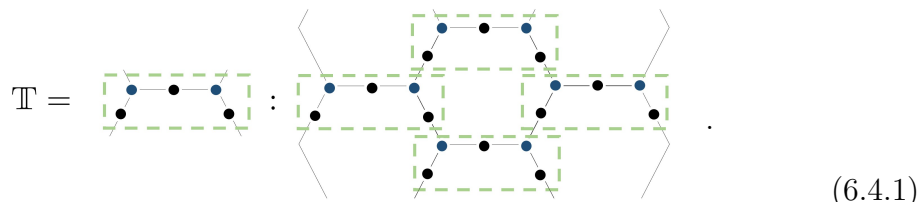
We study the model introduced in Chapter 2 corresponding to a Toric code decorated by cluster state loops which is called $|SET\rangle$ (2.6.15). At this time, our findings are mainly numerical due to the difficulty of proofs with the PEPS construction. We present the numerical study first, and give an outline of how we expect an analytic part to follow.

6.4.1 Numerical study

We now consider the action of noise on the model introduced in Ref. §2.6.1 which can be understood as decorating a 2D Toric code with cluster state loops. We leverage the methods and numerical tools developed in Ref. [10], and modify them to explore the order parameter Λ under evolution by a channel of uncorrelated noise. We observe that depolarising noise, which is weakly symmetric, sends the order parameter to a positive value indicating the trivial phase. Dephasing noise, which is strongly symmetric, preserves the sign of the order parameter for finite times, which suggests the phase is preserved. This is shown in Fig. 6.6.

The steady state value in the weakly symmetric case is $\Lambda_{ss} = 5.623 \times 10^{-8}$ and in the strongly symmetric case is $\Lambda_{ss} = -0.0311$. The fully depolarising and fully dephasing channels reach the respective steady state values instantaneously (after just one time step), and notably have opposite sign. Recall that the fully dephasing (depolarising) channel represents the infinite time limit of the dephasing (depolarising) channel; this indicates that the sign of Λ , which is equivalent to the SET phase, characterises the SETO robustness. This is suggestive that a similar Conjecture §6.3.3 as for the 1D swap order parameter \mathcal{S} holds for the 2D SETO order parameter Λ .

We summarise the details of the methods in Ref. [10]. The ground state of H_{SET} can be found using the iPEPS variational algorithm, where bond dimension $D = 3$ is sufficient to characterise the entire phase diagram with a very high accuracy. There would generally be $3^4 \times 2^5$ variational parameters for this PEPS which makes this a hard numerical problem. We fortunately don't need to solve this because we are primarily interested in the ground state of H_{SET} which admits a TN representation with just $D = 3$. Numerics done here makes use of this exact PEPS, given in Appendix A of Ref. [10], as well as the PEPS for the Toric code to study the trivial SET phase. Notably, the PEPS generating $|SET\rangle$ resembles that of the cluster state, since it is a tensor product of Paulis and a junk subspace (as discussed in Chapter 3) which nods to the inherited fractionalisation properties [289]. The tensor networks are contracted by placing them on a cylinder which is infinite in one direction. The order parameter is then computed using boundary MPS methods for the fixed points [290]. Finally, for simplicity the PEPS representation is redefined to give a translation-invariant input, which the pure representation on the honeycomb lattice (with sub-lattices A and B) does not provide. This is done by redefining the PEPS into the translation-invariant tensor \mathbb{T} which is defined



$$\mathbb{T} = \text{[Diagram of tensor network]} \quad (6.4.1)$$

This tensor blocks together three edges and the two vertices they are incident on of the hexagonal lattice which generates the translation-invariant tensor.

The tensor network diagram for the order parameter under the general action

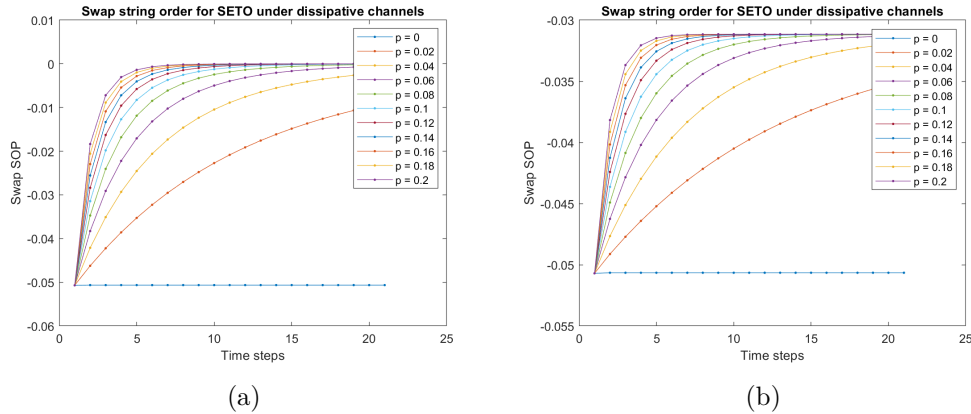


Figure 6.5: The SET order parameter (unnormalised) evolved under two channels of uncorrelated noise: (a) weakly symmetric depolarising noise and (b) strongly symmetric dephasing noise. For the SET phase, depolarising noise (weakly symmetric) causes the order parameter to decay to a finite positive value close to zero. The dephasing channel (strongly symmetric) causes the order parameter to decay slowly to a finite negative value.

of a channel is pictured in Fig. 6.6. For a more detailed reminder see Fig. 2.10 and Section §2.6. We may act with the channel on both vertex and edge qubits, as depicted, but it will be most interesting to focus on evolution which only affects the vertices and not the edges. This isolates the effect of the symmetry of the channel evolution to where the symmetry-enrichment is stored. Considering vertices and edges together takes into account the interplay with intrinsic topological order, i.e. the robustness of anyons of the Toric code, which are known to be unstable to sufficiently large amounts of thermal noise [61, 291]. This is a relevant question to the robustness of SETO, but in this part we choose to focus on the role of symmetries and here we share simulations of vertex-only evolution.

6.4.2 SETO robustness under strongly symmetric uncorrelated channels

The following Section describes a possible Conjecture about the robustness of SETO in open systems.

To understand the robustness of 2D SET phases, we have to ask two questions. We consider which are the conditions on open system evolution which preserve invariants of the phase, and vice versa, when the phase invariant is preserved by an evolution, which kinds of open system evolution are allowed? Based on the numerical evidence that preceded this, as well as the analytical proof for 1D SPTO, we are motivated that a similar Theorem may hold for SETO. We take the setting of G-injective PEPS for a “coherent SET phase”, meaning a class of coherent SET states with a given *pattern of signs*.

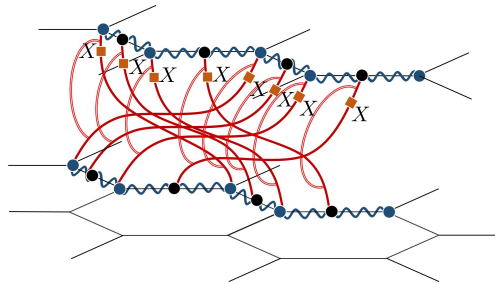


Figure 6.6: Evolving the order parameter for SETO (2.6.15) under channels. The evolution is depicted as a doubled red line going from a physical leg for a site on the bra to a physical leg for the same site on the ket.

Conjecture 3: *Fix any coherent SET phase. A semigroup of channels of uncorrelated noise generically preserves the phase at short times if and only if the semigroup is generated by a strongly symmetric Lindbladian.*

We outline how we might be able to show that SETO invariants are preserved by a channel iff that channel is strongly symmetric. Notably, this is only possible if the underlying topological anyons are still present, which may only occur for short times.

It was shown that for SET phases of quantum double models the order parameter Λ uniquely characterises the SET invariant $\omega(q, k)$ [11]. It does so with a pattern of signs. For example, in the state $|SET\rangle$ which has a global symmetry $\mathbb{Z}_2 \times \mathbb{Z}_2$, the SF class which classifies it corresponds to a D_8 gauge theory, and predicts $\Lambda = -1$ (normalised) for the order parameter of Eq. 2.6.15. On the other hand, for the Toric code $\Lambda = +1$. Conjecture 3 tells us that when the pattern of signs $\omega(q, k)$ is preserved, the SET phase is preserved also.

We investigate the quantity $\mathcal{E}^\dagger(\Lambda)$, in the case of uncorrelated noise where \mathcal{E} is a tensor product of single site channels. We study how $\mathcal{E}^\dagger(\Lambda)$ behaves under Heisenberg evolution by a channel \mathcal{E} with different degrees of symmetry, as previously.

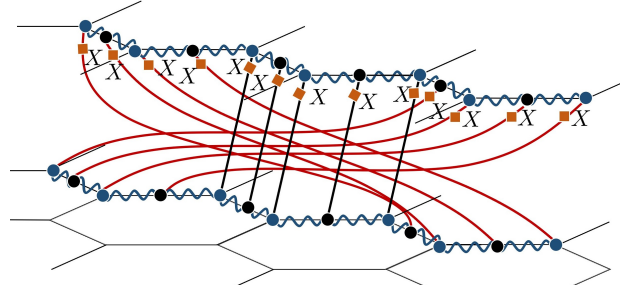
It may be helpful to modify the original SET order parameter (2.6.15) shown in Fig. 6.6 to include a string of symmetries in between the swapped sites which makes it more similar to the 1D swap order parameter \mathcal{S} . Such a modification doesn't change anything about the order parameter until a channel is applied; for a strongly symmetric channel, the modification again does nothing but add a phase, while for a weakly symmetric channel, the order parameter instantly vanishes, due to Chapter 4.

The modified version of Λ takes the form

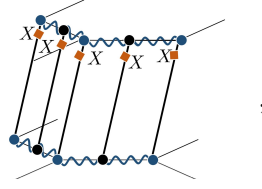
$$\tilde{\Lambda} = \langle SET | O_{\text{SWAP}}(g) \prod_{U_g} T_{U_g} O_{\text{SWAP}}(g)^\dagger | SET \rangle, \quad (6.4.2)$$

where T_{U_g} is the transfer operator on a symmetry element $g \in G$, and $O_{\text{SWAP}}(g)$ is the swap on a local patch which acts on some symmetry g , and X acts on all

sites of the bra and CZ operators are between all sites. In diagrammatic form the modified version $\tilde{\Lambda}$ reads


(6.4.3)

where T_{U_g} is


(6.4.4)

for an example length $l = 5$ sites, while $O_{\text{SWAP}}(g)$ is the SWAP from bra to ket, while its dagger goes from ket to bra.

This allows us to write $\tilde{\Lambda}$ simply, as we did previously for the 1D SPTO swap order parameter \mathcal{S} (6.3.4), as a dependence on the transfer operator and a SWAP

$$\tilde{\Lambda} := \tilde{\Lambda}(T_{U_g}, O_{\text{SWAP}}(g)), \quad (6.4.5)$$

Note that when $l = 0$, $\tilde{\Lambda} = \Lambda$. We know that in 1D $T_{\mathcal{E}^\dagger(U_g)}$ is preserved iff the channel is strongly symmetric.

Step 1 of proving the desired claim is to prove for G-injective PEPS that $\lambda_{\max}(T_{\mathcal{E}^\dagger(U_g)}) = 1$ iff \mathcal{E} is strongly symmetric. This follows from G-injectivity immediately due to the Cauchy-Schwarz proof of [Theorem 1](#). If a channel has $\lambda_{\max} = 1$ for a G-injective PEPS, then the channel must have been strongly symmetric and vice versa.

Step 2 of proving the desired claim is to consider the channel action on the swap operator in Λ which is written as $\mathcal{E}^\dagger(O_{\text{SWAP}}(g))$. If [Conjecture 2](#) is true, then it is reasonable that Step 2 towards would follow, such that the claim can be proven. This could be possible through a generalisation of [Eq. 6.3.5](#).

6.5 Discussion & Conclusions

We have made progress towards showing that certain 2D SET phases are robust to strongly symmetric noise. This work was motivated by the intuition that SET phases are protected by symmetry and so the allowed operations, even in open systems, should preserve that symmetry. We expect moreover that even channels with weak symmetry will illicit a profoundly different response from channels with strong symmetry, and will not preserve the phase. Our analysis for SETO has

been facilitated by the analogy with the 1D swap order parameter for SPTO in the framework of G -symmetric MPS. We investigate a similar order parameter for 2D SETO in the framework of G -injective PEPS. We present [Conjecture 3](#) which formalises this. We give numerical evidence to support the Conjecture, and outline how we hope to show this analytically.

Several points are still in development. The state $|SET\rangle$ has been a key character in our analysis of robustness of SETO. This state is a fixed point with zero correlation length. It would be prudent to consider the whole phase diagram of H_{SET} in order to understand the dependence of the phase robustness on correlation-length. It is likely, as hinted by the results of Ref. [10], that the order parameter will demonstrate a dependence on the blocking length L .

The missing link towards Step 2 in the proof of [Conjecture 3](#) for the SETO order parameter lies in developing an expression to describe the action of a channel on swap operations, which in brute force methods means computing the cross-terms of Kraus operators. This has not been completed in the 1D case, which would naturally lead to an extension to 2D. Furthermore this would more fully explain why the swap order parameter saturates at a finite value rather than zero at infinite time.

As an outlook to this work, it would be interesting to link the theoretical possibility for phase robustness to actual error correcting ability, and in particular also to SCQM. Does robustness of an SET phase at finite time translate to long coherence times in experiment? A particular point of interest is exploring models which theoretically host SCQM, especially of how the SCQM property survives noise which respects strong symmetry.

Chapter 7

Conclusions

We began this Thesis driven by a motivation to understand the entanglement structure which gives rise to emergent phenomena such as topological phases of matter, and moreover the robustness of these structures to noise. We have seen how symmetry and entanglement interplay in symmetry protected topological (SPT) phases and are characterised by certain fingerprints. The bulk of this Thesis was attacking the problem of how fingerprints of topological phases behave when coupled to an open system. We considered how to integrate symmetries with this setting, in which several notions of symmetry may be defined and which lead to fundamentally different phenomena. Crucially, we have leveraged the tool of tensor networks (TN), which has enabled us to systematically study phases by expressing global properties in a local manner.

There are many other approaches which one must tackle in order to formulate a complete picture of topological phases with symmetries in open systems, and hence several open questions left at the end of this Thesis. We will give some remarks on these questions, in addition to the open problems and outlook we have given at the end of every Chapter.

In Chapter 3 we studied the entanglement structure of SPT phases which led us to discover a new fingerprint for 1D SPTO, the inaccessible entanglement. This latent entanglement highlighted the intimate relationship between SPT phases and quantum computation. Namely, we determined a relation for a bound on the inaccessible entanglement, which directly includes the degeneracy of the topologically protected edge modes. Furthermore, all non-trivial SPT phases host some non-trivial amount of inaccessible entanglement, which may be connected to their computational power in measurement-based quantum computing (MBQC). This later led us to define the notion of SPT complexity which uniquely defines the computational power of the SPT phase.

In Chapter 4 we attacked the problem of the robustness of SPT phases of matter. We considered how SPTO states evolve under quantum channels with different notions of symmetry. We showed that weak symmetry instantly destroys the SPT phase ω . However, a strong symmetry condition on channels allows the SPT phase to persist at finite times. This highlights the importance of the interplay of entanglement and symmetry on the local level in SPT phases, since

weak symmetry does not satisfy all local symmetries.

A most important question in the classification of mixed state SPTO is to determine which is the class of mixed states with SPTO. We introduced coherent SPT mixed states, generalising certain symmetric matrix product states (MPS) which have a well-defined SPT phase $|\Psi_\omega\rangle$. It is open whether the class of coherent SPT states is complete, and whether it also includes thermal states or steady states. These would be useful questions to answer, as such states are the realisations of many physical processes, such as coupling to a thermal environment. This question has also recently been addressed for RG fixed points in Refs. [292, 293]. We comment that since thermal states of local, gapped Hamiltonians obey an entanglement area-law and as such are well-represented by TN [294–296], we expect that SPTO thermal states could be represented by matrix product density operators (MPDO), consistently extending from pure state SPT phases.

We have considered several indicators of SPTO including string order, edge modes and inaccessible entanglement. We gave numerical evidence on top of the analytic proof in the form of theorems. The fingerprints of SPTO which our approach has relied on were originally constructed for phases of pure states and detect entanglement structure, but in mixed states non-classicality can appear in more general ways than entanglement. This leaves the question: are there natural indicators for mixed state SPTO beyond entanglement-based fingerprints, and further, does SPTO manifest in mixed states beyond the cocycle classification ω ?

In Chapter 5 we considered which operations transmute between different SPT phases of mixed states, which is given by twisted versions of the strongly symmetric (SS) channels. We defined the SPT complexity, which is given by the degeneracy of topologically protected edge modes. This may either stay the same or be reduced by twisted-SS noise. Notably the SPT complexity determines the computational power in MBQC, which highlights the relationship between SPTO and quantum computation. We have left open several speculative questions, including how dissipation in the form of twisted-SS channels may contribute to a resource theory of MBQC. An additional question is what physical processes twisted-SS channels correspond to. It would be interesting to be able to distinguish these from channels which implement phase transitions through developing a structured framework, and to study invariants of mixed state under those phase transitions. Finally, how does this relate to a recent work which suggested that there are no dissipative phase transitions in local, commuting Hamiltonians under a particular Lindbladian evolution, by showing their rapid thermalisation [297].

Finally, in Chapter 6 we discussed how our findings for 1D SPTO could be applied to symmetry enriched topological (SET) phases. We numerically studied a particular model of 2D SETO [10]. The numerical evidence leads us to conjecture that SETO is protected by channels satisfying strong symmetry, and showing this analytically is ongoing work. This demonstrated that our work in Chapter 4 can be applied to higher-dimensional topological phases with symmetries, which is a promising future direction. A final question particularly relevant to the NISQ era is how the methods and results of Chapters 4 and 6 can be used to assess the fault-tolerance of phases of matter in practice: in particular, the robustness of

SPTO towards the MBQC protocol and of SETO towards topological quantum computing or self-correcting quantum memories.

Bibliography

- [1] M. A. Nielsen and I. Chuang, *Quantum computation and quantum information* (AAPT, 2002).
- [2] A. Kitaev, *Fault-tolerant quantum computation by anyons*, Ann. Phys. **303**, 2 (2003).
- [3] R. Raussendorf and H. J. Briegel, *A One-Way Quantum Computer*, Phys. Rev. Lett. **86**, 5188 (2001).
- [4] A. Coser and D. Pérez-García, *Classification of phases for mixed states via fast dissipative evolution*, Quantum **3**, 174 (2019).
- [5] J. Preskill, *Quantum Computing in the NISQ era and beyond*, Quantum **2**, 79 (2018).
- [6] D. T. Stephen, D.-S. Wang, A. Prakash, T.-C. Wei, and R. Raussendorf, *Computational Power of Symmetry-Protected Topological Phases*, Phys. Rev. Lett. **119**, 010504 (2017).
- [7] S. Bravyi and B. Terhal, *A no-go theorem for a two-dimensional self-correcting quantum memory based on stabilizer codes*, New Journal of Physics **11**, 043029 (2009).
- [8] S. Lieu, R. Belyansky, J. T. Young, R. Lundgren, V. V. Albert, and A. V. Gorshkov, *Symmetry Breaking and Error Correction in Open Quantum Systems*, Physical Review Letters **125** (2020).
- [9] H. Bombin, *Topological Order with a Twist: Ising Anyons from an Abelian Model*, Phys. Rev. Lett. **105**, 030403 (2010).
- [10] J. Garre-Rubio, M. Iqbal, and D. T. Stephen, *String order parameters for symmetry fractionalization in an enriched toric code*, Phys. Rev. B **103**, 125104 (2021).
- [11] J. Garre-Rubio and S. Iblisdir, *Local order parameters for symmetry fractionalization*, New Journal of Physics **21**, 113016 (2019).
- [12] X.-G. Wen, *Colloquium: Zoo of quantum-topological phases of matter*, Reviews of Modern Physics **89**, 041004 (2017).
- [13] H.-P. Breuer *et al.*, *The theory of open quantum systems* (Oxford University Press on Demand, 2002).
- [14] A. Acín *et al.*, *The quantum technologies roadmap: a European community view*, New Journal of Physics **20**, 080201 (2018).
- [15] M. A. Nielsen and I. Chuang, *Quantum computation and quantum information* (AAPT, 2002).

- [16] M.-O. Renou, D. Trillo, M. Weilenmann, T. P. Le, A. Tavakoli, N. Gisin, A. Acín, and M. Navascués, *Quantum theory based on real numbers can be experimentally falsified*, Nature **600**, 625 (2021).
- [17] Y. Ge and J. Eisert, *Area laws and efficient descriptions of quantum many-body states*, (2014).
- [18] D. N. Page, *Average entropy of a subsystem*, Phys. Rev. Lett. **71**, 1291 (1993).
- [19] M. B. Hastings and T. Koma, *Spectral Gap and Exponential Decay of Correlations*, Communications in Mathematical Physics **265**, 781 (2006).
- [20] D. Sauerwein, N. R. Wallach, G. Gour, and B. Kraus, *Transformations among Pure Multipartite Entangled States via Local Operations are Almost Never Possible*, Phys. Rev. X **8**, 031020 (2018).
- [21] B. Yan and S.-C. Zhang, *Topological materials*, Reports on Progress in Physics **75**, 096501 (2012).
- [22] B. Yan and C. Felser, *Topological materials: Weyl semimetals*, Annual Review of Condensed Matter Physics **8**, 337 (2017).
- [23] M. Vergniory, L. Elcoro, C. Felser, N. Regnault, B. A. Bernevig, and Z. Wang, *A complete catalogue of high-quality topological materials*, Nature **566**, 480 (2019).
- [24] R. P. Feynman, *Simulating physics with computers*, in *Feynman and computation*, pp. 133–153, CRC Press, 2018.
- [25] R. Raussendorf, D. E. Browne, and H. J. Briegel, *Measurement-based quantum computation on cluster states*, Phys. Rev. A **68**, 022312 (2003).
- [26] R. Raussendorf, C. Okay, D.-S. Wang, D. T. Stephen, and H. P. Nautrup, *Computationally Universal Phase of Quantum Matter*, Phys. Rev. Lett. **122**, 090501 (2019).
- [27] A. C. Doherty and S. D. Bartlett, *Identifying Phases of Quantum Many-Body Systems That Are Universal for Quantum Computation*, Phys. Rev. Lett. **103**, 020506 (2009).
- [28] D. V. Else, S. D. Bartlett, and A. C. Doherty, *Symmetry protection of measurement-based quantum computation in ground states*, New Journal of Physics **14**, 113016 (2012).
- [29] A. Miyake, *Quantum Computation on the Edge of a Symmetry-Protected Topological Order*, Phys. Rev. Lett. **105**, 040501 (2010).
- [30] S. D. Bartlett, G. K. Brennen, A. Miyake, and J. M. Renes, *Quantum Computational Renormalization in the Haldane Phase*, Phys. Rev. Lett. **105**, 110502 (2010).

- [31] D. V. Else, I. Schwarz, S. D. Bartlett, and A. C. Doherty, *Symmetry-Protected Phases for Measurement-Based Quantum Computation*, Phys. Rev. Lett. **108**, 240505 (2012).
- [32] H. Poulsen Nautrup and T.-C. Wei, *Symmetry-protected topologically ordered states for universal quantum computation*, Phys. Rev. A **92**, 052309 (2015).
- [33] J. Miller and A. Miyake, *Hierarchy of universal entanglement in 2D measurement-based quantum computation*, npj Quantum Information **2**, 16036 (2016).
- [34] T.-C. Wei and C.-Y. Huang, *Universal measurement-based quantum computation in two-dimensional symmetry-protected topological phases*, Phys. Rev. A **96**, 032317 (2017).
- [35] J. R. Wootton, *Demonstrating non-Abelian braiding of surface code defects in a five qubit experiment*, Quantum Science and Technology **2**, 015006 (2017).
- [36] C. Song *et al.*, *Demonstration of Topological Robustness of Anyonic Braiding Statistics with a Superconducting Quantum Circuit*, Phys. Rev. Lett. **121**, 030502 (2018).
- [37] C. K. Andersen *et al.*, *Repeated quantum error detection in a surface code*, Nature Physics **16**, 875 (2020).
- [38] K. J. Satzinger *et al.*, *Realizing topologically ordered states on a quantum processor*, Science **374**, 1237 (2021).
- [39] C.-Y. Lu, W.-B. Gao, O. Gühne, X.-Q. Zhou, Z.-B. Chen, and J.-W. Pan, *Demonstrating Anyonic Fractional Statistics with a Six-Qubit Quantum Simulator*, Phys. Rev. Lett. **102**, 030502 (2009).
- [40] J. K. Pachos, W. Wieczorek, C. Schmid, N. Kiesel, R. Pohlner, and H. Weinfurter, *Revealing anyonic features in a toric code quantum simulation*, New Journal of Physics **11**, 083010 (2009).
- [41] G. Feng, G. Long, and R. Laflamme, *Experimental simulation of anyonic fractional statistics with an NMR quantum-information processor*, Phys. Rev. A **88**, 022305 (2013).
- [42] A. J. Park, E. McKay, D. Lu, and R. Laflamme, *Simulation of anyonic statistics and its topological path independence using a seven-qubit quantum simulator*, New Journal of Physics **18**, 043043 (2016).
- [43] N. Kiesel, C. Schmid, U. Weber, G. Tóth, O. Gühne, R. Ursin, and H. Weinfurter, *Experimental Analysis of a Four-Qubit Photon Cluster State*, Phys. Rev. Lett. **95**, 210502 (2005).
- [44] N. Kiesel, C. Schmid, U. Weber, R. Ursin, and H. Weinfurter, *Linear Optics Controlled-Phase Gate Made Simple*, Phys. Rev. Lett. **95**, 210505 (2005).

- [45] P. Walther, K. J. Resch, T. Rudolph, E. Schenck, H. Weinfurter, V. Vedral, M. Aspelmeyer, and A. Zeilinger, *Experimental one-way quantum computing*, Nature **434**, 169 (2005).
- [46] K. Chen, C.-M. Li, Q. Zhang, Y.-A. Chen, A. Goebel, S. Chen, A. Mair, and J.-W. Pan, *Experimental Realization of One-Way Quantum Computing with Two-Photon Four-Qubit Cluster States*, Phys. Rev. Lett. **99**, 120503 (2007).
- [47] H. Wunderlich, G. Vallone, P. Mataloni, and M. B. Plenio, *Optimal verification of entanglement in a photonic cluster state experiment*, New Journal of Physics **13**, 033033 (2011).
- [48] M. V. Larsen, X. Guo, C. R. Breum, J. S. Neergaard-Nielsen, and U. L. Andersen, *Deterministic multi-mode gates on a scalable photonic quantum computing platform*, Nature Physics **17**, 1018 (2021).
- [49] M. Chen, N. C. Menicucci, and O. Pfister, *Experimental Realization of Multipartite Entanglement of 60 Modes of a Quantum Optical Frequency Comb*, Phys. Rev. Lett. **112**, 120505 (2014).
- [50] S. Yokoyama *et al.*, *Ultra-large-scale continuous-variable cluster states multiplexed in the time domain*, Nature Photonics **7**, 982 (2013).
- [51] C. González-Arciniegas, P. Nussenzeveig, M. Martinelli, and O. Pfister, *Cluster States from Gaussian States: Essential Diagnostic Tools for Continuous-Variable One-Way Quantum Computing*, PRX Quantum **2**, 030343 (2021).
- [52] O. Mandel, M. Greiner, A. Widera, T. Rom, T. W. Hänsch, and I. Bloch, *Controlled collisions for multi-particle entanglement of optically trapped atoms*, Nature **425**, 937 (2003).
- [53] C.-Y. Lu *et al.*, *Experimental entanglement of six photons in graph states*, Nature physics **3**, 91 (2007).
- [54] P. W. Shor, *Polynomial-Time Algorithms for Prime Factorization and Discrete Logarithms on a Quantum Computer*, SIAM Journal on Computing **26**, 1484 (1997).
- [55] S. Aaronson, *The Limits of Quantum Computers*, Scientific American **298**, 62 (2008).
- [56] J. von Neumann, *Probabilistic Logics and the Synthesis of Reliable Organisms From Unreliable Components* (Princeton University Press, 2016), pp. 43–98.
- [57] A. Y. Kitaev, *Quantum computations: algorithms and error correction*, Russian Mathematical Surveys **52**, 1191 (1997).
- [58] E. Knill, R. Laflamme, and W. H. Zurek, *Resilient quantum computation: error models and thresholds*, Proceedings of the Royal Society of London. Series A: Mathematical, Physical and Engineering Sciences **454**, 365 (1998).

- [59] D. Aharonov and M. Ben-Or, *Fault-Tolerant Quantum Computation With Constant Error Rate*, 1999.
- [60] X.-G. Wen, *Colloquium: Zoo of quantum-topological phases of matter*, Rev. Mod. Phys. **89**, 041004 (2017).
- [61] M. B. Hastings, *Topological Order at Nonzero Temperature*, Physical Review Letters **107** (2011).
- [62] C. Castelnovo and C. Chamon, *Topological order in a three-dimensional toric code at finite temperature*, Phys. Rev. B **78**, 155120 (2008).
- [63] S. Iblisdir, D. Pérez-García, M. Aguado, and J. Pachos, *Scaling law for topologically ordered systems at finite temperature*, Phys. Rev. B **79**, 134303 (2009).
- [64] O. Viyuela, A. Rivas, and M. Martin-Delgado, *Uhlmann Phase as a Topological Measure for One-Dimensional Fermion Systems*, Physical Review Letters **112** (2014).
- [65] O. Viyuela, A. Rivas, and M. Martin-Delgado, *Symmetry-protected topological phases at finite temperature*, 2D Materials **2**, 034006 (2015).
- [66] S. Diehl, E. Rico, M. A. Baranov, and P. Zoller, *Topology by dissipation in atomic quantum wires*, Nature Physics **7**, 971–977 (2011).
- [67] C.-E. Bardyn, M. A. Baranov, E. Rico, A. İmamoğlu, P. Zoller, and S. Diehl, *Majorana Modes in Driven-Dissipative Atomic Superfluids with a Zero Chern Number*, Phys. Rev. Lett. **109**, 130402 (2012).
- [68] C.-E. Bardyn, M. A. Baranov, C. V. Kraus, E. Rico, A. İmamoğlu, P. Zoller, and S. Diehl, *Topology by dissipation*, New Journal of Physics **15**, 085001 (2013).
- [69] M. McGinley and N. R. Cooper, *Classification of topological insulators and superconductors out of equilibrium*, Phys. Rev. B **99**, 075148 (2019).
- [70] A. T. K. Tan, S.-N. Sun, R. N. Tazhigulov, G. K.-L. Chan, and A. J. Minnich, *Realizing symmetry-protected topological phases in a spin-1/2 chain with next-nearest neighbor hopping on superconducting qubits*, 2021.
- [71] D. Azses, R. Haenel, Y. Naveh, R. Raussendorf, E. Sela, and E. G. Dalla Torre, *Identification of Symmetry-Protected Topological States on Noisy Quantum Computers*, Phys. Rev. Lett. **125**, 120502 (2020).
- [72] C. de Groot, D. T. Stephen, A. Molnar, and N. Schuch, *Inaccessible entanglement in symmetry protected topological phases*, Journal of Physics A: Mathematical and Theoretical **53**, 335302 (2020).
- [73] C. de Groot, A. Turzillo, and N. Schuch, *Symmetry Protected Topological Order in Open Quantum Systems*, (2022), 2112.04483.

- [74] C. de Groot, J. Garre Rubio, and A. Turzillo, *Symmetry Enriched Topological Order in Open Systems*, arxiv (in preparation).
- [75] B. Zeng, X. Chen, D.-L. Zhou, and X.-G. Wen, *Quantum information meets quantum matter: From Quantum Entanglement to Topological Phases of Many-Body Systems* (Springer, 2019).
- [76] J. C. Bridgeman and C. T. Chubb, *Hand-waving and Interpretive Dance: An Introductory Course on Tensor Networks*, *J. Phys. A: Math. Theor.* **50** (2017), arXiv:1603.03039.
- [77] I. Cirac, D. Perez-Garcia, N. Schuch, and F. Verstraete, *Matrix Product States and Projected Entangled Pair States: Concepts, Symmetries, and Theorems*, 2021, 2011.12127.
- [78] J. Eisert, M. Cramer, and M. B. Plenio, *Colloquium: Area laws for the entanglement entropy*, *Rev. Mod. Phys.* **82**, 277 (2010).
- [79] B. Zeng and X.-G. Wen, *Gapped quantum liquids and topological order, stochastic local transformations and emergence of unitarity*, *Phys. Rev. B* **91**, 125121 (2015).
- [80] K. G. Wilson, *The renormalization group: Critical phenomena and the Kondo problem*, *Rev. Mod. Phys.* **47**, 773 (1975).
- [81] F. Verstraete, J. I. Cirac, J. I. Latorre, E. Rico, and M. M. Wolf, *Renormalization-Group Transformations on Quantum States*, *Phys. Rev. Lett.* **94**, 140601 (2005).
- [82] Z.-C. Gu and X.-G. Wen, *Tensor-entanglement-filtering renormalization approach and symmetry-protected topological order*, *Phys. Rev. B* **80**, 155131 (2009).
- [83] M. A. Levin and X.-G. Wen, *String-net condensation: A physical mechanism for topological phases*, *Phys. Rev. B* **71**, 045110 (2005).
- [84] L. D. Landau, *On the theory of phase transitions*, *Ukr. J. Phys.* **11**, 19 (1937).
- [85] J. M. Kosterlitz and D. J. Thouless, *Ordering, metastability and phase transitions in two-dimensional systems*, *Journal of Physics C: Solid State Physics* **6**, 1181 (1973).
- [86] H. L. Stormer, D. C. Tsui, and A. C. Gossard, *The fractional quantum Hall effect*, *Rev. Mod. Phys.* **71**, S298 (1999).
- [87] X. G. Wen, *Vacuum degeneracy of chiral spin states in compactified space*, *Phys. Rev. B* **40**, 7387 (1989).
- [88] X.-G. Wen, *Topological orders in rigid states*, *International Journal of Modern Physics B* **4**, 239 (1990).

- [89] X. G. Wen and Q. Niu, *Ground-state degeneracy of the fractional quantum Hall states in the presence of a random potential and on high-genus Riemann surfaces*, Phys. Rev. B **41**, 9377 (1990).
- [90] M. Born and V. Fock, *Beweis des adiabatenatzes*, Zeitschrift für Physik **51**, 165 (1928).
- [91] X. Chen, Z.-C. Gu, and X.-G. Wen, *Local unitary transformation, long-range quantum entanglement, wave function renormalization, and topological order*, Phys. Rev. B **82**, 155138 (2010).
- [92] M. den Nijs and K. Rommelse, *Preroughening transitions in crystal surfaces and valence-bond phases in quantum spin chains*, Phys. Rev. B **40**, 4709 (1989).
- [93] A. Smith, B. Jobst, A. G. Green, and F. Pollmann, *Crossing a topological phase transition with a quantum computer*, (2019), arXiv:1910.05351.
- [94] M. Iqbal, K. Duivenvoorden, and N. Schuch, *Study of anyon condensation and topological phase transitions from a \mathbb{Z}_4 topological phase using the projected entangled pair states approach*, Phys. Rev. B **97**, 195124 (2018).
- [95] L. Tsui, H.-C. Jiang, Y.-M. Lu, and D.-H. Lee, *Quantum phase transitions between a class of symmetry protected topological states*, Nuclear Physics B **896**, 330 (2015).
- [96] M. B. Hastings and X.-G. Wen, *Quasiadiabatic continuation of quantum states: The stability of topological ground-state degeneracy and emergent gauge invariance*, Phys. Rev. B **72**, 045141 (2005).
- [97] S. Bachmann and B. Nachtergaele, *On Gapped Phases with a Continuous Symmetry and Boundary Operators*, Journal of Statistical Physics **154**, 91–112 (2013).
- [98] T. J. Osborne, *Simulating adiabatic evolution of gapped spin systems*, Physical review a **75**, 032321 (2007).
- [99] B. Nachtergaele, Y. Ogata, and R. Sims, *Propagation of Correlations in Quantum Lattice Systems*, Journal of Statistical Physics **124**, 1–13 (2006).
- [100] S. Bravyi, M. B. Hastings, and F. Verstraete, *Lieb-Robinson Bounds and the Generation of Correlations and Topological Quantum Order*, Phys. Rev. Lett. **97**, 050401 (2006).
- [101] M. Cheneau *et al.*, *Light-cone-like spreading of correlations in a quantum many-body system*, Nature **481**, 484 (2012).
- [102] X. Chen, Z.-C. Gu, and X.-G. Wen, *Classification of gapped symmetric phases in one-dimensional spin systems*, Phys. Rev. B **83**, 035107 (2011).

- [103] T. Scaffidi, D. E. Parker, and R. Vasseur, *Gapless Symmetry-Protected Topological Order*, Phys. Rev. X **7**, 041048 (2017).
- [104] R. Verresen, R. Thorngren, N. G. Jones, and F. Pollmann, *Gapless topological phases and symmetry-enriched quantum criticality*, (2019), arXiv:1905.06969.
- [105] R. Thorngren, A. Vishwanath, and R. Verresen, *Intrinsically Gapless Topological Phases*, (2020), arXiv:2008.06638.
- [106] D. Azses, E. G. D. Torre, and E. Sela, *Observing Floquet topological order by symmetry resolution*, 2021, 2109.01151.
- [107] A. Smith, M. S. Kim, F. Pollmann, and J. Knolle, *Simulating quantum many-body dynamics on a current digital quantum computer*, npj Quantum Information **5** (2019).
- [108] R. Alicki, M. Horodecki, P. Horodecki, and R. Horodecki, *On thermal stability of topological qubit in Kitaev's 4D model*, 2008, 0811.0033.
- [109] R. Raussendorf, S. Bravyi, and J. Harrington, *Long-range quantum entanglement in noisy cluster states*, Phys. Rev. A **71**, 062313 (2005).
- [110] D. Cavalcanti, L. Aolita, A. Ferraro, A. García-Saez, and A. Acín, *Macroscopic bound entanglement in thermal graph states*, New Journal of Physics **12**, 025011 (2010).
- [111] A. Kay, J. K. Pachos, W. Dür, and H.-J. Briegel, *Optimal purification of thermal graph states*, New Journal of Physics **8**, 147 (2006).
- [112] D. Markham, A. Miyake, and S. Virmani, *Entanglement and local information access for graph states*, New Journal of Physics **9**, 194–194 (2007).
- [113] D. Markham, J. Anders, V. Vedral, M. Muraio, and A. Miyake, *Survival of entanglement in thermal states*, EPL (Europhysics Letters) **81**, 40006 (2008).
- [114] M. Hajdušek and V. Vedral, *Entanglement in pure and thermal cluster states*, New Journal of Physics **12**, 053015 (2010).
- [115] Y. Li, D. E. Browne, L. C. Kwek, R. Raussendorf, and T.-C. Wei, *Thermal States as Universal Resources for Quantum Computation with Always-On Interactions*, Physical Review Letters **107** (2011).
- [116] K. Fujii, Y. Nakata, M. Ohzeki, and M. Muraio, *Measurement-Based Quantum Computation on Symmetry Breaking Thermal States*, Physical Review Letters **110** (2013).
- [117] S. Roberts, B. Yoshida, A. Kubica, and S. D. Bartlett, *Symmetry-protected topological order at nonzero temperature*, Physical Review A **96** (2017).
- [118] R. Roy and F. Harper, *Abelian Floquet symmetry-protected topological phases in one dimension*, Physical Review B **94**, 125105 (2016).

- [119] C. W. von Keyserlingk and S. L. Sondhi, *Phase structure of one-dimensional interacting Floquet systems. I. Abelian symmetry-protected topological phases*, Physical Review B **93**, 245145 (2016).
- [120] A. Kumar, P. T. Dumitrescu, and A. C. Potter, *String order parameters for one-dimensional Floquet symmetry protected topological phases*, Physical Review B **97**, 224302 (2018).
- [121] M. McGinley and N. R. Cooper, *Topology of One-Dimensional Quantum Systems Out of Equilibrium*, Phys. Rev. Lett. **121**, 090401 (2018).
- [122] M. McGinley and N. R. Cooper, *Fragility of time-reversal symmetry protected topological phases*, Nature Physics **16**, 1181–1183 (2020).
- [123] M. M. Wolf, *Quantum Channels & Operations Guided Tour*, 2012.
- [124] F. Verstraete and H. Verschelde, *On quantum channels*, arXiv preprint quant-ph/0202124 (2002).
- [125] L. Piroli and J. I. Cirac, *Quantum Cellular Automata, Tensor Networks, and Area Laws*, Phys. Rev. Lett. **125**, 190402 (2020).
- [126] T. S. Cubitt, A. Lucia, S. Michalakis, and D. Perez-Garcia, *Stability of Local Quantum Dissipative Systems*, Communications in Mathematical Physics **337**, 1275–1315 (2015).
- [127] R. König and F. Pastawski, *Generating topological order: No speedup by dissipation*, Phys. Rev. B **90**, 045101 (2014).
- [128] N. Schuch, D. Pérez-García, and I. Cirac, *Classifying quantum phases using matrix product states and projected entangled pair states*, Phys. Rev. B **84**, 165139 (2011).
- [129] H. A. Kramers and G. H. Wannier, *Statistics of the Two-Dimensional Ferromagnet. Part II*, Phys. Rev. **60**, 263 (1941).
- [130] G. Evenbly and G. Vidal, *Tensor Network Renormalization*, Phys. Rev. Lett. **115**, 180405 (2015).
- [131] M. Bal, M. Mariën, J. Haegeman, and F. Verstraete, *Renormalization Group Flows of Hamiltonians Using Tensor Networks*, Physical Review Letters **118** (2017).
- [132] M. B. Hastings, *An area law for one-dimensional quantum systems*, Journal of Statistical Mechanics: Theory and Experiment **2007**, P08024–P08024 (2007).
- [133] F. Verstraete and J. I. Cirac, *Matrix product states represent ground states faithfully*, Phys. Rev. B **73**, 094423 (2006).

- [134] I. Affleck, T. Kennedy, E. H. Lieb, and H. Tasaki, *Rigorous results on valence-bond ground states in antiferromagnets*, Phys. Rev. Lett. **59**, 799 (1987).
- [135] R. Raussendorf, D. E. Browne, and H. J. Briegel, *Measurement-based quantum computation on cluster states*, Physical Review A **68** (2003).
- [136] D. Perez-Garcia, F. Verstraete, M. M. Wolf, and J. I. Cirac, *Matrix Product State Representations*, Quantum Info. Comput. **7**, 401–430 (2007).
- [137] J. Biamonte and V. Bergholm, *Tensor Networks in a Nutshell*, 2017, 1708.00006.
- [138] R. Orús, *A practical introduction to tensor networks: Matrix product states and projected entangled pair states*, Annals of Physics **349**, 117 (2014).
- [139] F. Verstraete and J. I. Cirac, *Renormalization algorithms for Quantum-Many Body Systems in two and higher dimensions*, 2004.
- [140] F. Verstraete, J. J. García-Ripoll, and J. I. Cirac, *Matrix Product Density Operators: Simulation of Finite-Temperature and Dissipative Systems*, Phys. Rev. Lett. **93**, 207204 (2004).
- [141] F. Verstraete, D. Porras, and J. I. Cirac, *Density Matrix Renormalization Group and Periodic Boundary Conditions: A Quantum Information Perspective*, Phys. Rev. Lett. **93**, 227205 (2004).
- [142] F. Verstraete, M. M. Wolf, D. Perez-Garcia, and J. I. Cirac, *Criticality, the Area Law, and the Computational Power of Projected Entangled Pair States*, Phys. Rev. Lett. **96**, 220601 (2006).
- [143] N. Schuch, M. M. Wolf, F. Verstraete, and J. I. Cirac, *Computational Complexity of Projected Entangled Pair States*, Phys. Rev. Lett. **98**, 140506 (2007).
- [144] G. Vidal, *Classical Simulation of Infinite-Size Quantum Lattice Systems in One Spatial Dimension*, Phys. Rev. Lett. **98**, 070201 (2007).
- [145] J. Jordan, R. Orús, G. Vidal, F. Verstraete, and J. I. Cirac, *Classical Simulation of Infinite-Size Quantum Lattice Systems in Two Spatial Dimensions*, Phys. Rev. Lett. **101**, 250602 (2008).
- [146] R. Orús and G. Vidal, *Simulation of two-dimensional quantum systems on an infinite lattice revisited: Corner transfer matrix for tensor contraction*, Phys. Rev. B **80**, 094403 (2009).
- [147] K. G. Wilson, *Renormalization Group and Critical Phenomena. I. Renormalization Group and the Kadanoff Scaling Picture*, Phys. Rev. B **4**, 3174 (1971).

- [148] S. R. White, *Density matrix formulation for quantum renormalization groups*, Phys. Rev. Lett. **69**, 2863 (1992).
- [149] G. Vidal, *Efficient Classical Simulation of Slightly Entangled Quantum Computations*, Physical Review Letters **91** (2003).
- [150] A. Molnar, J. Garre-Rubio, D. Pérez-García, N. Schuch, and J. I. Cirac, *Normal projected entangled pair states generating the same state*, New J. Phys. **20**, 113017 (2018), arXiv:1804.04964.
- [151] N. Schuch, I. Cirac, and D. Pérez-García, *PEPS as ground states: Degeneracy and topology*, Annals of Physics **325**, 2153 (2010).
- [152] A. Y. Kitaev, *Fault-tolerant quantum computation by anyons*, Annals of Physics **303**, 2 (2003).
- [153] M. B. Şahinoğlu, D. Williamson, N. Bultinck, M. Mariën, J. Haegeman, N. Schuch, and F. Verstraete, *Characterizing Topological Order with Matrix Product Operators*, Annales Henri Poincaré **22**, 563 (2021).
- [154] X. Chen, Z.-C. Gu, Z.-X. Liu, and X.-G. Wen, *Symmetry protected topological orders and the group cohomology of their symmetry group*, Phys. Rev. B **87**, 155114 (2013).
- [155] Y. Ogata, *Classification of gapped ground state phases in quantum spin systems*, 2021, 2110.04675.
- [156] I. Marvian, *Symmetry-protected topological entanglement*, Phys. Rev. B **95**, 045111 (2017).
- [157] F. Pollmann and A. M. Turner, *Detection of symmetry-protected topological phases in one dimension*, Phys. Rev. B **86**, 125441 (2012).
- [158] F. Pollmann, A. M. Turner, E. Berg, and M. Oshikawa, *Entanglement spectrum of a topological phase in one dimension*, Phys. Rev. B **81**, 064439 (2010).
- [159] D. V. Else and C. Nayak, *Classifying symmetry-protected topological phases through the anomalous action of the symmetry on the edge*, Physical Review B **90** (2014).
- [160] S. Bravyi and R. Raussendorf, *Measurement-based quantum computation with the toric code states*, Physical Review A **76** (2007).
- [161] D. Gross, S. T. Flammia, and J. Eisert, *Most Quantum States Are Too Entangled To Be Useful As Computational Resources*, Physical Review Letters **102** (2009).
- [162] F. Pollmann, E. Berg, A. M. Turner, and M. Oshikawa, *Symmetry protection of topological phases in one-dimensional quantum spin systems*, Phys. Rev. B **85**, 075125 (2012).

- [163] D. T. Stephen, D.-S. Wang, A. Prakash, T.-C. Wei, and R. Raussendorf, *Computational Power of Symmetry-Protected Topological Phases*, Phys. Rev. Lett. **119**, 010504 (2017).
- [164] R. Raussendorf, D. E. Browne, and H. J. Briegel, *Measurement-based quantum computation on cluster states*, Phys. Rev. A **68**, 022312 (2003).
- [165] L. Fidkowski, J. Haah, and M. B. Hastings, *An Exactly Solvable Model for a 4 + 1D Beyond-Cohomology Symmetry Protected Topological Phase*, (2019), arXiv:1912.05565.
- [166] J. Garre-Rubio, L. Lootens, and A. Molnár, *Classifying phases protected by matrix product operator symmetries using matrix product states*, 2022.
- [167] T. Devakul, D. J. Williamson, and Y. You, *Classification of subsystem symmetry-protected topological phases*, Phys. Rev. B **98**, 235121 (2018).
- [168] D. Gottesman, *Stabilizer codes and quantum error correction*, (1997), arXiv:quant-ph/9705052.
- [169] D. Ben-Zion, D. Das, and J. McGreevy, *Exactly solvable models of spin liquids with spinons, and of three-dimensional topological paramagnets*, Phys. Rev. B **93**, 155147 (2016).
- [170] G. Karpilovsky, *Group representations*, 3 ed. (Elsevier, Amsterdam, 1994).
- [171] N. B. Backhouse and C. Bradley, *Projective representations of abelian groups*, Proceedings of the American Mathematical Society **36**, 260 (1972).
- [172] Y. G. Berkovich and E. M. Zhmud, *Characters of Finite Groups, Vol. 1* (American Mathematical Society, 1998).
- [173] A. Miyake, *Quantum Computation on the Edge of a Symmetry-Protected Topological Order*, Phys. Rev. Lett. **105**, 040501 (2010).
- [174] D. V. Else, I. Schwarz, S. D. Bartlett, and A. C. Doherty, *Symmetry-Protected Phases for Measurement-Based Quantum Computation*, Phys. Rev. Lett. **108**, 240505 (2012).
- [175] J. Miller and A. Miyake, *Resource Quality of a Symmetry-Protected Topologically Ordered Phase for Quantum Computation*, Phys. Rev. Lett. **114**, 120506 (2015).
- [176] J. Haegeman, D. Pérez-García, I. Cirac, and N. Schuch, *Order Parameter for Symmetry-Protected Phases in One Dimension*, Physical Review Letters **109** (2012).
- [177] M. den Nijs and K. Rommelse, *Preroughening transitions in crystal surfaces and valence-bond phases in quantum spin chains*, Phys. Rev. B **40**, 4709 (1989).

- [178] A. Elben, J. Yu, G. Zhu, M. Hafezi, F. Pollmann, P. Zoller, and B. Vermersch, *Many-body topological invariants from randomized measurements in synthetic quantum matter*, *Science advances* **6**, eaaz3666 (2020).
- [179] A. Elben, J. Yu, G. Zhu, M. Hafezi, F. Pollmann, P. Zoller, and B. Vermersch, *Many-body topological invariants from randomized measurements in synthetic quantum matter*, *Science Advances* **6** (2020).
- [180] A. Kitaev and J. Preskill, *Topological Entanglement Entropy*, *Phys. Rev. Lett.* **96**, 110404 (2006).
- [181] S. Papanikolaou, K. S. Raman, and E. Fradkin, *Topological phases and topological entropy of two-dimensional systems with finite correlation length*, *Phys. Rev. B* **76**, 224421 (2007).
- [182] N. Schuch, M. M. Wolf, F. Verstraete, and J. I. Cirac, *Entropy Scaling and Simulability by Matrix Product States*, *Phys. Rev. Lett.* **100**, 030504 (2008).
- [183] A. Kitaev, *Anyons in an exactly solved model and beyond*, *Annals of Physics* **321**, 2 (2006).
- [184] A. Hamma, R. Ionicioiu, and P. Zanardi, *Bipartite entanglement and entropic boundary law in lattice spin systems*, *Phys. Rev. A* **71**, 022315 (2005).
- [185] M. Barkeshli, P. Bonderson, M. Cheng, and Z. Wang, *Symmetry fractionalization, defects, and gauging of topological phases*, *Phys. Rev. B* **100**, 115147 (2019).
- [186] X. Chen, *Symmetry fractionalization in two dimensional topological phases*, *Reviews in Physics* **2**, 3 (2017).
- [187] N. Tarantino, N. H. Lindner, and L. Fidkowski, *Symmetry fractionalization and twist defects*, *New Journal of Physics* **18**, 035006 (2016).
- [188] M. B. Şahinoğlu, D. Williamson, N. Bultinck, M. Mariën, J. Haegeman, N. Schuch, and F. Verstraete, *Characterizing Topological Order with Matrix Product Operators*, *Annales Henri Poincaré* **22**, 563 (2021).
- [189] C.-Y. Huang, X. Chen, and F. Pollmann, *Detection of symmetry-enriched topological phases*, *Phys. Rev. B* **90**, 045142 (2014).
- [190] S. Roberts, B. Yoshida, A. Kubica, and S. D. Bartlett, *Symmetry-protected topological order at nonzero temperature*, *Phys. Rev. A* **96**, 022306 (2017).
- [191] A. Kómár, O. Landon-Cardinal, and K. Temme, *Necessity of an energy barrier for self-correction of Abelian quantum doubles*, *Phys. Rev. A* **93**, 052337 (2016).
- [192] H. Bombin and M. A. Martin-Delgado, *Family of non-Abelian Kitaev models on a lattice: Topological condensation and confinement*, *Phys. Rev. B* **78**, 115421 (2008).

- [193] D. Ben-Zion, D. Das, and J. McGreevy, *Exactly solvable models of spin liquids with spinons, and of three-dimensional topological paramagnets*, Phys. Rev. B **93**, 155147 (2016).
- [194] L. Cincio and Y. Qi, *Classification and detection of symmetry fractionalization in chiral spin liquids*, 2015.
- [195] M. P. Zaletel, Z. Zhu, Y.-M. Lu, A. Vishwanath, and S. R. White, *Space Group Symmetry Fractionalization in a Chiral Kagome Heisenberg Antiferromagnet*, Phys. Rev. Lett. **116**, 197203 (2016).
- [196] M. P. Zaletel, Y.-M. Lu, and A. Vishwanath, *Measuring space-group symmetry fractionalization in \mathbb{Z}_2 spin liquids*, Phys. Rev. B **96**, 195164 (2017).
- [197] L. Wang, A. Essin, M. Hermele, and O. Motrunich, *Numerical detection of symmetry-enriched topological phases with space-group symmetry*, Phys. Rev. B **91**, 121103 (2015).
- [198] S. N. Saadatmand and I. P. McCulloch, *Symmetry fractionalization in the topological phase of the spin- $\frac{1}{2}$ J_1 - J_2 triangular Heisenberg model*, Phys. Rev. B **94**, 121111 (2016).
- [199] A. Molnar, J. Garre-Rubio, D. Pérez-García, N. Schuch, and J. I. Cirac, *Normal projected entangled pair states generating the same state*, New Journal of Physics **20**, 113017 (2018).
- [200] A. Molnar, Y. Ge, N. Schuch, and J. I. Cirac, *A generalization of the injectivity condition for projected entangled pair states*, J. Math. Phys. **59**, 021902 (2018).
- [201] A. Mesaros and Y. Ran, *Classification of symmetry enriched topological phases with exactly solvable models*, Phys. Rev. B **87**, 155115 (2013).
- [202] C. de Groot, D. T. Stephen, A. Molnar, and N. Schuch, *Inaccessible entanglement in symmetry protected topological phases*, Journal of Physics A: Mathematical and Theoretical **53**, 335302 (2020).
- [203] C. H. Bennett, G. Brassard, C. Crépeau, R. Jozsa, A. Peres, and W. K. Wootters, *Teleporting an unknown quantum state via dual classical and Einstein-Podolsky-Rosen channels*, Phys. Rev. Lett. **70**, 1895 (1993).
- [204] A. K. Ekert, *Quantum cryptography based on Bell's theorem*, Phys. Rev. Lett. **67**, 661 (1991).
- [205] C. H. Bennett and S. J. Wiesner, *Communication via one- and two-particle operators on Einstein-Podolsky-Rosen states*, Phys. Rev. Lett. **69**, 2881 (1992).
- [206] H. Wiseman and J. A. Vaccaro, *Entanglement of indistinguishable particles shared between two parties*, Phys. Rev. Lett. **91**, 097902 (2003).

- [207] H. Barghathi, E. Casiano-Diaz, and A. Del Maestro, *Operationally accessible entanglement of one-dimensional spinless fermions*, Phys. Rev. A **100**, 022324 (2019).
- [208] H. Barghathi, E. Casiano-Diaz, and A. Del Maestro, *Operationally accessible entanglement of one-dimensional spinless fermions*, Phys. Rev. A **100**, 022324 (2019).
- [209] I. Klich and L. Levitov, *Scaling of entanglement entropy and superselection rules*, arXiv:0812.0006 (2008).
- [210] H. Barghathi, C. Herdman, and A. Del Maestro, *Rényi Generalization of the Accessible Entanglement Entropy*, Phys. Rev. Lett. **121**, 150501 (2018).
- [211] M. Goldstein and E. Sela, *Symmetry-resolved entanglement in many-body systems*, Phys. Rev. Lett. **120**, 200602 (2018).
- [212] J. Xavier, F. C. Alcaraz, and G. Sierra, *Equipartition of the entanglement entropy*, Phys. Rev. B **98**, 041106 (2018).
- [213] J. A. Vaccaro, F. Anselmi, H. M. Wiseman, and K. Jacobs, *Tradeoff between extractable mechanical work, accessible entanglement, and ability to act as a reference system, under arbitrary superselection rules*, Phys. Rev. A **77**, 032114 (2008).
- [214] G.-C. Wick, A. S. Wightman, and E. P. Wigner, *Superselection rule for charge*, Phys. Rev. D **1**, 3267 (1970).
- [215] N. Schuch, F. Verstraete, and J. I. Cirac, *Quantum entanglement theory in the presence of superselection rules*, Phys. Rev. A **70**, 042310 (2004).
- [216] F. Verstraete and J. I. Cirac, *Quantum nonlocality in the presence of superselection rules and data hiding protocols*, Phys. Rev. Lett. **91**, 010404 (2003).
- [217] D. Azses, R. Haenel, Y. Naveh, R. Raussendorf, E. Sela, and E. G. D. Torre, *Identification of symmetry-protected topological states on noisy quantum computers*, (2020), arXiv:2002.04620.
- [218] S. Fraenkel and M. Goldstein, *Symmetry resolved entanglement: Exact results in 1D and beyond*, arXiv:1910.08459 (2019).
- [219] P. Calabrese, M. Collura, G. D. Giulio, and S. Murciano, *Full counting statistics in the gapped XXZ spin chain*, (2020), arXiv:2002.04367.
- [220] E. Cornfeld, L. A. Landau, K. Shtengel, and E. Sela, *Entanglement spectroscopy of non-Abelian anyons: Reading off quantum dimensions of individual anyons*, Phys. Rev. B **99**, 115429 (2019).
- [221] S. D. Bartlett and H. M. Wiseman, *Entanglement constrained by superselection rules*, Phys. Rev. Lett. **91**, 097903 (2003).

- [222] S. Murciano, G. D. Giulio, and P. Calabrese, *Symmetry resolved entanglement in gapped integrable systems: a corner transfer matrix approach*, (2019), arXiv:1911.09588.
- [223] N. Laflorencie and S. Rachel, *Spin-resolved entanglement spectroscopy of critical spin chains and Luttinger liquids*, Journal of Statistical Mechanics: Theory and Experiment **2014**, P11013 (2014).
- [224] S. Ghosh, R. M. Soni, and S. P. Trivedi, *On the entanglement entropy for gauge theories*, Journal of High Energy Physics **2015**, 69 (2015).
- [225] K. Van Acoleyen, N. Bultinck, J. Haegeman, M. Marien, V. B. Scholz, and F. Verstraete, *Entanglement of Distillation for Lattice Gauge Theories*, Phys. Rev. Lett. **117**, 131602 (2016).
- [226] R. M. Soni and S. P. Trivedi, *Aspects of entanglement entropy for gauge theories*, Journal of High Energy Physics **2016**, 136 (2016).
- [227] X.-G. Wen, *Choreographed entangle dances: topological states of quantum matter*, arXiv:1906.05983 (2019).
- [228] B. Zeng, X. Chen, D.-L. Zhou, and X.-G. Wen, *Quantum Information Meets Quantum Matter—From Quantum Entanglement to Topological Phase in Many-Body Systems*, arXiv:1508.02595 (2015).
- [229] K. Duivenvoorden, M. Iqbal, J. Haegeman, F. Verstraete, and N. Schuch, *Entanglement phases as holographic duals of anyon condensates*, Phys. Rev. B **95**, 235119 (2017).
- [230] R. Verresen, R. Moessner, and F. Pollmann, *One-dimensional symmetry protected topological phases and their transitions*, Phys. Rev. B **96**, 165124 (2017).
- [231] X.-G. Wen, *Quantum order: a quantum entanglement of many particles*, Physics Letters A **300**, 175 (2002).
- [232] D. T. Stephen, H. Dreyer, M. Iqbal, and N. Schuch, *Detecting subsystem symmetry protected topological order via entanglement entropy*, Phys. Rev. B **100**, 115112 (2019).
- [233] Y. You, T. Devakul, F. J. Burnell, and S. L. Sondhi, *Subsystem symmetry protected topological order*, Phys. Rev. B **98**, 035112 (2018).
- [234] D. T. Stephen, H. P. Nautrup, J. Bermejo-Vega, J. Eisert, and R. Raussendorf, *Subsystem symmetries, quantum cellular automata, and computational phases of quantum matter*, Quantum **3**, 142 (2019).
- [235] M. M. Wilde, *Quantum information theory* (Cambridge University Press, 2013).

- [236] C. H. Bennett, H. J. Bernstein, S. Popescu, and B. Schumacher, *Concentrating partial entanglement by local operations*, Phys. Rev. A **53**, 2046 (1996).
- [237] U. Schollwöck, *The density-matrix renormalization group in the age of matrix product states*, Annals of Physics **326**, 96 (2011).
- [238] H. J. Briegel and R. Raussendorf, *Persistent entanglement in arrays of interacting particles*, Phys. Rev. Lett. **86**, 910 (2001).
- [239] W. Son, L. Amico, and V. Vedral, *Topological order in 1D Cluster state protected by symmetry*, Quantum Information Processing **11**, 1961 (2012).
- [240] D. V. Else, S. D. Bartlett, and A. C. Doherty, *Symmetry protection of measurement-based quantum computation in ground states*, New Journal of Physics **14**, 113016 (2012).
- [241] T. Devakul and D. J. Williamson, *Universal quantum computation using fractal symmetry-protected cluster phases*, Phys. Rev. A **98**, 022332 (2018).
- [242] A. K. Daniel, R. N. Alexander, and A. Miyake, *Computational universality of symmetry-protected topologically ordered cluster phases on 2D Archimedean lattices*, Quantum **4**, 228 (2020).
- [243] D. T. Stephen, D.-S. Wang, A. Prakash, T.-C. Wei, and R. Raussendorf, *Computational Power of Symmetry-Protected Topological Phases*, Physical Review Letters **119** (2017).
- [244] F. Verstraete, M. Popp, and J. I. Cirac, *Entanglement versus Correlations in Spin Systems*, Phys. Rev. Lett. **92**, 027901 (2004).
- [245] K. Choo, C. W. Von Keyserlingk, N. Regnault, and T. Neupert, *Measurement of the entanglement spectrum of a symmetry-protected topological state using the IBM quantum computer*, Phys. Rev. Lett. **121**, 086808 (2018).
- [246] D. P. DiVincenzo, D. W. Leung, and B. M. Terhal, *Quantum data hiding*, IEEE Transactions on Information Theory **48**, 580 (2002).
- [247] F. Haldane, *Continuum dynamics of the 1-D Heisenberg antiferromagnet: Identification with the $O(3)$ nonlinear sigma model*, Physics Letters A **93**, 464 (1983).
- [248] F. D. M. Haldane, *Nonlinear Field Theory of Large-Spin Heisenberg Antiferromagnets: Semiclassically Quantized Solitons of the One-Dimensional Easy-Axis Néel State*, Phys. Rev. Lett. **50**, 1153 (1983).
- [249] I. Affleck, T. Kennedy, E. H. Lieb, and H. Tasaki, *Rigorous results on valence-bond ground states in antiferromagnets*, Phys. Rev. Lett. **59**, 799 (1987).
- [250] T. Kennedy and H. Tasaki, *Hidden $\mathbb{Z}_2 \times \mathbb{Z}_2$ symmetry breaking in Haldane-gap antiferromagnets*, Phys. Rev. B **45**, 304 (1992).

- [251] F. Verstraete and J. I. Cirac, *Matrix product states represent ground states faithfully*, Phys. Rev. B **73**, 094423 (2006), cond-mat/0505140.
- [252] N. Schuch, M. M. Wolf, F. Verstraete, and J. I. Cirac, *Entropy scaling and simulability by Matrix Product States*, Phys. Rev. Lett. **100**, 30504 (2008), arXiv:0705.0292.
- [253] X. Chen, Z.-C. Gu, Z.-X. Liu, and X.-G. Wen, *Symmetry protected topological orders in interacting bosonic systems*, Science **338**, 1604 (2012), arXiv:1301.0861.
- [254] B. Kraus, H. P. Büchler, S. Diehl, A. Kantian, A. Micheli, and P. Zoller, *Preparation of entangled states by quantum Markov processes*, Physical Review A **78** (2008).
- [255] L. Zhou, S. Choi, and M. D. Lukin, *Symmetry-protected dissipative preparation of matrix product states*, 2017, 1706.01995.
- [256] S. Lieu, R. Belyansky, J. T. Young, R. Lundgren, V. V. Albert, and A. V. Gorshkov, *Symmetry Breaking and Error Correction in Open Quantum Systems*, Phys. Rev. Lett. **125**, 240405 (2020).
- [257] V. V. Albert, *Lindbladians with multiple steady states: theory and applications*, 2018, 1802.00010.
- [258] B. Buča and T. Prosen, *A note on symmetry reductions of the Lindblad equation: transport in constrained open spin chains*, New Journal of Physics **14**, 073007 (2012).
- [259] V. V. Albert and L. Jiang, *Symmetries and conserved quantities in Lindblad master equations*, Phys. Rev. A **89**, 022118 (2014).
- [260] M. M. Wolf, *Quantum Channels and Operations: Guided Tour*, 2012.
- [261] G. Benenti, G. Casati, and G. Strini, *Principles of Quantum Computation and Information* (World Scientific, 2004), <https://www.worldscientific.com/doi/pdf/10.1142/5528>.
- [262] W. Fulton and J. Harris, *Representation Theory: A First Course* (Springer New York, 2013).
- [263] K. Shiozaki and S. Ryu, *Matrix product states and equivariant topological field theories for bosonic symmetry-protected topological phases in (1+1) dimensions*, J. High Energ. Phys. **100** (2017).
- [264] A. Kapustin, A. Turzillo, and M. You, *Topological field theory and matrix product states*, Phys. Rev. B **96**, 075125 (2017).
- [265] J. I. Cirac, D. Perez-Garcia, N. Schuch, and F. Verstraete, *Matrix product unitaries: structure, symmetries, and topological invariants*, Journal of Statistical Mechanics: Theory and Experiment **2017**, 083105 (2017).

- [266] M. B. Şahinoğlu, S. K. Shukla, F. Bi, and X. Chen, *Matrix product representation of locality preserving unitaries*, Phys. Rev. B **98**, 245122 (2018).
- [267] D. Gross, V. Nesme, and H. Vogts, *Index Theory of One Dimensional Quantum Walks and Cellular Automata*, Commun. Math. Phys. **310**, 419–454 (2012).
- [268] Z. Gong, C. Sünderhauf, N. Schuch, and J. I. Cirac, *Classification of Matrix-Product Unitaries with Symmetries*, Phys. Rev. Lett. **124**, 100402 (2020).
- [269] D. Pérez-García, M. M. Wolf, M. Sanz, F. Verstraete, and J. I. Cirac, *String Order and Symmetries in Quantum Spin Lattices*, Phys. Rev. Lett. **100**, 167202 (2008).
- [270] J. Haah, *An Invariant of Topologically Ordered States Under Local Unitary Transformations*, Communications in Mathematical Physics **342**, 771 (2016).
- [271] M. Vojta, *Quantum phase transitions*, Reports on Progress in Physics **66**, 2069 (2003).
- [272] X. Chen, F. Wang, Y.-M. Lu, and D.-H. Lee, *Critical theories of phase transition between symmetry protected topological states and their relation to the gapless boundary theories*, Nuclear Physics B **873**, 248 (2013).
- [273] T. Grover and A. Vishwanath, *Quantum phase transition between integer quantum Hall states of bosons*, Phys. Rev. B **87**, 045129 (2013).
- [274] Y.-M. Lu and D.-H. Lee, *Quantum phase transitions between bosonic symmetry-protected topological phases in two dimensions: Emergent QED₃ and anyon superfluid*, Phys. Rev. B **89**, 195143 (2014).
- [275] F. Verstraete, M. M. Wolf, and J. Ignacio Cirac, *Quantum computation and quantum-state engineering driven by dissipation*, Nature Physics **5**, 633 (2009).
- [276] Z. Gong, C. Sünderhauf, N. Schuch, and J. I. Cirac, *Classification of Matrix-Product Unitaries with Symmetries*, Physical Review Letters **124** (2020).
- [277] K. Duivenvoorden, M. Iqbal, J. Haegeman, F. Verstraete, and N. Schuch, *Entanglement phases as holographic duals of anyon condensates*, Phys. Rev. B **95**, 235119 (2017).
- [278] J. Garre-Rubio, S. Iblisdir, and D. Pérez-García, *Symmetry reduction induced by anyon condensation: A tensor network approach*, Phys. Rev. B **96**, 155123 (2017).
- [279] J. Goold, M. Huber, A. Riera, L. del Rio, and P. Skrzypczyk, *The role of quantum information in thermodynamics—a topical review*, Journal of Physics A: Mathematical and Theoretical **49**, 143001 (2016).

- [280] S. Vinjanampathy and J. Anders, *Quantum thermodynamics*, Contemporary Physics **57**, 545 (2016).
- [281] P. Strasberg and A. Winter, *First and Second Law of Quantum Thermodynamics: A Consistent Derivation Based on a Microscopic Definition of Entropy*, PRX Quantum **2**, 030202 (2021).
- [282] J. Gemmer, M. Michel, and G. Mahler, *Quantum thermodynamics: Emergence of thermodynamic behavior within composite quantum systems*, 784 ed. (Springer, 2009).
- [283] R. Raussendorf, *Quantum computation via translation-invariant operations on a chain of qubits*, Phys. Rev. A **72**, 052301 (2005).
- [284] R. Raussendorf, J. Harrington, and K. Goyal, *A fault-tolerant one-way quantum computer*, Annals of Physics **321**, 2242 (2006).
- [285] R. Raussendorf, J. Harrington, and K. Goyal, *Topological fault-tolerance in cluster state quantum computation*, New Journal of Physics **9**, 199 (2007).
- [286] R. Raussendorf, D.-S. Wang, A. Prakash, T.-C. Wei, and D. T. Stephen, *Symmetry-protected topological phases with uniform computational power in one dimension*, Phys. Rev. A **96**, 012302 (2017).
- [287] M. S. Kesselring, F. Pastawski, J. Eisert, and B. J. Brown, *The boundaries and twist defects of the color code and their applications to topological quantum computation*, Quantum **2**, 101 (2018).
- [288] C. Delaney and Z. Wang, *Symmetry defects and their application to topological quantum computing*, Contemporary Mathematics , 121–151 (2020), arXiv:1811.02143.
- [289] D. Gross, J. Eisert, N. Schuch, and D. Perez-Garcia, *Measurement-based quantum computation beyond the one-way model*, Phys. Rev. A **76**, 052315 (2007).
- [290] J. Haegeman and F. Verstraete, *Diagonalizing Transfer Matrices and Matrix Product Operators: A Medley of Exact and Computational Methods*, Annual Review of Condensed Matter Physics **8**, 355 (2017).
- [291] C. Castelnovo and C. Chamon, *Topological order in a three-dimensional toric code at finite temperature*, Phys. Rev. B **78**, 155120 (2008).
- [292] A. R. de Alarcón, J. Garre-Rubio, A. Molnár, and D. Pérez-García, *Matrix Product Operator Algebras II: Phases of Matter for 1D Mixed States*, 2022.
- [293] A. R. de Alarcón, J. Garre-Rubio, A. Molnár, and D. Pérez-García, *Matrix Product Operator Algebras II: Phases of Matter for 1D Mixed States*, 2022.
- [294] M. B. Hastings, *Solving gapped Hamiltonians locally*, Phys. Rev. B **73**, 085115 (2006).

- [295] M. M. Wolf, F. Verstraete, M. B. Hastings, and J. I. Cirac, *Area Laws in Quantum Systems: Mutual Information and Correlations*, Phys. Rev. Lett. **100**, 070502 (2008).
- [296] A. Bluhm, Á . Capel, and A. Pérez-Hernández, *Exponential decay of mutual information for Gibbs states of local Hamiltonians*, Quantum **6**, 650 (2022).
- [297] I. Bardet, A. Capel, L. Gao, A. Lucia, D. Perez Garcia, and C. Rouze, *Rapid thermalization of spin chain commuting Hamiltonians*, 2021.